Lactococcal extracellular vesicles deliver vitamin K2 to human cells Yue Liu 2022

Good things come in small packages - delivery of vitamin K2 to human cells by extracellular vesicles from *Lactococcus lactis*

Yue Liu

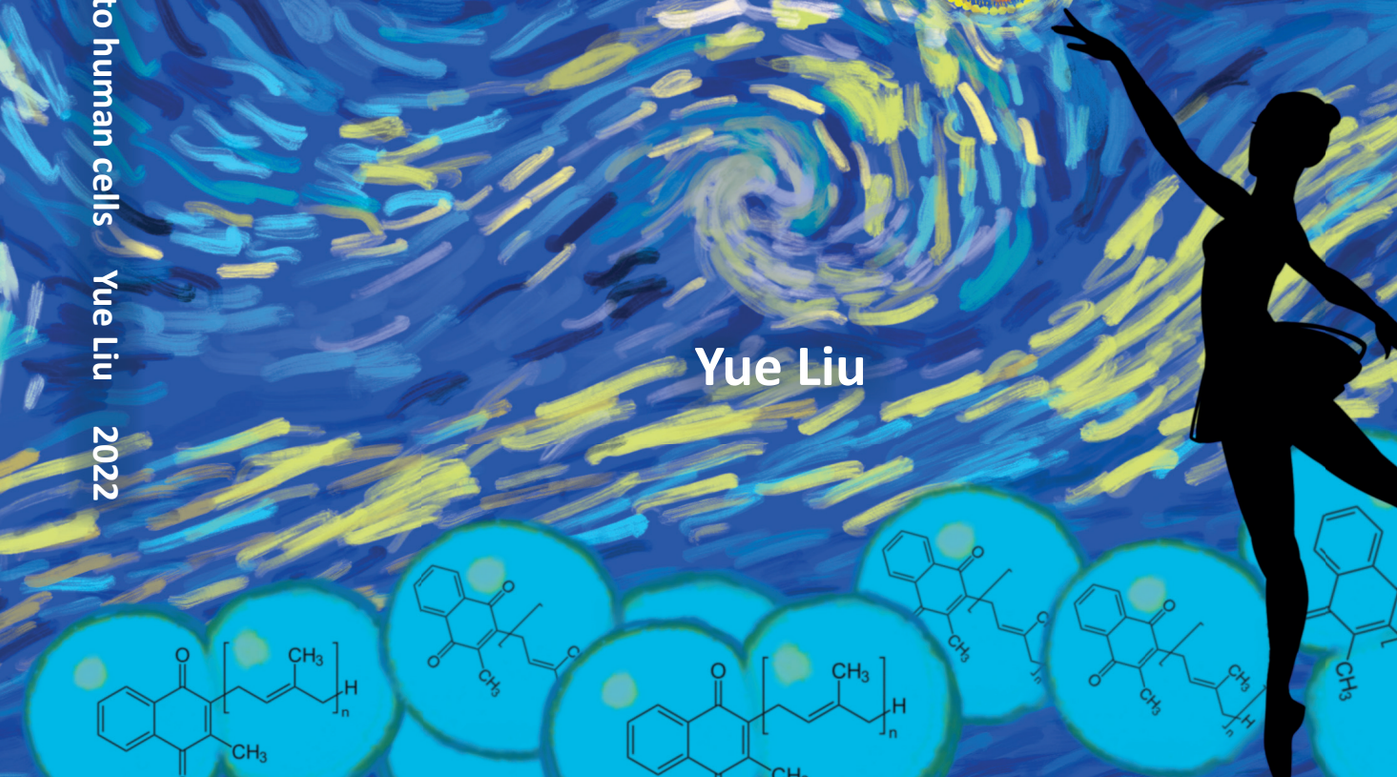

Invitation

To the public defence of my PhD thesis entitled:

Good things come in small packages – delivery of vitamin K2 to human cells by extracellular vesicles from *Lactococcus lactis*

On Friday 18 February 2022 at 1:30 p.m. in the Aula of Wageningen University, Generaal Foulkesweg 1, Wageningen

Yue Liu
yue1.liu@wur.nl

Paranymphs

Pjotr Middendorf
pjotr.middendorf@wur.nl

Oscar van Mastrigt
oscar.vanmastrigt@wur.nl

Propositions

1. Prophage activation stimulates bacterial extracellular vesicle production.
   (this thesis)

2. Bacterial extracellular vesicles deliver vitamin K2 to human cells.
   (this thesis)

3. Educated assumptions lead to delays in discoveries.

4. Knowledge on human gut bacteriophage diversity (Camarillo-Guerrero et al., Cell, 2021) sheds new light on interactions between the gut microbiota and human host.

5. The public perceptions of GMOs and vitamins stand at the opposite, but equally wrong ends.

6. Overcorrections in gender and race diversity reinforce the impostor syndrome.

Propositions belonging to the thesis, entitled

Good things come in small packages - delivery of vitamin K2 to human cells by extracellular vesicles from *Lactococcus lactis*

Yue Liu

Wageningen, 18 February 2022

Good things come in small packages - delivery of vitamin K2 to human cells by extracellular vesicles from *Lactococcus lactis*

Yue Liu

Thesis committee

Promotors
Prof. Dr E. J. Smid
Personal chair at the Laboratory of Food Microbiology
Wageningen University & Research

Prof. Dr T. Abee
Personal chair at the Laboratory of Food Microbiology
Wageningen University & Research

Other members
Prof. Dr M. Kleerebezem, Wageningen University & Research
Prof. Dr E. B. Hansen, Technical University of Denmark, Kongens Lyngby, Denmark
Prof. Dr J. Mahony, University College Cork, Ireland
Prof. Dr J. M. Geleijnse , Wageningen University & Research

This research was conducted under the auspice of Graduate School VLAG
(Advanced studies in Food Technology, Agrobiotechnology, Nutrition and Health Sciences)

Good things come in small packages - delivery of vitamin K2 to human cells by extracellular vesicles from *Lactococcus lactis*

Yue Liu

Thesis

submitted in fulfilment of the requirements for the degree of doctor
at Wageningen University
by the authority of the Rector Magnificus,
Prof. Dr A. P. J. Mol,
in the presence of the
Thesis Committee appointed by the Academic Board
to be defended in public
on Friday 18 February 2022
at 1:30 p.m. in the Aula.

Yue Liu
Good things come in small packages - delivery of vitamin K2 to human cells by extracellular vesicles from *Lactococcus lactis*
300 pages

PhD thesis, Wageningen University, Wageningen, the Netherlands (2022)
With references, with summary in English

ISBN 978-94-6447-080-2
DOI https://doi.org/10.18174/561776

Table of contents

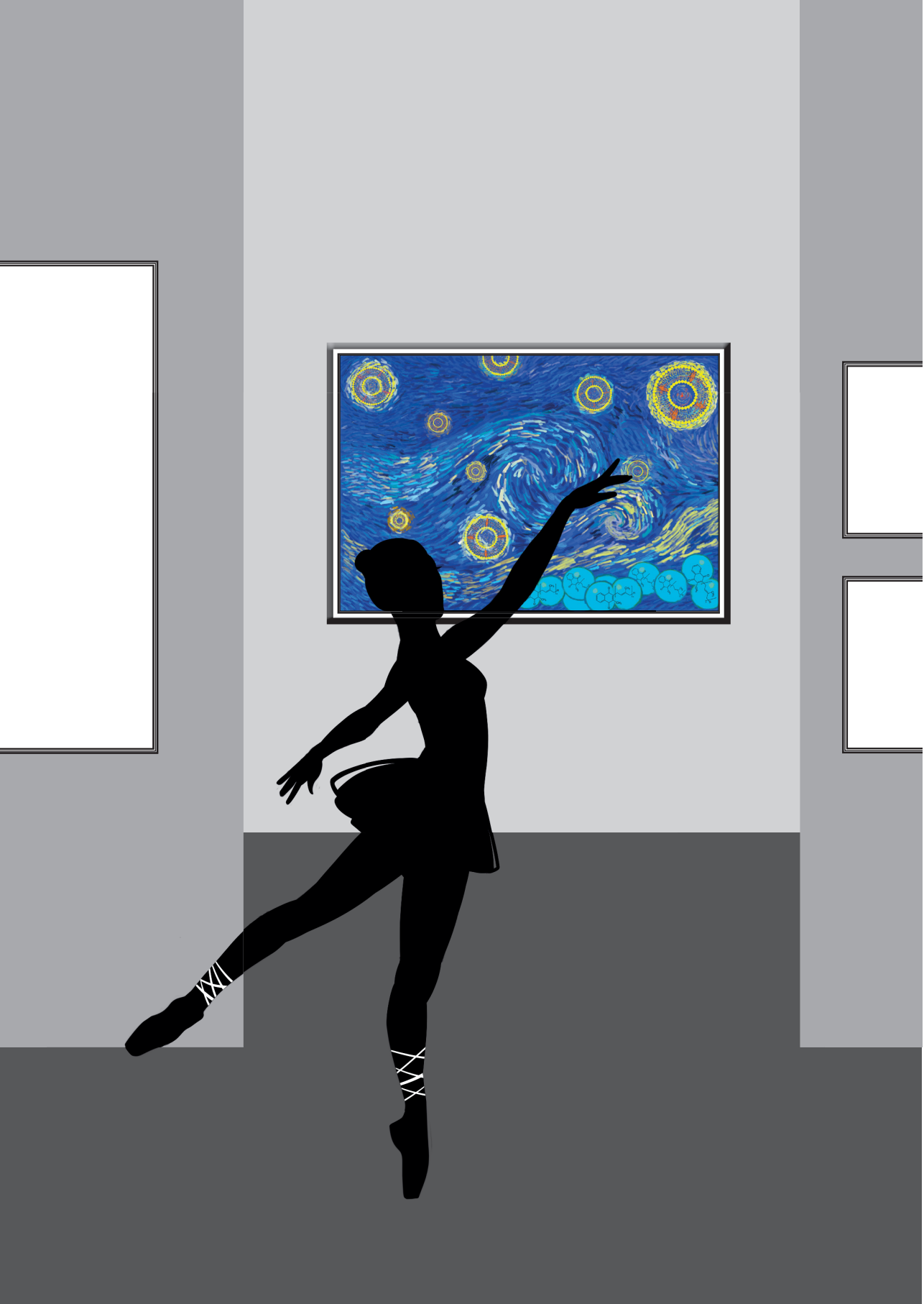

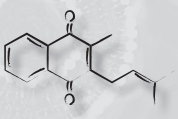

Chapter 1

General introduction

Yue Liu

Vitamins, including fat-soluble vitamins A, D, E, K and water-soluble vitamin B group and vitamin C, are micronutrients essential for proper development and function of the human body (Maqbool and Aslam, 2017; Akram et al., 2020). Vitamins cannot be synthesized by the human body to adequate levels and need to be supplied via diets. Vitamin fortification of foods is therefore of great interest for human health. Vitamin producing microorganisms offer opportunities for natural and effective vitamin enrichment in foods via fermentation, especially for members in the vitamin B group and vitamin K2 (Linares et al., 2017; Walther and Schmid, 2017). Selection of microbial species and strains, cultivation conditions, etc., have all been considered relevant aspects for vitamin fortification in foods. Furthermore, increased knowledge on microbial physiology in relation to vitamin production can be continuously translated into (novel) applications not only for enriched vitamin content, but also for efficient compound delivery to the human host to achieve the desired biological activities.

The research described in this thesis covers relevant areas including assessment of underlying mechanisms and optimization of vitamin K2 (menaquinone) production in the food fermentation key player *Lactococcus lactis*, as well as the production and characterization of bacterial extracellular vesicles (EVs) for optimized vitamin K2 delivery to the human host.

Vitamin K is essential for human health

The discovery of vitamin K dates back to the early 1930s, when the Danish scientist Henrik Dam originally set out to investigate the essentiality of cholesterol in chicken diet (Suttie, 1978). It was observed by Dam and other scientists that chickens fed on fat-depleted diets extracted with organic solvents suffered from hemorrhage and difficulty in blood clotting (McFarlane et al., 1931; Dam and Schönheyder, 1934). Addition of several known nutritional components such as pure cholesterol and ascorbic acid to the chicken diets did not restore these defects. However, anti-hemorrhage effect was observed from lipid extracts of animal liver, green plant and foods that were subjected to microbial actions (Almquist and Stokstad, 1935; Dam, 1935). Dam named this new, fat-soluble nutrient vitamin K, where the letter K was from the German word “Koagulation”, for its effect in blood coagulation. In 1943, the Nobel prize for Physiology or Medicine was rewarded to Dam and Doisy for the discovery of vitamin K and the chemical structure of it (NobelPrize.org, 2021).

Studies to date have established the basic biological function of vitamin K in the human body as the co-factor for the integral membrane protein γ-glutamyl carboxylase, that functions in post-translational carboxylation of proteins in which the glutamate (Glu) residues are converted into γ-carboxyglutamate (Gla) (Almquist and Stokstad, 1935; Cranenburg et al., 2007; Parker et al., 2014). The vitamin K-dependent carboxylation is essential for the maturation and the calcium-binding functionality of Gla-proteins. In the human body, important Gla-proteins include not only coagulation factors, but also osteocalcin which is associated with bone assembly and turnover, matrix Gla protein and Gla-rich protein which are strong tissue/cardiovascular calcification inhibitors, and growth-arrest-specific gene

6 protein (Gas6) (Stenflo et al., 1974; Berkner, 2005; Cranenburg et al., 2007; Schurgers et al., 2013; Willems et al., 2014). The wide range of vitamin K-dependent Gla-proteins extends the involvement in physiological processes of vitamin K from hemostasis to bone metabolism, cardiovascular mineralization, cell growth and apoptosis and beyond (Booth, 2009; Shearer and Okano, 2018; Xiao et al., 2021).

Vitamin K exists in two groups, namely vitamin K1 and vitamin K2. Both groups share a 2-methyl-1,4-naphthoquinone (menadione) structure, but differ in the number and degree of saturation of the isoprenoid side chain units attached to the C3 position of the naphthoquinone ring (Suttie, 2009) (Fig. 1.1). Vitamin K1 is a single form also named phylloquinone, and is synthesized in green plants as a component for photosynthesis. It contains four isoprene side chain units, among which three are saturated. Vitamin K2 refers to a group of menaquinones (MKs) containing only unsaturated isoprene side chain units, and the different forms of menaquinones are defined by the side chain length (MK-n, where n depicts the number of side chain units). Vitamin K2 is produced primarily by bacteria, with MK-4 being the only exception which is synthesized in animal tissue by the conversion of phylloquinone or menadione (Shearer and Okano, 2018). Although sometimes referred to as (pro-) vitamin K3, menadione itself lacks biological activity before being converted to MK-4 in animal tissue and is thus not discussed as a K vitamer here.

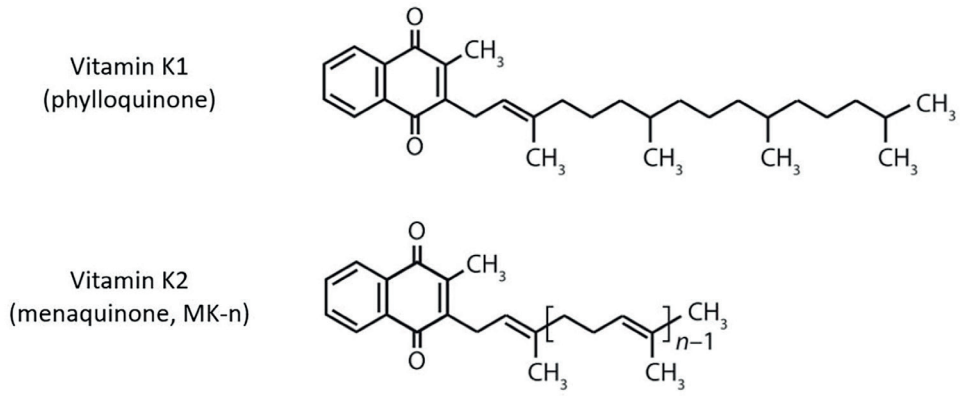

Figure 1.1. Chemical structure of vitamin K1 and vitamin K2. Modified from (Shearer and Okano, 2018).

The dietary source of vitamin K1 mainly includes green vegetables, some fruits and vegetable oils, while the source of vitamin K2 is more limited: MK-4 is mainly found in meat and meat products, egg yolk, milk and milk products; other long-chain MKs, namely MK-5 to MK-10, are found in fermented foods namely cheese and milk products, and the Japanese fermented soy bean product natto (Vermeer and Schurgers, 2000; Walther et al., 2013). In the western diet, the forms of vitamin K2 with highest amount of intake are MK-8 and MK-9 from fermented dairy products like cheese and curds, followed by MK-4 from meat (Shearer et al., 1996; Schurgers and Vermeer, 2000). In the Dutch and German diet, vitamin K2 was estimated to contribute to only 10% - 25% total vitamin K

content in the diet (Beulens et al., 2013). In addition, in a cohort of Dutch women, 9% of total dietary vitamin K content was estimated to be long-chain MKs in particular (Gast et al., 2009; Walther et al., 2013). Intestinal bacteria produce long-chain vitamin K2, and in human gut MK-10 was found to be the predominant form (Conly and Stein, 1992; Shearer, 1995). Vitamin K2 produced by intestinal bacteria showed a certain contribution to the vitamin K status in rats, but the colonic absorption was found to be extremely poor (Barnes and Fiala, 1959; Ichihashi et al., 1992; Groenen-Van Dooren et al., 1995). Therefore, dietary intake is an essential source to obtain vitamin K. A list of dietary sources of vitamin K is provided in Table 1.1.

Table 1.1. Vitamin K content in various dietary sources (µg/100g). Values collected from (Vermeer and Schurgers, 2000; Vermeer et al., 2018; Akbulut et al., 2020; Walther et al., 2021).

Food	Vitamin K1	MK-4	Long-chain MKs*
Fresh green vegetables	73 - 750	ND	ND
Sauerkraut	22	0.4	5
Natto	20 - 32	ND	800 - 1000
Fresh fruits	0.1 - 50	ND	ND
Nuts	10 - 74	ND	ND
Margarines (from plant oil)	80-110	ND	ND
Meat (including liver)	ND - 3	1 - 11	ND - 1
Fish	ND - 1.3	0.1 - 63	ND - 1.5
Milk	0.5 - 1	0.2 - 2	ND - 2
Yogurt	0.2 - 1	0.5 - 1	0.1 - 0.2
Butter	9 - 20	10 - 20	ND
Cheese and curd (all types)	0.2 - 15	ND - 21	ND - 123

*MK-5 to MK-10.

Currently, most dietary reference values for vitamin K are derived from data on vitamin K1 intake in the population. In 2017, the European Food Safety Authority (EFSA) Panel on Dietetic Products and Nutrition and Allergies (NDA) decided to maintain the proposed adequate intake (AI) values of vitamin K since 1993, in which 70 µg/day vitamin K1 for adults was recommended (EFSA Panel on Dietetic Products et al., 2017). According to the institute of Medicine (US) Panel on Micronutrients In the US, the AI for male and female adults was set to be 120 and 90 µg/day, respectively, based on the median dietary intake of vitamin K1 (Institute of Medicine (US) Panel on Micronutrients., 2001). So far there is no tolerable upper intake level (UL) derived for vitamin K: no toxicity or adverse effect in excessive doses of vitamin K1 or K2 has ever been reported for healthy individuals (Institute of Medicine (US) Panel on Micronutrients., 2001; EFSA Panel on Dietetic Products et al., 2017; Akbulut et al., 2020). However, it is relevant to mention that MK-7 supplementation interferes with anticoagulant therapy, and should be carefully considered for patients using vitamin K antagonists (Theuwissen et al., 2013).

Distinct features of vitamin K2

Although it is commonly accepted that the naphthoquinone group in all vitamin K forms endow the basic molecular function, and therefore all molecules belonging to the vitamin K forms share similar mechanisms of action, it has gradually been recognized that substantial differences can be expected with different vitamin K forms (Vermeer and Schurgers, 2000). Due to the difference in side chains and consequently the difference in lipophilicity of the molecule, the absorption, plasma transport, tissue distribution and bioavailability are expected to depend on the type of vitamin K ingested.

Vitamin K uptake is thought to follow the pathway used by most dietary lipids: first it gets solubilized by bile salts and pancreatic enzymes into mixed micelles, taken up into the enterocytes and incorporated into chylomicrons. Upon action of lipoprotein lipase on the chylomicrons, vitamin K enters the circulation and gets transported by triglyceride-rich lipoproteins to the liver (Shearer and Newman, 2008; Shearer et al., 2012). Thereafter, the fate of vitamin K1 and K2 differs. Vitamin K1 is almost exclusively retained in the liver, while vitamin K2, besides being partially available in the liver, is also transported by low-density lipoproteins to extrahepatic tissues in the whole body, including bones and arteries (Schurgers and Vermeer, 2002).

The absorption of vitamin K is generally influenced by the food matrices in which they are embedded. The uptake is improved when consumed along with fat, and detergent-solubilized vitamin K is more easily absorbed than the food-bounded fraction (Schurgers and Vermeer, 2000; Akbulut et al., 2020). Only 10% - 15% vitamin K1 contained in diet gets absorbed by the human body, possibly due to its tight association with the thylakoid membrane in the plant chloroplast. Vitamin K2 represented by MK-4 and MK-7 are considered to be more thoroughly absorbed from food (Schurgers and Vermeer, 2000). However, when administered as free, not food-bounded forms, vitamin K1 showed better absorption than MK-4 and MK-9, but MK-7 showed better absorption than vitamin K1 (Vermeer and Schurgers, 2000; Schurgers and Vermeer, 2002; Schurgers et al., 2007).

Following absorption, the plasma half-life of the various vitamin K forms also differs. The plasma half-life of vitamin K1 was estimated to be 1 - 3 hours with rapid clearance, similar to that of MK-4, while with MK-7 and MK-9 the half-life is around 3 days and they appear to accumulate to higher levels in the system from prolonged intake (Schurgers and Vermeer, 2000, 2002; Schurgers et al., 2007; Sato et al., 2012). As the long-chain vitamin K2 forms retain longer and with higher quantity in the circulation, they are more available for uptake by the target tissues in the whole body. Besides the higher bioavailability, the efficacy of long-chain vitamin K2 represented by MK-7 is higher than that of vitamin K1, as demonstrated by the carboxylation status of osteocalcin *in vivo* following intake of the respective vitamin K forms (Schurgers et al., 2007).

Due to the different absorption and bioavailability profiles, it was estimated that the total amount of absorbed vitamin K consist of 50% vitamin K1, 40% long-chain vitamin K2 and 10% MK-4 in most

diets (Akbulut et al., 2020). The long-chain vitamin K2 was hypothesized to provide 70% of the total extrahepatic activity while vitamin K1 contributing to only 5%.

Besides the well-recognized benefits in bone health of both vitamin K1 and K2 (Weber, 2001; Fusaro et al., 2017), additional, unique health benefits have been demonstrated for vitamin K2, with most evidence in cardiovascular health. In a study on a cohort of 7983 participants aged 55 years or more in Rotterdam, the Netherlands, a protective effect against coronary heart disease (CHD) has been suggested for dietary intake of vitamin K2, but not vitamin K1 (Geleijnse et al., 2004). Moreover, data from a cohort consisting of 16,057 Dutch women aged between 49 to 70 years revealed a dose-response relationship, where each 10 µg higher vitamin K2 intake is associated with a 9% lower risk of CHD, and this association was mainly due to the long-chain forms MK-7, MK-8 and MK-9; no significant association could be derived for vitamin K1 intake (Gast et al., 2009). Similar conclusions could be drawn when the study group was extended to 33,289 Dutch participants aged 20 - 70 years (Zwakenberg et al., 2017), as well as from a study on 2987 Norwegian participants aged 46 - 49 years (Haugsgjerd et al., 2020).

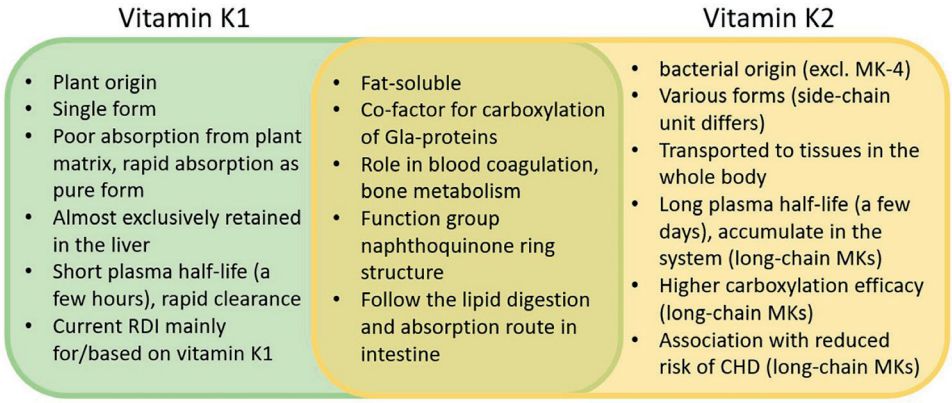

Figure 1.2. Common and unique features of vitamin K1 and vitamin K2.

In summary, vitamin K2 variants do have distinct features as compared to vitamin K1 (Fig. 1.2). It has been proposed that vitamin K2 needs a recommended daily intake value separate from vitamin K1 (Walther et al., 2013; Akbulut et al., 2020). The increasing attention and knowledge on vitamin K2 presence in fermented food products, its absorption, bioavailability and effects to the human body will eventually contribute to refined guidelines for vitamin K intake. In the meantime, efforts on vitamin K2 enrichment in food and supplements are desired for improved human nutrition and health.

Vitamin K2 produced by food grade bacteria

All forms of vitamin K2 or MKs, except for MK-4, are naturally synthesized by bacteria. The most studied function of MKs in the producing bacteria is as electron carriers in the cytoplasmic membrane, forming an essential component of the respiratory electron transport chain (Kurosu and Begari, 2010; Walther et al., 2013). The MK forms produced by a certain bacterial species are defined and unique, and in the past was even used as a chemotaxonomic marker (Collins and Jones, 1981). Mainly long-chain MKs, especially MK-7 to MK-10, are synthesized by bacteria.

Table 1.2. Menaquinone-producing bacteria applied in food fermentation. Information collected from (Hojo et al., 2007; Brooijmans et al., 2009; Walther et al., 2013; Liu et al., 2019). The bold letters highlight the major MK forms produced by the bacterial species.

Bacterial species	Application in food	MK forms (major forms shown in bold)
Lactococcus lactis* ssp. *lactis*, ssp. *cremoris	Cheese, buttermilk, sour cream, cottage cheese, cream cheese, kefir	MK-10, **MK-9**, MK-8, MK-7, MK-5, MK-3
Leuconostoc lactis	Cheese	MK-10, **MK-9**, MK-8, MK-7
Leuconostoc mesenteroids	Sauerkraut, kimchi	**MK-10**, MK-9, MK5
Propionibacterium freudenreichii	Cheese	**MK-9(H4)**
Propionibacterium shermanii	Cheese	**MK-9(H4)**
***Bacillus subtilis* "natto"**	Natto	**MK-7**
Brevibacterium linens	Cheese	**MK-8(H2)**
Brochontrix thermosphacta	Meat	**MK-7,** MK-6, MK-5
Hafnia alvei	Cheese	**MK-8**
Staphylococcus xylosus	Dairy, sausage	MK-8, **MK-7,** MK-6
Staphylococcus equorum	Dairy, meat	MK-8, **MK-7,** MK-6
Arthrobacter nicotinae	Cheese	MK-9, **MK-8,** MK-7

Obviously, vitamin K2 producing bacterial species that are commonly used in food fermentations are the most relevant for dietary vitamin K2 enrichment. A list of such bacteria, their applications in food fermentations, and the MK forms they produce, is presented in Table 1.2. Among these bacteria, *Bacillus subtilis* strains applied in Japanese natto fermentation is one of the most outstanding vitamin K2 (mainly MK-7) producers, that is able to fortify natto with up to 1000 µg MK-7 per 100 g product (Kamao et al., 2007; Walther et al., 2013). In a typical western diet, natto has not been a regular or well-accepted element so far, and the (long-chain) vitamin K2 is mostly obtained from fermented dairy products like cheese and curd (Schurgers and Vermeer, 2000; Vermeer et al., 2018). Key contributors to vitamin K2 in these food products are mainly restricted to *Lactococcus lactis* (ssp. *lactis* and ssp. *cremoris)*, *Leuconostoc lactis*, *Leuconostoc mesenteroides* and *Propionibacterium freudenreichii* (ssp. *freudenreichii* and ssp. *shermanii*) (Morishita et al., 1999; Walther et al., 2013; Chollet et al., 2017). Various studies on vitamin K2 content in cheese products revealed dramatically different content, depending on the type of cheese, strains in the starter cultures, ripening time and conditions, fat

content, season and geographic area of production, etc. (Vermeer et al., 2018; Walther et al., 2021). Although the vitamin K2 content in cheese was found to reach more than 100 µg per 100 g product, space for improvement is immense for vitamin K2 enrichment in fermented foods in the western diet considering the health benefits that vitamin K2 offers. To this end, understanding of strain variability, influencing factors and mechanisms of vitamin K2 production in food grade bacteria mentioned above is desirable. *Lactococcus lactis* is a particularly interesting species, for its relatively wide application and occurrence in various fermented food products.

Lactococcus lactis

Lactococcus lactis (Fig. 1.3A) is a Gram-positive, non-spore-forming bacterium that serves as a paradigm organism for lactic acid bacteria (LAB) (Cavanagh et al., 2015; Kleerebezem et al., 2020). *L. lactis* plays important roles in food fermentation processes, especially in dairy fermentations: it is the main constituent of dairy starter cultures used all over the world for the production of fermented dairy products including cheese, butter milk and sour cream (Cavanagh et al., 2015). In dairy fermentations, *L. lactis* converts lactose in milk to lactic acid, which inhibits the growth of pathogenic and spoilage organisms, therefore extending the shelf life of the fermented dairy products. Moreover, the texture and flavor characteristics of the fermented dairy products also benefit from the action of *L. lactis*. The long history of applying *L. lactis* in food fermentations not only endowed it the Generally Regarded As Safe (GRAS) status, but also made it the subject of fundamental research which has greatly advanced our knowledge on genetics, physiology and metabolism of this organism in particular and LAB in general (Cavanagh et al., 2015; Song et al., 2017; Kleerebezem et al., 2020).

Although *L. lactis* is best known for its application and occurrence in dairy products, its natural niches are extremely diverse besides milk, ranging from gastrointestinal tract of fish to plant materials (Cavanagh et al., 2015). In fact, the dairy isolates are believed to have evolved from plant isolates, with successful adaptations to thrive in the dairy environment (Kleerebezem et al., 2020). It has been suggested that the niche adaptation history is reflected by the lifestyle and adaptability of *L. lactis* in different environmental conditions. For instance, although *L. lactis* is classified as a facultative anaerobe with a fermentative metabolism (Fig. 1.3B), evidence has also been provided that in presence of oxygen and exogenous supplementation of heme, *L. lactis* can switch to aerobic respiration, a process enabled by the menaquinones (vitamin K2) produced by *L. lactis* as electron carriers (Fig. 1.3C) (Duwat et al., 2001; Brooijmans et al., 2009).

Among the subspecies (ssp.) of *L. lactis*, ssp. *lactis* and *cremoris* are most studied, both include dairy- and plant-derived strains (Kleerebezem et al., 2020). In fact, the ssp. *cremoris* has been promoted to species level (*Lactococcus cremoris*) very recently in 2021 (Li et al., 2021). For clarity, throughout this work we stick to the nomenclature used before this recent change.

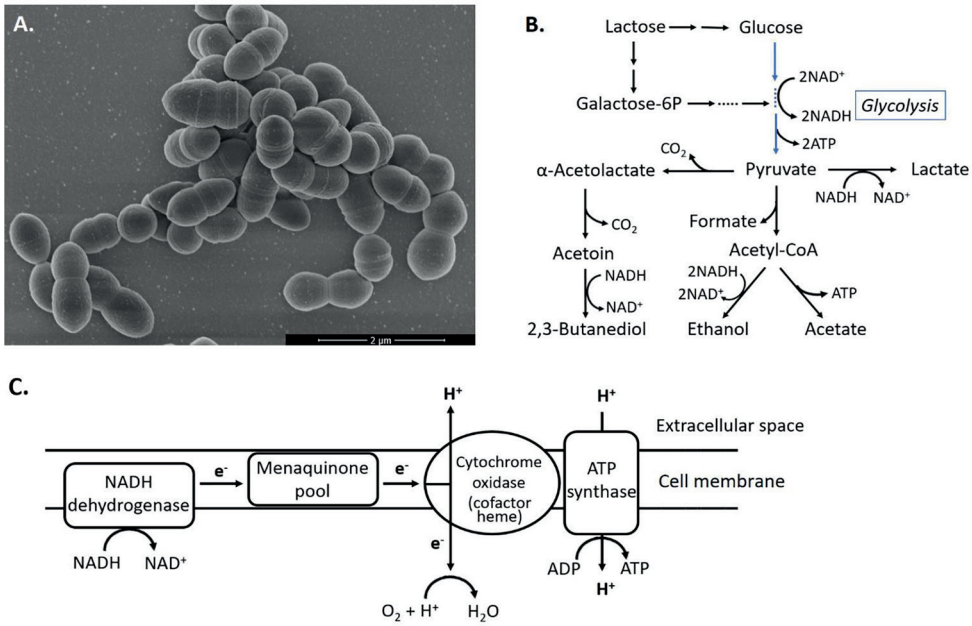

Figure 1.3. Important features of *Lactococcus lactis*. A) A scanning electron microscopic picture of *L. lactis* cells. B) Schematic representation of the primary metabolism pathway in *L. lactis*. Blue arrows show glycolysis pathway. Scheme modified from (Kleerebezem et al., 2020). Stoichiometries are not reflected in this scheme. C) Schematic representation of the heme- and oxygen-induced aerobic respiration in *L. lactis*. A NADH dehydrogenase, menaquinone pool (as electron carriers) and cytochrome oxidase form a simple electron transport chain that reduces oxygen and generates additional proton motive force for the ATP synthase. Scheme modified from (Brooijmans et al., 2009).

L. lactis ssp. *cremoris* MG1363 is a plasmid-free, prophage-cured strain derived from a dairy starter isolate, and has been used extensively as a model strain for fundamental research of *L. lactis* (Wegmann et al., 2007). Recent advance in research on the abundance of and functions encoded by plasmids and prophages in *L. lactis* (Alexeeva et al., 2018; van Mastrigt et al., 2018; Kelleher et al., 2019) also highlighted the interest of examining wildtype isolates, to expand our understanding in the lifestyle and adaptation of *L. lactis* in different environments, and to better apply this bacterium in food fermentation.

Delivery of lipophilic micronutrients, challenges and opportunities

While it is of interest to improve the content of vitamin K2 in food grade bacteria and eventually in the diet, the actual efficiency of its delivery to the human body is important as well. Vitamin K2 may not be readily absorbed by the human body due to the lipophilicity, which has been demonstrated especially for MK-9 (Schurgers and Vermeer, 2002), the major long-chain vitamin K2 form obtained from the western diet. Moreover, the location in the bacterial membrane could add difficulties for efficient

absorption of vitamin K2. Most bacteria that are commonly used in food fermentations (Table 1.2) are Gram-positive bacteria, of which the cell envelop contains a thick peptidoglycan layer (cell wall) outside the cytoplasmic membrane, adding an additional barrier for accessing vitamin K2. Notably, to our knowledge essentially nothing has been done to improve the delivery of bacterial membrane-bound vitamin K2 into the human host.

For other fat-soluble vitamins (vitamin A, E and D), enhanced absorption via a liposome formulation was observed after oral administration (Kirilenko and Gregoriadis, 1993). Liposomes are nano- or micro-sized, lumen-containing spheres, of which the shell is generally made of phospholipid bilayers (Mirafzali et al., 2014). With the hydrophilic head groups of phospholipids facing outwards and the hydrophobic tails facing inwards, the phospholipid bilayer structure allows liposomes to be water soluble, and can not only encapsulate hydrophilic compounds in the interior but also entrap hydrophobic compounds inside the bilayer (Fig. 1.4A). In fact, liposomes have been studied not only for (fat-soluble) vitamins, but also for other bioactive compounds like antioxidants, antimicrobials, as well as other nutritional and therapeutic molecules (Mirafzali et al., 2014; Sercombe et al., 2015; Simão et al., 2015; Emami et al., 2016). The liposome based delivery system offers advantages including protection against degradation of the delivered molecules, enhancing solubility, cellular uptake and bioavailability, and even achieving targeted delivery of compounds. In the human system, besides the digestion through bile and pancreatic enzymes followed by absorption in the intestine, liposomes have also been shown to deliver lipophilic substances to the hosts by membrane fusion or endocytosis (Yang et al., 2016; Kang et al., 2017; Liu et al., 2020).

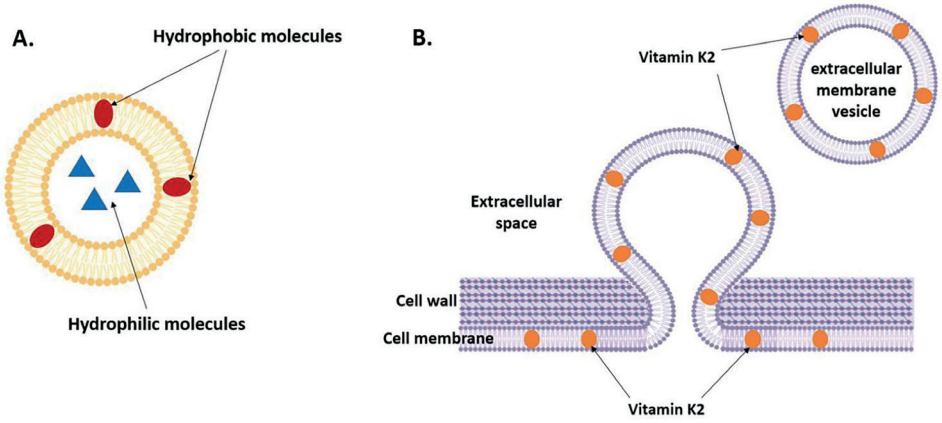

Figure 1.4. A) A liposome carrying compounds to be delivered. B) Hypothetical model: secretion of vitamin K2-containing extracellular membrane vesicles from Gram-positive bacteria. This figure was created with BioRender.com.

Liposomes are made artificially, but similar lipid particles can also be generated naturally: extracellular membrane vesicles (EVs) are known to be produced by members of all domains of life, including bacteria, both Gram-positive and Gram-negative (Kim et al., 2015; Gill et al., 2019; Toyofuku et al.,

2019; Nagakubo et al., 2020). These vesicles consist of lipid-bilayers forming enclosed spheres and are carriers for hydrophilic or lipophilic compounds and biomolecules (DNA, RNA, proteins, metabolites, etc.) supporting exchange between cells. Since vitamin K2 is present in the cell membrane of producing bacteria including *L. lactis*, the bacterial EVs are potentially ideal vehicles for continuous production of this essential vitamin and its efficient delivery to the human host (Fig. 1.4B). Both in fermented foods and in food supplements, the EVs are expected to improve the absorption of vitamin K2 by the human host presumably via similar processes as described in liposome studies including membrane fusion and endocytosis by the host cells, next to the established absorption pathway of fat-soluble vitamins based on bile-salt and pancreatic-dependent solubilization followed by the uptake of enterocytes.

Outline of this thesis

The research described in this thesis is dedicated to exploring the potential of optimized vitamin K2 delivery to human cells by EVs from *L. lactis*. In addition to the general background of research described in the current chapter, **Chapter 2** serves as an detailed introduction to Gram-positive bacterial EVs. It gives an overview of the compositions and roles of EVs produced by Gram-positive bacteria, including members from fermentation starters, gut bacteria, probiotics and pathogens, the cargo compounds of EVs, highlighting the implications of Gram-positive EVs in human health and disease and potential applications of EVs.

Further, the research of this thesis is documented in three parts (Fig. 1.5). **Part I (Chapter 3 - 5)** focuses on the production of vitamin K2 by *L. lactis*. Possibilities of improving the vitamin K2 content in *L. lactis* were investigated, and the biosynthetic pathway and physiological roles of vitamin K2 in *L. lactis* were elucidated. **Part II (Chapter 6 - 8)** focuses on the production of EVs in *L. lactis*. Using model strains isolated from cheese starters, the EV producing phenomenon was described for *L. lactis*, mechanisms of EV production especially in relation to bacteriophage activity were elucidated and composition of EVs determined. **Part III (Chapter 9)** brings the first two parts together by demonstrating that *L. lactis* EVs contain vitamin K2, and can facilitate the delivery of vitamin K2 to human cells.

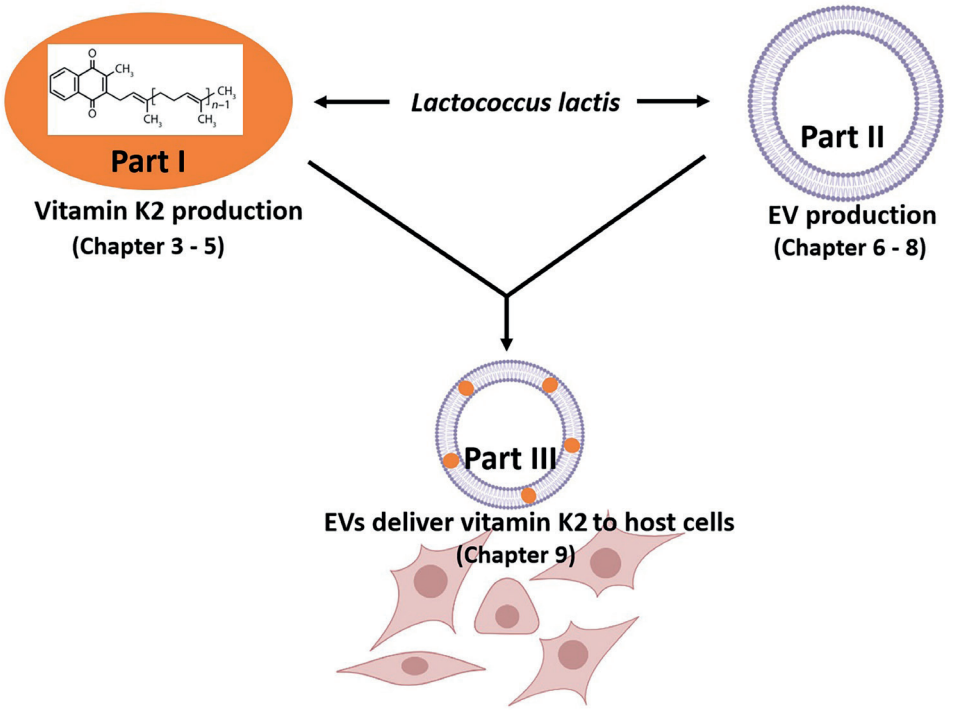

Figure 1.5. Structure of this thesis. This figure was created with BioRender.com

Chapter 3 describes the species and strain variability of vitamin K2 content in lactic acid bacteria, and the influence of cultivation conditions on vitamin K2 content in the model strain *L. lactis* ssp. *cremoris* MG1363. Improved vitamin K2 content was observed in oxygenated conditions compared to static cultivation conditions, and with carbon sources like fructose and trehalose compared to glucose. When applying strain MG1363 in quark fermentation, starters obtained from optimized cultivation conditions also resulted in higher vitamin K2 content in the quark product. Therefore, strain selection and optimization of growth conditions are viable strategies towards natural vitamin K2 enrichment in foods by improving the content in the producing bacteria.

Chapter 4 describes another strategy for improved vitamin K2 content in *L. lactis*: laboratory evolution. As the oxygenated cultivation conditions improved vitamin K2 content in *L. lactis* (Chapter 3), the model strain MG1363 was sequentially propagated under vigorous shaking condition for approximately 100 generations. Three selected evolved strains that displayed improved stationary phase survival in oxygenated conditions, showed considerable increase in vitamin K2 content and high resistance against hydrogen peroxide-induced oxidative stress. Genomic and proteomic analysis revealed the mutations and differential protein production in evolved strains compared to the original strain, and could largely explain the strong oxidative stress resistant phenotype of the evolved strains, but the increased vitamin K2 content could not be directly explained in this study. Nevertheless, this

study demonstrated laboratory evolution as a non-genetic engineering approach to obtain vitamin K2 overproducers that are of high interests for applications such as those described in **Chapter 3**.

Although strategies to improve the vitamin K2/MK content in *L. lactis* are described by **Chapter 3** and **4**, insights into the exact mechanisms were not obtained especially for the physiological roles of MKs in *L. lactis*. In the study described in **Chapter 5**, candidate genes in various stages of MK synthesis were deleted in *L. lactis* MG1363 to obtain mutants with no MK production or only short-chain MK production. As a result, the roles of several predicted genes in the MK synthesis were confirmed. By examining the phenotypes of the mutants and the original strain under various aeration conditions, the roles of short-chain and long-chain MKs in aerobic and anaerobic (extracellular) electron transfer were revealed. These findings add to our understanding of the evolutionary and physiological significance of MK production in facultative anaerobes, and may provide leads for strain selection and conditions for optimizing vitamin K2 accumulation in bacterial cells.

To achieve vitamin K2 enrichment in the diet, fermented foods like cheese are important sources and could provide the best opportunities. Therefore, studies on isolates from cheese starter cultures are highly relevant. *L. lactis* strains (TIFN1 to TIFN7) isolated from a complex dairy starter culture showed intriguing phenotypes in earlier research, where all these strains were reported to be lysogens, and tailless phage particles were released spontaneously and further stimulated by prophage inducing conditions without massive lysis of the host bacteria (Alexeeva et al., 2018). Analysis of the prophage genomes harbored by strains TIFN1 – TIFN7 revealed that most prophages had disruptions in the tail encoding genes and contained phage defense systems, explaining the tailless phenotype of phages and suggesting an evolutionary advantage of the observed phage-bacteria interaction (**Chapter 6**). Further, using model strain TIFN1, it was revealed that the released tailless phage particles were engulfed in lipid membranes, which could explain the non-lytic release phenotype (**Chapter 7**). As the complex cheese starter cultures are shaped by long-term back-slopping, the intriguing *L. lactis* bacteria-phage interaction in this microbial community is considered to be meaningful in microbial ecology and evolution.

To further understand the mechanism of bacteria-phage interactions, another isolate from artisanal cheese starter, *L. lactis* ssp. *cremoris* FM-YL11, was used that showed a similar growth profile and identical prophage sequence as strain TIFN1. In **Chapter 8**, extracellular membrane vesicle (EV) production is described for strain FM-YL11. It was found that massive EV production in *L. lactis* was stimulated by the prophage-encoded holin-lysin system, without causing massive, immediate cell lysis. A subpopulation of holin-lysin induced EVs conceivably contains phage particles as cargo.

As the vitamin K2 producer *L. lactis* is also found to produce EVs, the natural delivery tools are potentially provided for vitamin K2. The study described in **Chapter 9** revealed that holin-lysin induced EVs, or artificial EVs obtained from *L. lactis* mainly contained MK-8 and MK-9 forms of vitamin K2. Using the carboxylation status of osteocalcin produced by the *in vitro* grown osteosarcoma cells, evidence

was provided that EVs delivered bioactive vitamin K2 to the host cells, and the delivery efficiency was higher when the long-chain MKs are carried by EVs compared to the addition of solvent-dissolved MKs.

Finally, a general discussion is presented in **Chapter 10** and highlights the connections of the various parts/chapters in this research work as well as providing an overview of the current advances and future perspectives of vitamin K2 fortification of foods and delivery to the human body.

References

Akbulut, A. C., Pavlic, A., Petsophonsakul, P., Halder, M., Maresz, K., Kramann, R., et al. (2020). Vitamin K2 needs an RDI separate from vitamin K1. *Nutrients* 12, 1852.

Akram, M., Munir, N., Daniyal, M., Egbuna, C., Găman, M.-A., Onyekere, P. F., et al. (2020). "Vitamins and minerals: types, sources and their functions," in *Functional Foods and Nutraceuticals*, eds. C. Egbuna and G. Dable Tupas (Cham: Springer), 149–172.

Alexeeva, S., Guerra Martínez, J. A., Spus, M., and Smid, E. J. (2018). Spontaneously induced prophages are abundant in a naturally evolved bacterial starter culture and deliver competitive advantage to the host. *BMC Microbiol.* 18, 120.

Almquist, H. J., and Stokstad, E. L. R. (1935). Hemorrhagic chick disease of dietary origin. *J. Biol. Chem.* 111, 105–113.

Barnes, R. H., and Fiala, G. (1959). Effects of the prevention of coprophagy in the rat. *J. Nutr.* 68, 603–614.

Berkner, K. L. (2005). The vitamin K-dependent carboxylase. *Annu. Rev. Nutr.* 25, 127–149.

Beulens, J. W. J., Booth, S. L., van Den Heuvel, E. G. H. M., Stoecklin, E., Baka, A., and Vermeer, C. (2013). The role of menaquinones (vitamin K2) in human health. *Br. J. Nutr.* 110, 1357–1368.

Booth, S. L. (2009). Roles for vitamin K beyond coagulation. *Annu. Rev. Nutr.* 29, 89–110.

Brooijmans, R., Smit, B., Santos, F., van Riel, J., de Vos, W. M., and Hugenholtz, J. (2009). Heme and menaquinone induced electron transport in lactic acid bacteria. *Microb. Cell Fact.* 8, 28.

Cavanagh, D., Fitzgerald, G. F., and McAuliffe, O. (2015). From field to fermentation: The origins of *Lactococcus lactis* and its domestication to the dairy environment. *Food Microbiol.* 47, 45–61.

Chollet, M., Guggisberg, D., Portmann, R., Risse, M. C., and Walther, B. (2017). Determination of menaquinone production by *Lactococcus* spp. and propionibacteria in cheese. *Int. Dairy J.* 75, 1–9.

Collins, M. D., and Jones, D. (1981). Distribution of isoprenoid quinone structural types in bacteria and their taxonomic implications. *Microbiol. Rev.* 45, 316–354.

Conly, J. M., and Stein, K. (1992). Quantitative and qualitative measurements of K vitamins in human intestinal contents . *Am J Gastroenterol* 87, 311–316.

Cranenburg, E. C. M., Schurgers, L. J., and Vermeer, C. (2007). Vitamin K: the coagulation vitamin that became omnipotent. *Thromb. Haemost.* 98, 120–125.

Dam, H. (1935). The antihaemorrhagic vitamin of the chick. *Biochem. J.* 29, 1273–1285.

Dam, H., and Schönheyder, F. (1934). A deficiency disease in chicks resembling scurvy. *Biochem. J.* 28, 1355–1359.

Duwat, P., Sourice, S., Cesselin, B., Lamberet, G., Vido, K., Gaudu, P., et al. (2001). Respiration Capacity of the Fermenting Bacterium *Lactococcus lactis* and Its Positive Effects on Growth and Survival. *J. Bacteriol.* 183, 4509–4516.

Emami, S., Azadmard-Damirchi, S., Peighambardoust, S. H., Valizadeh, H., and Hesari, J. (2016). Liposomes as carrier vehicles for functional compounds in food sector. *J. Exp. Nanosci.* 11, 737–759.

Fusaro, M., Mereu, M. C., Aghi, A., Iervasi, G., and Gallieni, M. (2017). Vitamin K and bone. *Clin. Cases Miner. Bone Metab.* 14, 200–206.

Gast, G. C. M., de Roos, N. M., Sluijs, I., Bots, M. L., Beulens, J. W. J., Geleijnse, J. M., et al. (2009). A high menaquinone intake reduces the incidence of coronary heart disease. *Nutr. Metab. Cardiovasc. Dis.* 19, 504–510.

Geleijnse, J. M., Vermeer, C., Grobbee, D. E., Schurgers, L. J., Knapen, M. H. J., van Der Meer, I. M., et al. (2004). Dietary intake of menaquinone is associated with a reduced risk of coronary heart disease: The Rotterdam Study. *J. Nutr.* 134, 3100–3105.

Gill, S., Catchpole, R., and Forterre, P. (2019). Extracellular membrane vesicles in the three domains of life and beyond. *FEMS Microbiol. Rev.* 43, 273–303.

Groenen-van Dooren, M. M. C. L., Ronden, J. E., Soute, B. A. M., and Vermeer, C. (1995). Bioavailability of phylloquinone and menaquinones after oral and colorectal administration in vitamin K-deficient rats. *Biochem. Pharmacol.* 50, 797–801.

Haugsgjerd, T. R., Egeland, G. M., Nygård, O. K., Vinknes, K. J., Sulo, G., Lysne, V., et al. (2020). Association of dietary vitamin K and risk of coronary heart disease in middle-age adults: The Hordaland Health Study Cohort. *BMJ Open* 10, e035953.

Hojo, K., Watanabe, R., Mori, T., and Taketomo, N. (2007). Quantitative measurement of tetrahydromenaquinone-9 in cheese fermented by propionibacteria. *J. Dairy Sci.* 90, 4078–4083.

Ichihashi, T., Takagishi, Y., Uchida, K., and Yamada, H. (1992). Colonic absorption of menaquinone-4 and menaquinone-9 in rats. *J. Nutr.* 122, 506–512.

Institute of Medicine (US) Panel on Micronutrients. (2001). "Vitamin K," in *Dietary Reference Intakes for Vitamin A, Vitamin K, Arsenic, Boron, Chromium, Copper, Iodine, Iron, Manganese, Molybdenum, Nickel, Silicon, Vanadium, and Zinc.* (Washington (DC): National Academies Press (US)).

Kamao, M., Suhara, Y., Tsugawa, N., Uwano, M., Yamaguchi, N., Uenishi, K., et al. (2007). Vitamin K content of foods and dietary vitamin K intake in Japanese young women. *J. Nutr. Sci. Vitaminol. (Tokyo).* 53, 464–470.

Kang, J. H., Jang, W. Y., and Ko, Y. T. (2017). The effect of surface charges on the cellular uptake of liposomes investigated by live cell imaging. *Pharm. Res.* 34, 704–717.

Kelleher, P., Mahony, J., Bottacini, F., Lugli, G. A., Ventura, M., and van Sinderen, D. (2019). The *Lactococcus lactis* Pan-Plasmidome. *Front. Microbiol.* 10, 707.

Kim, J. H., Lee, J., Park, J., and Gho, Y. S. (2015). Gram-negative and Gram-positive bacterial extracellular vesicles. *Semin. Cell Dev. Biol.* 40, 97–104.

Kirilenko, V., and Gregoriadis, G. (1993). Fat soluble vitamins in liposomes: studies on incorporation efficiency and bile salt induced vesicle disintegration. *J. Drug Target.* 1, 361–368.

Kleerebezem, M., Bachmann, H., van Pelt-KleinJan, E., Douwenga, S., Smid, E. J., Teusink, B., et al. (2020). Lifestyle, metabolism and environmental adaptation in *Lactococcus lactis*. *FEMS Microbiol. Rev*. 44, 804–820.

Kurosu, M., and Begari, E. (2010). Vitamin K2 in electron transport system: are enzymes involved in vitamin K2 biosynthesis promising drug targets? *Molecules* 15, 1531–1553.

Linares, D. M., Fitzgerald, G., Hill, C., Stanton, C., and Ross, P. (2017). "Production of vitamins, exopolysaccharides and bacteriocins by probiotic bacteria," in *Probiotic Dairy Products*, eds. A. Y. Tamime and L. V. Thomas (Chichester, UK: John Wiley & Sons), 359–388.

Li, T. T., Wen L. T., and Chun T. G. (2021). Elevation of *Lactococcus lactis* subsp. *cremoris* to the species level as *Lactococcus cremoris* sp. nov. and transfer of *Lactococcus lactis* subsp. *tructae* to *Lactococcus cremoris* as *Lactococcus cremoris* subsp. *tructae* comb. nov. *Int. J. Syst. Evol.* 71, 004727.

Liu, W., Hou, Y., Jin, Y., Wang, Y., Xu, X., and Han, J. (2020). Research progress on liposomes: Application in food, digestion behavior and absorption mechanism. *Trends Food Sci. Technol.* 104, 177–189.

Liu, Y., van Bennekom, E. O., Zhang, Y., Abee, T., and Smid, E. J. (2019). Long-chain vitamin K2 production in *Lactococcus lactis* is influenced by temperature, carbon source, aeration and mode of energy metabolism. *Microb. Cell Fact.* 18, 129.

Maqbool, M. A., and Aslam, M. (2017). Biological importance of vitamins for human health: A review. *J. Agric. Basic Sci.* 2, 50–58.

McFarlane, W. D., Graham, W. R., and Richardson, F. (1931). The fat-soluble vitamin requirements of the chick: the vitamin A and vitamin D content of fish meal and meat meal. *Biochem. J.* 25, 358–366.

Mirafzali, Z., Thompson, C. S., and Tallua, K. (2014). "Application of liposomes in the food industry," in *Microencapsulation in the Food Industry*, eds. A. G. Gaonkar, N. Vasisht, A. R. Khare, and R. Sobel (Elsevier), 139–150.

Morishita, T., Tamura, N., Makino, T., and Kudo, S. (1999). Production of menaquinones by lactic acid bacteria. *J. Dairy Sci.* 82, 1897–1903.

Nagakubo, T., Nomura, N., and Toyofuku, M. (2020). Cracking open bacterial membrane vesicles. *Front. Microbiol.* 10, 3026.

NobelPrize.org (2021). The Nobel Prize in Physiology or Medicine 1943. *Nobel Media AB*. Available at: https://www.nobelprize.org/prizes/medicine/1943/summary/ [Accessed April 20, 2021].

Parker, C. H., Morgan, C. R., Rand, K. D., Engen, J. R., Jorgenson, J. W., and Stafford, D. W. (2014). A conformational investigation of propeptide binding to the integral membrane protein γ-glutamyl carboxylase using nanodisc hydrogen exchange mass spectrometry. *Biochemistry* 53, 1511–1520.

Products, E. P. on D., (NDA), N. and A., Turck, D., Bresson, J., Burlingame, B., Dean, T., et al. (2017). Dietary reference values for vitamin K. *EFSA J.* 15, 4780.

Sato, T., Schurgers, L. J., and Uenishi, K. (2012). Comparison of menaquinone-4 and menaquinone-7 bioavailability in healthy women. *Nutr. J.* 11, 93.

Schurgers, L. J., Teunissen, K. J. F., Hamulyák, K., Knapen, M. H. J., Vik, H., and Vermeer, C. (2007). Vitamin K-containing dietary supplements: comparison of synthetic vitamin K1 and natto-derived menaquinone-7. *Blood* 109, 3279–3283.

Schurgers, L. J., Uitto, J., and Reutelingsperger, C. P. (2013). Vitamin K-dependent carboxylation of matrix Gla-protein: a crucial switch to control ectopic mineralization. *Trends Mol. Med.* 19, 217–226.

Schurgers, L. J., and Vermeer, C. (2000). Determination of phylloquinone and menaquinones in food. Effect of food matrix on circulating vitamin K concentrations. *Haemostasis* 30, 298–307.

Schurgers, L. J., and Vermeer, C. (2002). Differential lipoprotein transport pathways of K-vitamins in healthy subjects. *Biochim. Biophys. Acta* 1570, 27–32.

Sercombe, L., Veerati, T., Moheimani, F., Wu, S. Y., Sood, A. K., and Hua, S. (2015). Advances and challenges of liposome assisted drug delivery. *Front. Pharmacol.* 6, 286.

Shearer, M. J. (1995). Vitamin K. *Lancet* 345, 229–234.

Shearer, M. J., Bach, A., and Kohlmeier, M. (1996). Chemistry, nutritional sources, tissue distribution and metabolism of vitamin K with special reference to bone health. *J. Nutr.* 126, 1181S-1186S.

Shearer, M. J., Fu, X., and Booth, S. L. (2012). Vitamin K nutrition, metabolism, and requirements: current concepts and future research. *Adv. Nutr.* 3, 182–195.

Shearer, M. J., and Newman, P. (2008). Metabolism and cell biology of vitamin K. *ThrombHaemost* 100, 530–547.

Shearer, M. J., and Okano, T. (2018). Key pathways and regulators of vitamin K function and intermediary metabolism. *Annu. Rev. Nutr.* 38, 127–151.

Simão, A. M. S., Bolean, M., Cury, T. A. C., Stabeli, R. G., Itri, R., and Ciancaglini, P. (2015). Liposomal systems as carriers for bioactive compounds. *Biophys. Rev.* 7, 391–397.

Song, A. A.-L., In, L. L. A., Lim, S. H. E., and Rahim, R. A. (2017). A review on *Lactococcus lactis*: from food to factory. *Microb. Cell Fact.* 16, 55.

Stenflo, J., Fernlund, P., Egan, W., and Roepstorff, P. (1974). Vitamin K dependent modifications of glutamic acid residues in prothrombin. *Proc. Natl. Acad. Sci. U. S. A.* 71, 2730–2733.

Suttie, J. W. (1978). "Vitamin K," in *The Fat-Soluble Vitamins. Handbook of Lipid Research, vol 2.*, ed. H. F. DeLuca (Boston, MA: Springer), 211–277.

Suttie, J. W. (2009). *Vitamin K in health and disease*. 1st Editio. CRC Press.

Theuwissen, E., Teunissen, K. J., Spronk, H. M. H., Hamulyák, K., Ten Cate, H., Shearer, M. J., et al. (2013). Effect of low-dose supplements of menaquinone-7 (vitamin K_2) on the stability of oral anticoagulant treatment: dose-response relationship in healthy volunteers. *J. Thromb. Haemost.* 11, 1085–1092.

Toyofuku, M., Nomura, N., and Eberl, L. (2019). Types and origins of bacterial membrane vesicles. *Nat. Rev. Microbiol.* 17, 13–24.

van Mastrigt, O., Di Stefano, E., Hartono, S., Abee, T., and Smid, E. J. (2018). Large plasmidome of dairy *Lactococcus lactis* subsp. *lactis* biovar diacetylactis FM03P encodes technological functions and appears highly unstable. *BMC Genomics* 19, 620.

Vermeer, C., Raes, J., van 't Hoofd, C., Knapen, M. H. J., and Xanthoulea, S. (2018). Menaquinone content of cheese. *Nutrients* 10, 446.

Vermeer, C., and Schurgers, L. J. (2000). A comprehensive review of vitamin K and vitamin K antagonists. *Hematol. Oncol. Clin. North Am.* 14, 339–353.

Walther, B., Guggisberg, D., Schmidt, R. S., Portmann, R., Risse, M. C., Badertscher, R., et al. (2021). Quantitative analysis of menaquinones (vitamin K2) in various types of cheese from Switzerland. *Int. Dairy J.* 112, 104853.

Walther, B., Philip Karl, J., Booth, S. L., and Boyaval, P. (2013). Menaquinones, bacteria, and the food supply: the relevance of dairy and fermented food products to vitamin K requirements. *Adv. Nutr.* 4, 463–473.

Walther, B., and Schmid, A. (2017). "Effect of fermentation on vitamin content in food," in *Fermented Foods in Health and Disease Prevention*, eds. J. Frias, C. Martinez-Villaluenga, and E. Peñas (Elsevier Inc.), 131–157.

Weber, P. (2001). Vitamin K and bone health. *Nutrition* 17, 880–887.

Wegmann, U., O'Connell-Motherway, M., Zomer, A., Buist, G., Shearman, C., Canchaya, C., et al. (2007). Complete genome sequence of the prototype lactic acid bacterium *Lactococcus lactis* subsp. *cremoris* MG1363. *J. Bacteriol.* 189, 3256–3270.

Willems, B. A. G., Vermeer, C., Reutelingsperger, C. P. M., and Schurgers, L. J. (2014). The realm of vitamin K dependent proteins: Shifting from coagulation toward calcification. *Mol. Nutr. Food Res.* 58, 1620–1635.

Xiao, H., Chen, J., Duan, L., and Li, S. (2021). Role of emerging vitamin K-dependent proteins: Growth arrest-specific protein 6, Gla-rich protein and periostin (Review). *Int. J. Mol. Med.* 47, 2.

Yang, J., Bahreman, A., Daudey, G., Bussmann, J., Olsthoorn, R. C. L., and Kros, A. (2016). Drug delivery via cell membrane fusion using lipopeptide modified liposomes. *ACS Cent. Sci.* 2, 621–630.

Zwakenberg, S. R., den Braver, N. R., Engelen, A. I. P., Feskens, E. J. M., Vermeer, C., Boer, J. M. A., et al. (2017). Vitamin K intake and all-cause and cause specific mortality. *Clin. Nutr.* 36, 1294–1300.


1

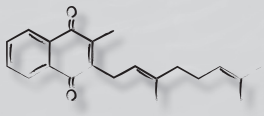

Chapter 2

Gram-positive bacterial extracellular vesicles and their impact on health and disease

Yue Liu, Kyra A. Y. Defourny, Eddy J. Smid & Tjakko Abee

Published in

Frontiers in Microbiology, 2018, 9:1502

Abstract

During recent years it has become increasingly clear that the release of extracellular vesicles (EVs) is a feature inherent to all cellular life forms. These lipid bilayer-enclosed particles are secreted by members of all domains of life: Eukarya, Bacteria and Archaea, being similar in size, general composition, and potency as a functional entity. Noticeably, the recent discovery of EVs derived from bacteria belonging to the Gram-positive phyla Actinobacteria and Firmicutes has added a new layer of complexity to our understanding of bacterial physiology, host interactions and pathogenesis. Being nano-sized structures, Gram-positive EVs carry a large diversity of cargo compounds, including nucleic acids, viral particles, enzymes and effector proteins. The diversity in cargo molecules may point to roles of EVs in bacterial competition, survival, material exchange, host immune evasion and modulation, as well as infection and invasion. Consequently, the impact of Gram-positive EVs on health and disease are being revealed gradually. These findings have opened up new leads for the development of medical advances, including strategies for vaccination and anti-bacterial treatment. The rapidly advancing research into Gram-positive EVs is currently in a crucial phase, therefore this review aims to give an overview of the groundwork that has been laid at present and to discuss implications and future challenges of this new research field.

Gram-positive bacterial EVs: an upcoming research area

Although discovered thirty years later than their Gram-negative counterparts, Gram-positive bacterial extracellular membrane vesicles (EVs) have been drawing more attention in recent years (Brown et al., 2015; Kim et al., 2015). Budding events of spherical particles and their release into the surrounding environment of the cells have been observed for a wide range of bacterial species belonging to the Gram-positive phyla Firmicutes and Actinobacteria (Table 2.1). These particles could be isolated using common EV isolation strategies and reflected lipid bilayer-enclosed structures that are morphologically similar to Gram-negative or eukaryotic EVs (Lee et al., 2009; Lee J.H. et al., 2013; Lee J. et al., 2013; Brown et al., 2014; Olaya-Abril et al., 2014; Haas and Grenier, 2015; Schrempf and Merling, 2015; Kim J.-H. et al., 2016; Resch et al., 2016; Jeon et al., 2017). Consistent with other classical EVs, Gram-positive EVs were within a nano-scale size range of about 10 - 400 nm.

The expanding research field on Gram-positive EVs has so far revealed possible roles of EVs in bacterial ecology, physiology, and host-microbe interactions linked to health and disease depending on the bacterial species. In this light, EVs are also of potential value in medical and clinical applications. In this article we will provide new insights into the diversity, functionality and possible applications of Gram-positive EVs.

Physiological roles of Gram-positive EVs

The biogenesis mechanism of Gram-positive EVs was not instantly evident as for the outer membrane vesicles (OMVs) produced by Gram-negative bacteria. While OMVs are generated by pinching off the outer membrane, the generation and release of Gram-positive EVs through the thick cell wall is still being disputed. The current evidence-supported hypothesis involves the action of cell wall-degrading enzymes that weaken the peptidoglycan layer and facilitate the release of EVs (Brown et al., 2015; Toyofuku et al., 2017; Wang et al., 2018).

Similar to OMVs, Gram-positive EVs carry a wide range of cargo molecules including nucleic acids, proteins, lipids, viruses, enzymes and toxins (Brown et al., 2015; Kim et al., 2015). Nevertheless, Gram-positive EVs can still be distinguished from OMVs since the latter typically contain lipopolysaccharide (LPS) and encapsulate periplasmic components. Experimental evidence has indicated that EV release is overall an active metabolic process and that dedicated sorting mechanisms are conceivably involved in determining the content of EVs (Athman et al., 2015; Brown et al., 2014; Liao et al., 2014; Prados-Rosales et al., 2011; Resch et al., 2016). This implies physiological or ecological importance of EV release in bacteria. An extensive overview of the possible physiological roles of Gram-positive EVs is presented in Fig. 2.1.

Table 2.1. Gram-positive organisms for which EV release has been demonstrated.

Phyla	Species	Evidence
Firmicutes	*Staphylococcus aureus*	TEM of budding events and EV isolates, protein characterization (SDS-PAGE, MS), fluorescence microscopy (lipid staining) (Lee et al., 2009; Gurung et al., 2011)
	Streptococcus pneumoniae	TEM of EV isolates, SEM of budding events, protein characterization (SDS-PAGE, MS), lipid characterization (Olaya-Abril et al., 2014)
	Streptococcus mutans	TEM of EV isolates, protein characterization (SDS-PAGE) (Liao et al., 2014)
	Streptococcus suis	TEM of cell culture and EV isolates, protein characterization (MS) (Haas and Grenier, 2015)
	Streptococcus pyogenes / Group A streptococci	TEM, SEM and AFM of budding events and EV isolates, protein characterization (SDS-PAGE, MS), lipid characterization (Resch et al., 2016)
	Streptococcus agalactiae/ Group B streptococci	TEM, SEM and AFM of EV isolates or budding events, protein characterization (SDS-P, MS), lipid characterization (Surve et al., 2016)
	Listeria monocytogenes	TEM of EV isolates, protein characterization (MS) (Lee J.H. et al., 2013)
	Propionibacterium acnes	TEM of EV isolates, protein characterization (SDS-PAGE, MS) (Jeon et al., 2017)
	Bacillus anthracis	TEM of EV isolates, flow cytometry (Rivera et al., 2010)
	Bacillus subtilis	TEM and SEM of budding events and EV isolates, protein characterization (SDS-PAGE, MS) (Brown et al., 2014; Kim Y. et al., 2016)
	Clostridium perfringens	TEM of EV isolates, protein characterization (SDS-PAGE, MS) (Jiang et al., 2014)
	Lactiplantibacillus plantarum [previously referred to as *Lactobacillus plantarum* (Zheng et al., 2020)]	TEM of EV isolates, protein characterization (MS) (Li et al., 2017)
	Lacticaseibacillus rhamnosus [previously referred to as *Lactobacillus rhamnosus* (Zheng et al., 2020)]	TEM of EV isolates (Behzadi et al., 2017)
	Limosilactobacillus reuteri [previously referred to as *Lactobacillus reuteri* (Zheng et al., 2020)]	SEM and TEM of budding events or EV isolates (Grande et al., 2017)
	Lacticaseibacillus casei [previously referred to as *Lactobacillus casei* (Zheng et al., 2020)]	TEM and AFM of EV isolates, CLSM of budding events, protein characterization (SDS-PAGE, MS) (Domínguez Rubio et al., 2017)
	Bifidobacterium longum	TEM of EV isolates, protein characterization (SDS-PAGE, MS) (Kim J.-H. et al., 2016)
	Enterococcus faecalis	TEM of EV isolates, protein characterization (SDS-PAGE, MS) (Kim J.-H. et al., 2016)

Actinobacteria	*Mycobacterium tuberculosis*	TEM of budding events and EV isolates, protein characterization (MS), lipid characterization immunofluorescence (Athman et al., 2015, 2017; Prados-Rosales et al., 2014; Lee et al., 2015)
	Mycobacterium smegmatis	TEM of EV isolates, protein characterization (MS) (Prados-Rosales et al., 2011)
	Mycobacterium avium	TEM of EV isolates (Prados-Rosales et al., 2011)
	Mycobacterium kansasii	TEM of EV isolates (Prados-Rosales et al., 2011)
	Mycobacterium phlei	TEM of EV isolates (Prados-Rosales et al., 2011)
	Mycobacterium bovis Bacillus Calmette□Guérin (BCG)	TEM of budding events and EV isolates, protein characterization (MS), lipid characterization (Prados-Rosales et al., 2011)
	Mycobacterium ulcerans	SEM, protein characterization (MS) (Marsollier et al., 2007)
	Streptomyces lividans	TEM of culture supernatant, lipid staining, protein characterization (MS) (Schrempf and Merling, 2015)
	Streptomyces coelicolor	TEM of culture supernatant and EV isolates, cryo-EM and cryo-electron tomography, protein characterization (SDS-PAGE, MS) (Schrempf et al., 2011)

TEM, transmission electron microscopy; SDS-PAGE, sodium dodecyl sulfate-polyacrylamide gel electrophoresis; MS, mass spectrometry; SEM, scanning electron microscopy; AFM, atomic force microscope; CLSM, confocal laser scanning microscopy.

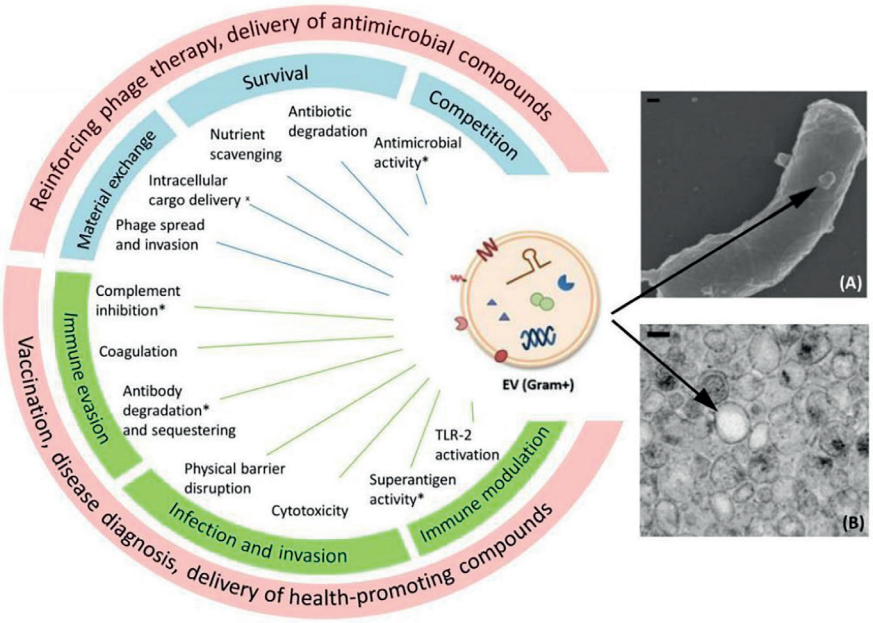

Figure 2.1. Proposed functions and potential medical applications of Gram-positive EVs. On the left side a schematic drawing of EVs carrying different types of cargo is shown. Functions marked with an asterisk (*) have been proposed on the basis of EV protein content, but a functional effect remains to confirmed. (ˣ) Bacterial cell-cell communication supported by membrane fusion assays. Blue boxes show EV roles in bacterial physiology and ecology, green boxes show EV roles in microbe-host interaction, and red boxes show proposed applications of EVs. On the right side a SEM picture (A) of EV production from *B. subtilis* and a TEM picture (B) of isolated *B. subtilis* EVs are shown as examples (Brown et al., 2014). Copyright 2018 Wiley-Blackwell. EM pictures used with permission. Scale bars 100 nm.

Obviously, the type of cargo determines the role of EVs to a large extent. Gram-positive EVs have been suggested, among others, to play a role in horizontal gene transfer. In addition to the transfer of bacterial chromosomal DNA, which was revealed in *Ruminococcus* spp. (Klieve et al., 2005), EVs may also facilitate gene transfer by mediating bacteriophage (phage) infection. It was observed in *Bacillus subtilis* that phage-resistant cells acquired phage sensitivity by receiving phage receptors carried by EVs generated from susceptible bacteria (Tzipilevich et al., 2017). The same mechanism even enabled *B. subtilis* phages to attach to non-host species *Bacillus cereus* and *Bacillus amyloliquefaciens*, providing the initial step for phages to adapt to new hosts and exchange genetic material. Moreover, phage particles were found inside EVs (Toyofuku et al., 2017), and these EVs could potentially provide a novel route for phages to enter bacterial hosts, that is, their intracellular release following membrane fusion which was demonstrated in *B. subtilis* (Kim Y. et al., 2016). Thus, EV-mediated horizontal gene transfer among different bacterial strains and species, contributes to bacterial DNA transfer and to phage spreading and invasion (Fig. 2.1).

EVs can also contribute to microbial survival or competition. To explicate the former, the scavenging properties of EVs support the uptake of nutrient molecules from the environment. For example, EVs derived from *Mycobacterium tuberculosis*, *Streptomyces coelicolor* as well as *Staphylococcus aureus* were shown to contain iron-binding factors that contribute to bacterial survival under iron-limited conditions (Rodriguez and Prados-Rosales, 2016; Lee et al., 2009, 2015; Schrempf et al., 2011; Jeon et al., 2016). Proteomic analysis also revealed the presence of beta-lactamase in *S. aureus* EVs. As a result, EVs produced by resistant bacteria could protect susceptible bacteria by degrading ampicillin in the environment (Lee J. et al., 2013). Although so far EV-conferred protection was restricted to this particular resistance factor, it is conceivable that EVs could be involved in the establishment of antibiotic resistant subpopulations via horizontal gene transfer and/or the transfer of antimicrobial factors. Competition is also believed to occur via antimicrobial factors released in EVs. The presence of autolysins in EVs points to a role in lytic attack on targeted bacteria (Olaya-Abril et al., 2014; Haas and Grenier, 2015; Lee et al., 2015) (Fig. 2.1).

Gram-positive EVs in bacteria-host interactions

In addition to the physiological roles of Gram-positive EVs, their functions in interacting with the human host are also revealed. Interestingly, Gram-positive EVs were shown to be internalized by eukaryotic cells via endocytosis in multiple epithelial and macrophage cell lines (Mulcahy et al., 2014; Surve et al., 2016; Brown et al., 2014; Hong et al., 2014; Kim et al., 2012). Moreover, the fusion of bacterial EVs with eukaryotic cell membranes has also been clearly demonstrated (Thay et al., 2013). In addition, EVs can directly interact with receptors on the surface of host cells to initiate intracellular signaling cascades (Prados-Rosales et al., 2014; Kim et al., 2012). Surface-exposed enzymes linked to EVs can function similarly to extracellular and cell surface-associated enzymes. Notably, it has been proposed that rupture of EVs facilitates targeted or delayed release of enzymes contained within vesicles, leading to a locally high and hence biologically active concentration of the released agent (Thay et al., 2013).

EV-associated virulence

Since virulence factors can form a large constituent of the protein content of EVs, a strong interest is focused on the role of Gram-positive EVs during infection (Lee J. et al., 2013) (Fig. 2.1). This not only relates to abundance, ranking among the top protein hits, but also the diversity of virulence factors found in EVs (Lee et al., 2009; Haas and Grenier, 2015) including so-called superantigens, capable of a-specifically activating a substantial portion of the human T cell repertoire (Lee J.H. et al., 2013; Jeon et al., 2016). Virulence factors specifically aimed at promoting invasion and spread throughout tissues have also been identified in EVs. Examples include collagenase and hyaluronate lyase that disrupts the extracellular matrix (ECM), and serine proteases, such as exfoliative toxins, which aid in the disruption of physical barriers (Jeon et al., 2016; Surve et al., 2016; Jeon et al., 2017). Functional effects of EV-incorporated virulence factors have so far most clearly been demonstrated for cytotoxic factors

(Rivera et al., 2010; Thay et al., 2013). EVs produced by *Bacillus anthracis*, *S. aureus*, *Streptococcus pneumoniae*, *Streptococcus pyogenes* and *Streptococcus agalactiae* were shown to carry a range of hemolysins and/or pore forming toxins (Olaya-Abril et al., 2014; Surve et al., 2016; Resch et al., 2016; Rivera et al., 2010; Jeon et al., 2016; Thay et al., 2013). Notably, the activity of such toxins can be altered or enhanced by enclosure inside or in membranes of EVs. Whereas soluble α-hemolysin induced apoptosis-like cell death, necrosis was caused following exposure to EV-enclosed α-hemolysin (Hong et al., 2014). This feature can be the result of a more preferable molecular organization of toxins in EVs or alternatively, by increased delivery to target cells.

Gram-positive EVs can contain an array of molecules involved in immune evasion (Fig. 2.1). EVs of *S. aureus* bear coagulase enzymes and factors that can mediate clot formation upon addition of EVs to serum (Lee et al., 2009; Sugimoto et al., 2016). EVs can thus aid in the formation of fibrin networks surrounding pathogens, thereby forming a protective environment with limited access to the innate immune system. Also an efficient humoral immune response can be subverted by EVs. *M. tuberculosis*-derived EVs carrying lipoglycans were shown to inhibit T cell responses (Athman et al., 2017). Multiple protein-disrupting key steps of the complement cascade have been identified in EV preparations (Lee et al., 2009; Resch et al., 2016). In addition, an IgM protease as well as functional IgG binding factors could be retrieved from these samples (Lee et al., 2009; Gurung et al., 2011; Haas and Grenier, 2015). These factors would allow EVs to actively clear antibodies in the surroundings, in addition to their natural decoy ability due to antigenic similarity with the secreting pathogen.

EVs in clinical disease

Given the virulence factors harbored in EVs, it is not surprising that EV exposure has been linked with the exacerbation or induction of a variety of disease states. For instance, the exposure of fetal-maternal structures to *S. agalactiae*-derived EVs can lead to fetal compromise and preterm termination of the pregnancy, as evidenced using mice models (Surve et al., 2016). Interestingly, EVs were able to travel along the female mouse reproductive tract towards the uterus. This phenomenon could provide an explanation for the paradoxical link between reproductive tract colonization and the occurrence of complications at the sterile fetal-maternal interface (Surve et al., 2016). These findings suggest that via the transfer of EVs, even infection or colonization at a distant site can contribute to disease development. Likewise, challenge with EVs can even occur via environmental exposure. *S. aureus* EVs were found in house dust, and in this form, bacterial products are thought to be more easily inhaled than whole bacteria (Kim et al., 2012). Incidental or repeated inhalation of *S. aureus* EVs was shown to cause airway inflammation in mice. Importantly, when EV exposure in the lungs was combined with allergens, a stronger sensitization occurred compared to the allergen exposure alone. EV exposure thereby enhanced a hypersensitivity response to the allergen in question (Kim et al., 2012). Gram-positive EVs therefore seem to represent an unforeseen contributor to frequently occurring, and seemingly unrelated disease conditions.

EVs in health benefits

Although a number of studies focus on EVs derived from pathogens and hence associate them with health threats, evidence of EV production by probiotic bacteria is also emerging and drawing attention to the health benefits conferred by EVs (Ilinskaya et al., 2017, Liu et al., 2018). Strains of *Bifidobacterium longum*, *Lacticaseibacillus rhamnosus* [previously referred to as *Lactobacillus rhamnosus* (Zheng et al., 2020)]*, Lacticaseibacillus casei* (previously referred to as *Lactobacillus casei*) and *Lactiplantibacillus plantarum* (previously referred to as *Lactobacillus plantarum*) were shown to produce EVs carrying effector molecules that are associated with the probiotic effects of the producing bacteria (Kim J.-H. et al., 2016; Behzadi et al., 2017; Domínguez Rubio et al., 2017; Li et al., 2017). EVs from *B. longum* effectively alleviated food allergy response in a mouse model; purified *L. rhamnosus* EVs were shown to have significant cytotoxic effect on hepatic cancer cells; *L. casei*-derived EVs carry proteins that offer the host intestinal epithelial cells protective, anti-apoptotic effects; *L. plantarum*-derived EVs provided protection to the host against pathogenic bacteria. Often these effects could be observed with EVs but not with complete bacterial cells, possibly due to the fact that EVs can penetrate the intestinal epithelial barrier and migrate to the other organs or interact with the immune system of the host (Kim J.-H. et al., 2016; Behzadi et al., 2017). These insights into the mechanisms of previously observed beneficial properties of probiotic microorganisms further highlight the importance of EVs.

Repurposing bacterial EVs in medical applications

Based on the revealed cargo components and speculated roles of Gram-positive EVs in microbe-microbe as well as microbe-host interactions, we propose several medical or biotechnological applications for Gram-positive EVs, including delivery of antimicrobial compounds, reinforcing phage therapy, vaccination, disease diagnosis and delivery of health-promoting compounds (Fig. 2.1).

Delivery of antimicrobial compounds

The role of Gram-positive EVs in cargo exchange among bacteria suggests that they could serve to deliver compounds that have difficulties to pass the cell membrane, such as antibiotics. Liposome incorporation of the antibiotic tobramycin was shown to greatly increase the efficacy against *S. aureus*, implicating EV-mediated delivery of antimicrobials as an interesting therapeutic approach (Beaulac et al., 1998). Many strategies have been proposed for the artificial loading of vesicles, which could enable the delivery of antibiotics or other chemical compounds via natural EVs to enhance uptake and targeting compared to synthetic structures (Vader et al., 2016). Local concentration and simultaneous release of two or more compounds via EV-incorporation could enable synergy of drug actions. In the case of autolysins, joined release with other compounds might aid in the passage of drugs, or maybe even whole EVs, through the cell wall. As EVs offer protection to the cargos, they may indeed show advantage in delivery of compounds susceptible to degradation, for example antimicrobial peptides (Moncla et al., 2011).

Reinforcing phage therapy

Phage therapy is being revisited frequently nowadays as an alternative to antibiotics for treating bacterial infections due to the increasing severity of antibiotic resistance (Lin et al., 2017; Nobrega et al., 2015). However, a challenge posed to phage therapy is the narrow host-range of phages (Koskella and Meaden, 2013). To tackle this, the use of phage cocktails (Sadekuzzaman et al., 2017, Yen et al., 2017) or engineering phages with broad host ranges has been reported (Pires et al., 2016; Ando et al., 2015). As Gram-positive EVs can have a role in promoting the spread of phages and invasion of novel bacterial hosts by transferring phage receptors (Tzipilevich et al., 2017), EVs might provide extra opportunities in phage therapy too. EVs derived from phage-sensitive bacteria can be administered prior to the phages, to enhance the targeting of bacteria and even enable the infection of novel bacterial host targets.

Another challenge in phage therapy is the reduction in activity in the case of orally administered phages through the gastrointestinal tract (GIT), where factors such as low pH have a large impact on phage activity (Ly-Chatain 2014). Liposome encapsulation was shown to improve phage stability in GIT both in simulated gastric fluid and *in vivo* (Colom et al., 2015). Similarly, we speculate that EV-engulfed phages may demonstrate improved tolerance to hostile conditions, and therefore show higher efficacy after (oral) administration. In addition, EV-mediated transfer of phages themselves could serve as a potential receptor-independent delivery route, although this theory remains to be confirmed experimentally.

Vaccination

Since EVs can transport bacterial products to the host, large efforts are being undertaken to study the EV-mediated delivery of immunogenic antigens. Initial steps towards the clinical use of Gram-positive EVs as disease prophylaxis are currently being evaluated. A patent has already been filed claiming ownership of the method of immune induction via Gram-positive EVs, thereby aiming to develop a new vaccination strategy (Gho et al., 2016). So far, beneficial effects of vaccination with Gram-positive EVs have been demonstrated for *Clostridium perfringens*, *S. pneumoniae*, *B. anthracis*, *M. tuberculosis*, and *S. aureus*. In mice models, the above mentioned EV vaccination prolonged survival time or increased the survival rate upon lethal challenge (Olaya-Abril et al., 2014; Rivera et al., 2010; Jiang et al., 2014; Choi et al., 2015). In addition, the bacterial burden to the host immune system and the degree of inflammation could be reduced upon a sub-lethal challenge (Choi et al., 2015; Prados-Rosales et al., 2011). While Wang et al. (2018) employed genetic engineering to ensure the production of non-toxic *S. aureus* EVs as effective vaccines in mice, another study showed that also non-engineered *S. aureus* EVs did not cause notable toxicity in mice despite the potent immune activation (Choi et al., 2015). This is in contrast to OMV-based vaccines, for which toxicity of LPS constituents hampers the vaccine application (Acevedo et al., 2014). Gram-positive EVs might thus form an even more potent vaccination strategy than currently licensed vaccines.

Disease diagnosis

The link between gut microbiota composition and human health or diseases is being revealed gradually in recent years (Yamashiro, 2017; Marchesi et al., 2016; Chelakkot et al., 2018). Studies show that EVs derived from the gut microbiota are distributed throughout the human body including the blood and urine, and they reflect the composition of the microbiota to a great extent (Kang et al., 2013; Yoo et al., 2016; Jang et al., 2015). This observation opens doors to novel methods of disease diagnosis or assessment. As an example, Lee and co-workers successfully developed a rapid, non-invasive assessment method on microbiota profiles in autism spectrum disorder patients by examining the 16S rRNA gene sequences in bacterial EVs isolated from urine samples (Lee et al., 2017). Since EV release is often the result of active metabolism in bacteria, EVs may form a better indication of the microbiota activities in the hosts than the bacterial populations themselves, and therefore provide more insights into the links between microbiota and the disease or health status of the hosts.

Delivery vehicles of health-promoting compounds

As EVs were shown to play important roles in realizing the anti-allergy, anti-inflammation and cancer-inhibiting effects of several probiotic bacteria (Li et al., 2017; Behzadi et al., 2017; Kim J.H. et al., 2016), the opportunity of using EVs as a booster or even substitute for bacteria to achieve probiotic effects becomes attractive. Moreover, EVs may offer protection and serve to deliver beneficial nutritional compounds, namely proteins or vitamins, to the hosts in an efficient manner (Liu et al., 2018). The same effect might not be attained by ingesting the pure compounds or whole-cell bacteria due to degradation of the effector molecules or limited accessibility to the targeted tissue or cells. Therefore, bacterial EVs may contribute to novel formulations of probiotics or food supplements.

Concluding remarks

Gram-positive bacteria constitute a large and widely diverse group, including species that are extensively used in food fermentations and as probiotics, whereas other species are known to be pathogenic causing a range of foodborne and clinical infections. So far, a clear picture has emerged showing that Gram-positive EVs may play a role in a wide range of biological events and consequently in human health and disease. These initial indications form a strong framework that can guide new research lines focused on the mechanistic understanding of these events and the translation of individual examples to general concepts and applications. Yet, many enigmatic puzzles regarding the underlying biology of Gram-positive EVs still remain unsolved, especially in EV biogenesis and uptake. Elucidation of these aspects may further stimulate innovative medical and biotechnological applications.

Acknowledgements

The work described in this article was subsidized by the Netherlands Organization for Scientific Research (NWO) through the Graduate Program on Food Structure, Digestion and Health.

References

Acevedo, R., Fernández, S., Zayas, C., Acosta, A., Sarmiento, M. E., Ferro, V. A., et al. (2014). Bacterial outer membrane vesicles and vaccine applications. *Front. Immunol.* 5:121.

Ando, H., Lemire, S., Pires, D. P., and Lu, T. K. (2015). Engineering modular viral scaffolds for targeted bacterial population editing. *Cell Syst.* 1, 187–196.

Athman J. J., Sande O. J., Groft S. G., Reba S. M., Nagy N., Wearsch P. A., et al. (2017) *Mycobacterium tuberculosis* membrane vesicles inhibit T cell activation. *J. Immunol*. 198, 2028-2037.

Athman, J. J., Wang, Y., McDonald, D. J., Boom W. H., Harding, C. V., and Wearsch, P. A. (2015) Bacterial membrane vesicles mediate the release of *Mycobacterium tuberculosis* lipoglycans and lipoproteins from infected macrophages. *J. Immunol.* 195, 1044–1053.

Beaulac, C., Sachetelli, S., and Lagace, J. (1998) *In-vitro* bactericidal efficacy of sub-MIC concentrations of liposome-encapsulated antibiotic against Gram-negative and Gram-positive bacteria. *J. Antimicrob. Chemother*. 41, 35–41

Behzadi, E., Mahmoodzadeh Hosseini, H., and Imani Fooladi, A. A. (2017) The inhibitory impacts of *Lactobacillus rhamnosus* GG-derived extracellular vesicles on the growth of hepatic cancer cells. *Microb. Pathog.* 110, 1–6.

Brown, L., Kessler A., Cabezas-Sanchez, P., Luque-Garcia, J. L., and Casadevall, A. (2014) Extracellular vesicles produced by the Gram-positive bacterium *Bacillus subtilis* are disrupted by the lipopeptide surfactin. *Mol. Microbiol*. 93, 183–198.

Brown, L., Wolf, J. M., Prados-Rosales, R., and Casadevall, A. (2015) Through the wall: extracellular vesicles in Gram-positive bacteria, mycobacteria and fungi. *Nat. Rev. Microbiol.* 13, 620–630.

Chelakkot C., Choi Y., Kim D.K., Park H. T., Ghim J., Kwon Y., et al. (2018) *Akkermansia muciniphila*-derived extracellular vesicles influence gut permeability through the regulation of tight junctions. *Exp. Mol. Med*. 50:e450.

Choi, S. J., Kim M.-H., Jeon, J., Kim, O. Y., Choi, Y., Seo, J., et al. (2015) Active immunization with extracellular vesicles derived from *Staphylococcus aureus* effectively protects against staphylococcal lung infections, mainly via Th1 cell-mediated immunity. *PLoS One* 10:e0136021.

Colom, J., Cano-Sarabia, M., Otero, J., Cortés, P., Maspoch, D., and Llagostera, M. (2015) Liposome-encapsulated bacteriophages for enhanced oral phage therapy against *Salmonella* spp. *Appl. Environ. Microbiol*. 81, 4841–4849.

Domínguez Rubio, A. P., Martínez, J. H., Martínez Casillas, D. C., Coluccio Leskow, F., Piuri, M., and Pérez, O. E. (2017) *Lactobacillus casei* BL23 produces microvesicles carrying proteins that have been associated with its probiotic effect. *Front. Microbiol.* 8:1783.

Gho, Y. S., Kim, Y. K., Lee, E. Y., Hong, S. W., Kim, J. H., and Choi, S. J. Extracellular vesicles derived from gram-positive bacteria, and use thereof. United States patent US9273359B2 (2016)

Grande, R., Celia, C., Mincione, G., Stringaro, A., Di Marzio, L., Colone, M., et al. (2017) Detection and physicochemical characterization of membrane vesicles (MVs) of *Lactobacillus reuteri* DSM 17938. *Front. Microbiol.* 8:1040.

Gurung, M., Moon, D. C., Choi, C. W., Lee, J. H., Bae, Y. C., Kim, J., et al. (2011) *Staphylococcus aureus* produces membrane-derived vesicles that induce host cell death. *PLoS One* 6:e27958.

Haas, B., and Grenier, D. (2015) Isolation, characterization and biological properties of membrane vesicles produced by the swine pathogen *Streptococcus suis*. *PLoS One* 10:e0130528.

Hong, S.-W., Choi, E.-B., Min, T.-K., Kim, J.-H., Kim, M.-H., Jeon, S. G., et al. (2014) An important role of α-hemolysin in extracellular vesicles on the development of atopic dermatitis induced by *Staphylococcus aureus*. *PLoS One* 9:e100499.

Ilinskaya O. N., Ulyanova V. V., Yarullina D. R. and Gataullin I. G. (2017) Secretome of intestinal *Bacilli*: a natural guard against pathologies. *Front. Microbiol.* 8:1666.

Jang, S. C., Kim, S. R., Yoon, Y. J., Park, K.-S., Kim, J. H., Lee, J., et al. (2015) *In vivo* kinetic biodistribution of nano-sized outer membrane vesicles derived from bacteria. *Small* 11, 456–461.

Jeon, H., Oh, M. H., Jun, S. H., Kim, S. I., Choi, C. W., Kwon, H. I., et al. (2016) Variation among *Staphylococcus aureus* membrane vesicle proteomes affects cytotoxicity of host cells. *Microb. Pathog*. 93, 185–193.

Jeon, J., Mok, H. J., Choi, Y., Park, S. C., Jo, H., Her, J., et al. (2017) Proteomic analysis of extracellular vesicles derived from *Propionibacterium acnes*. *Proteomics Clin. Appl.* 11:1600040.

Jiang, Y., Kong, Q., Roland, K. L., and Curtiss, R. 3rd. (2014) Membrane vesicles of *Clostridium perfringens* type a strains induce innate and adaptive immunity. *Int. J. Med. Microbiol*. 304, 431–443.

Kang, C.-s., Ban, M., Choi, E.-J., Moon, H.-G., Jeon, J.-S., Kim, D.-K., et al. (2013). Extracellular vesicles derived from gut microbiota, especially *Akkermansia muciniphila*, protect the progression of dextran sulfate sodium-induced colitis. *PLoS One* 8:e76520.

Kim, J.-H., Jeun, E.-J., Hong, C.-P., Kim, S.-H., Jang, M. S., Lee, E.-J., et al. (2016) Extracellular vesicle–derived protein from *Bifidobacterium longum* alleviates food allergy through mast cell suppression. *J. Allergy Clin. Immunol.* 137, 507–516.

Kim, J. H., Lee, J., Park, J. and Gho, Y. S. (2015) Gram-negative and gram-positive bacterial extracellular vesicles. *Semin. Cell Dev. Biol*. 40, 97–104.

Kim, M.-R., Hong, S.-W., Choi, E.-B., Lee, W.-H., Kim, Y.-S., Jeon, S. G., et al. (2012) *Staphylococcus aureus*-derived extracellular vesicles induce neutrophilic pulmonary inflammation via both Th1 and Th17 cell responses. *Allergy* 67, 1271–1281.

Kim, Y., Edwards, N., and Fenselau, C. (2016) Extracellular vesicle proteomes reflect developmental phases of *Bacillus subtilis*. *Clin. Proteomics* 13:6.

Klieve, A. V., Yokoyama, M. T., Forster, R. J., Ouwerkerk, D., Bain, P. A., and Mawhinney, E. L. (2005) Naturally occurring DNA transfer system associated with membrane vesicles in cellulolytic *Ruminococcus* spp. of ruminal origin. *Appl. Environ. Microbiol.* 71, 4248–4253.

Koskella, B., and Meaden, S. (2013) Understanding bacteriophage specificity in natural microbial communities. *Viruses* 5, 806–823.

Lee, E.-Y., Choi, D.-Y., Kim, D.-K., Kim, J.-W., Park, J. O., Kim, S., et al. (2009) Gram-positive bacteria produce membrane vesicles: proteomics-based characterization of *Staphylococcus aureus*-derived membrane vesicles. *Proteomics* 9, 5425–5436.

Lee, J., Kim, S.-H., Choi, D.-S., Lee, J. S., Kim, D.-K., Go, G., et al. (2015) Proteomic analysis of extracellular vesicles derived from *Mycobacterium tuberculosis*. *Proteomics* 15, 3331–3337.

Lee, J., Lee, E.-Y., Kim, S.-H., Kim, D.-K., Park, K.-S., Kim, K. P., et al. (2013) *Staphylococcus aureus* extracellular vesicles carry biologically active β-lactamase. *Antimicrob. Agents Chemother.* 57, 2589–2595.

Lee, J. H., Choi, C.-W., Lee, T., Kim, S. I., Lee, J.-C., and Shin, J.-H. (2013) Transcription factor σb plays an important role in the production of extracellular membrane-derived vesicles in *Listeria monocytogenes*. *PLoS One* 8:e73196.

Lee, Y., Park, J.-Y., Lee, E.-H., Yang, J., Jeong, B.-R., Kim, Y.-K., et al. (2017) Rapid assessment of microbiota changes in individuals with autism spectrum disorder using bacteria-derived membrane vesicles in urine. *Exp. Neurobiol*. 26, 307–317.

Li, M., Lee, K., Hsu, M., Nau, G., Mylonakis, E., and Ramratnam, B. (2017) *Lactobacillus*-derived extracellular vesicles enhance host immune responses against vancomycin-resistant enterococci. *BMC Microbiol.* 17:66.

Liao, S., Klein, M. I., Heim, K. P., Fan, Y., Bitoun, J. P., Ahn, S.-J. et al. (2014) *Streptococcus mutans* extracellular DNA is upregulated during growth in biofilms, actively released via membrane vesicles, and influenced by components of the protein secretion machinery. *J. Bacteriol.* 196, 2355–2366.

Lin, D. M., Koskella, B., and Lin, H. C. (2017) Phage therapy: an alternative to antibiotics in the age of multi-drug resistance. *World J. Gastrointest. Pharmacol. Ther.* 8, 162-173.

Liu, Y., Alexeeva, S., Defourny, K. A. Y., Smid, E. J., and Abee, T. (2018) Tiny but mighty: bacterial membrane vesicles in food biotechnological applications. *Curr. Opin. Biotechnol*. 49, 179–184.

Ly-Chatain, M. H. (2014) The factors affecting effectiveness of treatment in phages therapy. *Front Microbiol*. 5:51.

Marchesi, J. R., Adams, D. H., Fava, F., Hermes, G. D. A., Hirschfield, G. M., Hold, G., et al. (2016) The gut microbiota and host health: a new clinical frontier. *Gut* 65, 330–339.

Marsollier, L., Brodin, P., Jackson, M., Korduláková, J., Tafelmeyer, P., Carbonnelle, E., et al. (2007) Impact of *Mycobacterium ulcerans* biofilm on transmissibility to ecological niches and buruli ulcer pathogenesis. *PLoS Pathog*. 3:e62.

Moncla, B. J., Pryke, K., Rohan, L. C., and Graebing, P. W. (2011) Degradation of naturally occurring and engineered antimicrobial peptides by proteases. *Adv Biosci Biotechnol*. 2, 404–408.

Mulcahy, L. A., Pink, R. C., and Carter, D. R. F. (2014) Routes and mechanisms of extracellular vesicle uptake. *J. Extracell. Vesicles* 3:24641.

Nobrega, F. L., Costa, A. R., Kluskens, L. D., and Azeredo, J. (2015) Revisiting phage therapy: new applications for old resources. *Trends Microbiol*. 23, 185–191.

Olaya-Abril, A., Prados-Rosales, R., McConnell, M. J., Martín-Peña, R., González-Reyes, J. A., Jiménez-Munguía, I., et al. (2014) Characterization of protective extracellular membrane-derived vesicles produced by *Streptococcus pneumoniae*. *J. Proteomics*. 106, 46–60.

Pires, D. P., Cletoa, S., Sillankorvac, S., Azeredoc, J. and Lu, T. K. (2016) Genetically Engineered Phages: a Review of Advances over the Last Decade. *Microbiol. Mol. Biol. Rev*. 80, 523-543.

Prados-Rosales, R., Carreño, L. J., Batista-Gonzalez, A., Baena, A., Venkataswamy, M. M., Xu, J., et al. (2014) Mycobacterial membrane vesicles administered systemically in mice induce a protective immune response to surface compartments of *Mycobacterium tuberculosis*. *MBio* 5:e01921-14.

Prados-Rosales, R., Baena, A., Martinez, L. R., Luque-Garcia, J., Kalscheuer, R., Veeraraghavan, U., et al. (2011) Mycobacteria release active membrane vesicles that modulate immune responses in a TLR2-dependent manner in mice. *J. Clin. Invest*. 121, 1471–1483.

Resch, U., Tsatsaronis, J. A., Le Rhun, A., Stübiger, G., Rohde, M., Kasvandik, S., et al. (2016) A two-component regulatory system impacts extracellular membrane-derived vesicle production in Group A *Streptococcus*. *MBio* 7:e00207-16.

Rivera, J., Cordero, R. J. B., Nakouzi, A. S., Frases, S., Nicola, A., and Casadevall, A. (2010) *Bacillus anthracis* produces membrane-derived vesicles containing biologically active toxins. *Proc. Natl. Acad. Sci. U. S. A*.107, 19002–19007.

Rodriguez, G. M. and Prados-Rosales, R. (2016) Functions and importance of mycobacterial extracellular vesicles. *Appl Microbiol Biotechnol*. 100, 3887–3892.

Sadekuzzaman, M., Yang, S., Mizan Md. F. R., Kim H.-S. and Ha S.-D. (2017) Effectiveness of a phage cocktail as a biocontrol agent against *L. monocytogenes* biofilms. *Food Control* 78, 256-263.

Schrempf, H., Koebsch, I., Walter, S., Engelhardt, H., and Meschke, H. (2011) Extracellular *Streptomyces* vesicles: amphorae for survival and defence. *Microb. Biotechnol.* 4, 286–299.

Schrempf, H., and Merling, P. (2015) Extracellular *Streptomyces lividans* vesicles: composition, biogenesis and antimicrobial activity. *Microb. Biotechnol*. 8, 644–658.

Sugimoto, S., Okuda, K., Miyakawa, R., Sato, M., Arita-Morioka, K., Chiba, A., et al. (2016) Imaging of bacterial multicellular behaviour in biofilms in liquid by atmospheric scanning electron microscopy. *Sci Rep*. 6:25889.

Surve, M. V., Anil, A., Kamath, K. G., Bhutda, S., Sthanam, L. K., Pradhan, A., et al. (2016) Membrane vesicles of Group B *Streptococcus* disrupt feto-maternal barrier leading to preterm birth. *PLoS Pathog*. 12:e1005816.

Thay, B., Wai, S. N., and Oscarsson, J. (2013) *Staphylococcus aureus* α-toxin-dependent induction of host cell death by membrane-derived vesicles. *PLoS One.* 8:e54661.

Toyofuku, M., Cárcamo-Oyarce, G., Yamamoto, T., Eisenstein, F., Hsiao, C.-C., Kurosawa, M., et al. (2017) Prophage-triggered membrane vesicle formation through peptidoglycan damage in *Bacillus subtilis*. *Nat. Commun*. 8:481.

Tzipilevich, E., Habusha, M., and Ben-Yehuda, S. (2017). Acquisition of phage sensitivity by bacteria through exchange of phage receptors. *Cell* 168, 186–199.

Vader, P., Mol, E. A., Pasterkamp, G., and Schiffelers, R. M. (2016) Extracellular vesicles for drug delivery. *Adv. Drug Deliv. Rev.* 106 (Pt A), 148–156.

Wang, X., Thompson, C. D., Weidenmaier, C., and Lee, J. C. (2018) Release of *Staphylococcus aureus* extracellular vesicles and their application as a vaccine platform. *Nat. Commun.* 9:1379.

Yamashiro, Y. (2017) Gut microbiota in health and disease. *Ann. Nutr. Metab*. 71, 242–246.

Yen, M., Cairns, L. S. and Camilli, A. (2017) A cocktail of three virulent bacteriophages prevents *Vibrio cholerae* infection in animal models. *Nat. Commun*. 8:14187.

Yoo, J. Y., Rho, M., You, Y.-A., Kwon, E. J., Kim, M.-H., Kym, S., et al. (2016) 16S rRNA gene-based metagenomic analysis reveals differences in bacteria-derived extracellular vesicles in the urine of pregnant and non-pregnant women. *Exp. Mol. Med.* 48:e208.

Zheng, J., Wittouck, S., Salvetti, E., Franz, C. M. A. P., Harris, H. M. B., Mattarelli, P., et al. (2020). A taxonomic note on the genus *Lactobacillus*: Description of 23 novel genera, emended description of the genus *Lactobacillus Beijerinck* 1901, and union of *Lactobacillaceae* and *Leuconostocaceae*. *Int. J. Syst. Evol. Microbiol.* 70, 2782–2858.


2

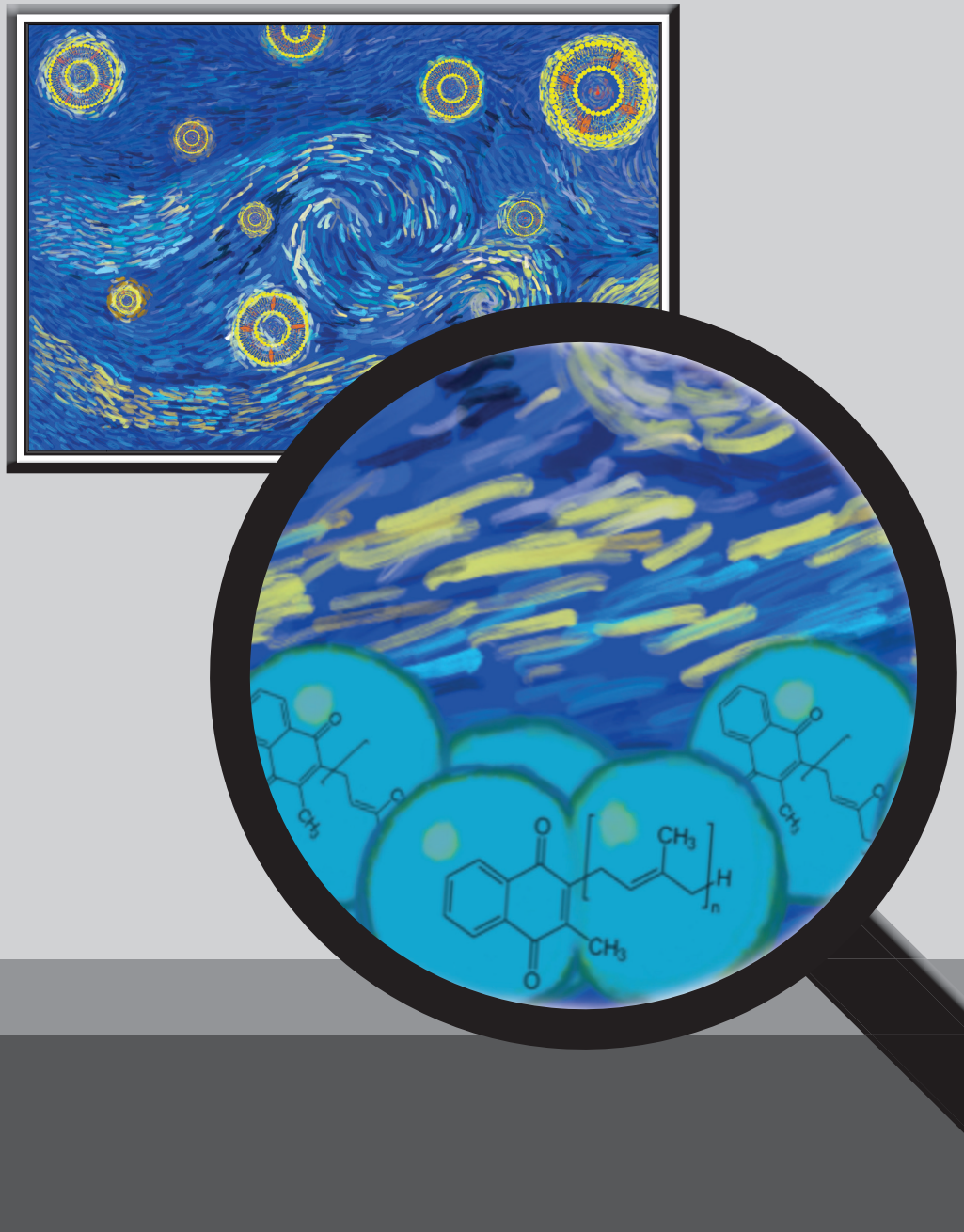
CH3
O
O
CH3
H
n
CH3
O
O
CH3

Chapter 3

Long-chain vitamin K2 production in *Lactococcus lactis* is influenced by temperature, carbon source, aeration and mode of energy metabolism

Yue Liu, Eric O. van Bennekom, Yu Zhang, Tjakko Abee & Eddy J. Smid

Published in
Microbial Cell Factories, 2019, 18:129

Abstract

Vitamin K2 (menaquinone, MK-n) is a lipid-soluble vitamin that functions as a carboxylase co-factor for maturation of proteins involved in many vital physiological processes in humans. Notably, long-chain vitamin K2 is produced by bacteria, including some species and strains belonging to the group of lactic acid bacteria (LAB) that play important roles in food fermentation processes. This study was performed to gain insights into the natural long-chain vitamin K2 production capacity of LAB and the factors influencing vitamin K2 production during cultivation, providing a basis for biotechnological production of vitamin K2 and *in situ* fortification of this vitamin in food products.

We observed that six selected *Lactococcus lactis* strains produced MK-5 to MK-10, with MK-8 and MK-9 as the major MK variant. Significant diversities between strains was observed in terms of specific concentrations and titers of vitamin K2. *L. lactis* ssp. *cremoris* MG1363 was selected for more detailed studies of the impact of selected carbon sources tested under different growth conditions [ie., static fermentation (oxygen absent, heme absent); aerobic fermentation (oxygen present, heme absent) and aerobic respiration (oxygen present, heme present)] on vitamin K2 production in M17 media. Aerobic fermentation with fructose as a carbon source resulted in the highest specific concentration of vitamin K2: 3.7-fold increase compared to static fermentation with glucose, whereas aerobic respiration with trehalose resulted in the highest titer: 5.2-fold increase compared to static fermentation with glucose. When the same strain was applied to quark fermentation, we consistently observed that altered carbon source (fructose) and aerobic cultivation of the pre-culture resulted in efficient vitamin K2 fortification in the quark product.

With this study we demonstrate that certain LAB strains can be employed for efficient production of long-chain vitamin K2. Strain selection and optimization of growth conditions offer a viable strategy towards natural vitamin K2 enrichment of fermented foods, and to improved biotechnological vitamin K2 production processes.

Introduction

Vitamin K is a fat-soluble vitamin that is essential for human health (Vermeer and Schurgers, 2000). It functions as an enzyme cofactor for γ-carboxylation of glutamate (Gla) residues in Gla-proteins, which play key roles in a number of vital physiological processes including hemostasis, calcium and bone metabolism, as well as cell growth regulation (Vermeer and Schurgers, 2000; Wen et al., 2018). Vitamin K exists naturally in two forms: vitamin K1 (phylloquinone) and vitamin K2 (menaquinones). Vitamin K1 is abundantly present in green leafy vegetables and found in some vegetable oils and is the predominant form of vitamin K in our daily diet. Vitamin K2 refers to a group of menaquinones (MKs) varying in side chain length. Different forms of MKs are written as MK-n, where n indicates the number of isoprenoid residues in its side chain (Walther et al., 2013). MK-4 is the most common form of short-chain MKs, and is produced in human and animal tissues by converting vitamin K1 or analogs of MK-precursors. Meats, eggs and milk are the common dietary sources of MK-4. The long-chain MKs, namely MK-5 to MK-13, are uniquely synthesized by bacteria. The main dietary sources of long-chain MKs are fermented foods (Walther et al., 2013; Fu et al., 2017).

The dietary intake of vitamin K2 covers only 10% to 25% of the total vitamin K intake in the Dutch and German population (Beulens et al., 2013) and is assumed to be even lower in many other countries. The bioavailability of vitamin K2 is thought to be higher than that of vitamin K1 (Geleijnse et al., 2004). Compared to vitamin K1, the co-factor efficacy of vitamin K2 for protein carboxylation has been shown to be higher (Schurgers et al., 2007). Notably, some forms of vitamin K2 with long side chains, e.g., MK-7 and MK-9, have been found to have longer plasma half-life times than vitamin K1 and MK-4, suggesting advantages for their uptake and utilization by the human body (Schurgers and Vermeer, 2002; Schurgers et al., 2007; Sato et al., 2012). Moreover, indications have been found that dietary intake of vitamin K2, especially in the form of MK-7, MK-8 and MK-9, is associated with a reduced risk of coronary heart disease (Geleijnse et al., 2004; Gast et al., 2009; Rees et al., 2010). Vitamin K2 intake is also involved in normal bone growth and development, whereas its deficiency is associated with increased risk of fracture and low bone mineral density (Booth et al., 2003; Fujita et al., 2012; Beulens et al., 2013; Wen et al., 2018). Some intestinal bacteria also produce vitamin K2, but in animal studies the absorption of this vitamin in the colon was found to be limited (Groenen-Van Dooren et al., 1995) and hence dietary intake is an essential source to obtain this vitamin. This information, combined with advances in nutrition research, underline the importance of fortifying food products with vitamin K2, especially the long-chain forms, in food products and supplements.

Production of long-chain vitamin K2 has been observed in a variety of bacteria involved in well-known food fermentation processes, and the specific structure of menaquinones produced by these bacteria has been determined (Collins and Jones, 1981; Walther et al., 2013). These food grade bacteria can be seen as potential candidates for *in situ* fortification in fermented foods and biotechnological production of long-chain MKs. *Bacillus subtilis* produces MK-7 and some strains are used to make fermented soybean food products, among which the Japanese natto is well-known (Walther et al.,

2013). However, fermented food products involving *B. subtilis* are mostly appreciated in certain regions in Asia and do not contribute to the western diet. Several studies have been performed to optimize biotechnological production of MK-7 in *B. subtilis* (Berenjian et al., 2011, 2012, 2014). Propionibacteria, producing MK-9 (4H), are used to produce Swiss-type cheeses (Hojo et al., 2007; Chollet et al., 2017) and are applied in biotechnological MK-9 (4H) production processes (Furuichi et al., 2006). Lactic acid bacteria (LAB) are key players in various food fermentation processes as starter cultures, probiotics and producers of vitamins. Among LAB, *Lactococcus lactis* ssp. *cremoris*, *L. lactis* ssp. *lactis*, *Leuconostoc lactis* and *Leuconostoc mesenteroides* are the reported producers of mainly MK-8, MK-9 and MK-10 (Morishita et al., 1999). In spite of the wide applications of LAB, studies were mainly conducted to reveal vitamin K2 levels in fermented dairy products (Chollet et al., 2017; Fu et al., 2017) and only a few studies (Morishita et al., 1999; Brooijmans et al., 2009) collected information on vitamin K2 production in LAB in laboratory conditions. Therefore, long-chain vitamin K2 production in LAB definitely deserves more investigation.

Vitamin K2 is present in the cytoplasmic membranes of producing bacteria, acting as an electron carrier in the respiratory electron transport chain (ETC) (Kurosu and Begari, 2010). Although LAB have been classified as non-respiring, facultative anaerobes, conclusive evidence has been found for functional respiration in various lactococci, lactobacilli, and pediococci in response to heme supplementation (Brooijmans et al., 2009). Menaquinones, together with the NADH dehydrogenase complex and the *bd*-type cytochrome complex (where heme functions as an essential cofactor), form a simple electron transport chain that enables aerobic respiration in these strains when oxygen is present. Nevertheless, it was found that menaquinone is produced in *L. lactis* continuously, under conditions including static fermentation (no oxygen or heme present), aerobic fermentation (oxygen present, no heme) and aerobic respiration (both oxygen and heme present) (Brooijmans et al., 2009). The role of menaquinones in the fermentative metabolism of producing bacteria remains unclear so far.

The vitamin K2 biosynthesis pathway begins with chorismite (Nowicka and Kruk, 2010). Chorismate is generated from shikimate pathway, that is supplied with precursors derived from glycolysis and the pentose phosphate pathway (Herrmann and Weaver, 1999; KEGG, 2018), and thus linking the production of menaquinone, to the central carbon metabolism. Therefore, the type of carbon source as well as the mode of energy metabolism potentially affects vitamin K2 synthesis in bacteria.

In this study, we focus on long-chain MKs as they are uniquely produced by bacteria and are thought to deliver additional health benefits in comparison to other vitamin K forms (Schurgers and Vermeer, 2002; Geleijnse et al., 2004; Schurgers et al., 2007; Sato et al., 2012). We aim to provide insights into the natural long-chain vitamin K2 producing capacity in different LAB strains and the influences of cultivation conditions on vitamin K2 production. To this end, we first examined the MK forms and quantity produced by different *L. lactis* and *Lc. mensenteroides* strains. Next, we selected *L. lactis* ssp. *cremoris* MG1363 to investigate changes in MK profile and levels in response to various growth conditions (i.e., different growth temperatures, degrees of aeration, types of carbon sources and

modes of energy metabolism), and used selected parameters for vitamin K2 enrichment in a quark product.

Materials and methods

Bacterial strains and culture conditions

For strain screening, we examined *L. lactis* ssp. *lactis* strains FM03, FM04, DSM20481, *L. lactis* ssp. *cremoris* strains MG1363, YL11, YL12 and *Lc. mesenteroides* strains DSM20343, FM06 , and FM08. *L. lactis* strains were cultivated in M17 media (Oxoid LOT2216165) supplemented with 0.5% (w/v) glucose (GM17), and *Lc. mesenteroides* strains were cultivated in MRS (De Man, Rogosa and Sharpe) media. The inoculum of each biological replicate was a single colony of the corresponding strain. Fifty-milliliter centrifuge tubes were filled with 50 mL media and statically incubated at 30 °C for 48 hours.

L. lactis ssp. *cremoris* MG1363 was used to examine the effect of cultivation conditions. A single colony was inoculated into GM17 media and incubated at 30 °C overnight. Ten microliter of the overnight culture was inoculated in 50 mL M17 media supplemented with 0.5% (w/v) carbon source. The carbon source was glucose unless specified otherwise. For static fermentation, 50 mL cultures were incubated statically in 50 mL centrifuge tubes. For aerobic fermentation, 50 mL cultures were placed in 500 mL Erlenmeyer flasks and shaken at one of the following shaking speeds: 60 rpm, 120 rpm and 200 rpm. For aerobic respiration, 50 mL cultures supplemented with 2 μg/mL hemin (heme) (Sigma) were shaken at 120 rpm in 500 mL Erlenmeyer flasks. Bacteria were cultivated for 48 hours at 30 °C, unless the temperature was otherwise stated.

Quark fermentation

Pre-cultures for quark fermentation were obtained by inoculating *L. lactis* ssp. *cremoris* MG1363 in M17 media supplemented with 0.5% (w/v) carbon source and incubated overnight at 30 °C, with aeration (aerobic fermentation at 120 rpm) or without aeration (static fermentation). The quark making procedure is modified from Binda and Ouwehand (2019). Together with 45 mL pasteurized skim milk (Jumbo Biologische houdbare Magere Melk, Netherlands), 0.5% (w/v) carbon source, 1% (w/v) casein tryptone (Sigma) and 1% (v/v) pre-culture were added to 50 mL centrifuge tubes. Fermentation took place at 20 °C or 30 °C for 20 h, and the pH values of samples were checked to be similar to traditional quark products (4.6). After centrifugation at 3000 x *g* for 10 min, the whey was discarded to obtain quark products.

Vitamin K2 extraction

For extraction from bacterial biomass, bacteria were harvested by centrifugation at 8000 x *g* for 15 min. The supernatant was discarded. The cell pellet was washed twice with 1 x volume of phosphate-buffered saline (PBS). The pellet was then re-suspended in 1.5 mL PBS that contained 10 mg/mL lysozyme (Sigma) and incubated at 37 °C for 1 hour. The cell suspension was vigorously mixed on a

vortex at the beginning and after 30 min of incubation. An extraction buffer was made with n-hexane and 2-peopanol at ratio 2:1 (v/v). Four volumes of extraction buffer was added to the lysozyme-treated bacterial suspension and the mixture was vigorously vortexed for 30 sec. The mixture was then centrifuged at 3000 x *g* for 10 min, and the (upper) organic phase was collected. Equal volume (as extraction buffer) of n-hexane was added to the remaining lower phase, and the extraction step was repeated twice.

For vitamin K2 extraction from quark samples, the method was adapted from Manoury et al. (2013). Four grams of quark sample was mixed with 10 mL MQ water and vigorously vortexed for 30 sec. Then 5 mL of 1 M HCl was added to the mixture, and the sample was heated at 99 °C for 30 min in a water bath and cooled in tap water. Ten milliliters iso-propanol and 4 mL hexane were added to the sample. The mixture was vigorously vortexed for 30 sec and centrifuged at 3000 x *g* for 10 min. The organic phase was collected. The extraction was repeated once with 4 mL hexane.

After extraction from bacteria or quark, organic phases from each sample were combined and evaporated under N_2 gas. Iso-propanol was then added to the sample vials to dissolve the extracted vitamin K2 by shaking at 160 rpm for 1 hour. All samples were diluted in methanol and subjected to high performance liquid chromatograph - mass spectrophotometry (HPLC-MS) analysis.

Determination of vitamin K2 content

Vitamin K2 extraction samples were analyzed on a HPLC (UFLC, Shimadzu, Japan) system coupled with a Micromass Quattro Ultima MS (Waters, USA). Fifty-microliter of each sample was injected on a Symmetry C18, 5 µm, 150 × 3 mm column (Waters, USA). Elution of compounds followed a gradient that started with 100% methanol (solvent A), 0% 2-propanol/hexane 50/50 (solvent B), and changed to 25% solvent A and 75% solvent B in 10 min. Then the gradient changed to 1% solvent A and 99% solvent B in 2 min and remained for another 2 min. The flow rate was 0.4 mL/min and oven temperature was 40 °C. Eluted compounds were detected by the MS system with an APCI (Atmospheric Pressure Chemical Ionization) source in the positive mode. The corona current was 5 µA. The APCI source temperature was 120 °C and probe temperature 500 °C. Details of MRM (multiple reaction monitoring) are presented in supplementary Table S3.1. Standards of MK-1 (Santa Cruz Biotechnology), MK-4 (Sigma), MK-7 (Sigma), MK-9 (Santa Cruz Biotechnology) and vitamin K1 (Sigma) in the concentration range from1 ng/mL to 3 µg/mL were analyzed to obtain the calibration curves. Except for the strain screening experiment, vitamin K1 was added at a concentration of 300 ng/mL as an internal standard in each sample.

Quantification of biomass

Biomass accumulation was quantified by cell dry weight (CDW) determination. The cells were harvested and washed twice in PBS as described in the vitamin K2 extraction protocol. Water content in the cell pellets was evaporated at 80 °C for 48 - 72 hours. The dried biomass was then weighed.

Determination of growth rate

Overnight cultures of bacteria in GM17 media, incubated statically at 30 °C were diluted in fresh GM17 to an optical density (OD) value of 0.2 measured at 600 nm. The diluted cultures were incubated statically at specific temperatures. The OD_{600} were measured every 30 min for in total 6 hours. Growth rates were calculated by plotting the natural logarithm values of the OD_{600} values; slopes of the linear range from each plot were used to determine the specific growth rates.

Data analysis

HPLC-MS data was processed in MassLynx software (Waters). Quantities of MK-5 and MK-6 were estimated using the formulas derived from MK-4 and MK-7 calibration curves, respectively; quantities of MK-8 and MK10 were estimated using the formula derived from MK-9 calibration curve. Where applicable, the peak areas in samples were corrected based on the measurement of vitamin K1 internal standards.

Vitamin K2 levels were presented in specific concentrations and titers. Specific concentrations were obtained by calculating total vitamin K2 (MK-5 to MK-10) content per unit biomass (nmol/mg CDW) while titers were obtained by calculating total vitamin K2 content per volume medium that was used to harvest the biomass (nmol/mL medium). In fold change calculations the control group was in all cases *L. lactis* MG1363 cultivated in GM17 media, statically at 30 °C for 48 hours.

Statistical significance analysis was performed in IBM SPSS Statistics (version 23) using one-way or two-way analysis of variance (ANOVA). Original values of measurement were used for ANOVA. Homogeneity of variance was examined using Levene's test ($\alpha = 0.05$). Unless stated otherwise, the post hoc multiple comparisons were conducted using Dunnett test (2-sided) and in all cases the control group was *L. lactis* MG1363 cultivated in GM17 media, statically at 30 °C for 48 hours (*, $P \leq 0.05$; **, $P \leq 0.01$; ***, $P \leq 0.001$).

Results

Strain diversity in vitamin K2 production

To reveal the natural capacity of vitamin K2 production in different LAB strains, we examined MK forms and levels in strains *of L. lactis* ssp. *lactis, L. lactis* ssp. *cremoris* and *Lc. mesenteroides* (Fig. 3.1). Strains of *L. lactis* ssp. *lactis* and *L. lactis* ssp. *cremoris* produced vitamin K2 in the form of MK-5 to MK-10 (Fig. 3.1C). MK-9 was the most abundant followed by MK-8. Among the *L. lactis* strains, large diversity of vitamin K2 producing capacity was demonstrated by the specific concentrations: *L. lactis* ssp. *cremoris* MG1363 and *L. lactis* ssp. *lactis* FM03 produced the highest amount of vitamin K2, reaching 125 nmol/g CDW; *L. lactis* ssp. *cremoris* DSM20481 produced the lowest amount, 13 nmol/g CDW (Fig. 3.1A). The strain diversity was also evident as reflected by the titers (Fig. 3.1B). *L. lactis* ssp. *cremoris* MG1363 showed the highest titer of about 95 nmol/L medium while *L. lactis* ssp.

lactis DSM20481 showed the lowest titer of 7 nmol/L medium. *Lc. mesenteroides* strains FM06 and DSM20343 did not produce detectable amounts of vitamin K2. *Lc. mesenteroides* FM08 produced a very low amount: about 3 nmol/g CDW in specific concentration and 2.5 nmol/L medium in titer (Fig. 3.1A & B). The MK composition produced in *Lc. mesenteroides* FM08 was also different from *L. lactis*: MK-10 was the major form followed by MK-9, and MK-5 to MK-8 in low abundance (Fig. 3.1C). Since *L. lactis* ssp. *cremoris* MG1363 produced the highest specific concentrations and titers of vitamin K2 in the tested conditions, this strain was selected for more detailed studies.

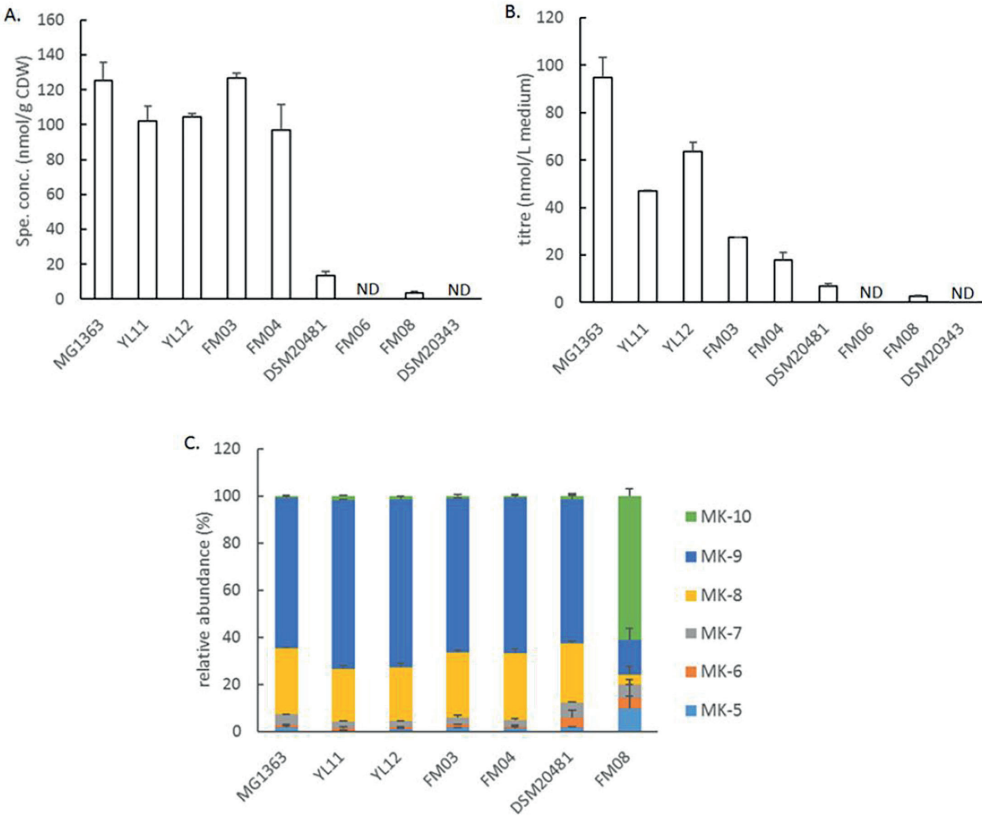

Figure 3.1. Vitamin K2 production in different LAB strains. (A) Specific concentrations of total vitamin K2. (B) Titers of total vitamin K2. (C) Relative abundance of MKs. MG1363, YL11 and YL12 are *L. lactis* ssp. *cremoris* strains; FM03, FM04 and DSM20481 are *L. lactis* ssp. *lactis* strains; FM06, FM08 and DSM20343 are *Lc. mesenteroides* strains. *L. lactis* strains were cultivated in GM17 and *Lc. mesenteroides* in MRS media, all statically incubated at 30 °C for 48 h. Values shown are from averages of biological triplicates for MG1363 and duplicates for the other strains. Error bars represent standard errors of the means (SEMs).

Effect of temperature on vitamin K2 production

L. lactis ssp. *cremoris* MG1363 was cultivated at different temperatures and the MK levels and forms were measured (Fig. 3.2). Significant differences were observed for specific concentrations ($P = 0.001$) and titers ($P < 0.001$) as a result of varied temperatures. At 30 °C and 33.5 °C, the specific concentrations and titers were the highest, about two-times higher than the lowest values obtained at 37 °C (Fig. 3.2A & B). The relative abundance of different MK-n forms also changed under altered temperatures (Fig. 3.2C), and from 20 °C to 37 °C, the relative abundance of MK-9 gradually decreased from 80% to 50%, while other shorter-chained forms, i.e. MK-5 to MK-8, increased.

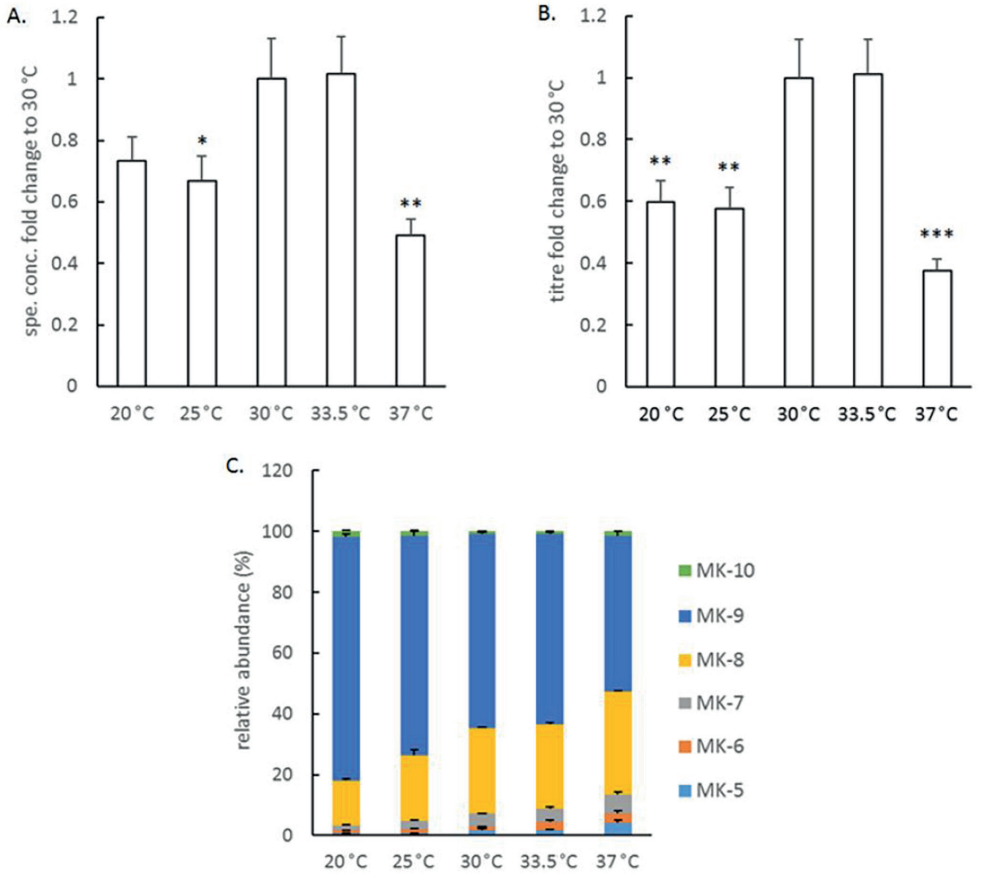

Figure 3.2. Effect of temperature on vitamin K2 production in *L. lactis* ssp. *cremoris* MG1363. (A) Fold changes in specific concentrations with respect to the control group (30 °C). (B) Fold changes in titers with respect to the control group (30 °C). (C) Relative abundance of MKs. Strain MG1363 was cultivated in GM17, statically incubated for 48 h at indicated temperature. Values shown are from averages ± SEMs of biological triplicates. For Dunnett test (2-sided) the control group was 30 °C (*, $P \leq 0.05$; **, $P \leq 0.01$; ***, $P \leq 0.001$).

Impact of carbon sources on vitamin K2 production

To examine the effect of carbon source on vitamin K2 production, *L. lactis* ssp. *cremoris* MG1363 was cultivated in M17 supplemented with different carbon sources and the MK levels and forms were measured (Fig. 3.3). Significant differences in specific concentrations and titers of vitamin K2 production were observed ($P = 0.021$ and $P < 0.000$ respectively) as a result of the varied carbon source supplementation. Fructose, trehalose, maltose and mannitol all resulted in an approximately 1.8-fold increase in specific concentrations compared to glucose (Fig. 3.3A). A similar increase in titers was also observed for the above mentioned carbon sources, with the exception of trehalose which resulted in a 2.4-fold increase compared to glucose (Fig. 3.3B). The relative abundance of different MKs was slightly influenced by the carbon source (Fig. 3.3C). Mannitol and galactose resulted in the lowest relative abundance of MK-9, ~60%, while mannose resulted in the highest MK-9 abundance, ~70%. Glucose, fructose, trehalose and maltose resulted in similar MK compositions, with ~65% MK-9.

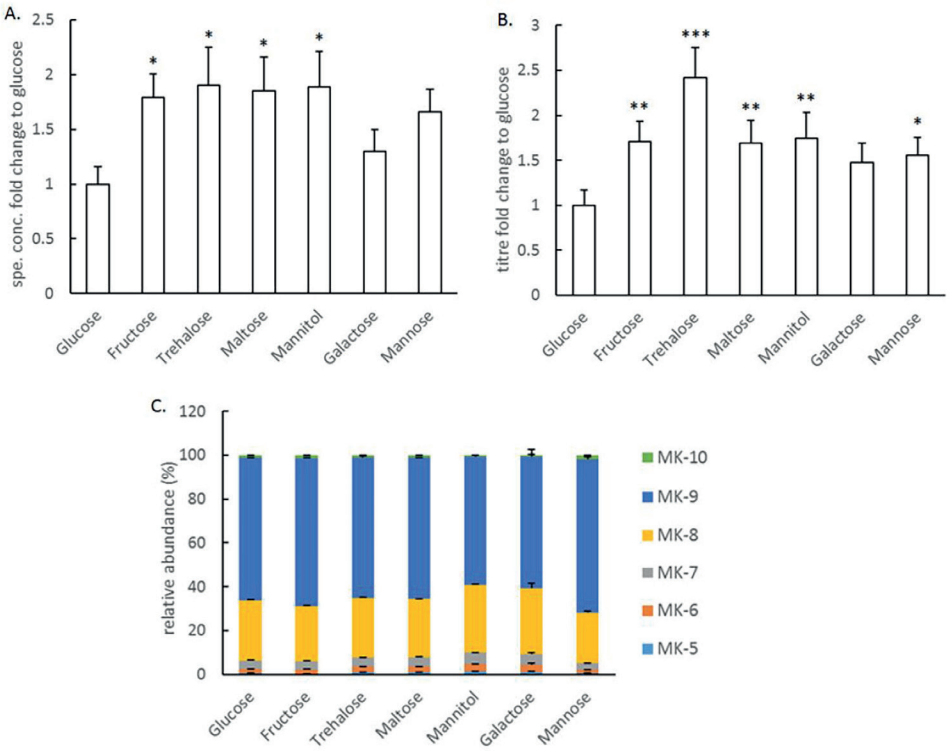

Figure 3.3. Effect of carbon source on vitamin K2 production in *L. lactis* ssp. *cremoris* MG1363. (A) Fold changes in specific concentrations with respect to the control group (glucose). (B) Fold changes in titers with respect to the control group (glucose). (C) Relative abundance of MKs. Strain MG1363 was cultivated in M17 supplemented with indicated carbon source, statically incubated at 30 °C for 48 h. Values shown are from averages ± SEMs of biological triplicates. For Dunnett test (2-sided) the control group was glucose (*, $P \leq 0.05$; **, $P \leq 0.01$; ***, $P \leq 0.001$).

Aerobic cultivation leads to elevated vitamin K2 levels

To examine the effect of aeration and respiratory metabolism on vitamin K2 production, *L. lactis* ssp. *cremoris* MG1363 was cultivated under conditions of static fermentation, aerobic fermentation and aerobic respiration. Specific concentrations as well as titers differed significantly among these three conditions ($P = 0.034$ and $P < 0.000$ respectively). Aerobic fermentation resulted in a 1.9-fold increase in specific concentration, and a 2.8-fold increase in titer compared to static fermentation (Fig. 3.4A & B). Aerobic respiration resulted in a 4-fold increase in titer compared to static fermentation. Aerobic fermentation resulted in a shift towards longer-chained MKs (25% MK-8, 67% MK-9 and 3% MK-10) in comparison to static fermentation (31% MK-8, 58% MK-9 and 1% MK-10) (Fig. 3.4C), and similar MK compositions were found with aerobic respiration.

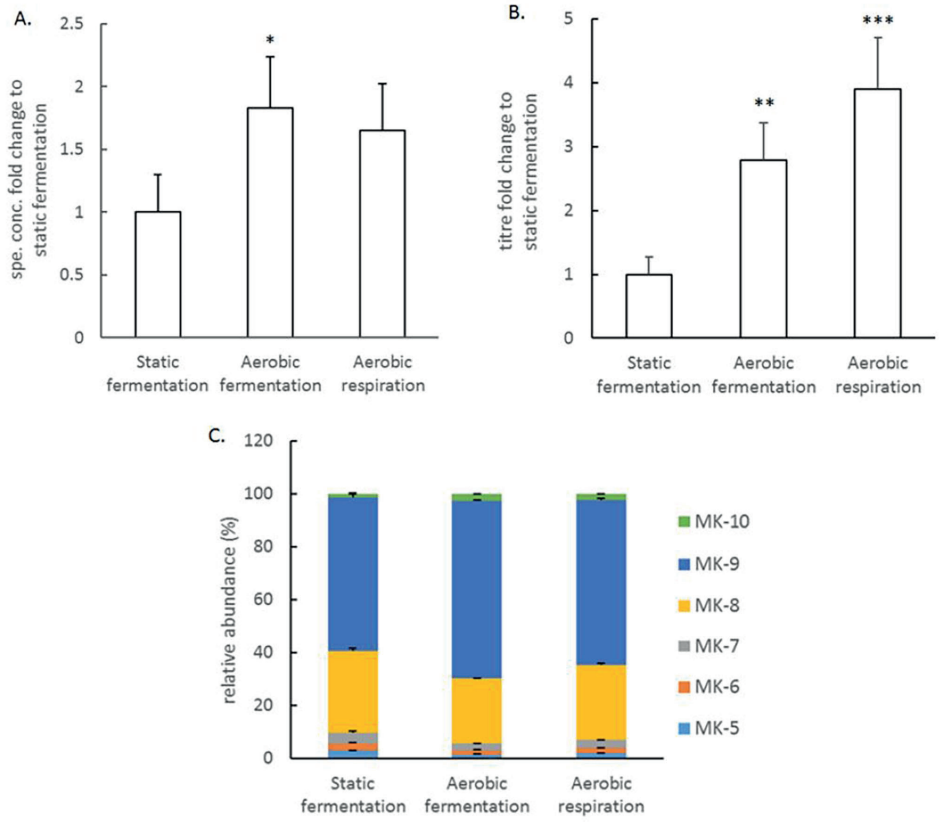

Figure 3.4. Effect of aeration and respiration on vitamin K2 production in *L. lactis* ssp. *cremoris* MG1363. (A) Fold changes in specific concentrations with respect to the control group (static fermentation). (B) Fold changes in titers with respect to the control group (static fermentation). (C) Relative abundance of MKs. Strain MG1363 was cultivated in GM17 at 30 °C for 48 h. For static fermentation, full tube of culture was statically incubated. For aerated fermentation, bacterial culture was incubated in flasks with head space, shaken at 120 rpm. For respiration, bacterial culture was incubated in flasks with head space, shaken at 120 rpm and with 2 µg/mL heme added. Values shown are from averages ± SEMs of biological triplicates. For Dunnett test (2-sided) the control group was static fermentation (*, $P \leq 0.05$; **, $P \leq 0.01$; ***, $P \leq 0.001$).

The effect of degree of aeration on vitamin K2 production was further examined by cultivating bacteria at different shaking speeds. Aerobic fermentation at all three tested shaking speeds resulted in increased vitamin K2 specific concentrations and titers (Fig. 3.5A & B). The highest amount was obtained at 60 rpm, 2.8-fold increase in specific concentration and 4.3-fold increase in titer compared to static fermentation, followed by 200 rpm and 120 rpm. The values obtained at 60 rpm were also significantly higher compared to aeration at 120 rpm (Tukey HSD P = 0.037 and P = 0.006), but not compared to 200 rpm (Tukey HSD P = 0.595 and P = 0.322). The relative abundances of MKs were identical in aerated conditions with all three tested shaking speeds, all resulted in a shift towards longer-chained MKs compared to static fermentation (Fig. 3.5C).

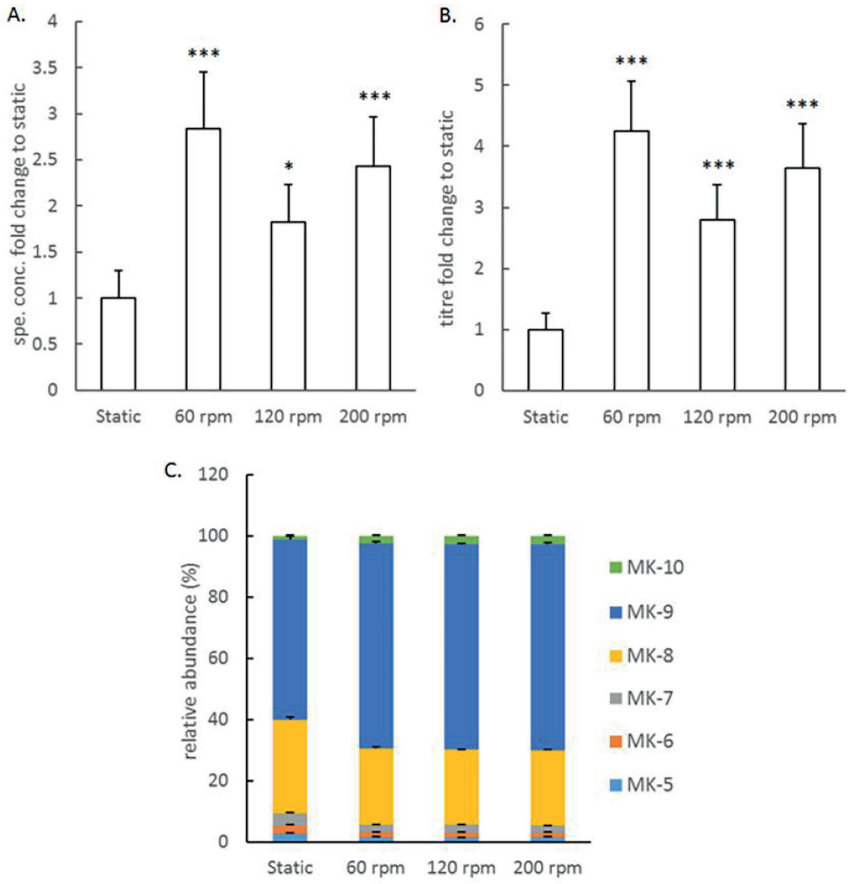

Figure 3.5. Effect of degree of aeration on vitamin K2 production in *L. lactis* ssp. *cremoris* MG1363. (A) Fold changes in specific concentrations with respect to the control group (static fermentation). (B) Fold changes in titers with respect to the control group (static fermentation). (C) Relative abundance of MKs. Strain MG1363 was cultivated in GM17 at 30 °C for 48 h. For static fermentation, full tube of culture was statically incubated. For aerated fermentation, bacterial culture was incubated in flasks with head space, shaken at indicated speeds. Values shown are from averages ± SEMs of biological triplicates. For Dunnett test (2-sided) the control group was static (*, P ≤ 0.05; **, P ≤ 0.01; ***, P ≤ 0.001).

Effect of aerobic cultivation on vitamin K2 production is carbon source-dependent

Observing that aerobic cultivations (aerobic fermentation and aerobic respiration) lead to increased vitamin K2 production when glucose was the carbon source, we further examined whether the same effect remained when other carbon sources such as fructose and trehalose were used. The effects of carbon source and aerobic cultivation were analyzed by two-way ANOVA. A significant main effect of carbon source was observed ($P < 0.000$ for specific concentration, $P = 0.001$ for titer), and so was a significant main effect of aerobic cultivation ($P = 0.002$ for specific concentration, $P = 0.001$ for titer). Moreover, a significant interaction between carbon source and aerobic cultivation was found ($F(4, 21) = 4.804$, $P = 0.007$ for specific concentration; $F(4, 21) = 7.719$, $P = 0.001$ for titer). When fructose was the carbon source, the specific concentration and titer were both highest with aerobic fermentation while aerobic respiration resulted in similar level as static fermentation; when trehalose was the carbon source, aerobic respiration resulted in lower vitamin K2 production than static and aerobic fermentation (Fig. 3.6A & B). Comparing all combinations, aerobic fermentation with fructose resulted in the highest specific concentration, i.e., a 3.7-fold increase compared to static fermentation with glucose. Aerobic fermentation with trehalose resulted in the highest titer, 5.2-fold compared to the same control group. The change in relative abundance of MKs in the three carbon sources across different conditions were similar: static fermentation resulted in the lowest abundance of MK-9, MK-10 and highest abundance of MK-8; a shift towards longer-chained MKs was observed in aerobic respiration and further in aerobic fermentation (Fig. 3.6C).

Vitamin K2 fortification in quark

Quark products were made from pasteurized milk using *L. lactis* ssp. *cremoris* MG1363 as the starter culture. We varied carbon sources and aeration conditions for making the pre-cultures, as well as the carbon sources and temperatures in quark fermentation. All quark samples showed pH values around 4.9. All quark samples were fortified with vitamin K2 compared to unfermented milk (1.4 ± 0.1 ng/g), with MK-7 to MK-10 being the detectable forms (Table 3.1). Fermentation at 30 °C (B, 72.1 ± 12.9 ng/g) resulted in a 61% increase of total vitamin K2 content in the quark samples compared to fermentation at 20 °C (A, 44.9 ± 10.6 ng/g). Under the same pre-culturing condition, using fructose as a carbon source for fermentation, we found an 18% to 73% increase in the vitamin K2 content in quark samples compared to using glucose as the carbon source (B vs. C, D vs. E and F vs. G). Moreover, the use of aerated pre-cultures resulted in 35% to 79% increased vitamin K2 content in quark samples compared to static pre-cultures (D vs. F, E vs. G).

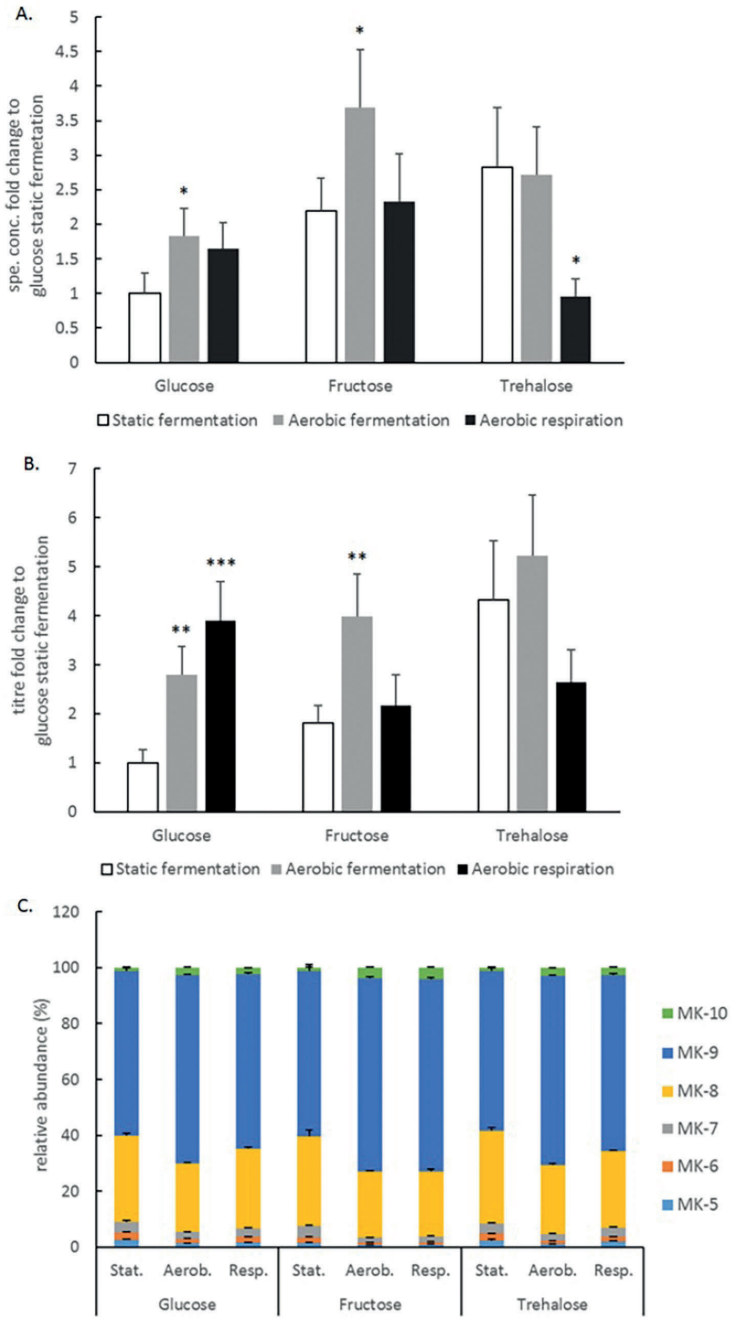

Figure 3.6. Effect of carbon source and aeration/respiration on vitamin K2 production in *L. lactis* MG1363. (A) Fold changes in specific concentrations with respect to glucose, static fermentation. (B) Fold changes in titers with respect to glucose, static fermentation. (C) Relative abundance of MKs. Strain MG1363 was cultivated in M17 with indicated carbon source at 30 °C for 48 h. For static fermentation, full tube of culture was statically incubated.

For aerated fermentation, bacterial culture was incubated in flasks with head space, shaken at 120 rpm. For respiration, bacterial culture was incubated in flasks with head space, shaken at 120 rpm and with 2 µg/mL heme added. Values shown are from averages ± SEMs of biological triplicates. Dunnett test (2-sided) was performed within each carbon source group, and the control groups were in all cases static fermentation (*, P ≤ 0.05; **, P ≤ 0.01; ***, P ≤ 0.001).

Table 3.1. Vitamin K2 content in quark samples.

No.[1]	Pre-culture		Quark		MK-7	MK-8	MK-9	MK-10	Total VK2
	C source[2]	Aeration	C source	Temp.[3]	(ng/g of quark; means ± SEMs[4])				
A	glucose	no	glucose	20 °C	0.8 ± 0.3	5.4 ± 0.8	36.7 ± 10.0	0.4 ± 0.1	44.9 ± 10.6
B	glucose	no	glucose	30 °C	1.0 ± 0.3	16.0 ± 5.8	52.1 ± 8.6	1.5 ± 1.2	72.1 ± 12.9
C	glucose	no	fructose	30 °C	1.0 ± 0.3	16.2 ± 2.2	64.8 ± 8.2	1.0 ± 0.5	85.0 ± 10.3
D	fructose	no	glucose	30 °C	0.7 ± 0.2	7.5 ± 1.5	36.3 ± 10.4	1.8 ± 1.1	48.8 ± 13.0
E	fructose	no	fructose	30 °C	2.0 ± 0.5	18.8 ± 5.2	59.9 ± 9.6	0.9 ± 0.4	84.4 ± 15.6
F	fructose	yes	glucose	30 °C	1.9 ± 0.3	15.9 ± 3.3	64.9 ± 5.8	1.4 ± 0.1	87.3 ± 9.1
G	fructose	yes	fructose	30 °C	1.7 ± 0.4	18.9 ± 4.8	88.1 ± 8.8	2.6 ± 1.1	1.8 ± 9.8

[1]Each combination of cultivation condition was given a number for easy reference in the text.

[2]Carbon source.

[3]Temperature.

[4]All conditions was tested in biological triplicates, except for B which was in duplicate.

Discussion

Long-chain vitamin K2 production in LAB is of interest for food industry, but there has not been much effort made to optimize conditions for vitamin K2 production and to elucidate the influencing environmental factors. In this study we examined the levels and forms of MKs (MK-5 to MK-10) from different LAB strains, and the influence of cultivation conditions. In our study, the levels of total vitamin K2 production are expressed as specific concentrations (in nmol vitamin K2 per mg cell dry weight). The values of specific concentrations show the natural vitamin K2 producing capacity of bacteria and may provide insights into the bacterial physiology related to the synthesis of these membrane-embedded menaquinones. Titers were derived from the amount of vitamin K2 recovered from the biomass harvested from the culture medium, expressed as nmol vitamin K2/mL medium, and therefore showed a combined effect of vitamin K2 accumulation in the cells and biomass accumulation in the media. The values of titers provide clear information on the product output for a certain amount of medium/material input, and therefore is of strong industrial interest.

We screened *L. lactis* ssp. *cremoris*, *L. lactis* ssp. *lactis* and *Lc. mesenteroides* strains, as these LAB (sub)species are known to possess the complete set of genetic elements for menaquinone synthesis (Pedersen et al., 2012) and are frequently used in food fermentation processes. From each (sub)

species, the prototype (MG1363) or type strain (DSM20481, DSM20343), together with two other strains isolated from fermented foods, were selected to show a representative picture of the diversity among vitamin K2-producing LAB species and strains. Comparative analysis of vitamin K2 production showed that the specific concentrations and titers of the six selected *L. lactis* strains varied largely, demonstrating a wide strain diversity in the natural vitamin K2 producing capacity (Fig. 3.1A & B). The specific concentration values were in the same order of magnitude as reported previously for *L. lactis* (Morishita et al., 1999). It is also clear that specific concentrations and titers may not show the same trend. As vitamin K2 is cell membrane-associated, the titer is not only determined by specific concentrations but also biomass yield. For example, strain FM03 showed one of the highest specific concentrations but its titer value was among the lowest due to its low biomass accumulation in the culture media (supplementary Fig. S3.1). We detected no significant amounts of vitamin K2 in *Lc. mesenteroides* FM06 and DSM20343 and only very minor amounts in FM08 in the tested conditions. Although a complete set of menaquinone-synthesis genes have been identified in *Lc. mesenteroides*, Brooijmans et al. (2009) also observed the discrepancy that they could not induce respiratory growth in the tested *Lc. mesenteroides* strain.

Analysis of the relative abundance of long-chain MKs in *L. lactis* strains showed very similar distributions, and MK-8 and MK-9 were found to be the most abundant (Fig. 3.1C). The minor amount of vitamin K2 produced by *Lc. mesenteroides* strain FM08 was found to contain MK-10 as the major form. Given the large strain diversity, strain selection can be an efficient first step towards improved vitamin K2 fortification in fermented foods or food supplements. Both high vitamin K2 producing capacity and high biomass accumulation under selected cultivation conditions should be criteria for strain selection to achieve vitamin K2 fortification. For this reason, we selected prototype strain *L. lactis* MG1363, which showed both high specific concentration and high titer, to further analyze the impact of selected cultivation parameters on vitamin K2 production in *L. lactis*.

Using *L. lactis* MG1363 as the model strain, we demonstrated that vitamin K2 production is influenced by temperature, carbon source, aeration and mode of energy metabolism. Temperature influenced both the total amount and relative abundance of different long-chain MK forms in MG1363. At 30 °C to 33.5 °C the specific concentrations and titers were the highest (Fig. 3.2A & B), temperatures above or below this range resulted in lower vitamin K2 production. As the temperature increased from 20 °C to 37 °C, MK-8 became more abundant and MK-9 less (Fig. 3.2C). This could be caused by the influence of temperature on the activity of the enzyme that controls the isoprenoid side chain elongation during menaquinone synthesis. As MKs are membrane embedded, their relative abundance could also be influenced by the dynamics in biomass accumulation, including the growth rate (supplementary Table S3.2), composition of lipids and fatty acid side chains, and membrane fluidity, which are all affected by temperature.

The impact of different carbon sources on vitamin K2 production was also significant. Fructose, trehalose, maltose and mannitol all resulted in about 2-fold increase of vitamin K2 production

compared to glucose (Fig. 3.3A & B). Trehalose stood out for the highest titer level, as it also lead to the highest biomass accumulation (supplementary Fig. S3.3). This is one of the first studies to examine the effect of using trehalose for metabolite production in LAB. Our study demonstrates a positive effect of various carbon sources compared to glucose, on vitamin K2 production in *L. lactis*.

Vitamin K2 is known for its function as electron carrier in the bacterial ETC, and *L. lactis* can switch to respiratory metabolism when both oxygen and heme are supplied (Brooijmans et al., 2009). Moreover, the presence of oxygen alone has impact on metabolism by altering the balance of redox cofactors, as well as expression and activity of key enzymes (Nordkvist et al., 2003). Therefore, it was highly relevant to examine whether vitamin K2 production was influenced by aeration only (fermentation under aerobic conditions) and respiratory metabolism (aerobic respiration). We demonstrated production of MK-5 to MK-10 under static fermentation, aerobic fermentation and aerobic respiration conditions, and a shift towards longer chained MKs under the two aerobic conditions (Fig. 3.4). This is in agreement with the study from Brooijmans et al. (2009) regarding the quantity of MK-5 to MK-10. We observed increased specific concentrations of MK-5 to MK-10 under both aerobic conditions compared to static fermentation, which could suggest specific roles of long-chain MKs in aerobic conditions. Moreover, as the increase was observed for both aerobic fermentation and aerobic respiration, it is likely that MK production responded to oxygen, and not necessarily a functional respiratory ETC. A transcriptomic analysis (Cretenet et al., 2014) also revealed that the first gene in menaquinone-synthesis pathway, *menF*, is upregulated by 2.7-fold during the early stage of cultivation under oxygen condition compared to anaerobic condition in MG1363. A previous study (Pedersen et al., 2008) also detected up-regulation of another menaquinone-synthesis enzyme, *menB*, under aerobic condition compared to static cultivation in a *L. lactis* strain. Increased activity of the menaquinone-synthesis pathway could explain the increased vitamin K2 content in aerobically cultivated *L. lactis* MG1363 cells. The increase of MK production was even more obvious in terms of titers, since besides higher specific concentrations, the biomass accumulations in aerobic fermentation and aerobic respiration were also higher than in static fermentation (supplementary Fig. S3.4). A higher biomass yield under aerobic conditions was also reported, and it was proposed that this was because of less energy limitation for biomass synthesis (Nordkvist et al., 2003). Respiratory metabolism is known to enhance the growth efficiency in *L. lactis* (Brooijmans et al., 2009), and indeed we obtained the highest biomass accumulation with aerobic respiration, reaching a more than 2-fold increase compared to static fermentation.

When we further examined the aerobic fermentation conditions by applying different degree of aeration, we observed that all aerobic fermentation conditions clearly resulted in enhanced vitamin K2 production compared to static fermentation (Fig. 3.5A & B), and the enhancement did not seem to be a function of the degree of aeration.

When the effects of aeration and respiratory metabolism were examined with carbon sources other than glucose, differences in response were observed (Fig. 3.6A & B). With fructose as the carbon source, aerobic fermentation resulted in the highest vitamin K2 production, while aerobic respiration

was similar to static fermentation. When trehalose was used, aerobic fermentation resulted in similar level as static fermentation, while aerobic respiration resulted in much lower vitamin K2 production. Therefore, the effect of aerobic fermentation and aerobic respiration on vitamin K2 production was found to be carbon source-dependent. It was found to be consistent though, for all 3 carbon sources tested, the biomass accumulation was highest under aerobic respiration, followed by aerobic fermentation, and lowest under static fermentation (supplementary Fig. S3.6). The MK profile also reflected that for all 3 carbon sources, aerated conditions lead to a shift towards longer chained MKs compared to static fermentation (Fig. 3.6C).

The reason why each carbon source or cultivation condition influenced vitamin K2 production in this way remains to be elaborated. As a secondary metabolite, the metabolic fluxes towards vitamin K2 are complicated with a variety of enzymatic reactions involved. The flux towards chorismate, which is the first compound in menaquinone biosynthesis pathway, could be influenced by the central carbon metabolism. As different carbon sources are taken up, converted and directed to the central carbon metabolism, the conversion rate, energy transduction, redox factor regeneration and regulation of the sugar catabolism all vary (Neves et al., 2005; Kowalczyk and Bardowski, 2007). This could globally explain why the amount of vitamin K2 production in *L. lactis* responded to aeration as well as respiration in a carbon source-dependent manner. A series of genes are required for menaquinone synthesis, some dedicated to the naphthoquinone synthesis, some to the elongation of the isoprenoid tail. Together, they influence the quantity and composition of the menaquinone pool. However, to date, regulations of these genes under different conditions have been hardly investigated (Miller et al., 1988), and little is known about feedback regulation in this pathway, especially in LAB. A mechanistic explanation for the response towards each specific carbon source or cultivation condition requires further studies and the construction of a comprehensive metabolic model.

We further demonstrated that the obtained knowledge can be transferred to food fermentation processes by fortifying quark with vitamin K2. Consistently, cultivation temperature of 30 °C, altered carbon source (fructose) and aerobic cultivation of the pre-culture, resulted in higher vitamin K2 content in the quark product.

The insights obtained from this study show a proof of principle that strain selection and combination of favorable cultivation parameters, namely temperature, aeration, carbon source and mode of energy metabolism, can contribute to improved production of long-chain vitamin K2 in LAB strains. As hydrophobic, membrane-embedded compounds, menaquinones are not produced extracellularly and continuously, but remain cell-associated in all producing bacteria. Nevertheless, simple and efficient procedures are being continuously developed and optimized for extracting vitamin K2 and other valuable cell-associated molecules from biomass (Wei et al., 2018; Chronopoulou et al., 2019; Fang et al., 2019), that, together with the knowledge obtained from this study, will facilitate the biotechnological production of long-chain vitamin K2.

The effect of different carbon sources also demonstrate the potential of long-chain vitamin K2 fortification during fermentation of different raw food materials, enabling utilization of low-value substrates in industrial processes or development of vitamin K2-enriched fermentation-based food products as exemplified in the current study with the production of vitamin K2-fortified quark. Since vegetables like cabbage (Hughes and Lindsay, 1985), beetroots and carrots (Dolores Rodríguez-Sevilla et al., 1999) contain high levels of fructose, they could serve as excellent sources for *in situ* vitamin K2 fortification through fermentation with selected LAB.

Conclusion

In this study, we demonstrated a large species and strain diversity in LAB for vitamin K2 producing capacity. Furthermore, the influence of relevant cultivation conditions on vitamin K2 production in *L. lactis* MG1363 has been studied in detail. We concluded that vitamin K2 production is already significantly affected when a single factor among temperature, carbon source, aeration and mode of metabolism, is changed. The highest specific concentration of vitamin K2 was achieved under aerobic fermentation with fructose, reaching 3.7-fold increase compared to static fermentation with glucose; the highest titer was found under aerobic respiration with trehalose, reaching 5.2-fold increase compared to static fermentation with glucose. The ratios of MK-8 to MK-10 increased in response to aerobic cultivations. Knowledge obtained from this study can contribute to biotechnological production of vitamin K2 supplements as well as to strategies for natural enrichment of vitamin K2 in fermented foods, and together with further studies lead to better understanding of the regulation of vitamin K2 production and its role in LAB metabolism and physiology.

Acknowledgements

The work described in this article was subsidized by the Netherlands Organization for Scientific Research (NWO) through the Graduate Program on Food Structure, Digestion and Health.

The authors would like to express their gratitude towards Tina Zuidema (BU Veterinary Drugs, RIKILT, Wageningen University and Research) for her support and assistance in developing and performing the HPLC analysis. We also thank master student Daniel Román Pizarro (Food Microbiology, Wageningen University) for his contribution in the trial experiments for this study.

Supplementary materials

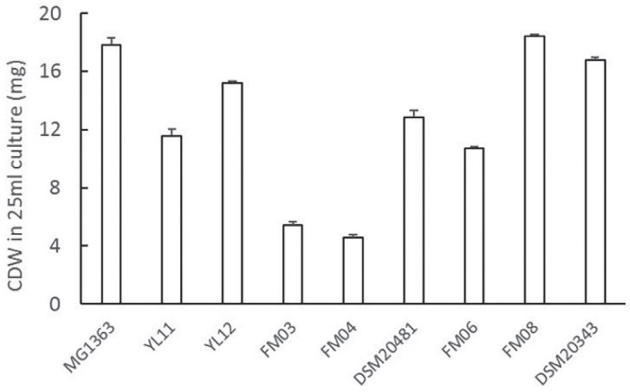

Figure S3.1. Biomass accumulation in different LAB strains. *L. lactis* strains were cultivated in GM17 and *Leu. mesenteroides* in MRS media, all statically incubated at 30 °C for 48 h. Values shown are from averages of biological triplicates for MG1363 and duplicates for the other strains. Error bars represent standard errors (SEs).

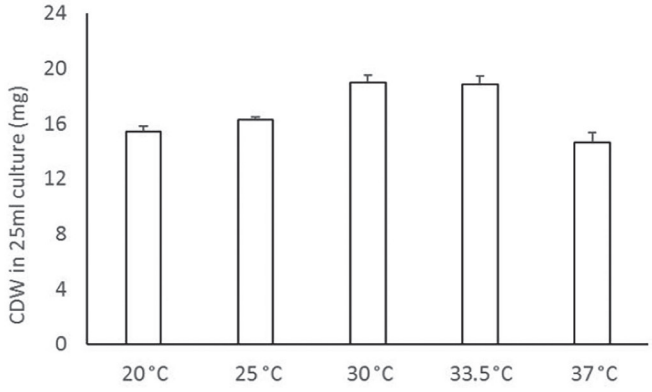

Figure S3.2. Effect of temperature on biomass accumulation in *L. lactis* ssp. *cremoris* MG1363. Strain MG1363 was cultivated in GM17, statically incubated for 48 h at indicated temperature. Values shown are from averages ± SEs of biological triplicates.

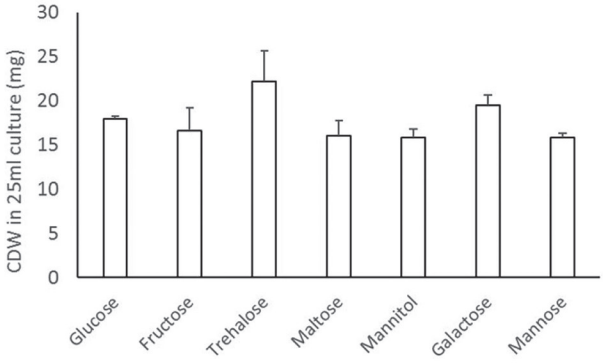

Figure S3.3. Effect of carbon source on biomass accumulation in *L. lactis* ssp. *cremoris* MG1363. Strain MG1363 was cultivated in M17 supplemented with indicated carbon source, statically incubated at 30 °C for 48 h. Values shown are from averages ± SEs of biological triplicates.

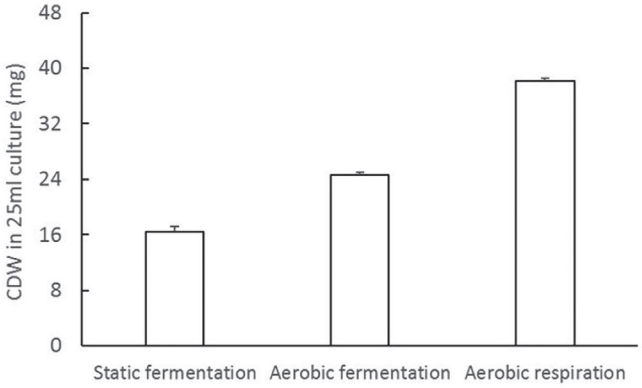

Figure S3.4. Effect of aeration and respiration on biomass accumulation in *L. lactis* ssp. *cremoris* MG1363. Strain MG1363 was cultivated in GM17 at 30 °C for 48 h. For static fermentation, full tube of culture was statically incubated. For aerated fermentation, bacterial culture was incubated in flasks with head space, shaken at 120 rpm. For respiration, bacterial culture was incubated in flasks with head space, shaken at 120 rpm and with 2 μg/mL hemin added. Values shown are from averages ± SEs of biological triplicates.

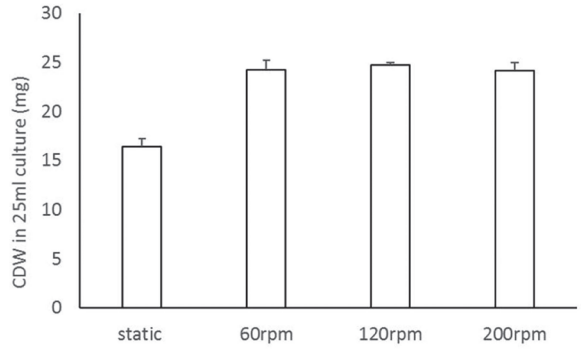

Figure S3.5. Effect of degree of aeration on biomass accumulation in *L. lactis* ssp. *cremoris* MG1363. Strain MG1363 was cultivated in GM17 at 30 °C for 48 h. For static fermentation, full tube of culture was statically incubated. For aerated fermentation, bacterial culture was incubated in flasks with head space, shaken at indicated speeds. Values shown are from averages ± SEs of biological triplicates.

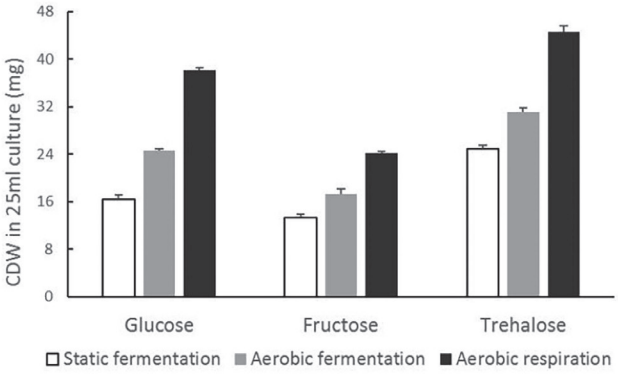

Figure S3.6. Effect of different carbon source and aeration/respiration on biomass accumulation in *L. lactis* ssp. *cremoris* MG1363. Strain MG1363 was cultivated in M17 with indicated carbon source at 30 °C for 48 h. For static fermentation, full tube of culture was statically incubated. For aerated fermentation, bacterial culture was incubated in flasks with head space, shaken at 120 rpm. For respiration, bacterial culture was incubated in flasks with head space, shaken at 120 rpm and with 2 μg/mL hemin added. Values shown are from averages ± SEs of biological triplicates.

Table S3.1. Details of MRM analysis.

Function	Molecule	Parent ion (Da)	Daughter ion (Da)	Collision energy (eV)
2	Vitamin K1	451.55	187.25	25.00
2	Vitamin K1	451.55	227.28	20.00
2	MK-5	513.37	187.25	25.00
2	MK-5	513.37	227.28	20.00
2	MK-6	581.44	187.25	25.00
2	MK-6	581.44	227.28	20.00
2	MK-7	649.76	187.25	25.00
2	MK-7	649.76	227.28	20.00
2	MK-8	717.56	187.25	25.00
2	MK-8	717.56	227.28	20.00
3	MK-9	785.72	187.25	35.00
3	MK-9	785.72	227.28	30.00
3	MK-10	853.69	187.25	35.00
3	MK-10	853.69	227.28	30.00

Different forms of MKs were detected in 3 functions. Dwell time was in all cases 0.08 s in function 1 and 2, and 0.10 s in function 3. Cone voltage was 30.00 V in all cases.

Table S3.2. Specific growth rate of *L. lactis* ssp. *cremoris* MG1363 at different temperatures.

Growth temperature (°C)	Growth rate (h^{-1})
20	0.54
25	0.72
30	0.87
37	1.07

Strain MG1363 was cultivated in GM17 at 30 °C with a starting OD = 0.2. Growth was followed by OD measurement for 5 hours, and maximum growth rates were determined for the exponential phase of each culture.

References

Berenjian, A., Mahanama, R., Talbot, A., Biffin, R., Regtop, H., Valtchev, P., et al. (2011). Efficient media for high menaquinone-7 production: response surface methodology approach. *N. Biotechnol.* 28, 665–672.

Berenjian, A., Mahanama, R., Talbot, A., Regtop, H., Kavanagh, J., and Dehghani, F. (2012). Advances in menaquinone-7 production by *Bacillus subtilis* natto: fed-batch glycerol addition. *Am. J. Biochem. Biotechnol.* 8, 105–110.

Berenjian, A., Mahanama, R., Talbot, A., Regtop, H., Kavanagh, J., and Dehghani, F. (2014). Designing of an intensification process for biosynthesis and recovery of menaquinone-7. *Appl. Biochem. Biotechnol.* 172, 1347–1357.

Beulens, J. W. J., Booth, S. L., Heuvel, E. G. H. M. van den, Stoecklin, E., Baka, A., and Vermeer, C. (2013). The role of menaquinones (vitamin K2) in human health. *Br. J. Nutr.* 110, 1357–1368.

Binda, S., and Ouwehand, A. C. (2019). "Lactic acid bacteria for fermented dairy products," in *Lactic Acid Bacteria*, eds. G. Vinderola, A. C. Ouwehand, S. Salminen, and A. von Wright (Boca Raton: CRC Press), 175–198.

Booth, S. L., Broe, K. E., Gagnon, D. R., Tucker, K. L., Hannan, M. T., McLean, R. R., et al. (2003). Vitamin K intake and bone mineral density in women and men. *Am. J. Clin. Nutr.* 77, 512–516.

Brooijmans, R., Smit, B., Santos, F., van Riel, J., de Vos, W. M., and Hugenholtz, J. (2009). Heme and menaquinone induced electron transport in lactic acid bacteria. *Microb. Cell Fact.* 8, 28.

Chollet, M., Guggisberg, D., Portmann, R., Risse, M.-C., and Walther, B. (2017). Determination of menaquinone production by *Lactococcus* spp. and propionibacteria in cheese. *Int. Dairy J.* 75, 1–9.

Chronopoulou, L., Bosco, C. D., Di Caprio, F., Prosini, L., Gentili, A., Pagnanelli, F., et al. (2019). Extraction of carotenoids and fat-soluble vitamins from tetradesmus obliquus microalgae: an optimized approach by using supercritical CO2. *Molecules* 24, 2581.

Collins, M. D., and Jones, D. (1981). Distribution of isoprenoid quinone structural types in bacteria and their taxonomic implication. *Microbiol. Rev.* 45, 316–54.

Cretenet, M., Le Gall, G., Wegmann, U., Even, S., Shearman, C., Stentz, R., et al. (2014). Early adaptation to oxygen is key to the industrially important traits of *Lactococcus lactis* ssp. *cremoris* during milk fermentation. *BMC Genomics* 15, 1054.

Dolores Rodríguez-Sevilla, M., Villanueva-Suárez, M. J., and Redondo-Cuenca, A. (1999). Effects of processing conditions on soluble sugars content of carrot, beetroot and turnip. *Food Chem.* 66, 81–85.

Fang, Z., Wang, L., Zhao, G., Liu, H., Wei, H., Wang, H., et al. (2019). A simple and efficient preparative procedure for menaquinone-7 from *Bacillus subtilis* (natto) using two-stage extraction followed by microporous resins. *Process Biochem.* 83, 183–188.

Fu, X., Harshman, S. G., Shen, X., Haytowitz, D. B., Karl, J. P., Wolfe, B. E., et al. (2017). Multiple vitamin K forms exist in dairy foods. *Curr. Dev. Nutr.* 1, e000638.

Fujita, Y., Iki, M., Tamaki, J., Kouda, K., Yura, A., Kadowaki, E., et al. (2012). Association between vitamin K intake from fermented soybeans, natto, and bone mineral density in elderly Japanese men: the Fujiwara-kyo Osteoporosis Risk in Men (FORMEN) study. *Osteoporos. Int.* 23, 705–714.

Furuichi, K., Hojo, K. ichi, Katakura, Y., Ninomiya, K., and Shioya, S. (2006). Aerobic culture of *Propionibacterium freudenreichii* ET-3 can increase production ratio of 1,4-dihydroxy-2-naphthoic acid to menaquinone. *J. Biosci. Bioeng.* 101, 464–470.

Gast, G. C. M., de Roos, N. M., Sluijs, I., Bots, M. L., Beulens, J. W. J., Geleijnse, J. M., et al. (2009). A high menaquinone intake reduces the incidence of coronary heart disease. *Nutr. Metab. Cardiovasc. Dis.* 19, 504–510.

Geleijnse, J. M., Vermeer, C., Grobbee, D. E., Schurgers, L. J., Knapen, M. H. J., van der Meer, I. M., et al. (2004). Dietary intake of menaquinone is associated with a reduced risk of coronary heart disease: The Rotterdam Study. *J. Nutr.* 134, 3100–3105.

Groenen-van Dooren, M. M. C. L., Ronden, J. E., Soute, B. A. M., and Vermeer, C. (1995). Bioavailability of phylloquinone and menaquinones after oral and colorectal administration in vitamin K-deficient rats. *Biochem. Pharmacol.* 50, 797–801.

Herrmann, K. M., and Weaver, L. M. (1999). The shikimate pathway. *Annu. Rev. Plant Physiol. Plant Mol. Biol.* 50, 473–503.

Hojo, K., Watanabe, R., Mori, T., and Taketomo, N. (2007). Quantitative measurement of tetrahydromenaquinone-9 in cheese fermented by propionibacteria. *J. Dairy Sci.* 90, 4078–4083.

Hughes, A., and Lindsay, R. C. (1985). Liquid chromatographic analysis of sugars and mannitol in cabbage and fermenting sauerkraut. *J. Food Sci.* 50, 1662–1667.

KEGG (2018). KEGG MODULE: M00022. Available at: https://www.genome.jp/kegg-bin/show_module?M00022 [Accessed December 2, 2018].

Kowalczyk, M., and Bardowski, J. (2007). Regulation of Sugar Catabolism in *Lactococcus lactis*. *Crit. Rev. Microbiol.* 33, 1–13.

Kurosu, M., and Begari, E. (2010). Vitamin K2 in electron transport system: are enzymes involved in vitamin K2 biosynthesis promising drug targets? *Molecules* 15, 1531–53.

Manoury, E., Jourdon, K., Boyaval, P., and Fourcassié, P. (2013). Quantitative measurement of vitamin K2 (menaquinones) in various fermented dairy products using a reliable high-performance liquid chromatography method. *J. Dairy Sci.* 96, 1335–1346.

Miller, P., Mueller, J., Hill, K., and Taber, H. (1988). Transcriptional regulation of a promoter in the men gene cluster of *Bacillus subtilis*. *J. Bacteriol.* 170, 2742–2748.

Morishita, T., Tamura, N., Makino, T., and Kudo, S. (1999). Production of menaquinones by lactic acid bacteria. *J. Dairy Sci.* 82, 1897–1903.

Neves, A. R., Pool, W. A., Kok, J., Kuipers, O. P., and Santos, H. (2005). Overview on sugar metabolism and its control in – The input from in vivo NMR. *FEMS Microbiol. Rev.* 29, 531–554.

Nordkvist, M., Jensen, N. B. S., and Villadsen, J. (2003). Glucose metabolism in *Lactococcus lactis* MG1363 under different aeration conditions: requirement of acetate to sustain growth under microaerobic conditions. *Appl. Environ. Microbiol.* 69, 3462–8.

Nowicka, B., and Kruk, J. (2010). Occurrence, biosynthesis and function of isoprenoid quinones. *Biochim. Biophys. Acta* 1797, 1587–1605.

Pedersen, M. B., Garrigues, C., Tuphile, K., Brun, C., Vido, K., Bennedsen, M., et al. (2008). Impact of aeration and heme-activated respiration on *Lactococcus lactis* gene expression: identification of a heme-responsive operon. *J. Bacteriol.* 190, 4903–4911.

Pedersen, M. B., Gaudu, P., Lechardeur, D., Petit, M.-A., and Gruss, A. (2012). Aerobic respiration metabolism in lactic acid bacteria and uses in biotechnology. *Annu. Rev. Food Sci. Technol.* 3, 37–58.

Rees, K., Guraewal, S., Wong, Y. L., Majanbu, D. L., Mavrodaris, A., Stranges, S., et al. (2010). Is vitamin K consumption associated with cardio-metabolic disorders? A systematic review. *Maturitas* 67, 121–128.

Sato, T., Schurgers, L. J., and Uenishi, K. (2012). Comparison of menaquinone-4 and menaquinone-7 bioavailability in healthy women. *Nutr. J.* 11, 93.

Schurgers, L. J., Teunissen, K. J. F., Hamulyák, K., Knapen, M. H. J., Vik, H., and Vermeer, C. (2007). Vitamin K-containing dietary supplements: comparison of synthetic vitamin K1 and natto-derived menaquinone-7. *Blood* 109, 3279–3283.

Schurgers, L. J., and Vermeer, C. (2002). Differential lipoprotein transport pathways of K-vitamins in healthy subjects. *Biochim. Biophys. Acta* 1570, 27–32.

Vermeer, C., and Schurgers, L. J. (2000). A comprehensive review of vitamin K and vitamin K antagonists. *Hematol. Oncol. Clin. North Am.* 14, 339–353.

Walther, B., Karl, J. P., Booth, S. L., and Boyaval, P. (2013). Menaquinones, bacteria, and the food supply: the relevance of dairy and fermented food products to vitamin K requirements. *Adv. Nutr.* 4, 463–73.

Wei, H., Zhao, G., Liu, H., Wang, H., Ni, W., Wang, P., et al. (2018). A simple and efficient method for the extraction and separation of menaquinone homologs from wet biomass of *Flavobacterium*. *Bioprocess Biosyst. Eng.* 41, 107–113.

Wen, L., Chen, J., Duan, L., and Li, S. (2018). Vitamin K-dependent proteins involved in bone and cardiovascular health. *Mol. Med. Rep.* 18, 3–15.


3

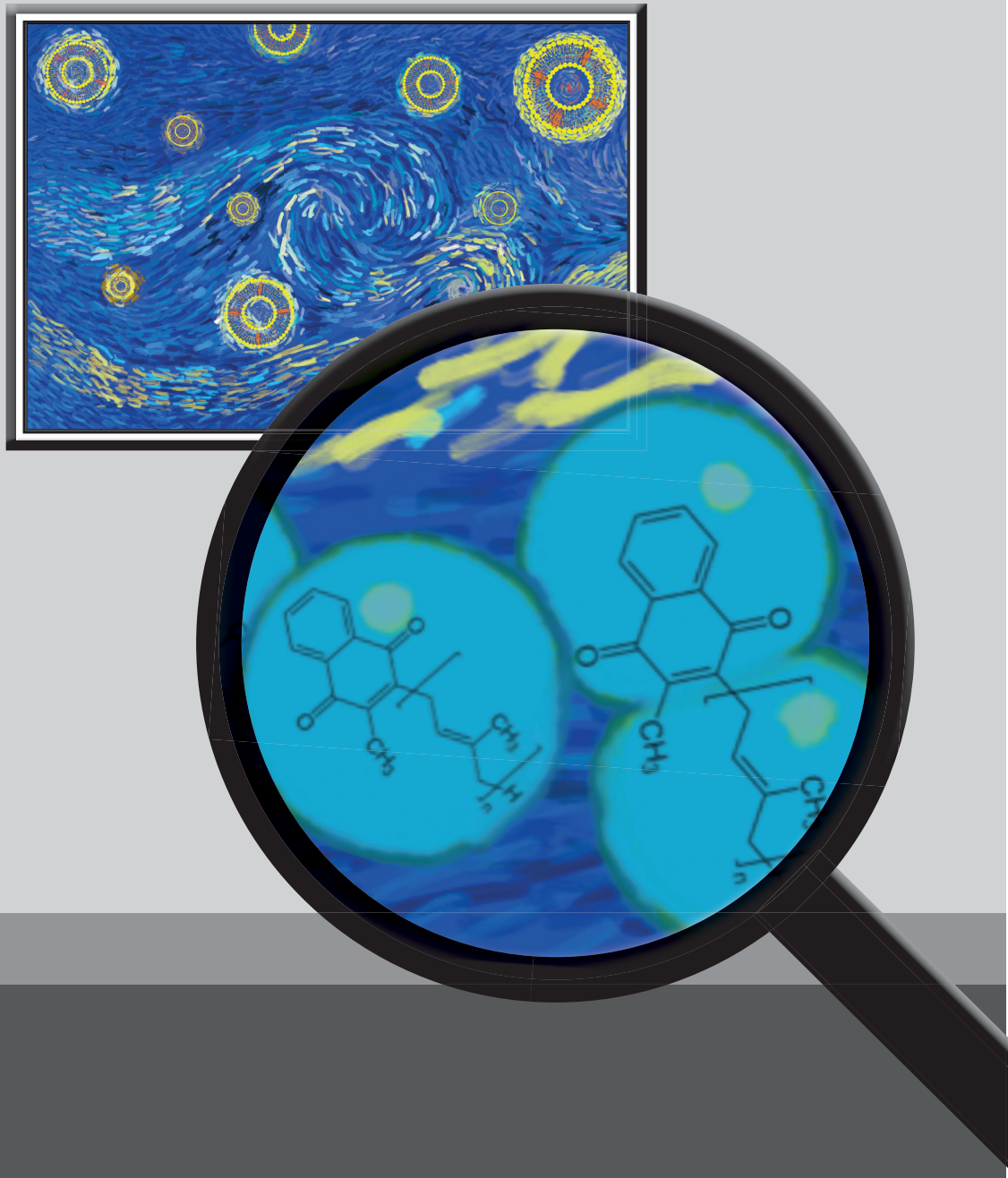

Chapter 4

Lactococcus lactis mutants obtained from laboratory evolution show elevated vitamin K2 content and enhanced resistance to oxidative stress

Yue Liu, Anteun de Groot, Sjef Boeren, Tjakko Abee & Eddy J. Smid

Published in
Frontiers in Microbiology, 2021, 12:746770

Abstract

Vitamin K2 is an important vitamin for human health. Vitamin K2 enrichment in the human diet is possible by using vitamin K2-producing bacteria such as *Lactococcus lactis* in food fermentations. Based on previous observations that aerated cultivation conditions improved vitamin K2 content in *L. lactis*, we performed laboratory evolution on *L. lactis* model strain MG1363 by cultivating it under vigorous shaking condition and transferred it every 72 hours to propagate in fresh medium. After 100 generations of propagation, we selected three evolved strains that showed improved stationary phase survival in oxygenated conditions.

In comparison to the original strain MG1363, the evolved strains showed 50% - 110% increased vitamin K2 content and exhibited high resistance against hydrogen peroxide-induced oxidative stress. Genome sequencing of the evolved strains revealed common mutations in the genes *ldh* and *gapB*. Proteomics analysis revealed overproduction of GapA, UspA2 and MutM under aerated conditions in evolved strains, proteins with putative functions in redox reactions, universal stress response and DNA damage repair, all of which could contribute to the enhanced oxidative stress resistance. The improvement in vitamin K2 content in the evolved strains remains to be understood. Two out of the three evolved strains performed similar to the original strain MG1363 in terms of growth and acidification of culture media. In conclusion, this study demonstrated a natural selection approach without genetic manipulations to obtain vitamin K2 overproducers that are highly relevant for food applications, and contributed to the understanding of oxidative stress resistance in *L. lactis*.

Introduction

Vitamin K2 is an essential vitamin for human health. It functions as an enzyme co-factor for the carboxylation of proteins with γ-carboxyglutamate domains (Gla-proteins) that are involved in biological processes such as blood coagulation, calcium metabolism and cell growth (Vermeer and Schurgers, 2000; Vermeer, 2012). In addition, a higher intake of vitamin K2 was found to be associated with a reduced risk of coronary heart disease and improved bone health (Beulens et al., 2013; Geleijnse et al., 2004; Myneni and Mezey, 2018; Plaza and Lamson, 2005).

Vitamin K2, also referred to as menaquinones, is a group of compounds sharing a naphthoquinone ring structure but differing in the number of the isoprene units in the side chain (Vermeer and Schurgers, 2000). The specific form is expressed as MK-n where n depicts the number of the side chain isoprene units. Vitamin K2 is produced by bacteria, and *Lactococcus lactis* is one of the producers (Chapter 3 of this thesis - Liu et al., 2019; Morishita et al., 1999). *L. lactis* produces mainly MK-9 and MK-8, the long-chain MK forms that are shown to have higher contributions to the vitamin K2 status in human body (Geleijnse et al., 2004; Schurgers et al., 2007; Schurgers and Vermeer, 2002). This is of great interest, as *L. lactis* is widely applied in various food fermentation or biotechnological production processes (Song et al., 2017), allowing opportunities for vitamin K2 enrichment in food products or supplements.

The possibility to obtain vitamin K2 overproducers by genetic engineering has been demonstrated in *L. lactis* (Bøe and Holo, 2020), but practical applications could be limited due to the strict rules in the European Union regarding the use of genetically modified organisms (GMOs) (Eriksson et al., 2020; Sybesma et al., 2006). Therefore, an approach without genetic modification (non-GM) is preferred to obtain vitamin K2 overproducers. In this regard, some studies employed an MK analogue to select for vitamin K2 overproducers of *Bacillus subtilis*, and these studies reported 30% - 100% increased production (Sato et al., 2001; Tsukamoto et al., 2001). Efforts have also been made to reveal the cultivation conditions that improve vitamin K2 content in bacteria: for *L. lactis*, Liu et al. observed that aerobic fermentation increased vitamin K2 content compared to static fermentation (Chapter 3 of this thesis - Liu et al., 2019).

It is known that menaquinones function as electron carriers in the respiratory electron transport chain in the cytoplasmic membranes of the producing bacteria. In *L. lactis*, it has been shown that menaquinones, together with an NADH dehydrogenase complex and the bd-type cytochrome complex, form a simple electron transport chain that enables aerobic respiration when heme (co-factor of cytochrome) and oxygen are supplemented (Rezaïki et al., 2008; Brooijmans et al., 2009). However, not much is known about the roles of menaquinones in *L. lactis* under aerobic (fermentation) conditions without heme-induced respiration. Evidence has been provided in some bacteria that quinones contribute to defense against oxidative stress (Søballe and Poole, 2000; Maruyama et al., 2003; Wang and Maier, 2004). The same protective effect was suggested, although not experimentally confirmed, for menaquinone in *L. lactis* (Vido et al., 2005), where menaquinone is the sole quinone

form produced even under non-respiration conditions (Morishita et al., 1999). Although the exact mechanism is not yet revealed, combining these suggestions and the findings by Liu et al. where vitamin K2 content is improved under aerobic fermentation (Chapter 3 of this thesis - Liu et al., 2019), we hypothesized that applying aerated conditions could lead to the selection of natural vitamin K2 overproducers.

In this study, laboratory evolution under aerated conditions was performed on *L. lactis* ssp. *cremoris* model strain MG1363, aiming to explore the possibility of an non-GM approach to obtain vitamin K2 overproducers. After propagating approximately hundred generations under intensively aerated conditions, we examined three obtained evolved strains closely for their vitamin K2 (menaquinone) content and other physiological characteristics, as well as the genetic and proteome changes compared to the original strain. Relevant test conditions employed in this study were static fermentation (ST), aerated (AE) and respiration-permissive (RES) condition.

Materials & methods

Strains and conditions

Lactococcus lactis ssp. *cremoris* MG1363 and evolved strains were cultivated in M17 medium (Oxoid™) supplemented with 0.5 % glucose (w/v) (named GM17) at 30 °C. For static fermentation condition (ST), the cultures were statically incubated in closed, full filled tubes. For aerated conditions (AE), the cultures were incubated in Erlenmeyer flasks filled with 10% volume media, shaking at 200 rpm. For respiration-permissive condition (RES), 2 µg/mL heme was added to the cultures besides the settings of the aerated conditions.

Laboratory evolution

The evolution was carried out in 100 mL flasks filled with 10 mL GM17 media, shaking at 200 rpm at 30 °C. The first culture was obtained by inoculating a colony of strain MG1363 in the medium. Thereafter every 72 h, a passage was made by transferring 1/100 volume of the old culture into fresh medium in a new 100 mL flask. In total 14 passages were made before evolved strains were isolated for analysis. The cultures from the 14th passage were plated, and single colonies were purified. In total 2 independent cultures (A and B) were successfully maintained throughout all the passages, with 9 mutants screened in culture A and 5 mutants in culture B for vitamin K2 content (specific concentration) under static fermentation conditions. Five out of 9 mutants from culture A and all 5 mutants from culture B showed similar (no increase or less than 30% increase) vitamin K2 content as the wildtype strain, and we selected all 3 mutants (Evo1 - 3) from culture A showing significant increase in vitamin K2 content for further comparative analysis with the wildtype strain.

Determination of bacterial growth and survival

To obtain growth curves, overnight cultures of each strain were diluted to OD_{600} = 0.1 (600 nm; path length 10 mm) in 50 mL fresh GM17, and subjected to desired cultivation conditions (ST, AE or RES). Samples were taken every half hour for optical density (OD) measurement at 600 nm by a spectrophotometer. To determine the survival of bacteria, viable plate counts were determined at indicated time points.

H_2O_2 treatment

An overnight culture of each strain, obtained from static cultivation, was diluted to OD_{600} = 0.2 with fresh GM17 in a 15 mL centrifugal tube and incubated at 30 °C for 1 hour statically. Then 5 mM hydrogen peroxide was added (t = 0) and the viable plate count of bacteria was determined every 30 minutes for 2 hours in total. To stop the action of hydrogen peroxide, 2 µL catalase ($1.3*10^6$ U/mL) was added to the sample that was examined.

Acidification test

An overnight culture of each strain, obtained from static cultivation, was diluted to OD_{600} = 0.1 with fresh GM17 in a 50 mL centrifugal tube and then incubated statically at 30 °C. Thereafter the pH of the culture was measured by a pH probe every hour, for 6 hours in total.

Vitamin K2 extraction and analysis

L. lactis cells were cultivated in GM17 media at 30 °C for 48 h under static fermentation conditions and harvested for vitamin K2 analysis. Vitamin K2 was extracted from cells as described by Liu et al (Chapter 3 of this thesis - Liu et al., 2019). Briefly, PBS washed biomass was incubated with 10 mg/mL lysozyme (Sigma) at 37 °C for 1 h. Four volumes of extraction buffer [n-hexane and 2-propanol at a ratio of 2:1 (v/v)] was added to the lysozyme-treated bacterial suspension and vigorously mixed by vortexing. After centrifugation at 3000 × *g* for 10 min, the (upper) organic phase was collected. Equal volume (as extraction buffer) of n-hexane was added to the remaining lower phase, and the extraction step was repeated twice. The organic phases from each sample were combined and evaporated under a flow of N_2 gas, and re-dissolved in iso-propanol. All samples were diluted in methanol and subjected to liquid chromatography–mass spectrometry (LC–MS) analysis for identification and quantification of different forms of vitamin K2.

Samples from two experiments were analyzed exactly as described in a previous study (Chapter 3 of this thesis - Liu et al., 2019) by a HPLC (UFLC, Shimadzu, Japan) system coupled with a Micro-mass Quattro Ultima MS (Waters, USA). Samples from another two experiments were analyzed using a UPLC (Thermo Scientific Vanquish) coupled with MS (Thermo Q-Exactive hybrid quadrupole-Orbitrap) as follows: one µL sample was injected into an Acquity BEH C18 column (50 mm x 2.1 mm, 1.7 µm particle, 130A, Waters) and compounds were eluted with a gradient starting from 100% methanol to methanol/isopropanol (75%/25%) in 13.7 min and maintained for 5.5 min before going back to 100% methanol in 1.1 min. The flow rate was 0.4 mL/min and column compartment temperature was kept

at 40 °C. The MS system was equipped with a heated electrospray ionization (ESI) source that was set at positive ionization mode. The capillary temperature was 150 °C and the source temperature was 450 °C. The sheath gas (nitrogen) was set to 40 arbitrary units and the ion spray voltage was 4.5 kV. Data were processed using software Xcalibur (Thermo Scientific, version 2.2).

Analytical standards containing MK-1 (Santa Cruz Biotechnology), MK-4 (Sigma), MK-7 (Sigma), MK-9 (Santa Cruz Biotechnology) and vitamin K1 (Sigma) were mixed in the concentration range from 1 ng/mL to 3 µg/mL. Vitamin K1 (phylloquinone) was added at a concentration of 150 ng/mL as an internal standard in each sample. Quantities of MK-5 and MK-6 were estimated using the formulas derived from MK-4 and MK-7 calibration curves, respectively; quantities of MK-8 and MK10 were estimated using the formula derived from MK-9 calibration curve. Values were corrected based on measurement of vitamin K1 internal standards.

Oxygen consumption rate analysis

Strains were all cultivated under anaerobic conditions overnight in GM17 to obtain biomass for oxygen consumption analysis. For the test under respiration-permissive conditions, 2 µg/mL heme was supplemented to obtain cells with functional cytochrome *bd* oxidase. The cells were harvested and washed in PBS once, and OD was standardized to 2 in PBS that had already been saturated with dissolved oxygen (by shaking for 30 min at 180 rpm in flasks). Bacterial suspension (20 mL) was placed in infusion bottles (volume 25 mL) with a layer of mineral oil on top to prevent exchange of gas. An oxygen microsensor (Needle-type PSt7-02, PreSens, Germany) was inserted into the bacterial suspension. The reaction was initiated by adding glucose to a concentration of 1% in the bacterial suspension. Dissolved oxygen in the bacterial suspension was followed at room temperature by an Microx 4 oxygen meter (PreSens, Germany) for 20 min with an interval of 1 min. The absolute value of the slope of the linear correlation between oxygen concentration and time for each measurement was taken as the oxygen consumption rate.

Primary metabolite analysis

Lactate, formate, acetate, acetoin and ethanol were analyzed by high-performance liquid chromatography (HPLC). The strains were incubated in GM17 media at 30 °C overnight under static or aerobic conditions. Cell free culture supernatant was obtained by pelleting the cells at 17000 x *g* for 5 min. To remove proteins, the supernatant was first mixed with 0.5 volume cold Carrez A solution [0.1 M $K_4Fe(CN)_6$] and then mixed with 0.5 volume cold Carrez B solution (0.2 M $ZnSO_4$), and centrifuged at 17000 x *g* for 5 min. The supernatant was subjected to HPLC analysis as described by van Mastrigt et al (van Mastrigt et al., 2018). Briefly, 25 µL sample was injected into HPLC system Ultimate 3000 (Dionex, Idstein, Germany) equipped with an Aminex HPX-87H column (300 × 7.8 mm). Compounds were eluted by 5 mM sulphuric acid at a flow rate of 0.6 mL/min at 40 °C, identified by UV detectors at 220, 250 and 280 nm and quantified by a refractive index detector Shodex RI-101 (Showa Denko K.K., Tokyo, Japan). The quantity of metabolites detected in un-inoculated GM17 medium was used as the initial level to calculate the production/consumption of bacterial metabolites.

Genome sequencing

The original strain MG1363 and three selected evolved strains, Evo1, Evo2 and Evo3 were subjected to genome sequencing. For genomic DNA isolation, cells collected from 1 mL of an overnight culture (static incubation in GM17) of each strain was used. DNeasy Blood & Tissue Kit (Qiagen, Germany) was used to extract DNA according to the manufacture's instruction. DNA was sequenced using the Illumina HiSeq Genome Sequencing System (GATC Biotech, Germany), read length 2 x 150 bp. The sequencing reads were deposit under BioProject with accession number PRJNA765529 at National Center for Biotechnology Information (NCBI) Sequence Read Archive (SRA).

Sequenced reads from each genome was mapped to the reference sequence of *L. lactis* ssp. *cremoris* MG1363 (NCBI accession No. AM406671_1) using BWA (Li and Durbin, 2009) with default parameters. In all strains, more than 99.9% of all reads were mapped. The removal of PCR duplicates was carried out using Picard ("Picard Toolkit," 2019). In the four sequenced strains, 935 - 1141 x coverage depths were reached. Variant analysis was performed using GATK's Haplotype Caller (DePristo et al., 2011; McKenna et al., 2010) to identify single nucleotide polymorphism (SNP) and insertion and deletion (InDel).

Proteomics analysis

Strains were cultivated in GM17 media at 30 °C overnight (16h) under desired conditions (ST, AE and RES). Cells were harvested from 1 mL cultures, washed and resuspended in 100 mM Tris (pH 8), lysed by a sonication probe twice for 45 s. For each strain and condition combination, samples were collected from three independent experiments. For all samples 40 µg proteins were used for sample preparation and analysis. Sample preparation followed the filter assisted sample preparation protocol (FASP) (Wiśniewski et al., 2009). In brief, proteins were reduced with 15 mM dithiothreitol, alkylated with 20 mM acrylamide, and digested with trypsin. Maximally 5 µL prepared sample was injected into a 0.10 x 250 mm ReproSil-Pur 120 C18-AQ 1.9 µm beads analytical column (prepared in-house) at a constant pressure of 825 bar using a 1 h gradient from 9 to 34% acetonitrile in water with 0.1% formic acid in 50 minutes by a nanoLC-MS/MS (Thermo nLC1000 coupled to a Q Exactive-HFX). MS and MSMS AGC targets were set to 3106 and 50000 respectively or maximum ion injection times of 50 ms (MS) and 25 ms (MSMS) were used. HCD fragmented (Isolation width 1.2 m/z, 24% normalized collision energy) MSMS scans of the 25 most abundant 2-5+ charged peaks in the MS scan were recorded in data dependent mode (Threshold 1.2e5, 15 s exclusion duration for the selected m/z +/- 10 ppm).

The MaxQuant quantitative proteomics software package was used to analyze LCMS data with all MS/MS spectra as described previously (Cox et al., 2014), the proteome of *L. lactis* MG1363 (UniProt ID UP000000364) was used as the protein database. Perseus was employed for filtering and further bioinformatics and statistical analysis of the MaxQuant ProteinGroups files (Tyanova et al., 2016). Reverse hits were removed; identified protein groups should contain minimally two peptides, of which at least one is unique and one unmodified. The LFQ (label-free quantitation) intensity values were used for t-test; protein groups differing by a factor of 2 or more (log fold change ≤ -0.3 or ≥ 0.3) and a

p-value of 0.05 or less (−log p-value ≥ 1.3) were considered significantly different. The quality of nLC-MS/MS system was checked with PTXQC using the MaxQuant result files (Bielow et al., 2016). The MS proteomics data have been deposited to the ProteomeXchange Consortium via the PRIDE (Vizcaíno et al., 2016) partner repository with the dataset identifier PXD028721.

Data analysis

Where applicable, statistical significance analysis was performed in JASP (0.11.1) (Love et al., 2019) using analysis of variance (ANOVA) unless specified otherwise. Post hoc multiple comparisons were conducted using Tukey's test (2-sided) and in all cases the control group was *L. lactis* MG1363 (* $P \leq 0.05$).

Results

Three evolved strains showed better survival and higher vitamin K2 production

After sequential propagation of a culture of *L. lactis* ssp. *cremoris* MG1363 for 100 generations under intensively aerated conditions (shaking at 200 rpm in flasks with 10x headspace of the culture) for 72 hours in glucose supplemented M17 media, we isolated three strains and examined them closely. All three strains (Evo1, Evo2 and Evo3) showed considerably better survival compared to the original strain MG1363 under aerated conditions, as reflected by viable plate count: when all strains were cultivated in GM17 under the aerated conditions employed in the evolution experiment for 72 hours, the culturability was tested at 24, 48 and 72 hours (Fig. 4.1A). While the viable plate count of strain MG1363 dropped to 10^5 CFU/mL after 48 hours in aerated conditions from the initial 10^9 CFU/mL (not shown), the three evolved strains all maintained at 10^9 CFU/mL. After 72 hours aerated cultivation, viable plate count of strain MG1363 further dropped to 10^2 – 10^3 CFU/mL, while strain Evo1, Evo2 and Evo3 were still at 10^6 CFU/mL, 10^9 CFU/mL and 10^4 CFU/mL, respectively.

Next, we examined the vitamin K2 content in three evolved strains in comparison to the original strain under static fermentation conditions, as this is the most relevant condition for applications. The total vitamin K2 content in MG1363 was 80 ± 19 nmol/g cell dry weight. The three evolved strains showed 50% - 110% higher average total vitamin K2 content than the original strain (Fig. 4.1B). The relative abundance of MK forms produced by evolved strains are similar to MG1363: 65 - 70% MK-9, 20% MK-8, 5 - 9% MK-3 and minor amount of other forms including MK-10, MK-5 to MK-7 (Fig. 4.1C).

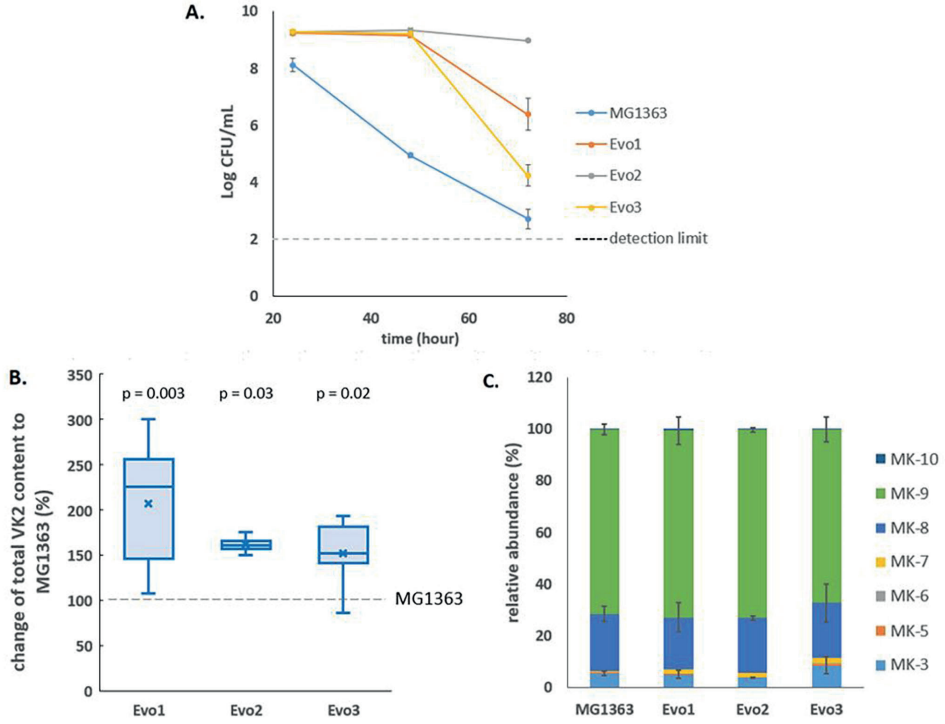

Figure 4.1. Selection of strains. A) Viable plate count of MG1363 and three evolved strains under aerated conditions after 24, 48 and 72 hours cultivation in GM17 media at 30 °C. Data from biological triplicates, error bars represent standard deviation (SD). B) Differences of vitamin K2 (VK2) content in three evolved strains comparing to strain MG1363, under static fermentation condition for 48 hours in GM17 media at 30 °C. Data from four independent experiments, differences in percentage were calculated from each experiment. Crosses represent mean values in the graph, p-values of each strain compared to MG1363 were calculated by paired t-tests. C) Relative abundance of different menaquinone forms in strain MG1363 and evolved strains under static fermentation condition for 48 hours in GM17 media at 30 °C. Data from two independent experiments, error bars represent standard error of the mean (SEM).

Growth and survival of evolved strains in various conditions

As the evolved strains showed favorable traits mentioned above, we further examined the growth and survival of evolved strains under various conditions namely static, aerated and respiration-permissive condition (Fig. 4.2). Under static and aerated conditions, the evolved strains behaved similar to MG1363: they all reached stationary phase (around OD 3.0 - 3.5) in 5 hours, and Evo3 showed slightly lower turbidity (about 0.5 lower in OD) than the other strains when reaching stationary phase under static cultivation. Under respiration-permissive condition, MG1363, Evo1 and Evo2 all reached OD values of 4.5 - 5.0 in 5 hours, while Evo3 only reached OD of 3.0 at stationary phase.

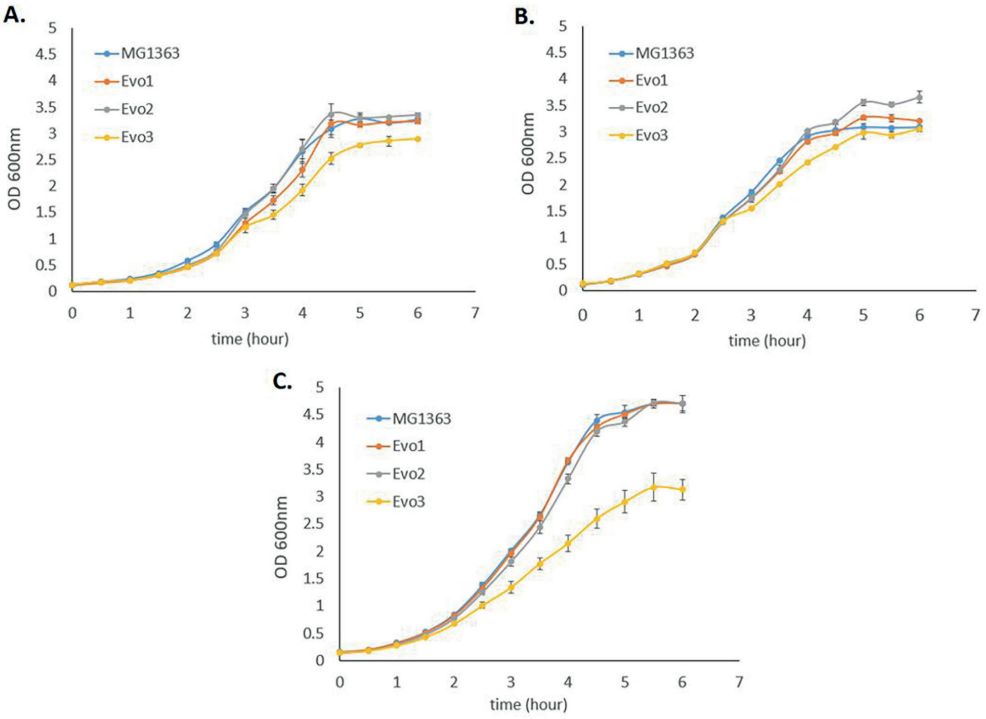

Figure 4.2. Growth curves based on OD_{600} of MG1363 and evolved strains under static fermentation (A), aerated (B) and respiration-permissive (C) conditions in GM17 media at 30 °C. Data from biological triplicates, error bars represent SD.

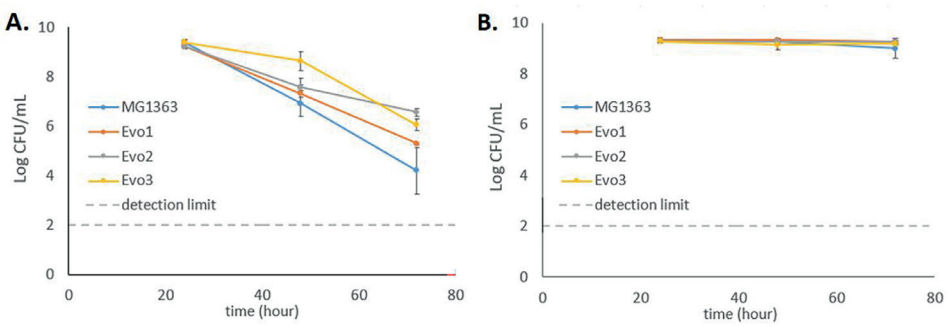

Figure 4.3. Viable plate counts of MG1363 and evolved strains throughout 72 hours under static fermentation (A) and respiration-permissive (B) conditions in GM17 media at 30 °C. Data from biological triplicates, error bars represent SD.

Besides survival under aerated conditions that was used for the selection of evolved strains (Fig. 4.1A), the survival (reflected by viable plate counts) of evolved strains and MG1363 were also tested under static and respiration-permissive conditions for 72 hours (Fig. 4.3).

Under static condition, the viable counts of MG1363 dropped to 10^7 CFU/mL at 48 hours from the initial 10^9 CFU/mL, and further decreased to 10^4 CFU/mL at 72 hours. All three evolved strains showed similar decrease along time, but were constantly 0.5 - 2 log CFU/mL higher than MG1363 at 48 hours and 72 hours ($p < 0.05$ for Evo2 and Evo3). Under respiration-permissive condition, all strains maintained high viable counts at 10^9 CFU/mL throughout the 72 hours.

Oxygen consumption rate in evolved strains

As the evolved strains were obtained from aerated conditions, oxygen consumption by each strain was a relevant phenotype. The oxygen consumption rates in evolved strains and MG1363 were examined under aerobic and respiration-permissive conditions (Fig. 4.4). The biomass was obtained by cultivating each strain in GM17 media overnight anaerobically (heme added to the biomass for respiration-permissive condition), washed and resuspended in air-saturated PBS for the oxygen consumption test. Under aerobic condition, MG1363, Evo1 and Evo2 showed similar oxygen consumption rate of about 70 nmol/(min x OD unit), while Evo3 showed a significantly lower rate of 40 nmol/(min x OD unit). Under respiration-permissive condition, the oxygen consumption rates of all strains were doubled compared to the values found under aerobic condition: MG1363, Evo1 and Evo2 reached 140-160 nmol/(min x OD unit), while Evo3 reached 80 nmol/(min x OD unit).

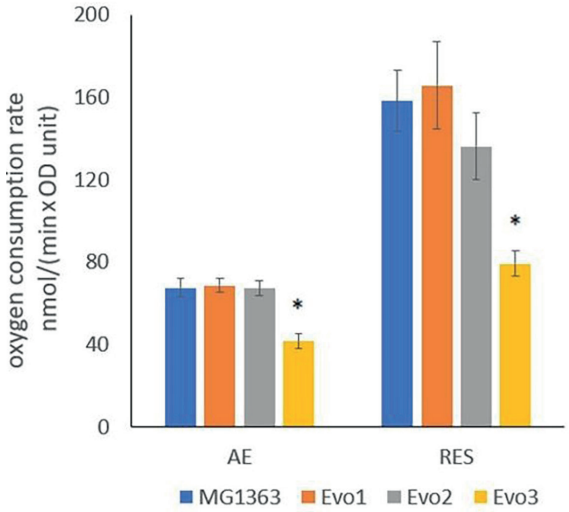

Figure 4.4. Oxygen consumption rate of strain MG1363 and evolved strains under aerobic and respiration-permissive conditions. Cells for this test were obtained from overnight cultures in GM17 media at 30 °C under anaerobic condition, and in addition 2 μg/mL heme was supplemented to the culture for obtaining cells used for RES condition oxygen consumption test. PBS-washed cells were suspended in air-saturated PBS (OD standardized all to 2) for oxygen consumption test at room temperature. Reaction was initiated by adding 1% glucose. Data from four independent experiments, error bars represent SEM. *indicate significant difference compared to MG1363 under the same condition ($p \leq 0.05$).

Evolved strains showed high resistance to H_2O_2

In addition to the previous observation that the evolved strains maintained high survival under aerated cultivation condition, we also tested the strains for resistance to oxidative stress caused by H_2O_2. Cells from early log phase (OD_{600} = 0.2) from each strain were exposed to 5 mM H_2O_2 in GM17 media and the viable plate count was monitored for 2 hours (Fig. 4.5). The viable plate count of MG1363 kept decreasing after 0.5-hour exposure to H_2O_2, and dropped to 10^4 CFU/mL after 2 hours. In contrast, all evolved strains maintained viable counts of 10^9 CFU/mL throughout the 2-hour exposure to H_2O_2.

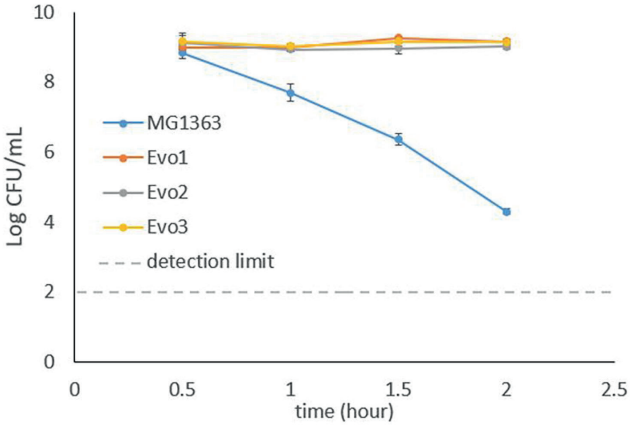

Figure 4.5. Viable plate counts of strain MG1363 and evolved strains after exposure to 5mM H_2O_2. Cells in the early exponential phase were treated with H_2O_2 in GM17 media, incubated statically at 30 °C. Data from biological triplicates, error bars represent SD.

Acidification capacity of evolved strains

As the acidification capacity is an important feature for lactic acid bacteria as starter cultures, we also examined the evolved strains for their ability to lower the pH in GM17 media. Cells from each strain were inoculated at OD of 0.1 in GM17 media and the pH was followed for 6 hours. MG1363, Evo1 and Evo2 lowered the pH from 7 to below 6 in 4 hours, while Evo3 showed 1-hour delay than the other strains in reducing the pH to lower than 6 (Fig. 4.6).

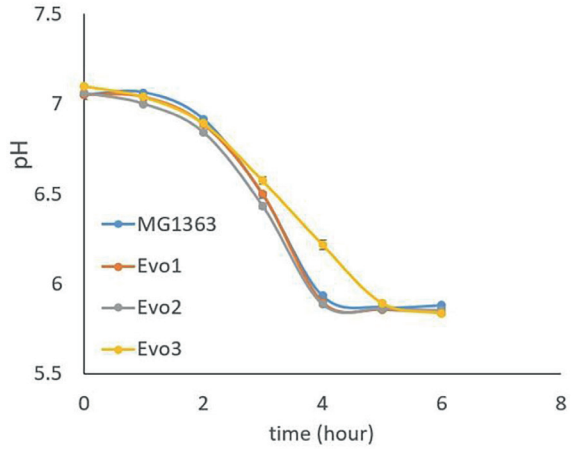

Figure 4.6. Acidification capacity of MG1363 and evolved strains. Test started with cells at OD = 0.1 in GM17 media, incubated statically at 30 °C.

Evo1 and Evo2 produced less lactate and more acetate under aerobic condition

The primary metabolites were examined in the overnight cultures of original and evolved strains under static and aerobic condition in GM17 media. Among all tested metabolites, namely lactate, acetate, formate, acetoin and ethanol, significant differences between strain MG1363 and evolved strains were observed for lactate and acetate under aerobic condition (Fig. 4.7). Under anaerobic condition, all strains produced about 32 mM lactate and 0.5 - 1 mM acetate. Under aerobic condition, MG1363 produced 25 mM lactate and 6.5 mM acetate, Evo3 produced the same amount of lactate as MG1363 and about 1 mM more acetate, while Evo1 and Evo2 produced 2.5 mM less lactate but 2 mM more acetate than MG1363.

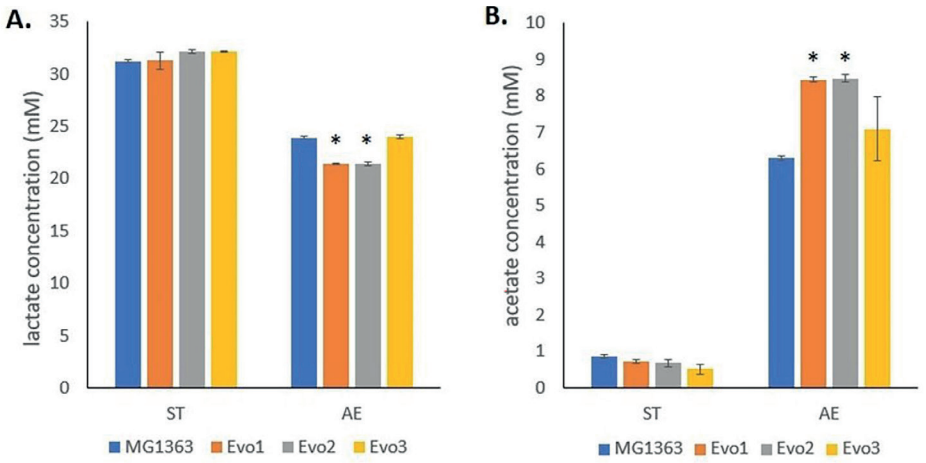

Figure 4.7. Primary metabolites produced by MG1363 and evolved strains. A) lactate and B) acetate concentration from the supernatant of cultures in GM17 at 30 °C under indicated conditions. Data from three independent experiments, error bars represent SEM. *indicate significant difference compared to MG1363 under the same condition ($p \leq 0.05$).

Evolved strains showed common mutations in *ldh* and *gapB* gene

Whole genome sequencing revealed the mutations in evolved strains comparing to strain MG1363 (Table 4.1). All three evolved strains contained single nucleotide polymorphisms (SNPs) in genes *ldh* (*llmg_1120*), *ps435* (*llmg_2107*) and *gapB* (*llmg_2539*) encoding proteins L-lactate dehydrogenase, hypothetical protein and glyceraldehyde 3-phosphate dehydrogenase, respectively. Evo1 and Evo2 shared a SNP in llmg_0907 encoding an YlbN-like protein. Evo3 contained two unique mutations: a SNP in *ftsL* (*llmg_1680*) encoding a cell division protein and a deletion in *purR* (*llmg_2551*) encoding a *pur* operon repressor. A few more unique mutations in Evo2 and Evo3 were revealed, but these were in pseudogenes or noncoding sequences; except for a SNP in Evo2 that could be in the promoter region of *rplA* (*llmg_2276*), the rest were not expected to have regulatory effects on gene expression. No mutations were identified in genes that are predicted to be involved in vitamin K2 biosynthesis in any of the evolved strains.

Table 4.1. Mutations in evolved strains compared to MG1363.

	Strain	Position	Variation	Sequence change	Gene	Protein and ID	Function	Amino acid change
Unique mutations	Evo2	670701	INS	G-> GGA	*llmg_pseudo_18*	pseudo	Transposase and inactivated derivatives	Non-coding
	Evo2	2233340	SNP	T -> A	20bp downstream of *llmg_2275*, 43bp upstream of *rplA* (*llmg_2276*)	Downstream of: putative membrane protein (A2RNF2) Upstream of:50S ribosomal protein L1 (A2RNF3)	putative membrane protein/Ribosomal protein L1	Non-coding
	Evo3	612538	SNP	G -> T	295bp up stream of *llmg_pseudo_14*, 19 bp downstream of *llmg_0623*	Downstream of: abortive phage resistance protein abiP (A2RIX6)	abortive phage resistance protein	Non-coding
	Evo3	1655780	SNP	G -> A	*ftsL* (*llmg_1680*)	cell division protein (A2RLT3)	Protein required for the initiation of cell division	L69F
	Evo3	2510291	DEL	AT -> A	*purR* (*llmg_2551*)	pur operon repressor (P0A400)	Adenine/guanine phosphoribosyltransferases and related PRPP-binding proteins	frameshift (last 13 amino acids)
Common mutations	Evo1, Evo2	873610	SNP	C -> A	*llmg_0907*	hypothetical protein, YlbN-like protein (A2RJP8)	Predicted metal-binding, possibly nucleic acid-binding protein	T9K
	Evo1, Evo2,	1081552	SNP	T -> A	*ldh* (*llmg_1120*)	L-lactate dehydrogenase (A2RKA4)	Malate/lactate dehydrogenases	V212D
	Evo3	1081502		A -> T				K195N
	Evo1, Evo2, Evo3	2090425	SNP	C -> G	*ps435* (*llmg_2107*)	hypothetical protein (A2RMY7)		K13N
	Evo1, Evo2, Evo3	2492912	SNP	G -> A	*gapB* (*llmg_2539*)	glyceraldehyde 3-phosphate dehydrogenase (A2RP55)	Glyceraldehyde-3-phosphate dehydrogenase/ erythrose-4-phosphate dehydrogenase	A203V

Proteomes of evolved strains differed most from MG1363 under aerobic condition

The proteomes of evolved strains and strain MG1363 were examined when cells were cultivated under static, aerobic and respiration-permissive conditions in GM17 media overnight. In total 1387 proteins were quantified by the proteomics analysis, out of the 2383 proteins predicted for MG1363 proteome (UniProt proteome ID UP000000364).

Table 4.2. Numbers of differentially produced proteins in the evolved strains compared to MG1363 under different cultivation conditions.

No. of proteins \ Conditions		ST	AE	RES
Evo1	overproduction	0	5	1
	underproduction	2	12	1
	total different	2	17	2
Evo2	overproduction	2	6	1
	underproduction	1	10	2
	total different	3	16	3
Evo3	overproduction	126	172	160
	underproduction	108	128	132
	total different	234	300	292

Among the three tested cultivation conditions, all three evolved strains showed the highest numbers of proteins with significantly different production level (cut-off $p \leq 0.05$, fold change ≥ 2) compared to MG1363 under aerobic conditions (Table 4.2). Evo1 and Evo2 had 17 and 16 proteins differently produced compared to MG1363 under the aerobic condition, while under static and respiration-permissive condition only 2-3 proteins were identified to be differently produced. Evo3 showed the biggest proteome change compared to MG1363, and the numbers of differentially produced proteins under static, aerobic and respiration-permissive conditions were 234, 300 and 292 respectively. Under all tested conditions, a significant number of the differentially produced proteins in Evo3 compared to MG1363 are identified to be ribosomal proteins and proteins involved in purine nucleotide and amino acids biosynthesis (supplementary Fig. S4.1 and Fig. S4.2).

Table 4.3. Common proteins overproduced in all mutants compared to MG1363 under aerated conditions.

Protein ID	Protein name/Gene name (GN)	GO terms and functions
A2RIN9	Glyceraldehyde 3-phosphate dehydrogenase GN=*gapA*	Oxidoreductase activity, acting on the aldehyde or oxo group of donors, NAD or NADP as acceptor. Glucose metabolic process.
A2RK64	Universal stress protein A2 GN=*uspA2*	
A2RI84	Formamidopyrimidine-DNA glycosylase GN=*mutM*	Involved in base excision repair of DNA damaged by oxidation or by mutagenic agents. Acts as DNA glycosylase that recognizes and removes damaged bases.

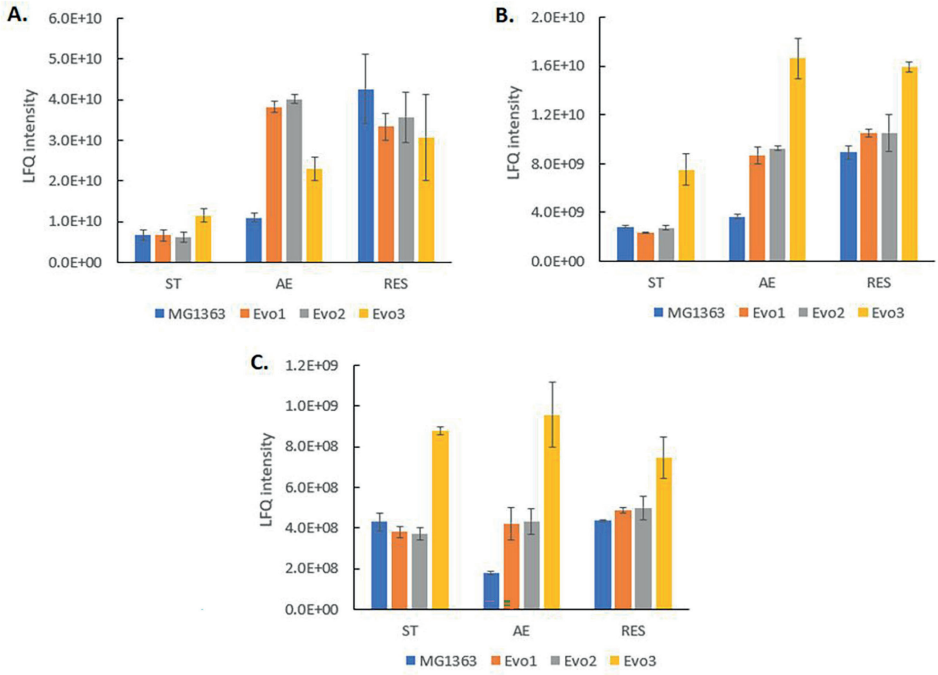

Figure 4.8. Quantity of common differentially produced proteins in evolved strains than MG1363 under different cultivation conditions. LFQ intensities of A) Glyceraldehyde 3-phosphate dehydrogenase, GapA (A2RIN9), B) Universal stress protein A2, UspA2 (A2RK64), and C) Formamidopyrimidine-DNA glycosylase, MutM (A2RI84). Samples were from three independent experiments, error bars represent SEM.

Under the aerobic condition, three proteins were identified to be significantly ($p \leq 0.05$, fold change ≥ 2) overproduced in all evolved strains compared to MG1363 (supplementary Fig. S4.3): glyceraldehyde 3-phosphate dehydrogenase (A2RIN9), universal stress protein A2 (A2RK64) and formamidopyrimidine-DNA glycosylase (A2RI84) (Table 4.3). Quantities of these three proteins in all strains under different cultivation conditions were examined closely (Fig. 4.8). Under static condition, the levels of the three proteins in Evo1, Evo2 were similar to that in MG1363, while Evo3 showed doubled amount compared to the rest. Under aerated conditions, the levels of the three proteins in the evolved strains were in general 2 - 4 times higher than in MG1363. Under respiration-permissive condition, the amounts of the three proteins in MG1363 were close to the evolved stains, about 2 - 4 times higher than that of MG1363 under aerobic conditions.

Proteomics analysis did not reveal many cases of differential production of proteins encoded by genes with mutations in evolved strains compared to MG1363 in all cultivation conditions (supplementary Table S4.1), with the exception that *purR* encoded protein was at least 10 times less in Evo3 than the other strains in all conditions. Moreover, we also did not observe significant changes in proteins that are predicted to be involved in the vitamin K2 biosynthesis pathway among all strains in the three tested cultivation conditions: static, aerobic and respiration-permissive condition (supplementary Table S4.2).

Discussion

Enhancing vitamin K2 content in lactic acid bacteria represented by *L. lactis* via non-GM approaches is highly relevant for enrichment of this valuable vitamin in fermented foods and supplements. Since in previous studies, it was observed that aerated cultivation conditions increased vitamin K2 content in *L. lactis* (Chapter 3 of this thesis - Liu et al., 2019), and because vitamin K2 has been suggested to contribute to oxidative stress resistance in bacteria (Søballe and Poole, 2000; Vido et al., 2005), we performed laboratory evolution through aerated cultivation using the model strain *L. lactis* MG1363. Prolonged cultivation time (72 h) in aerobic conditions was applied for each passage during the evolution experiment, to impose strong selection pressure as evidenced by the decline in culturable cells of the original wild type cells along this time line.

The evolved strains did not only show significantly higher stationary phase survival under aerated conditions, but also showed 50% - 110% higher total vitamin K2 content than the original strain under static fermentation condition, which is the most relevant cultivation condition for (food) fermentations with *L. lactis*. This increase is considerable, comparing to the 30% - 100% increase obtained by selecting resistant mutant against a menaquinone analogue for *Bacillus subtilis* (Sato et al., 2001; Tsukamoto et al., 2001). Liu et al. reported that aerated cultivation conditions and a different carbon source such as fructose, improved vitamin K2 content in MG1363 compared to static cultivation with glucose (Chapter 3 of this thesis - Liu et al., 2019). Here we could reproduce this result in strain MG1363, but

not with the evolved variants of this strains (supplementary Fig. S4.4). Aeration and different carbon source did not result in the same level of increase of vitamin K2 content in the evolved strains as they did for MG1363, and in some cases even lowered the vitamin K2 content in the evolved strains.

As the evolved strains showed desirable traits in vitamin K2 content, essential aspects for application of these strains, such as growth performance, acidification capacity and oxidative stress resistance, were studied. Evo1 and Evo2 performed as good as MG1363 in growth and acidification in static fermentation, while Evo3 showed a slightly lower turbidity and a delay in acidifying the culture medium. This could be explained by the unique mutation in Evo3 in the cell division protein encoding gene *ftsL* and the *pur* operon repressor *purR*, the latter supported also by proteomics analysis, showing a big global proteome change in ribosomal proteins, purine and amino acid synthesis proteins in Evo3 compared to the other strains. The PurR regulon has indeed been shown to include promoters in nucleotide metabolism, (p)ppGpp metabolism, translation-related functions and more (Jendresen et al., 2012), and mutations in *purR* can thus influence the cell growth, metabolism and stress response. The mutation in *ftsL* can result in hindered cell growth as well as morphological changes (Guzman et al., 1992), and both factors may contribute to the slightly lower turbidity of Evo3 comparing to other strains under static fermentation. Evo3 also differed from the other strains with respect to growth under respiration-permissive condition. MG1363, Evo1 and Evo2 all showed nearly doubled biomass in respiration-permissive conditions as compared to static and aerated cultivation, which is a well-known effect of aerobic respiration in *L. lactis*. Evo3 did not show increased biomass under respiration-permissive condition. An explanation for this observation can be derived from the proteome data (supplementary Table S4.3): Evo3 showed a 4 - 6 times lower amount in NADH dehydrogenase NoxA and slightly less NoxB than the other strains under all tested conditions. NoxA and NoxB, are membrane bound type II NADH dehydrogenases in *L. lactis* which, together with menaquinone and cytochrome bd forms functional electron transport chain (ETC) (Brooijmans et al., 2007; Tachon et al., 2010). The reduced amount of NoxA and NoxB in Evo3 could have compromised the efficiency of the ETC under respiration-permissive condition. Moreover, Evo3 also produced about 50% less NoxE (supplementary Table S4.3), another NADH dehydrogenase that directly donates electrons from NADH to oxygen. Together with the reduced amount in NoxA and NoxB, this could explain the lower oxygen consumption rate in Evo3 under aerobic and respiration-permissive conditions compared to the other strains.

Given the conditions used during the laboratory evolution process, the evolved mutants were selected for both resistance to acid and starvation stress in stationary phase, as well as to oxidative stress. For the improved stationary phase survival, it is likely that the 3 evolved strains adopted different approaches: Evo1 and Evo2 produced less lactate in aerated conditions (Fig 4.7), which could be beneficial for reducing acid stress for the two strains. Evo3 showed unique proteome profile, where a whole group of proteins involved in arginine biosynthesis/metabolism were differentially produced comparing to the other strains (supplementary Fig. S4.2). *L. lactis* is known to utilize arginine as an alternative energy source when the sugar source is deprived (Brandsma et al., 2012), and the unique

profile of arginine biosynthesis/metabolism proteins of Evo3 could offer advantage to this strain when facing starvation stress in the stationary phase. This was also in line with the observation that Evo3 was one of the best survivors throughout prolonged cultivation in static fermentation conditions (Fig. 4.3A).

The high resistance of evolved strains against oxidative stresses was also confirmed separately by exposing bacteria to hydrogen peroxide, and putative factors involved were identified in our proteomics analysis. In the proteomics analysis, the three proteins that were found to be overproduced in each of the evolved strains under aerated conditions were identified (supplementary Fig. S4.3). These three proteins, glyceraldehyde 3-phosphate dehydrogenase (GapA), universal stress protein A2 (UspA2) and formamidopyrimidine-DNA glycosylase (MutM) could explain the oxidative stress-resistant phenotype of the evolved strains. Solem et al. reported that gapA is only expressed under certain stress conditions (Solem et al., 2003), and Rochat et al. reported that overproduction of GapA led to increased resistance to H_2O_2 in MG1363 (Rochat et al., 2012). In this study, proteomics analysis revealed that in MG1363, GapA production was low in static condition, increased 2-fold in aerated conditions and 8-fold in respiration-permissive conditions, where in evolved strains GapA was produced at very high level in both aerated and respiration-permissive conditions. Similar trends were also observed for UspA2 and MutM, proteins involved in universal stress response and DNA repair upon oxidative damages, respectively. In the evolved strains, these proteins were produced at high levels in both the aerated conditions and respiration-permissive conditions, but in MG1363 they were only present at high levels under respiration. A high degree of resistance against stresses is one of the known traits for *L. lactis* when achieving functional respiration (Duwat et al., 2001; Rezaïki et al., 2004); this was confirmed for MG1363 in this study, and also supports the explanation on the oxidative stress-resistant phenotype of the evolved strains: key proteins represented by GapA, UspA2 and MutM were overproduced in these strains upon oxidative stress, to a similar level as in cells undergoing respiration, and that most likely offered protection to cells.

Common mutations in genes *ldh* and *gapB* were identified in the evolved strains, but the encoded proteins produced in evolved strains were at a similar level as in MG1363 (supplementary Table S4.4). However, the protein quantity does not always reflect possible changes in the activity and functionality caused by the mutations, and further studies are required to obtain a more detailed characterization of relevant enzyme activities. It is conceivable that the difference in lactate and acetate production in Evo1 and Evo2 compared to the wildtype under aerobic condition could be a result of the SNP in the lactate dehydrogenase encoding gene, as the quantity of other proteins involved in pyruvate metabolism could not explain the difference in lactate and acetate production otherwise (supplementary Table S4.4). Moreover, the mutation in GapB could influence the level of GapA, of which a higher protein quantity was observed in the evolved strains under the aerated conditions. It has been reported that *gapA* and *gapB* both encode glyceraldehyde 3-phosphate dehydrogenases (GAPDH), and that GapB mainly performs GAPDH activity in *L. lactis* during normal growth while GapA activity increases under stressed conditions (Willemoës et al., 2002).

Although most phenotypes of the evolved strains, especially the high resistance against oxidative stresses, could be explained by genomics or proteomics data, we could not fully elucidate the mechanism explaining increased vitamin K2 content in the evolved strains with the same collection of data: the evolved strains did not show any difference in gene sequence or protein production in the vitamin K2 synthesis pathway compared to strain MG1363 (supplementary Table S4.2). However, proteomics data obtained in this study were from stationary phase cells to avoid variations caused by the timing of protein production and different growth rates of the strains, and thus do not reflect the dynamics during cell growth. Gene expression data in exponential phase cells could provide extra insight into any possible difference in regulation of vitamin K2 production in evolved strains. Moreover, vitamin K2 is a group of secondary metabolites. Its production is not only determined by expression level or activity of genes and proteins directly involved in vitamin K2-specific biosynthesis pathway, but also by fluxes towards the precursors or competing reactions. Therefore, the increased vitamin K2 content in evolved strains can be best understood by using a genome-scale metabolic model in future studies.

Despite a clear correlation, the high resistance against oxidative stresses in the evolved strains could not be linked directly to the elevated vitamin K2 content in *L. lactis*. Given the challenges of exogenously supplementing the hydrophobic long-chain MKs, opportunities could be provided by supplementing additional short-chain MKs to *L. lactis*, as previously reported by (Rezaïki et al., 2008), who showed that exchange/exogenous supplementation of short-chain MKs in bacteria can activate respiration and stimulate growth in Group B Streptococcus. Supplemented short-chain MKs can possibly be converted to the native long-chain MK forms in bacteria including *L. lactis*, by a widely conserved isoprenyl diphosphate synthase (part of MK biosynthesis pathway, homologs of IspB described in *Escherichia coli*) (Wang and Ohnuma, 2000; Franza et al., 2016; Bøe and Holo, 2020), allowing investigation on the effect of elevated vitamin K2 content in *L. lactis*. Nevertheless, to confirm the physiological roles of vitamin K2/MKs in *L. lactis*, studies can be best performed using dedicated *L. lactis* mutants with different MK profiles but otherwise identical genetical background.

Given the wide applications in fermented food products, *L. lactis* provides unique opportunities for vitamin K2 fortification in our diets. This holds particularly true for the long-chain vitamin K2 forms, which shows a longer half-life in the human body allowing contributions to additional health benefits in vascular and bone health associated with vitamin K2 intake (Gast et al., 2009; Beulens et al., 2013; Schwalfenberg, 2017; Zwakenberg et al., 2017). Although the delivery of these hydrophobic molecules by bacteria cells to the human body remains a challenge and also deserves future attention, efforts to increase the content of vitamin K2 in food grade producers like *L. lactis* is a valuable first step to take.

The evolved *L. lactis* strains obtained and their reported phenotypes, highlight the potential of laboratory evolution as a non-GM approach to obtain dairy starters with desired functions in industrial applications. Firstly, the evolved strains, especially Evo1 and Evo2, retained essential features of the original strain in terms of growth and acidification capacity; secondly, the increased vitamin K2 content

in the evolved strains enables better fortification of this valuable vitamin in fermented products; finally, the high resistance to oxidative stresses in the evolved strains is desirable for optimal performance of starter cultures (Cretenet et al., 2014; Dijkstra et al., 2014; Ghandi et al., 2012), as *L. lactis* is often subjected to oxidative stresses associated with preservation procedures like spray drying, or linked to processing operations such as stirring in the first stages of cheese manufacturing.

Conclusions

In this study, we obtained three strains evolved from *L. lactis* ssp. *cremoris* MG1363 by sequential aerated cultivation. Most evolved strains retained essential features of the original strain in terms of growth and acidification performance. In addition, the evolved strains showed not only increased vitamin K2 content but also high resistance against oxidative stresses comparing to the original strain. Genome and proteome analysis provided explanations for most of the phenotypes observed for evolved strains. The laboratory evolution approach therefore showed great potential in obtaining non-GM dairy starters in fermentation industry, where traits of starter cultures such as resistance to oxidative stress, and potentials for enrichment of valuable vitamins like K2, are desired. In conclusion, this study demonstrated a non-genetical modifying approach to obtain vitamin K2 overproducers that are highly relevant for food applications, and contributed to the understanding of oxidative stress resistance in *L. lactis*.

Acknowledgements

The authors would like to thank Yu Zhang (Food Microbiology, Wageningen University) for her involvement at the early stage of the laboratory evolution experiment, Jeroen Koomen (Food Microbiology, Wageningen University) for his kind help in analyzing proteomics data and Alberto Garre Perez (Food Microbiology, Wageningen University) for his advice in statistics analysis. The authors would also like to thank Mark Sanders (Food Chemistry, Wageningen University) and Eric van Bennekom (RIKILT, Wageningen University and Research) for their assistance in vitamin K2 analysis.

The work was subsidized by the Netherlands Organization for Scientific Research (NWO) through the Graduate Program on Food Structure, Digestion and Health.

Supplementary materials

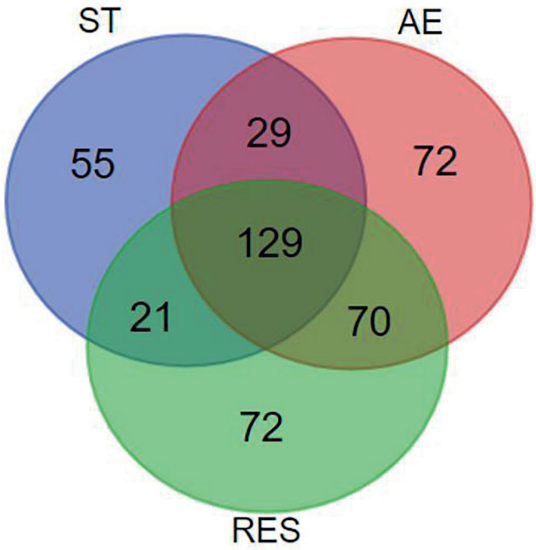

Figure S4.1. Venn graph showing the differentially produced proteins in Evo3 versus MG1363 in all three tested conditions. There are 129 proteins showing differential production between the two stains in all three conditions. ST, static; AE, aerobic; RES, respiration-permissive condition.

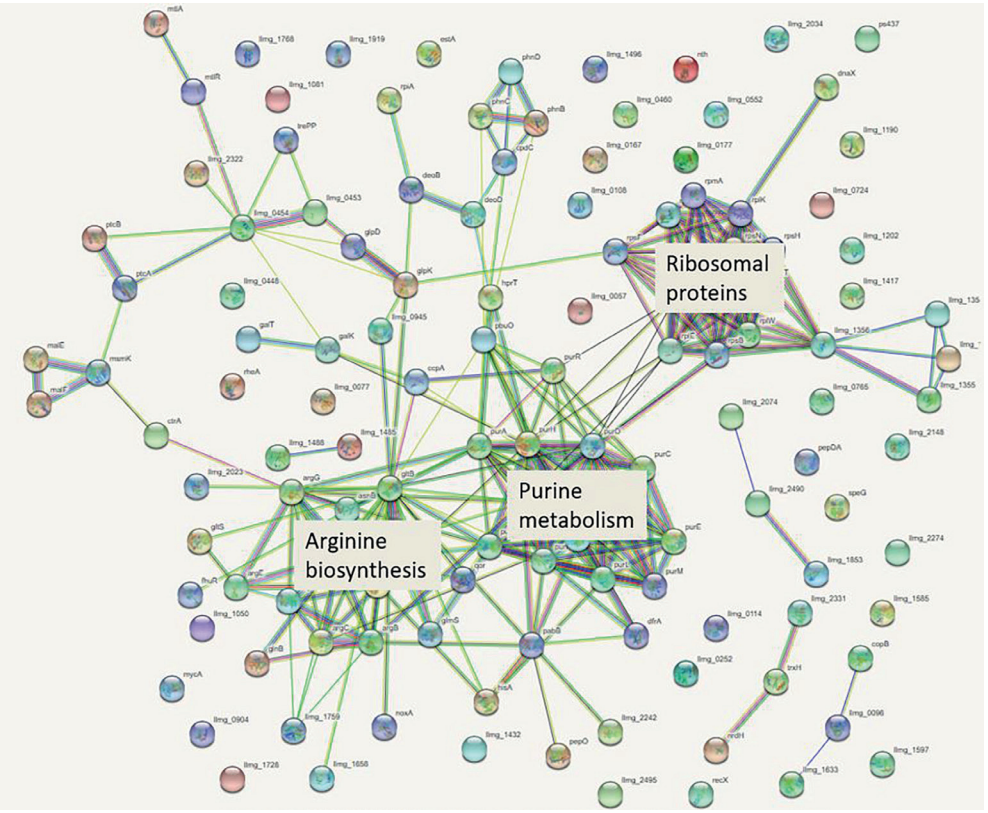

Figure S4.2. Protein network/associations of the 129 proteins differentially produced in Evo3 versus MG1363 under all conditions.

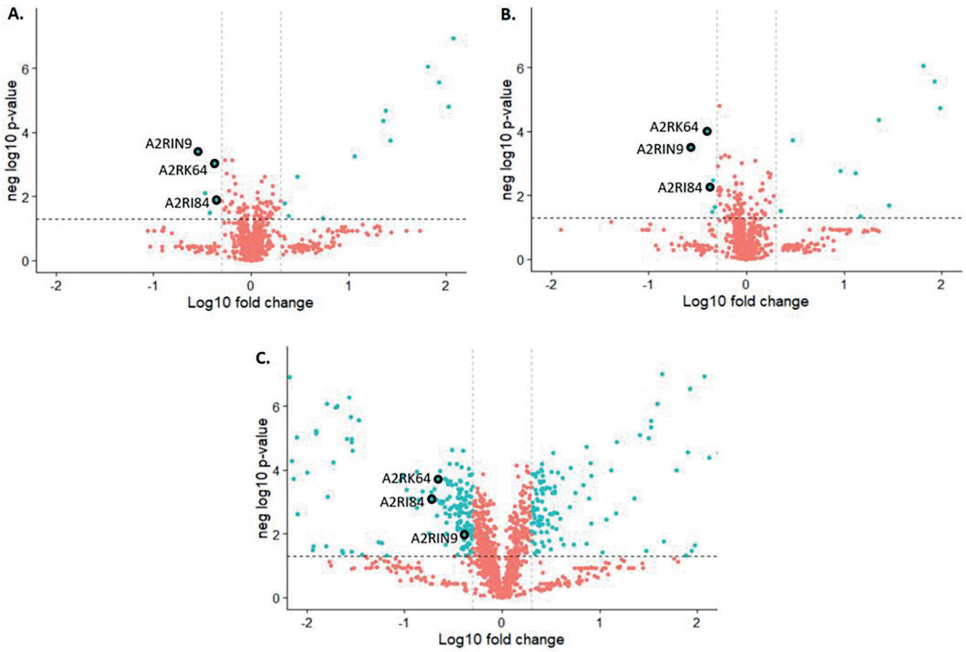

Figure S4.3. Volcano plots of proteome changes between evolved strains and MG1363 under aerobic condition. A) MG1363 vs. Evo1; B) MG1363 vs. Evo2; C) MG1363 vs. Evo3. In all three comparisons, proteins A2RK64, A2RI84 and A2RIN9 were significantly ($p \leq 0.05$, fold change ≥ 2) overproduced in the evolved strains compared to MG1363 (i.e. underproduced in MG1363 compared to evolved strains), as indicated by black circles. Data from three independent experiments.

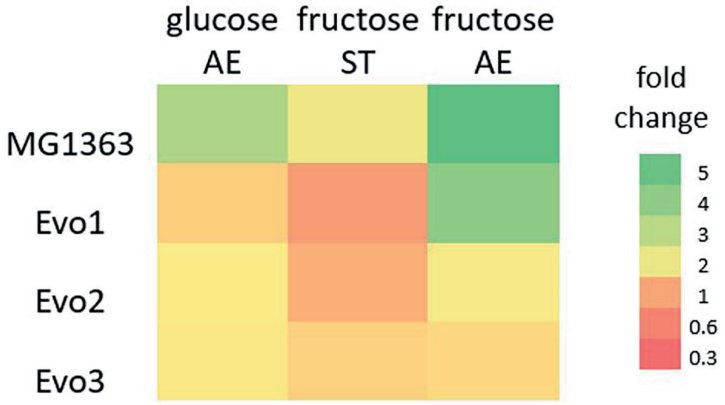

Figure S4.4. Changes in the total vitamin K2 production under varied conditions in respective strains. MG1363 and evolved strains were cultivated in M17 media supplemented with 0.5% (w/v) indicated carbon source (glucose or fructose), under indicated conditions (ST or AE), at 30 °C for 48 h. Fold changes were calculated taking values of "glucose ST" condition as the reference of respective strains.

Table S4.1. Quantity (Log LFQ intensity) of proteins encoded by mutated genes in evolved strains compared to strain MG1363 under various cultivation conditions.

Gene name (locus)	Protein ID	ST				AE				RES			
		MG1363	Evo1	Evo2	Evo3	MG1363	Evo1	Evo2	Evo3	MG1363	Evo1	Evo2	Evo3
***rplA* (*llmg_2276*)**	A2RNF3	10.78	10.81	10.85	10.61	10.84	10.85	10.83	10.52	10.76	10.78	10.77	10.46
		(0.03)	(0.01)	(0.05)	(0.03)	(0.03)	(0.03)	(0.03)	(0.03)	(0.04)	(0.02)	(0.03)	(0.07)
***ftsL* (*llmg_1680*)**	A2RLT3	ND	ND	ND	ND	ND	ND	ND	ND	ND	ND	ND	ND
		-	-	-	-	-	-	-	-	-	-	-	-
***purR* (*llmg_2551*)**	P0A400	9.28	9.27	9.32	8.12	9.22	9.17	9.22	7.70	9.28	9.26	9.27	8.35
		(0.01)	(0.04)	(0.04)	(0.15)	(0.04)	(0.03)	(0.04)	(0.03)	(0.03)	(0.02)	(0.04)	(0.07)
llmg_0907	A2RJP8	8.77	8.84	8.87	8.95	8.82	8.88	8.86	8.91	8.85	8.90	8.93	9.00
		(0.03)	(0.02)	(0.02)	(0.02)	(0.01)	(0.02)	(0.05)	(0.07)	(0.01)	(0.01)	(0.03)	(0.03)
***ldh* (*llmg_1120*)**	A2RKA4	10.92	10.93	10.89	11.15	10.76	10.74	10.76	10.91	10.65	10.68	10.67	10.95
		(0.01)	(0.03)	(0.04)	(0.01)	(0.01)	(0.02)	(0.02)	(0.02)	(0.00)	(0.00)	(0.01)	(0.01)
***ps435* (*llmg_2107*)**	A2RMY7	ND	ND	ND	ND	ND	ND	ND	ND	ND	ND	ND	ND
		-	-	-	-	-	-	-	-	-	-	-	-
***gapB* (*llmg_2539*)**	A2RP55	11.46	11.51	11.48	11.74	11.51	11.57	11.56	11.63	11.46	11.50	11.49	11.84
		(0.04)	(0.02)	(0.04)	(0.09)	(0.03)	(0.03)	(0.02)	(0.05)	(0.02)	(0.03)	(0.04)	(0.04)

Values are average from samples collected from 3 independent experiments, SEM values are shown in brackets. Detection limit in Log LFQ intensity: 6.3; ND = not detected, and "-" indicates that SEM values are not applicable in this case.

Table S4.2. Quantity (Log LFQ intensity) of proteins involved in the vitamin K2 synthesis pathway (kegg pathway llm00130) in strain MG1363 and evolved strains under various cultivation conditions.

Gene name (locus)	Protein ID	ST				AE				RES			
		MG1363	Evo1	Evo2	Evo3	**MG1363**	**Evo1**	**Evo2**	**Evo3**	**MG1363**	**Evo1**	**Evo2**	**Evo3**
menF	A2RM72	8.32	8.24	8.32	8.14	8.18	8.28	8.26	7.52	8.07	8.20	8.06	8.00
(***llmg_1828***)		(0.03)	(0.04)	(0.07)	(0.07)	(0.03)	(0.04)	(0.04)	(0.61)	(0.04)	(0.03)	(0.03)	(0.05)
menD	A2RM73	9.03	8.96	8.96	8.94	9.00	8.96	9.00	8.99	8.88	8.88	8.94	8.86
(***llmg_1829***)		(0.02)	(0.01)	(0.01)	(0.02)	(0.03)	(0.02)	(0.01)	(0.05)	(0.01)	(0.03)	(0.02)	(0.04)
menX	A2RM74	ND	ND	ND	ND	ND	ND	ND	ND	ND	ND	ND	ND
(***llmg_1830***)		-	-	-	-	-	-	-	-	-	-	-	-
menC	A2RM77	8.29	8.19	8.25	8.40	8.11	8.29	8.25	8.40	8.23	8.25	8.25	8.33
(***llmg_1833***)		(0.06)	(0.02)	(0.07)	(0.03)	(0.03)	(0.00)	(0.04)	(0.05)	(0.04)	(0.05)	(0.06)	(0.08)
menE	A2RM76	8.55	8.44	8.54	8.72	8.48	8.40	8.38	8.71	8.48	8.50	8.47	8.61
(***llmg_1832***)		(0.03)	(0.02)	(0.01)	(0.01)	(0.02)	(0.09)	(0.04)	(0.06)	(0.02)	(0.02)	(0.03)	(0.05)
menB	A2RM75	9.87	9.83	9.86	9.74	9.98	10.01	9.95	9.79	9.98	9.97	10.01	9.95
(***llmg_1831***)		(0.02)	(0.04)	(0.04)	(0.06)	(0.01)	(0.01)	(0.04)	(0.06)	(0.01)	(0.00)	(0.01)	(0.04)
menA	A2RHR6	ND	ND	ND	ND	ND	ND	ND	ND	ND	ND	ND	ND
(***llmg_0197***)		-	-	-	-	-	-	-	-	-	-	-	-
menG	A2RJA5	8.74	8.71	8.81	8.89	8.81	8.79	8.77	8.96	8.73	8.70	8.74	8.84
(***llmg_0753***)		(0.03)	(0.03)	(0.02)	(0.05)	(0.04)	(0.05)	(0.02)	(0.05)	(0.01)	(0.01)	(0.01)	(0.04)
llmg_0196	A2RHR5	8.84	8.87	8.83	8.93	8.88	8.89	8.88	8.95	8.81	8.85	8.80	8.95
		(0.02)	(0.02)	(0.01)	(0.01)	(0.02)	(0.01)	(0.01)	(0.03)	(0.01)	(0.01)	(0.02)	(0.03)
ispB	A2RK94	8.61	8.57	8.62	8.43	8.50	8.42	8.52	8.52	8.38	8.37	8.38	8.33
(***llmg_1110***)		(0.03)	(0.04)	(0.03)	(0.14)	(0.04)	(0.08)	(0.05)	(0.07)	(0.05)	(0.05)	(0.10)	(0.10)
gerCA	A2RK95	ND	ND	ND	ND	ND	ND	ND	ND	ND	ND	ND	ND
(***llmg_1111***)		-	-	-	-	-	-	-	-	-	-	-	-
mvk	A2RID4	9.27	9.22	9.23	9.14	9.23	9.20	9.21	9.21	9.09	9.09	9.08	9.12
(***llmg_0425***)		(0.03)	(0.04)	(0.04)	(0.02)	(0.00)	(0.03)	(0.01)	(0.05)	(0.02)	(0.01)	(0.01)	(0.05)

Values are average from samples collected from 3 independent experiments, SEM values are shown in brackets. Detection limit in Log LFQ intensity: 6.3; ND = not detected, and "-" indicates that SEM values are not applicable in this case.

Table S4.3. Quantity (Log LFQ intensity) of NADH dehydrogenases in strain MG1363 and evolved strains under various cultivation conditions.

Gene name (locus)	Protein ID	ST				AE				RES			
		MG1363	Evo1	Evo2	Evo3	MG1363	Evo1	Evo2	Evo3	MG1363	Evo1	Evo2	Evo3
***noxA* (*llmg_1735*)**	A2RLY1	9.79	9.76	9.79	8.92	9.86	9.82	9.84	9.03	9.62	9.64	9.62	9.01
		(0.03)	(0.05)	(0.05)	(0.05)	(0.01)	(0.02)	(0.02)	(0.07)	(0.00)	(0.02)	(0.02)	(0.06)
***noxB* (*llmg_1734*)**	A2RLY0	10.17	10.17	10.18	9.93	10.14	10.14	10.16	9.96	10.02	10.03	10.03	9.84
		(0.04)	(0.02)	(0.07)	(0.04)	(0.02)	(0.02)	(0.02)	(0.04)	(0.03)	(0.02)	(0.01)	(0.03)
***noxC* (*llmg_1770*)**	A2RM15	9.11	9.03	9.06	9.26	9.09	9.08	9.05	9.14	9.18	9.18	9.15	9.18
		(0.04)	(0.05)	(0.05)	(0.07)	(0.02)	(0.02)	(0.08)	(0.02)	(0.01)	(0.01)	(0.02)	(0.05)
***noxE* (*llmg_0408*)**	A2RIB7	10.11	10.12	10.11	9.92	10.41	10.35	10.37	10.20	9.76	9.81	9.83	9.90
		(0.05)	(0.07)	(0.06)	(0.05)	(0.02)	(0.00)	(0.01)	(0.05)	(0.02)	(0.01)	(0.03)	(0.03)

Values are average from samples collected from 3 independent experiments, SEM values are shown in brackets. Detection limit in Log LFQ intensity: 6.3; ND = not detected, and "-" indicates that SEM values are not applicable in this case.

Table S4.4. Quantity (Log LFQ intensity) of proteins involved in pyruvate metabolism in strain MG1363 and evolved strains under various cultivation conditions.

Gene name (locus)	Protein ID	ST				AE				RES			
		MG1363	Evo1	Evo2	Evo3	MG1363	Evo1	Evo2	Evo3	MG1363	Evo1	Evo2	Evo3
***pfl* (*llmg_0629*)**	O32799	10.37	10.27	10.31	10.28	9.88	9.87	9.91	10.11	10.39	10.50	10.53	10.48
		(0.03)	(0.04)	(0.02)	(0.04)	(0.02)	(0.01)	(0.00)	(0.03)	(0.04)	(0.02)	(0.01)	(0.03)
***pflA* (*llmg_1997*)**	A2RMN3	8.93	8.93	8.98	9.23	7.39	ND	7.36	9.01	8.28	8.41	8.47	9.15
		(0.03)	(0.03)	(0.02)	(0.01)	(0.55)	-	(0.54)	(0.04)	(0.04)	(0.06)	(0.08)	(0.04)
***ldhB* (*llmg_0392*)**	P0CI34	6.76	7.28	7.27	ND	6.77	6.77	7.27	6.71	6.69	6.76	ND	ND
		(0.45)	(0.49)	(0.48)	-	(0.47)	(0.47)	(0.49)	(0.41)	(0.39)	(0.46)	-	-
***ldhX* (*llmg_1429*)**	A2RL45	8.54	8.49	8.45	8.01	8.06	7.84	7.91	7.91	7.98	7.96	7.96	8.00
		(0.06)	(0.07)	(0.06)	(0.06)	(0.01)	(0.04)	(0.07)	(0.02)	(0.02)	(0.02)	(0.08)	(0.02)
***ldh* (*llmg_1120*)**	A2RKA4	10.92	10.93	10.89	11.15	10.76	10.74	10.76	10.91	10.65	10.68	10.67	10.95
		(0.01)	(0.03)	(0.04)	(0.01)	(0.01)	(0.02)	(0.02)	(0.02)	(0.00)	(0.00)	(0.01)	(0.01)
***pdhD* (*llmg_0071*)**	A2RHE1	10.42	10.41	10.40	10.37	10.56	10.59	10.60	10.36	10.69	10.69	10.70	10.47
		(0.02)	(0.02)	(0.01)	(0.02)	(0.00)	(0.02)	(0.02)	(0.02)	(0.01)	(0.01)	(0.01)	(0.03)
***pdhC* (*llmg_0072*)**	A2RHE2	10.61	10.60	10.58	10.58	10.81	10.81	10.85	10.55	10.91	10.93	10.94	10.62
		(0.04)	(0.03)	(0.03)	(0.07)	(0.01)	(0.02)	(0.01)	(0.01)	(0.02)	(0.00)	(0.01)	(0.02)
***pdhB* (*llmg_0073*)**	A2RHE3	10.70	10.69	10.67	10.79	10.81	10.83	10.85	10.67	10.91	10.94	10.92	10.78
		(0.03)	(0.02)	(0.03)	(0.06)	(0.03)	(0.03)	(0.02)	(0.01)	(0.01)	(0.02)	(0.01)	(0.03)
***pdhA* (*llmg_0074*)**	A2RHE4	10.28	10.28	10.27	10.24	10.42	10.42	10.41	10.15	10.56	10.54	10.59	10.29
		(0.02)	(0.04)	(0.02)	(0.03)	(0.01)	(0.01)	(0.01)	(0.02)	(0.02)	(0.02)	(0.02)	(0.05)

Values are average from samples collected from 3 independent experiments, SEM values are shown in brackets. Detection limit in Log LFQ intensity: 6.3; ND = not detected, and "-" indicates that SEM values are not applicable in this case.

References

Beulens, J. W. J., Booth, S. L., van den Heuvel, E. G. H. M., Stoecklin, E., Baka, A., and Vermeer, C. (2013). The role of menaquinones (vitamin K2) in human health. *Br. J. Nutr.* 110, 1357–1368.

Bielow, C., Mastrobuoni, G., and Kempa, S. (2016). Proteomics quality control: quality control software for MaxQuant results. *J. Proteome Res.* 15, 777–787.

Bøe, C. A., and Holo, H. (2020). Engineering *Lactococcus lactis* for increased vitamin K2 production. *Front. Bioeng. Biotechnol.* 8, 191.

Brandsma, J. B., van de Kraats, I., Abee, T., Zwietering, M. H., and Meijer, W. C. (2012). Arginine metabolism in sugar deprived *Lactococcus lactis* enhances survival and cellular activity, while supporting flavour production. *Food Microbiol.* 29, 27–32.

Brooijmans, R. J. W., Poolman, B., Schuurman-Wolters, G. K., de Vos, W. M., and Hugenholtz, J. (2007). Generation of a membrane potential by *Lactococcus lactis* through aerobic electron transport. *J. Bacteriol.* 189, 5203–5209.

Brooijmans, R., Smit, B., Santos, F., van Riel, J., de Vos, W. M., and Hugenholtz, J. (2009). Heme and menaquinone induced electron transport in lactic acid bacteria. *Microb. Cell Fact.* 8, 28.

Cox, J., Hein, M. Y., Luber, C. A., Paron, I., Nagaraj, N., and Mann, M. (2014). Accurate proteome-wide label-free quantification by delayed normalization and maximal peptide ratio extraction, termed MaxLFQ. *Mol. Cell. Proteomics* 13, 2513–2526.

Cretenet, M., Le Gall, G., Wegmann, U., Even, S., Shearman, C., Stentz, R., et al. (2014). Early adaptation to oxygen is key to the industrially important traits of *Lactococcus lactis* ssp. *cremoris* during milk fermentation. *BMC Genomics* 15, 1054.

DePristo, M. A., Banks, E., Poplin, R., Garimella, K. V, Maguire, J. R., Hartl, C., et al. (2011). A framework for variation discovery and genotyping using next-generation DNA sequencing data. *Nat. Genet.* 43, 491–498.

Dijkstra, A. R., Setyawati, M. C., Bayjanov, J. R., Alkema, W., van Hijum, S. A. F. T., Bron, P. A., et al. (2014). Diversity in robustness of *Lactococcus lactis* strains during heat stress, oxidative stress, and spray drying stress. *Appl. Environ. Microbiol.* 80, 603–611.

Duwat, P., Sourice, S., Cesselin, B., Lamberet, G., Vido, K., Gaudu, P., et al. (2001). Respiration capacity of the fermenting bacterium *Lactococcus lactis* and its positive effects on growth and survival. *J. Bacteriol.* 183, 4509–4516.

Eriksson, D., Custers, R., Edvardsson Björnberg, K., Hansson, S. O., Purnhagen, K., Qaim, M., et al. (2020). Options to reform the European Union legislation on GMOs: scope and definitions. *Trends Biotechnol.* 38, 231–234.

Franza, T., Delavenne, E., Derré-Bobillot, A., Juillard, V., Boulay, M., Demey, E., et al. (2016). A partial metabolic pathway enables group b streptococcus to overcome quinone deficiency in a host bacterial community. *Mol. Microbiol*. 102, 81–91.

Gast, G. C. M., De Roos, N. M., Sluijs, I., Bots, M. L., Beulens, J. W. J., Geleijnse, J. M., et al. (2009). A high menaquinone intake reduces the incidence of coronary heart disease. *Nutr. Metab. Cardiovasc. Dis.* 19, 504–510.

Geleijnse, J. M., Vermeer, C., Grobbee, D. E., Schurgers, L. J., Knapen, M. H. J., van Der Meer, I. M., et al. (2004). Dietary intake of menaquinone is associated with a reduced risk of coronary heart disease: the Rotterdam Study. *J. Nutr.* 134, 3100–3105.

Ghandi, A., Powell, I. B., Howes, T., Chen, X. D., and Adhikari, B. (2012). Effect of shear rate and oxygen stresses on the survival of *Lactococcus lactis* during the atomization and drying stages of spray drying: A laboratory and pilot scale study. *J. Food Eng.* 113, 194–200.

Guzman, L. M., Barondess, J. J., and Beckwith, J. (1992). FtsL, an essential cytoplasmic membrane protein involved in cell division in *Escherichia coli*. *J. Bacteriol.* 174, 7717–7728.

Jendresen, C. B., Martinussen, J., and Kilstrup, M. (2012). The PurR regulon in *Lactococcus lactis* - transcriptional regulation of the purine nucleotide metabolism and translational machinery. *Microbiology* 158, 2026–2038.

Li, H., and Durbin, R. (2009). Fast and accurate short read alignment with Burrows – Wheeler transform. *Bioinformatics* 25, 1754–1760.

Liu, Y., van Bennekom, E. O., Zhang, Y., Abee, T., and Smid, E. J. (2019). Long-chain vitamin K2 production in *Lactococcus lactis* is influenced by temperature, carbon source, aeration and mode of energy metabolism. *Microb. Cell Fact.* 18, 129.

Love, J., Selker, R., Marsman, M., Jamil, T., Dropmann, D., Verhagen, J., et al. (2019). JASP: Graphical statistical software for common statistical designs. *J. Stat. Softw.* 88, 2.

Maruyama, A., Kumagai, Y., Morikawa, K., Taguchi, K., Hayashi, H., and Ohta, T. (2003). Oxidative-stress-inducible qorA encodes an NADPH-dependent quinone oxidoreductase catalysing a one-electron reduction in *Staphylococcus aureus*. *Microbiology* 149, 389–398.

McKenna, A., Hanna, M., Banks, E., Sivachenko, A., Cibulskis, K., Kernytsky, A., et al. (2010). The genome analysis toolkit : A MapReduce framework for analyzing next-generation DNA sequencing data. *Genome Res.* 20, 1297–1303.

Morishita, T., Tamura, N., Makino, T., and Kudo, S. (1999). Production of menaquinones by lactic acid bacteria. *J. Dairy Sci.* 82, 1897–1903.

Myneni, V., and Mezey, E. (2018). Immunomodulatory effect of vitamin K2 : Implications for bone health. *Oral Dis.* 24, 67–71.

Picard Toolkit (2019). *Broad Institute, GitHub Repos. Available at: https://broadinstitute.github.io/picard/ [Accessed July 23, 2020].*

Plaza, S. M., and Lamson, D. W. (2005). Vitamin K2 in bone metabolism and osteoporosis. *Altern. Med. Rev.* 10, 24–35.

Rezaïki, L., Cesselin, B., Yamamoto, Y., Vido, K., Van West, E., Gaudu, P., et al. (2004). Respiration metabolism reduces oxidative and acid stress to improve long-term survival of *Lactococcus lactis*. *Mol. Microbiol.* 53, 1331–1342.

Rezaïki, L., Lamberet, G., Derré, A., Gruss, A., and Gaudu, P. (2008). *Lactococcus lactis* produces short-chain quinones that cross-feed Group B Streptococcus to activate respiration growth. *Mol. Microbiol*. 67, 947–957.

Rochat, T., Boudebbouze, S., Gratadoux, J.-J., Blugeon, S., Gaudu, P., Langella, P., et al. (2012). Proteomic analysis of spontaneous mutants of *Lactococcus lactis*: Involvement of GAPDH and arginine deiminase pathway in H2O2 resistance. *Proteomics* 12, 1792–805.

Sato, T., Yamada, Y., Ohtani, Y., Mitsui, N., Murasawa, H., and Araki, S. (2001). Efficient production of menaquinone (vitamin K2) by a menadione-resistant mutant of *Bacillus subtilis*. *J. Ind. Microbiol. Biotechnol.* 26, 115–120.

Schurgers, L. J., Teunissen, K. J. F., Hamulyak, K., Knapen, M. H. J., Vik, H., and Vermeer, C. (2007). Vitamin K – containing dietary supplements: comparison of synthetic vitamin K1 and natto-derived menaquinone-7. *Blood* 109, 3279–3283.

Schurgers, L. J., and Vermeer, C. (2002). Differential lipoprotein transport pathways of K-vitamins in healthy subjects. *Biochim. Biophys. Acta* 1570, 27–32.

Schwalfenberg, G. K. (2017). Vitamins K1 and K2: The Emerging Group of Vitamins Required for Human Health. *J. Nutr. Metab.* 2017, 6254836.

Søballe, B., and Poole, R. K. (2000). Ubiquinone limits oxidative stress in *Escherichia coli*. *Microbiology* 146, 787–796.

Solem, C., Koebmann, B. J., and Jensen, P. R. (2003). Glyceraldehyde-3-phosphate dehydrogenase has no control over glycolytic flux in *Lactococcus lactis* MG1363. *J. Bacteriol.* 185, 1564–1571.

Song, A. A. L., In, L. L. A., Lim, S. H. E., and Rahim, R. A. (2017). A review on *Lactococcus lactis*: from food to factory. *Microb. Cell Fact.* 16, 55.

Sybesma, W., Hugenholtz, J., de Vos, W. M., and Smid, E. J. (2006). Safe use of genetically modified lactic acid bacteria in food. Bridging the gap between consumers, green groups, and industry. *Electron. J. Biotechnol.* 9, 424–448.

Tachon, S., Brandsma, J. B., and Yvon, M. (2010). NoxE NADH oxidase and the electron transport chain are responsible for the ability of *Lactococcus lactis* to decrease the redox potential of milk. *Appl. Environ. Microbiol.* 76, 1311–1319.

Tsukamoto, Y., Kasai, M., and Kakuda, H. (2001). Construction of a *Bacillus subtilis* (natto) with high productivity of vitamin K2 (menaquinone-7) by analog resistance. *Biosci. Biotechnol. Biochem.* 65, 2007–2015.

Tyanova, S., Temu, T., Sinitcyn, P., Carlson, A., Hein, M. Y., Geiger, T., et al. (2016). The Perseus computational platform for comprehensive analysis of (prote)omics data. *Nat. Methods* 13, 731–740.

van Mastrigt, O., Mager, E. E., Jamin, C., Abee, T., and Smid, E. J. (2018). Citrate, low pH and amino acid limitation induce citrate utilization in *Lactococcus lactis* biovar diacetylactis. *Microb. Biotechnol.* 11, 369–380.

Vermeer, C., and Schurgers, L. J. (2000). A comprehensive review of vitamin K and vitamin K antagonists. *Hematol. Oncol. Clin. North Am.* 14, 339–353.

Vermeer, C. V. (2012). Vitamin K: the effect on health beyond coagulation – an overview. *Food Nutr. Res.* 56, 5329.

Vido, K., van Dorsselaer, A., Leize, E., Juillard, V., Gruss, A., and Gaudu, P. (2005). Roles of thioredoxin reductase during the aerobic life of *Lactococcus lactis*. *J. Bacteriol.* 187, 601–610.

Vizcaíno J. A., Csordas A., del-Toro N., Dianes J. A., Griss J., Lavidas I., et al. (2016). 2016 update of the PRIDE database and related tools. *Nucleic Acids Res.* 44(D1): D447-D456.

Wang, G., and Maier, R. J. (2004). An NADPH quinone reductase of *Helicobacter pylori* plays an important role in oxidative stress resistance and host colonization. *Infect. Immun.* 72, 1391–1396.

Wang, K. C., and Ohnuma, S. ichi (2000). Isoprenyl diphosphate synthases. *Biochim. Biophys. Acta - Mol. Cell Biol. Lipids* 1529, 33–48.

Willemoës, M., Kilstrup, M., Roepstorff, P., and Hammer, K. (2002). Proteome analysis of a *Lactococcus lactis* strain overexpressing gapA suggests that the gene product is an auxiliary glyceraldehyde 3-phosphate dehydrogenase. *Proteomics* 2, 1041–6.

Wiśniewski, J. R., Zougman, A., Nagaraj, N., and Mann, M. (2009). Universal sample preparation method for proteome analysis. *Nat. Methods* 6, 359–362.

Zwakenberg, S. R., den Braver, N. R., Engelen, A. I. P., Feskens, E. J. M., Vermeer, C., Boer, J. M. A., et al. (2017). Vitamin K intake and all-cause and cause specific mortality. *Clin. Nutr.* 36, 1294–1300.

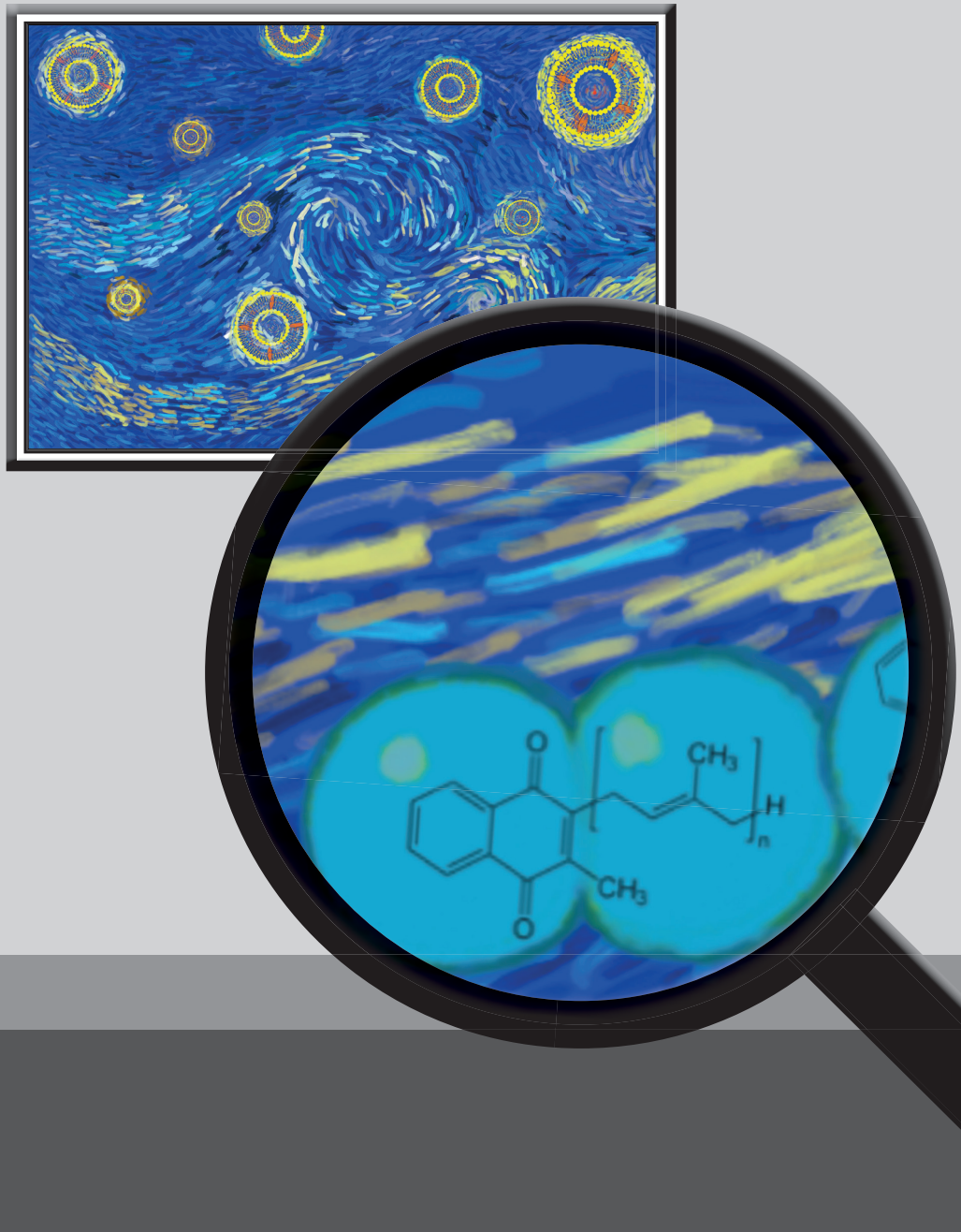
O
CH3
H
n
CH3
O

Chapter 5

Physiological roles of short-chain and long-chain menaquinones (vitamin K2) in *Lactococcus lactis*

Yue Liu, Nikolaos Charamis, Sjef Boeren, Joost Blok, Alisha Geraldine Lewis, Eddy J. Smid & Tjakko Abee

Accepted for publication in
Frontiers in Microbiology

Abstract

Lactococcus lactis is well-known for its occurrence and applications in dairy fermentations, but its niche extends to a range of natural and food production environments. *L. lactis* produces MKs (vitamin K2), mainly as the long-chain forms represented by MK-9 and MK-8, and a detectable amount of short-chain forms represented by MK-3. The physiological significance of the short-chain and long-chain MK forms in the lifestyle of *L. lactis* has not been investigated extensively. In this study, we used *L. lactis* MG1363 to construct mutants producing different MK profiles by deletion of genes encoding (i) a menaquinone-specific isochorismate synthase (*menF*), (ii) a geranyltranstransferase (*ispA*) and (iii) a prenyl diphosphate synthase (*llmg_0196*). These gene deletions resulted in (i) a non-MK producer (Δ*menF*), (ii) a presumed MK-1 producer (Δ*ispA*) and (iii) a MK-3 producer (Δ*llmg_0196*), respectively. By examining the phenotypes of the MG1363 wildtype strain and respective mutants, including biomass accumulation, stationary phase survival, oxygen consumption, primary metabolites, azo dye/copper reduction, and proteomes, under aerobic, anaerobic and respiration-permissive conditions, we could infer that short-chain MKs like MK-1 and MK-3 are preferred to mediate extracellular electron transfer (EET) and reaction with extracellular oxygen, while the long-chain MKs like MK-9 and MK-8 are more efficient in aerobic respiratory electron transport chain (ETC). The different electron transfer routes mediated by short-chain and long-chain MKs likely support growth and survival of *L. lactis* in a range of (transiently) anaerobic and aerobic niches including food fermentations, highlighting the physiological significance of diverse MKs in *L. lactis*.

Introduction

Lactococcus lactis is a lactic acid bacterium (LAB) that plays important roles in food fermentation processes, especially in the manufacturing of fermented dairy products: it is the main constituent of various dairy starter cultures used all over the world for the production of cheese, butter milk and sour cream (Cavanagh et al., 2015). The essential involvement of *L. lactis* in the fermentation of food raw materials highlights the interest in understanding the physiology and lifestyle of this bacterium.

Although *L. lactis* is best known for its application and occurrence in dairy products, it is found in a diverse range of natural niches such as the gastrointestinal tract of particular fish species and various plant materials (Cavanagh et al., 2015). In fact, the dairy isolates are believed to originate from plant isolates which successful adapted to thrive in the dairy environment (Kleerebezem et al., 2020). It has been suggested that the niche adaptation history is reflected in the lifestyle and adaptability of *L. lactis* in different environmental conditions. For instance, although *L. lactis* is classified as a facultative anaerobe with a fermentative metabolism, evidence has also been provided that in presence of oxygen and exogenous supplemented of heme, the organism can switch to aerobic respiration, a process enabled by the menaquinones (MKs, also referred to as vitamin K2) produced by *L. lactis* as electron carriers (Duwat et al., 2001; Brooijmans et al., 2009c). Notably, many other LAB species commonly applied in food fermentation processes, e.g., *Lactiplantibacillus plantarum* [previously referred to as *Lactobacillus plantarum* (Zheng et al., 2020)], have lost the ability to produce MKs (Pedersen et al., 2012). The ecological and physiological significance of MKs and their contribution to the successful applications of *L. lactis* in food fermentations is an interesting, but under-explored topic.

MKs accumulate in the cell membrane of producing bacteria (Walther et al., 2013). All MKs share a naphthoquinone structure but the variants differ in the length of sidechains consisting of isoprenyl units (Lenaz and Genova, 2013). In the abbreviation MK-n, the number of isoprenyl units in the side chain is indicated by n. The variants of MKs produced in different bacterial species are distinct and have even been proposed as taxonomic markers (Collins and Jones, 1981). For example, *Bacillus subtilis* produces MK-7, *Escherichia coli* produces mainly MK-8 and *Propionibacterium freudenreichii* produces MK-9(4H) (Walther et al., 2013). *L. lactis* is known to produce a range of MK variants, including MK-3, MK-5 through MK-10, among which MK-8 and MK-9 are the major forms (Brooijmans et al., 2009c; Chapter 3 of this thesis - Liu et al., 2019).

MK is the sole quinone that shuttles electrons in the respiratory electron transport chain (ETC) in Gram-positive bacteria, essential for both aerobic and anaerobic respiration processes (Kurosu and Begari, 2010). For respiring Gram-positive bacteria, MK is essential for growth and survival, and enzymes in the biosynthesis pathway in pathogens have therefore been considered as targets for developing antibacterial agents. As mentioned, functional respiration in response to oxygen and heme supplementation has been observed *L. lactis* strains, where the NADH dehydrogenase complex, MKs and the bd-type cytochrome complex (where heme is required as a cofactor) together form

a functional ETC in the cell membrane (Brooijmans et al., 2009c). *L. lactis* is not able to synthesis heme, thus heme has to be supplied exogenously to allow aerobic respiration in *L. lactis* (Pedersen et al., 2012). Nevertheless, heme is not considered to be present in dairy environment, and aerobic respiration is not a common or essential metabolic mode for *L. lactis* in food fermentations. In fact, in the production processes of fermented dairy product, *L. lactis* is considered to mainly encounter anaerobic conditions during the fermentation. However, *L. lactis* may be exposed to oxygen during starter culture production and during early stages in cheese production, i.e., aerobic conditions in absence of heme (Cretenet et al., 2014).

Under anaerobic conditions, MKs are known to endow some bacteria with the ability to utilize extracellular electron acceptors as alternative for oxygen, e.g., nitrate or fumarate, allowing anaerobic respiration as reported for *E. coli*, *Enterococcus faecalis* and *Lb. plantarum* (with exogenously supplied heme and MK). (Huycke et al., 2001; Brooijmans et al., 2009b; Kurosu and Begari, 2010). Moreover, MKs or precursors such as demethylmenaquinones (DMKs) or naphthoquinones were shown to be crucial for extracellular electron transfer (EET) in various Gram-positive bacteria species including *L. cremoris,* which has been shown to be able to reduce Cu^{2+} ions, transfer electrons to electrodes and decolorize azo dyes conceivably via flavin-based EET (Rezaïki et al., 2008; Freguia et al., 2009; Pérez-Díaz and McFeeters, 2009; Light et al., 2018, 2019).

Under aerobic conditions, *L. lactis* is known to be oxygen tolerant. (D)MKs were found to mediate reduction of exogenous oxygen to reactive oxygen species (ROS) such as superoxide in *L. lactis* and *En. faecalis* (Huycke et al., 2001; Rezaïki et al., 2008). On the other hand, Liu et al. obtained *L. lactis* vitamin K2 (MK) overproducers that showed high resistance to oxidative stress by laboratory evolution under aerobic conditions, although a direct relationship between elevated MK content and enhanced resistance to oxidative stress remains to be established (Chapter 4 of this thesis - Liu et al., 2021).

Interestingly, a significant amount of MKs was found in *L. lactis* stationary phase cells from different growth conditions: anaerobic/microaerophilic, aerobic and respiration-permissive (aerobic conditions with addition of heme) (Brooijmans et al., 2009c; Chapter 3 of this thesis - Liu et al., 2019). Notably, *L. lactis* produces multiple MK forms, whereas most MK producing bacteria are known to produce one specific form, or one major form with two adjacent forms in very minor amount. *L. lactis* produces noticeable amounts of both short-chain MKs represented by MK-3, and long-chain MKs represented by MK-8 and MK-9, and the distribution of the short-chain and long-chain MK forms alters depending on the growth conditions (Brooijmans et al., 2009c; Walther et al., 2013; Chapter 3 of this thesis - Liu et al., 2019). It remains to be elucidated whether the short-chain or long-chain forms of MKs are favored for particular functions under the different aeration conditions (anaerobic or aerobic) and metabolic modes (fermentation or respiration) that *L. lactis* could be exposed to in a range of natural and food production environments, for example in dairy fermentations.

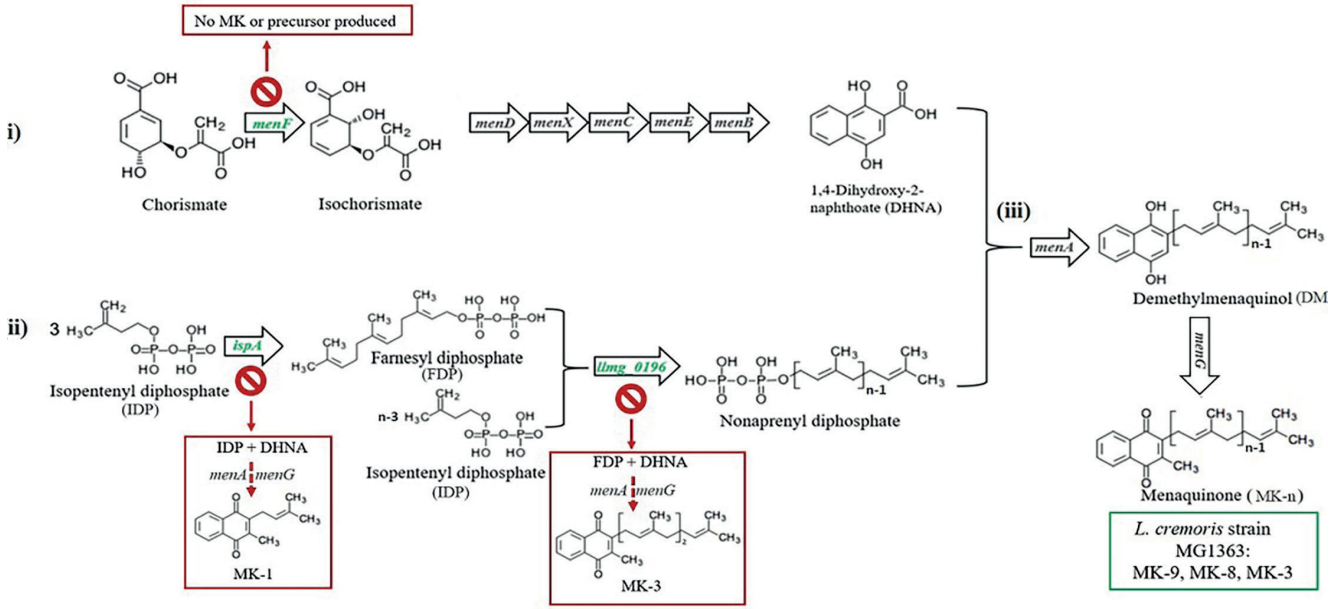

Figure 5.1. Predicted menaquinone biosynthesis pathway in *L. lactis* strain MG1363 and mutants. MK biosynthesis in *L. lactis* is predicted to follow a pathway consisting of three parts: (i) synthesis of the naphthoquinone structure (the head group), (ii) synthesis of the isoprenyl side chain (the tail group), and (iii) joining of the head and tail structures giving the MK. The head group synthesis starts with chorismate generated from the Shikimate pathway with the first step catalyzed by a menaquinone-specific isochorismate synthase (predicted encoding gene is *menF*), and the tail group synthesis starts with isopentenyl diphosphate (IPP), containing a single isoprene unit, generated from mevalonate pathway. For building the side chain, first a geranyltranstransferase (predicted encoding gene is *ispA*) is required to form farnesyl diphosphate (FPP) containing three isoprene units. More IPP is linked to FPP to form longer isoprene chains, and this step is catalyzed by a prenyl diphosphate synthase (predicted encoding gene is *llmg_0196*). The latter enzyme also is thought to play a role in determination of the length of the isoprene chain (Nagel et al., 2018; Johnston and Bulloch, 2020). Finally, the naphthoquinone head group - 1.4-dihydroxy-2-naphthoic acid (DHNA), and the polyprenyl tail group are combined by isoprenyl diphosphate:1,4-dihydroxy-2-naphthoate isoprenyltransferase to form *demethylmenaquinone (DMK), which* is methylated to give MK. Mainly MK-9, MK-8, MK-3 are formed in original *L. lactis* strain MG1363 (green box). Mutants Δ*menF,* Δ*ispA and* Δ*llmg_0196* are expected to produce no MK, only MK-1 and only MK-3, respectively. Genes targeted in this study shown in green color. Predicted MK production route and profiles in respective gene deletion mutants are shown in red boxes.

To examine the physiological significance of the short-chain and long-chain MKs in *L. lactis*, we constructed dedicated mutants using model strain *L. lactis* ssp. *cremoris* MG1363, based on annotation of putative genes in the MK biosynthesis pathway in *L. lactis* (Fig. 5.1) (Wegmann et al., 2007)(Brooijmans et al., 2009c): candidate genes encoding a menaquinone-specific isochorismate synthase (*menF*), a geranyltranstransferase (*ispA*) and a prenyl diphosphate synthase (*llmg_0196*) were deleted, with the prediction to create mutants producing no MK (Δ*menF*), only MK-1 (Δ*ispA*) and only MK-3 (Δ*llmg_0196*) respectively. These mutants, together with the original strain MG1363 producing mainly MK-9 and MK-8, allowed the study of functionality of short-chain and long-chain MK forms in *L. lactis* under anaerobic, aerobic and respiration-permissive conditions, where involvement of MKs in bacterial metabolism and physiology has been proposed. Under these conditions, relevant phenotypes including MK profile, biomass accumulation, viability/survival, oxygen consumption, electron transfer to extracellular acceptors (e.g., azo dye, Cu^{2+}), metabolites and proteomes were examined for strain MG1363 and mutants.

Materials and methods

Strains and conditions

Lactococcus lactis ssp. *cremoris* MG1363 and derived gene deletion mutants Δ*llmg_0196*, Δ*ispA* and Δ*menF* were cultivated in GM17 medium [M17 broth (Difco, BD Biosciences) supplemented with 0.5 % (w/v) glucose] at 30 °C. Cultivation times and conditions are specified in the Results section and figure legends for each particular case. For mutants with gene complementation, 5 µg/mL erythromycin was added to the medium.

For general static cultivation, cultures were incubated statically in closed Greiner tubes in maximal volume under normal atmosphere. For specified anaerobic cultivation, cultivation vessels with bacterial cultures were placed in anaerobic jars flushed with gas mix (10% CO_2, 10% H_2 and 80% N_2) using the anaerobic cycle programme by Anoxomat (WS9000, Mart Microbiology, Netherlands) unless specified otherwise. For aerobic cultivation, bacterial cultures filled up to 10% volume of Erlenmeyer flasks and were shaken at 180 rpm. Respiration-permissive cultivation conditions were the same as those applied for aerobic cultivations but with the addition of 2 µg/mL heme (hemin, Sigma).

E. coli strains used in the genetic modification procedures, harbouring plasmids with an erythromycin resistance gene (*ermAM*), were cultivated/selected in LB medium supplemented with 150 µg/mL erythromycin at 37 °C. Liquid cultures were shaken at 160 rpm with 90% headspace for no longer than 16 h, agar plates were incubated at normal atmosphere for maximal 22 h.

Genetic modification

Selection of targeted genes

The MK biosynthesis pathway in *L. lactis* MG1363 was predicted based on information retrieved from KEGG (Kanehisa and Goto, 2000) and genome of *L. lactis* MG1363 (Wegmann et al., 2007) and homology searches based on sequences from other bacteria with experimentally confirmed functions (Fig. 5.1). To obtain mutants of *L. lactis* MG1363 with different MK profiles, several genes were selected and subsequently targeted for gene deletion procedures. For the mutant producing no MK at all, it was decided that the gene involved in the first step of MK-specific synthesis pathway would be the target, to eliminate possible interference of intermediate products on the mutant phenotype (Fig. 5.1). We used BLAST to identify MenF homologs in the microbial protein database (Joint Genome Institute) (Chen et al., 2019). Gene product of *menF* (*llmg_1828*) in *L. lactis* MG1363 was identified with 26% identity with MenF protein sequence (Uniprot ID: P38051) from *E.coli* K12, for which the function has been confirmed (Daruwala et al., 1996), and was chosen as the first target gene to delete in strain MG1363. For the mutant producing short-chain MKs, genes encoding the geranyltranstransferase and prenyl diphosphate synthase were the targets. Combining previous knowledge (Kobayashi et al., 2003), sequences of genes *hepT* (P31114), *hepS* (P31112) and *yqiD* (P54383) from *Bacillus subtilis* 168 were used to search for homologs in *L. lactis* MG1363 using BLAST. No sequences similar to *B. subtilis hepS* were found in *L. lactis* MG1363. Moreover, *ispB* (*llmg_1110*), *llmg_0196* and *ispA* (*llmg_1689*) in *L. lactis* MG1363 were identified with 34%, 31% and 35% identity to *B. subtilis hepT* respectively. Finally, *ispB* (*llmg_1110*), *llmg_0196* and *ispA* (*llmg_1689*) were identified with 30%, 28% and 45% identity to *B. subtilis yqiD* respectively. Genes encoding *ispB* (*llmg_1110*), *llmg_0196* and *ispA* (*llmg_1689*) were all chosen as the target genes for modifying MK side chains to obtain mutants producing only MK-3 or MK-1 (Fig. 5.1). The *ispB* (*llmg_1110*) deletion mutant did not show any alteration in MK profile compared to MG1363 and will not be discussed in further details in this study.

Plasmid construction

Gene deletion in *L. lactis* MG1363 was achieved by homologous recombination. To construct the plasmids for gene deletion, the upstream and downstream homologous regions of 700 - 800 bp of the target genes were amplified, and desired restriction sites were introduced by PCR using primers listed in supplementary Table S5.1. Phusion High-fidelity PCR kit (Thermo Fisher Scientific) was used according to manufacturer's instruction. Both upstream and downstream homologous regions of each target gene were inserted in plasmid pCS1966 [gift from Solem et al. (Solem et al., 2008)] by restriction digestion and ligation following basic guidelines provided with the enzymes (Thermo Fisher Scientific). In brief, restriction site PstI was used to connect the upstream and downstream homologous regions of each target gene, HindIII and XbaI sites were used to insert the two homologous regions to the backbone of pCS1966. As a result, plasmid pYL005, pYL004 and pYL003 harboring the surrounding homologous regions of *menF*, *llmg_0196* and *ispA*, respectively, were constructed.

For gene complementation, promoter regions (ca. 50 bp upstream of the start codon) and open reading frames of *menF*, *llmg_0196* and *ispA* were amplified by PCR using primers listed in supplementary

Table S5.2. PCR products for each gene were inserted in the backbone (8301 bp fragment obtained by XbaI and BglII digestion) of plasmid pMSP3545 [gift from Gary Dunny (Bryan et al., 2000), Addgene plasmid # 46888] using NEBuilder HiFi DNA assembly cloning kit (New England Biolabs) according to manufacturer's instruction. As a result, p45-*menF*, p45-0196 and p45-*ispA* containing the promoter and gene sequences of *menF*, *llmg_0196* and *ispA*, respectively, were constructed.

Assembled plasmids were first transformed into *E. coli* competent cells Mix & Go Zymo 5α (Zymo research) according to product manuals, and transformed candidates were made into liquid culture for plasmid isolation. Assembled plasmids were checked for correctness by restriction digestion analysis after propagation in transformed *E. coli*. The correctness of PCR amplified sequences were checked by Sanger sequencing (BaseClear, Leiden, Netherlands).

Transformation and homologous recombination in L. lactis

For gene deletion, plasmid pYL005, pYL004 and pYL003 were separately transformed into MG1363 with the protocol described by (Holo and Nes, 1989) with the following modifications: MG1363 was cultured in SMGG media (M17, 0.5 M Sucrose, 0.5% Glucose and 0.5% Glycine) till mid-log phase (OD_{600} = 0.6 - 0.9). An additional washing step was performed in between the original two washing steps, with 0.5 volume EDTA washing buffer (0.05 M EDTA, 0.5 M sucrose, 10% glycerol). For transformation, 500 – 1000 ng plasmid pYL005, pYL004 or pYL003 in volume 1 - 2 µL was added. Electroporation was done using the Gene Pulser Xcell Electroporation Systems (Bio-Rad) at 2500 V, 25 µF, 200 Ω. Cells were plated on selection plates (GM17, 1.5% agar, 0.5 M sucrose and 3 µg/mL erythromycin), and were incubated at 30 °C for 2-3 days till colonies emerge.

At this stage the plasmids, having no replication origin in *L. lactis*, are integrated into the genome of MG1363 at either homologous region of the target genes. To eliminate the plasmid backbone and achieve gene deletion, transformants were inoculated in 2 mL SA medium (Jensen and Hammer, 1993) containing 1% glucose and incubated at 30 °C overnight. Then they were diluted 10x in SA (1% glucose) medium and incubated at 30 °C for 6 h. The culture was then plated on SA (1% glucose) agar plates supplemented with 10 µg/mL 5-Fluoroorotate (Sigma). Plates were incubated at 30 °C until colonies emerge. Due to the *oroP* gene on the plasmid of pCS1966, the presence of 5-fluoroorotate selects for mutants that have eliminated the plasmid backbone. From these mutants, the ones with gene deletion were selected by PCR (DreamTaq DNA polymerase, Thermo Fisher Scientific) using the primers listed in supplementary material Table S5.3.

For gene complementation, p45-*menF*, p45-0196 and p45-*ispA* were transformed into mutants Δ*menF*, Δ*ispA* and *llmg_0196* respectively with the electroporation protocol described above. Transformants were checked by PCR (DreamTaq DNA polymerase, Thermo Fisher Scientific) using the primers listed in supplementary material Table S5.2.

MK analysis

MKs were extracted from cells as described previously (Chapter 3 of this thesis - Liu et al., 2019). Briefly, the biomass was first treated with lysozyme and then MKs were extracted with organic solvent n-hexane and eventually dissolved in iso-propanol. All samples were diluted in methanol and subjected to analysis in the ultra-performance liquid chromatography (Thermo Scientific Vanquish) coupled with mass spectrometry (Thermo Q-Exactive hybrid quadrupole-Orbitrap) (UPLC–MS), exactly as described in (Chapter 4 of this thesis - Liu et al., 2021). Calculations from analytical standards were performed as described previously (Chapter 3 of this thesis - Liu et al., 2019).

Biomass quantification

For cell dry weight (CDW) determination, PBS washed cell pellets from bacterial cultures were kept at 80 °C for 48-72 h to evaporate water content. The dried biomass was then weighed.

For optical density (OD) determination, OD_{600} of cell cultures was measured by a spectrophotometer (600 nm; path length 10 mm).

Viable cell count enumeration

Bacterial cultures were subjected to serial dilution series in 96-well plates using PBS. Each dilution was spotted (10 µL) in triplicate on GM17 agar plates. Agar plates were incubated at 30 °C for 24 hours under microaerobic conditions before colonies were counted.

Oxygen consumption rate analysis

The measurement and calculation of oxygen consumption rate in *L. lactis* were performed exactly as described previously (Chapter 4 of this thesis - Liu et al., 2021).

Decolorization of azo dyes

Most azo dyes are not permeable to the cell membrane, and get decolorized upon reduction (Fang et al., 2019). Therefore, here we use the decolorization of an azo dye as an indicator for EET.

Strains were all cultivated under anaerobic conditions overnight in GM17 to obtain biomass for oxygen consumption analysis. The cells were harvested and washed in PBS once, and OD_{600} was standardized to 1 in PBS. Azo dye Reactive Black 5 (Sigma) was added to the cell suspension at a final concentration of 0.005%. The infusion bottles were flushed with N_2 gas for 2 min to ensure an anaerobic environment. Reaction was at 30 °C and was initiated by adding glucose to a final concentration of 1%. OD of cell-free supernatant was followed for 4 h with 1 h interval at 595 nm. The OD_{595} at time 0 h was regarded as 100% colour intensity. The absolute value of the initial slope of the linear correlation between colour intensity and time for each measurement was taken as the absolute azo dye decolorization rate. Thereafter, a relative azo dye reduction rate was calculated by comparing the absolute decolorization rate among the strains, setting the highest absolute decolorization rate as 100%.

Reduction of copper ions

The reduction of Cu^{2+} was measured indirectly in *L. lactis*. When Cu^{2+} is reduced to the toxic species Cu^{+}, growth of *L. lactis* will be inhibited (Abicht et al., 2013). Therefore, inhibition of growth of *L. lactis* was used as an indication of Cu^{2+} reduction.

Strains were cultivated statically in GM17 overnight, and then the cultures were diluted to an OD_{600} value of 0.1 in fresh GM17. For Cu^{2+} reduction tests, 300 nM $CuCl_2$ was added to the media, and for growth controls $CuCl_2$ was not added. For anaerobic cultivation, aliquots of 450 µL were brought into 100-well Honeycomb microplates (ThermoFisher) and incubated at 30 °C for 48 h in Bioscreen C (ThermoFisher), where the OD_{600} was measured at 1 h intervals. For aerobic cultivation, aliquots of 350 µL were transferred to microplates which were subsequently incubated with continuous shaking at medium intensity. For respiration-permissive conditions, cultures were incubated the same way as for aerobic conditions, albeit with the addition of 2 µg/mL heme (hemin, Sigma).

The time to reach (TTR) OD_{600} value 0.4 was used as a measurement of growth; the factor difference between TTRs in the test of 300 nM $CuCl_2$ and in the growth control without $CuCl_2$ was eventually used as the indicator of Cu^{2+} reduction-induced growth inhibition/toxicity.

Metabolite analysis

Metabolites including lactate, formate, acetate, acetoin, ethanol and succinate were measured in cell-free supernatant from overnight cultures by high-performance liquid chromatography (HPLC) analysis exactly as described previously (Chapter 4 of this thesis - Liu et al., 2021). The amount of each metabolite measured in uncultured GM17 medium was used as level zero to calculate the production or consumption of metabolites in the bacterial cultures.

Proteomics analysis

Cells from overnight culture (16 h) were used for proteomics analysis. For each strain and condition combination, samples were collected from three independent experiments. Sample preparation, LCMS analysis and data processing were performed exactly as described previously (Chapter 4 of this thesis - Liu et al., 2021). The proteome of *L. lactis* MG1363 (UniProt ID UP000000364) was used as the protein database.

Data analysis

Statistical significance analysis was performed in JASP (0.11.1) (Love et al., 2019) using two-way analysis of variance (ANOVA). Post hoc multiple comparisons were conducted using Tukey's test (2-sided) and in all cases the control group was *L. lactis* MG1363 (*$P \leq 0.05$).

Results

MK profiles in mutants Δ*menF*, Δ*ispA* and Δ*llmg_0196*

First, we evaluated the gene deletion mutants derived from *L. lactis* strain MG1363, by examining whether the MK profiles of the respective mutants were as predicted *in silico*. Wildtype strain MG1363 is known to produce mainly MK-8 and MK-9, but also MK-3 and a minor amount of other forms. The three gene deletion mutants were predicted to produce either no MK (Δ*menF*), only MK-1 (Δ*ispA*) or only MK-3 (Δ*llmg_0196*) based on the putative roles of respective gene products in the MK biosynthesis pathway (Fig. 5.1). The MK profiles as well as other phenotypes of strain MG1363 and the mutants were evaluated under three cultivation conditions (Fig. 5.2A): anaerobic, aerobic and respiration-permissive (meaning aerobic cultivation with heme supplementation).

Under all three tested cultivation conditions, substantial amounts of MKs mainly in the forms of MK-8 and MK-9, and noticeable amounts of MK-3 could be found in the biomass of wildtype strain MG1363. In addition, minor amounts of MK7 and MK-10 were also detected (Fig. 5.2A, supplementary Fig. S5.1A). The total amount of MKs in MG1363 was highest when cultivated under aerobic conditions, reaching 90 nmol/g cell dry weight (CDW), followed by respiration-permissive conditions of approximately 70 nmol/g CDW, while the amount found in cultures growing under anaerobic conditions was the lowest, less than 60 nmol/g CDW.

MG1363Δ*llmg_0196* produced solely MK-3 in the biomass, with the highest amount of about 25 nmol/g CDW was observed under aerobic and respiration-permissive conditions, and 12 nmol/g CDW under anaerobic conditions, confirming the hypothesis that gene *llmg_0196* encodes a (nona)prenyl diphosphate synthase. The molar amount of MK-3 produced in *Δllmg_0196* was higher than the MK-3 amount found in wildtype MG1363, but counted up to only one-third of the total MK amount in MG1363.

It was expected that mutant Δ*menF* would not produce MKs at all, and Δ*ispA* would produce only MK-1. Indeed, MG1363Δ*menF* showed no MK production except for trace amounts of MK-9 under anaerobic conditions (2 nmol/g CDW). MG1363Δ*ispA* showed low concentrations (3-5 nmol/g CDW) of MK-9 in all three conditions, while MK-1 was not detected.

Besides examining the MK profiles in the biomass of *L. lactis*, the cell-free supernatants of bacterial cultures were also examined for the presence of MKs. In all strains, no MK was detected in the culture supernatant except for Δ*llmg_0196* culture: a detectable amount of MK-3 was found in the supernatant, counting to 2% of the MK-3 quantity found in the cells obtained from the same culture.

When the mutants were complemented with the respective genes, the MK production levels were restored and profiles were similar to the original MG1363 (Fig. 5.2B, supplementary Fig. S5.1B).

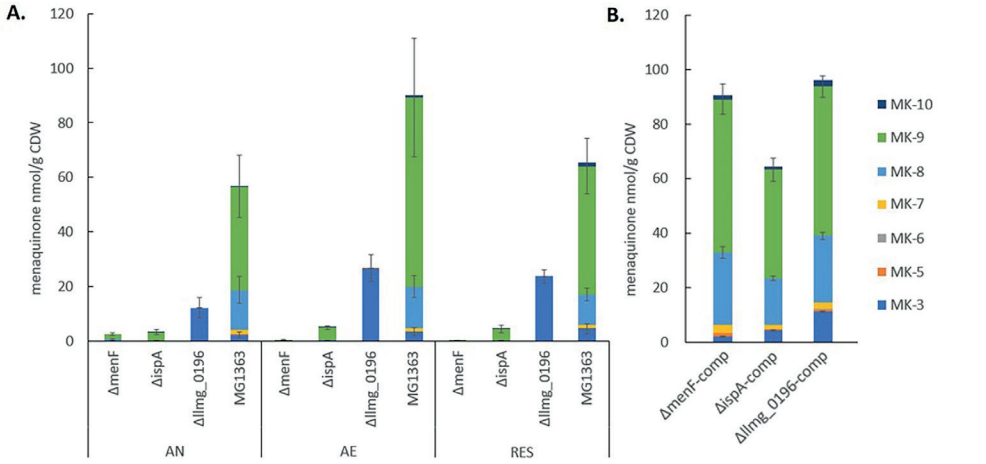

Figure 5.2. MK content in the biomass of *L. lactis* strains. A) MK content in strain MG1363 and mutants with gene deletions. All strains were cultivated in GM17 media under indicated conditions for 16-18 hours at 30 °C before MKs were extracted from the biomass. AN: anaerobic; AE: aerobic; RES: respiration-permissive, i.e. supplement of both heme and aeration. Data from three independent experiments. B) MK content in mutants with respective gene complementation. Strains were cultivated under anaerobic conditions. Data from four biological replicates. Error bars show SEM for MK-3, MK-8 and MK-9.

Anaerobic conditions: mutants showed distinct phenotypes in azo dye and Cu^{2+} reduction

Under anaerobic conditions, all mutants showed similar biomass accumulation as compared to wildtype MG1363 after overnight cultivation, which was about 1 g/L in cell dry weight (Fig. 5.3A, and OD measurement in supplementary Fig. S5.2A showed identical trend). The presumed MK-1 producer *ΔispA* and MK-3 producer *Δllmg_0196* showed 1-2 log higher survival than non-MK producer *ΔmenF* and wildtype MG1363 (MK-9, 8, 3 producer) after prolonged cultivation for 72 h (Fig. 5.3C).

The most distinct phenotypes among the mutants under the anaerobic conditions were observed when subjecting the mutants to an azo dye reduction (decolorization) and a Cu^{2+} reduction test. In these tests, indicators for the functionality of the different forms of MKs in *L. lactis* EET, which are mostly described for anaerobic conditions, were obtained. In the azo dye reduction test, *ΔispA* showed the highest rate of decolorization among all strains (Fig. 5.3D, and example pictures of azo dye discoloration are provided in supplementary Fig. S5.4). The reduction rates for strains MG1363, *Δllmg_0196* and *ΔmenF* were 65%, 75% and 30% as compared to *ΔispA*. Observations in line with the azo dye decolorization test were obtained from the Cu^{2+} reduction test, which was reflected by the degree of growth inhibition in presence of Cu^{2+} (Fig. 5.3E). Strain *ΔmenF* was least inhibited in growth (factor 2) and *ΔispA* was most inhibited (factor 8), while wildtype strain MG1363 and the MK-3 producer *Δllmg_0196* showed an intermediate degree of growth inhibition (factor 4) under anaerobic conditions.

The primary metabolite profiles of MG1363 and mutants were mostly similar among each other under anaerobic conditions: all strains produced mainly lactate (ca. 55 mM) and hardly any acetate or acetoin (Fig. 5.4A). The analysis of the succinate concentration in culture supernatants revealed that *ΔispA* produced noticeable amount of succinate (0.5 mM) while in cultures of the other strains succinate was not detectable indicating consumption of the small amount of succinate present in M17 media, and this effect is most pronounced under anaerobic conditions (Fig. 5.4B).

Aerobic conditions: mutants showed distinct phenotypes in long-term survival and Cu^{2+} reduction

Under aerobic conditions, all mutants showed similar biomass accumulation as compared to the wildtype strain MG1363 after overnight cultivation. The biomass yields were found to be at the same level as those observed under anaerobic conditions (Fig. 5.3A, supplementary Fig. S5.2A). Also the oxygen consumption rates for all strains were similar, ranging between 80 and 100 nmol/(min x OD unit) (Fig. 5.3B). The primary metabolite profiles of all strains cultivated under aerobic conditions were also similar to each other, with a small decrease in lactate (by 5 mM) and an increase in acetate (by 5 mM) concentration as compared to the anaerobic conditions (Fig. 5.4A).

The tested strains showed distinct phenotypes in survival when cultivated for a prolonged period of time under aerobic conditions (Fig. 5.3C): the presumed MK-1 producer *ΔispA* showed 1 log lower viability than the other strains after 24 h cultivation, and the difference even further increased after 48 h. While the culture of the non-MK producer *ΔmenF* remained at a viable plate count of 10 log CFU/mL, for strain *ΔispA* this value was lowered to 4 log CFU/mL, followed by the MK-3 producer *Δllmg_0196* and MK-9, 8, 3 producer MG1363 (6-7 log CFU/mL). After 72 h, none of the strains showed detectable viability (below 2 log CFU/mL) except strain *ΔmenF* which stood out with 8 log CFU/mL.

Big differences among the strains were also observed when the reduction of Cu^{2+} was tested under aerobic conditions (Fig. 5.3E). The growth inhibition, as reflected by the factor difference in the time it took the bacterial culture to grow from OD_{600} of 0.1 to 0.4 in absence and presence of Cu^{2+}, was used to indicate Cu^{2+} reduction as the reduced product Cu^{+} poses toxicity to the cells. The Cu^{2+} reduction induced growth inhibition was most severe with strain *ΔispA* (factor 11), even more than under anaerobic conditions. While *ΔmenF* remains the least inhibited (factor 2), *Δllmg_0196* showed less inhibition (factor 3) than under anaerobic conditions, followed by MG1363 (factor 4).

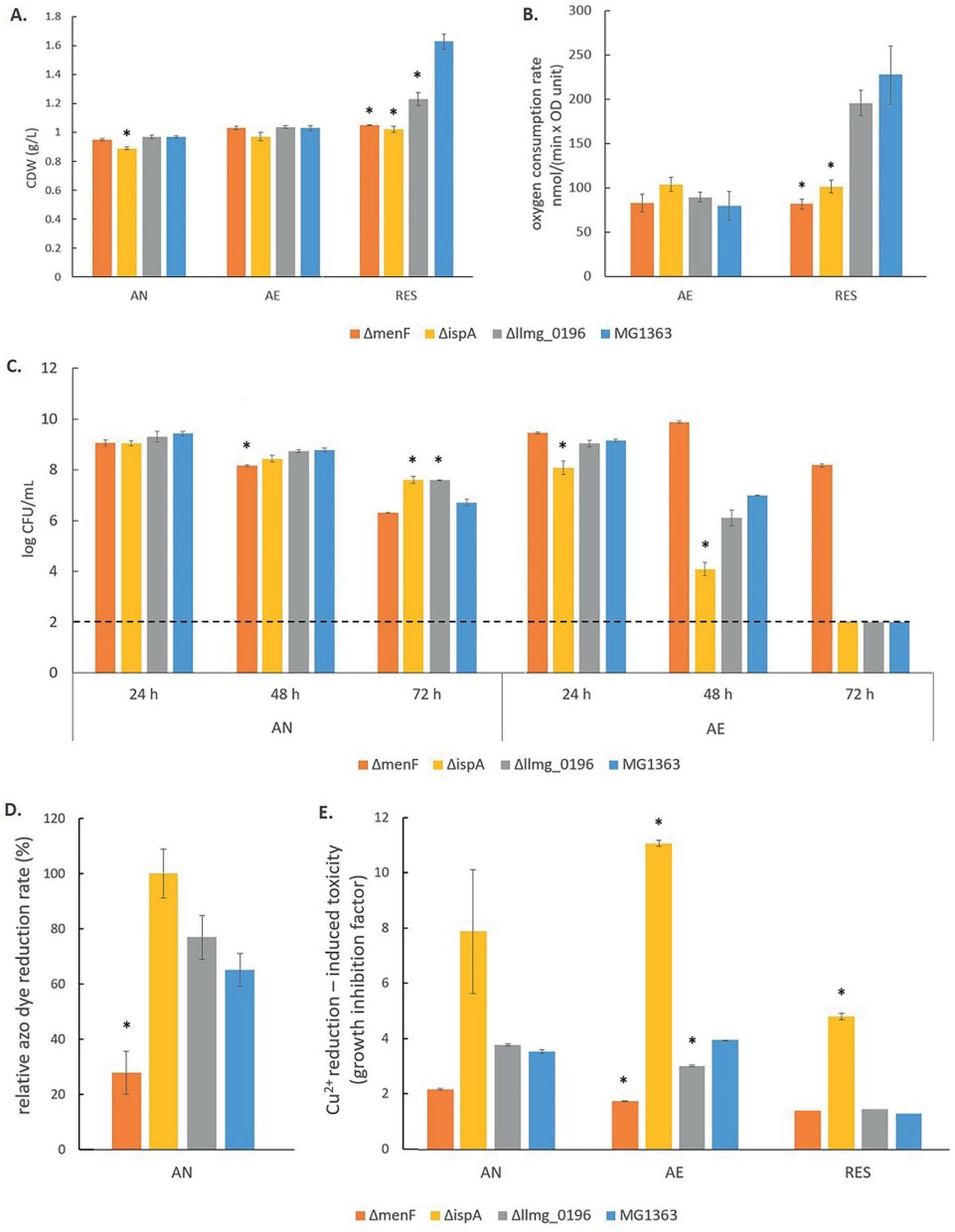

Figure 5.3. Phenotypical characterization of *L. lactis* MG1363 and mutants under anaerobic, aerobic and respiration-permissive conditions. A) Biomass accumulation. Cell dry weight (CDW) was measured for strains cultivated in GM17 medium under respective conditions for 16-18 hours at 30 °C. B) Oxygen consumption rate. For AE test, cells were obtained from overnight culture in GM17 media under anaerobic conditions. For RES test, cells were obtained from overnight culture in GM17 media supplemented with heme under anaerobic conditions. C) Viable plate count. All strains were cultivated in GM17 media under indicated conditions at 30 °C, culturability was determined at 24 h, 48 h and 72 h. All strains were inoculated at 10^6 CFU/mL at 0 h. The dotted line indicates the detection limit. D) Relative azo dye reduction rate. Biomass was obtained from overnight culture under anaerobic

conditions, washed and suspended in PBS. Initial azo dye reduction rate was measured by monitoring the decrease in color intensity (OD_{595}) for 1 hour, and the relative azo dye reduction rate was calculated by setting the initial azo dye reduction rate in Δ*ispA* as 100%. E) Cu^{2+} reduction-induced toxicity reflected by growth inhibition. Growth of strains in GM17 media was monitored in a Bioscreen at 30 °C in absence and presence of 300 nM $CuCl_2$, with initial OD = 0.1. The time to reach (TTR) OD = 0.4 was determined for each strain and condition, and the factor difference between the TTR in presence of 300 nM $CuCl_2$ and in absence of $CuCl_2$ is an indicator of growth inhibition, which reflects Cu^{2+} reduction. A) – D) data from three independent experiments, and E) data from biological triplicates. *shows significant ($p<0.05$) difference to MG1363. Error bars show SEM. AN: anaerobic; AE: aerobic; RES: respiration-permissive, i.e. heme and aeration.

Respiration-permissive conditions: mutants showed distinct phenotypes in biomass accumulation, oxygen consumption and metabolite profiles

Under respiration-permissive conditions, differences were observed among the tested strains in biomass accumulation after overnight cultivation (Fig. 5.3A, supplementary Fig. S5.2A). The MK-9, 8, 3 producer MG1363 reached about 1.7 g/L in cell dry weight, which is almost a doubling compared to the yield found in anaerobic and aerobic conditions. In the non-MK producer Δ*menF* and presumed MK-1 producer *ΔispA*, the biomass accumulation remained the same level (1 g/L dry weight) as in anaerobic and aerobic conditions. In the MK-3 producer *Δllmg_0196*, about 1.3 g/L dry weight was obtained under respiration-permissive conditions, which is significantly higher than in Δ*menF* and *ΔispA* but lower than MG1363. When the mutants were complemented with the respective genes, the biomass accumulations became similar to strain MG1363 (supplementary Fig. S5.3). The stationary phase survival for all strains under the respiration-permissive conditions were not significantly different throughout 72 h, all maintained at about 9 log CFU/mL (not shown).

The oxygen consumption rates in strain MG1363 and mutants under respiration-permissive conditions also showed differences. While *ΔmenF* and *ΔispA* remained at the same level as in aerobic conditions (80-100 nmol/(min x OD unit)), MG1363 and *Δllmg_0196* showed much higher oxygen consumption rates, reaching values over 200 nmol/(min x OD unit).

Less difference among the strains were observed for the Cu^{2+} reduction test under the respiration-permissive conditions, all strains showed no growth inhibition caused by Cu^{2+} reduction (factor 1) except for *ΔispA* which still showed an inhibition factor of 5.

The metabolite profiles of strain MG1363 and mutants differed the most under respiration-permissive conditions (Fig. 5.4A). Strain MG1363 produced the lowest concentration of lactate (ca. 20 mM) and the highest acetate (20 mM) and acetoin (10 mM) concentrations among all strains. The metabolite profiles of *ΔmenF* were similar under the respiration-permissive and aerobic conditions. For *ΔispA* and *Δllmg_0196,* about 40 mM lactate and ca. 10 mM acetate, 5 mM acetoin was observed under respiration-permissive conditions, showing differences in comparison to their own profiles under aerobic conditions. Moreover, the profiles of strains *ΔispA* and *Δllmg_0196* also differed largely from that of strain MG1363 under respiration-permissive conditions.

Additional insights provided by proteomics analysis

Finally, we examined the proteome profiles of strain MG1363 and mutants under anaerobic, aerobic and respiration-permissive conditions to further understand the phenotypic differences, which likely result from differences in bacterial metabolism, physiology and functionality caused by the short-chain and long-chain MK forms. Cells from stationary phase (16 h) were used for this analysis, and 1394 proteins in the sample set were quantified.

We examined changes in the proteome profile between the wildtype strain MG1363 and the MK mutants under the various cultivation conditions (Fig. 5.5). The proteome profiles obtained under anaerobic and aerobic conditions of cultures of the non-MK producer *ΔmenF* and the MK-3 producer *Δllmg_0196* were found to be very similar to that of strain MG1363. Under respiration-permissive conditions, *Δllmg_0196* showed a proteome profile similar to that of strain MG1363. In the comparison with strain MG1363, the presumed MK-1 producer *ΔispA* showed the most different proteome profile in all three conditions.

When closely examining the protein list, we identified proteins that are predicted to be involved in MK biosynthesis, aerobic respiration, aerobic growth and EET/anaerobic respiration (Table 5.1 – 5.4). Among proteins predicted to be part of the MK biosynthesis pathway (Table 5.1), we could first confirm that in respective mutants, the protein products of the deleted genes were indeed absent/ only showed signals at very low levels possibly due to cross contaminations in sample preparations and quantification errors. Most other MK biosynthesis proteins in this list showed constitutive presence in all strains and conditions, and for the protein product (A2RM75) of *menB* for example, a slightly higher level was observed under the aerobic conditions, which could contribute to the higher MK content in *L. lactis* under aerobic conditions observed in this study (Fig. 5.2). The protein product (A2RHR6) of the gene annotated as *menA* was not detected in all cases, but the homologous protein (A2RJB1) encoded by *ubiA* was present constitutively, suggesting that the gene annotated as *ubiA* is in fact functional in merging the head and tail group of MKs in strain MG1363 instead of the gene annotated as *menA*. The absence of protein product of *gerCA* (gene deletion mutant of *gerCA*) and *ispB* showed no influence on the MK profile) and inconsistent detection of *menX* product, also highlighted the necessity to experimentally confirm the functionality of the genes predicted in the MK biosynthesis pathway.

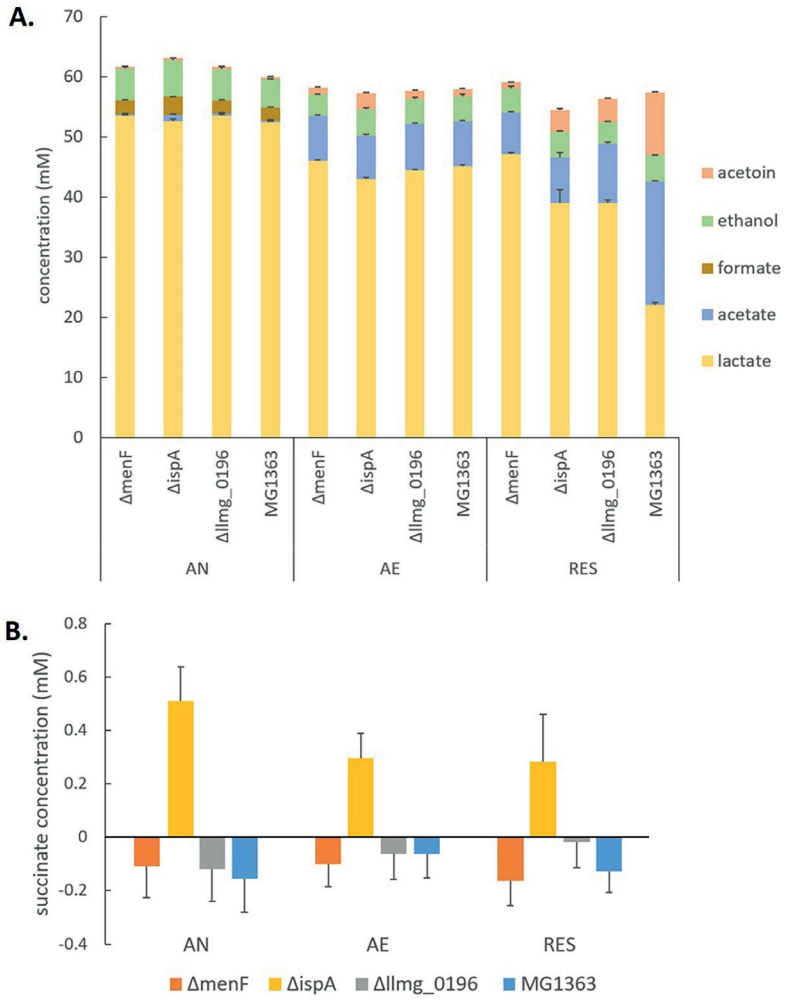

Figure 5.4. Metabolites in MG1363 and mutants. A) Concentration of primary metabolites including lactate, acetate, formate, acetoin and ethanol in the culture supernatant. B) Concentration of succinate in the culture supernatant. Metabolites were from the supernatant of cell cultures incubated in GM17 at 30 °C for 16-18 hours under indicated conditions. The concentration of metabolites in uncultured GM17 was used as level zero. A minor amount of succinate is present in GM17, and negative values from samples indicate consumption of the succinate present in GM17. AN: anaerobic; AE: aerobic; RES: respiration-permissive, i.e. heme and aeration. Data from three independent experiments, error bars show SEM.

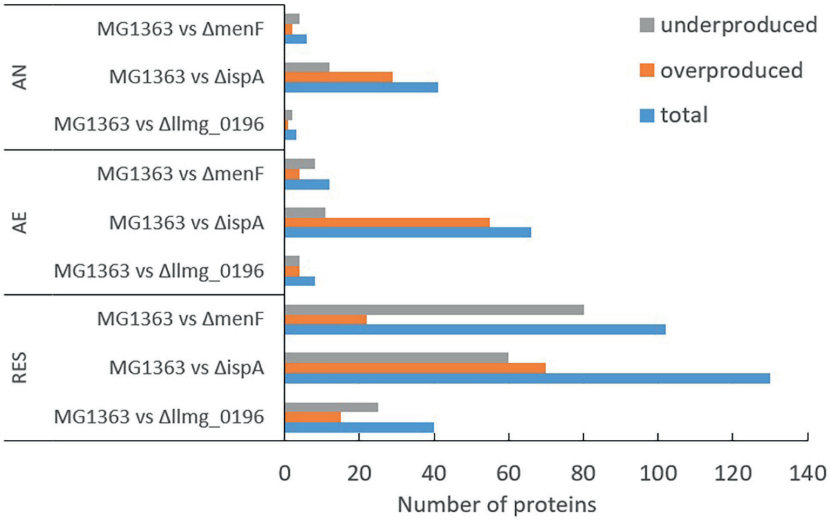

Figure 5.5. Differential proteome. Numbers of differentially produced proteins between MG1363 and mutants under each cultivation condition. Cells were obtained from cultures incubated in GM17 media at 30 °C for 16-18 hours under indicated conditions, samples from three independent experiments. AN: anaerobic; AE: aerobic; RES: respiration-permissive, i.e. heme and aeration. Proteins considered to be differently produced were selected when the LFQ intensity showed fold change ≥ 2 and $p \leq 0.05$.

When examining the proteins predicted to be involved in aerobic respiration (Table 5.2), including the NADH dehydrogenase and cytochrome *bd* oxidase in the respiratory ETC, we see that these proteins are present in all strains under all cultivation conditions at similar levels. Protein products of two heme traffic/synthesis genes *hemN* and *hemK* were constantly present in most cases. Two type II NADH dehydrogenases have been identified in the proteome, encoded by genes *noxA* and *noxB*.

We also examined other proteins relevant for the aerobic cultivation conditions (Table 5.3), including NADH oxidase and several oxidoreductases. In general proteins in this category were produced at higher levels under the aerobic conditions than anaerobic, as expected. The NADH oxidase (A2RIB7) in MG1363 and Δ*llmg_0196* was produced at a lower level in respiration-permissive conditions compared to aerobic conditions, which could be a result of the activated respiratory ETC taking over the reduction of oxygen in these two strains. Antioxidation proteins like thioredoxins (A2RIB5, A2RJC9, A2RI31) were in general more abundant under the aerobic conditions than anaerobic conditions. Moreover, the low level of glutaredoxin-like protein (Q48708) in the Δ*menF* under the aerobic conditions indeed reflects particular roles of MKs under oxidative/aerobic conditions.

Furthermore, we examined proteins predicted to be relevant for EET/anaerobic respiration (Table 5.4). While the NADH dehydrogenase encoded by *noxB* and most flavin synthesis or oxidoreduction related proteins were constantly present at similar levels in all strains and conditions, one riboflavin biosynthesis protein (A2RLE1) was more abundant in the MK-1 producer Δ*ispA* than other strains

under aerobic and respiration-permissive conditions. A fumarate reductase flavoprotein subunit protein (A2RL55) showed the highest level under anaerobic conditions in all strains, pointing to a potential role in anaerobic respiration.

Besides the proteins that are expected to be highly relevant for the several cultivation conditions and electron transfer pathways, much more information could be derived from the proteomics analysis. For example, when examining the proteins involved in primary metabolism (supplementary Table S5.4), we observed protein level changes across the three cultivation conditions in the tested strains, which corresponds to the production of primary metabolites (Fig. 5.4A). When examining the remainder of the proteins that showed significant changes across the strains or cultivation conditions, membrane proteins, oxidoreductases, stress proteins, metal ion (copper, iron, etc.) transporters, ATP-binding cassette (ABC) transporters were among the most often observed categories. A non-exhaustive list of these proteins is provided in supplementary Table S5.5.

Table 5.1. Quantity (Log LFQ intensity) of proteins predicted in the MK biosynthesis pathway in MG1363 and mutant under different cultivation conditions.

	Protein	Gene	AN				AE				RES			
	Function		MG1363	Δ*menF*	Δ*ispA*	Δ*0196*	MG1363	Δ*menF*	Δ*ispA*	Δ*0196*	MG1363	Δ*menF*	Δ*ispA*	Δ*0196*
Proteins predicted in the MK biosynthesis pathway in *L. lactis* MG1363	A2RM72	*menF*	8.30	**ND**	8.24	8.21	8.16	**ND**	8.23	8.16	8.07	**ND**	8.31	8.18
	Menaquinone-specific isochorismate synthase		(0.06)	-	(0.09)	(0.08)	(0.09)	-	(0.07)	(0.02)	(0.03)	-	(0.04)	(0.07)
	A2RM73	*menD*	8.95	**8.65**	9.08	9.02	9.09	8.84	9.17	9.11	9.05	8.86	9.11	9.04
	2-succinyl-5-enolpyruvyl-6-hydroxy-3-cyclohexene-1-carboxylate synthase		(0.04)	**(0.03)**	(0.01)	(0.01)	(0.04)	(0.00)	(0.02)	(0.06)	(0.02)	(0.03)	(0.02)	(0.02)
	A2RM74	*menX*	7.52	**ND**	7.53	6.96	7.46	6.93	7.70	7.23	ND	ND	**7.65**	6.94
	Putative 2-succinyl-6-hydroxy-2,4-cyclohexadiene-1-carboxylate synthase		(0.03)	-	(0.01)	(0.26)	(0.09)	(0.23)	(0.08)	(0.27)	-	-	**(0.03)**	(0.24)
	A2RM77	*menC*	8.13	8.12	8.03	8.10	8.09	8.02	8.17	8.05	8.12	8.15	8.18	8.22
	o-succinylbenzoate synthase		(0.04)	(0.05)	(0.01)	(0.08)	(0.02)	(0.05)	(0.04)	(0.04)	(0.05)	(0.01)	(0.04)	(0.03)
	A2RM76	*menE*	8.24	8.15	8.20	8.25	8.22	8.11	8.28	8.24	8.23	8.27	8.34	8.38
	2-succinylbenzoate--CoA ligase		(0.06)	(0.03)	(0.05)	(0.03)	(0.03)	(0.05)	(0.04)	(0.06)	(0.06)	(0.03)	(0.04)	(0.04)
	A2RM75	*menB*	9.65	9.59	9.59	9.67	9.90	9.85	9.80	9.93	9.91	9.87	9.82	9.88
	1,4-dihydroxy-2-naphthoyl-CoA synthase		(0.05)	(0.02)	(0.04)	(0.03)	(0.04)	(0.04)	(0.03)	(0.04)	(0.03)	(0.03)	(0.03)	(0.02)
	A2RHR5	*llmg_0196*	9.02	8.99	9.00	**7.07**	9.15	9.09	9.07	**8.00**	8.96	9.13	9.04	**7.16**
	Prenyl transferase		(0.04)	(0.04)	(0.02)	**(0.37)**	(0.03)	(0.01)	(0.06)	**(0.16)**	(0.04)	(0.02)	(0.05)	**(0.46)**
	A2RK94	*ispB*	8.66	8.58	8.73	8.73	8.74	8.69	8.74	8.71	8.57	8.66	8.66	8.63
	Similar to heptaprenyl diphosphate synthase component II		(0.02)	(0.04)	(0.03)	(0.01)	(0.02)	(0.04)	(0.03)	(0.04)	(0.03)	(0.05)	(0.03)	(0.02)
	A2RK95	*gerCA*	ND	ND	ND	ND	ND	ND	ND	ND	ND	ND	ND	ND
	Heptaprenyl diphosphate synthase component I		-	-	-	-	-	-	-	-	-	-	-	-
	A2RLU2	*ispA*	8.64	8.62	**ND**	8.59	8.58	8.54	**ND**	8.52	8.47	8.55	**ND**	8.53
	Geranyltranstransferase		(0.01)	(0.07)	-	(0.05)	(0.04)	(0.05)	-	(0.07)	(0.05)	(0.02)	**(0.00)**	(0.01)
	A2RHR6	*menA*	ND	ND	ND	ND	ND	ND	ND	ND	ND	ND	ND	ND
	Prenyltransferase, UbiA family		-	-	-	-	-	-	-	-	-	-	-	-
	A2RJB1	*ubiA*	7.87	7.85	7.88	7.90	7.91	7.88	7.82	7.91	7.84	7.92	7.92	7.87
	Putative prenyltransferase, UbiA family		(0.05)	(0.03)	(0.05)	(0.04)	(0.04)	(0.09)	(0.04)	(0.07)	(0.05)	(0.10)	(0.05)	(0.11)
	A2RJA5	*menG*	8.66	8.68	8.81	8.74	8.77	8.77	8.88	8.74	8.65	8.83	8.91	8.73
	Demethylmenaquinone methyltransferase		(0.04)	(0.05)	(0.03)	(0.05)	(0.03)	(0.04)	(0.03)	(0.05)	(0.03)	(0.03)	(0.03)	(0.02)

Values are average from samples collected from 3 independent experiments, SEM values are shown in brackets. Detection limit in Log LFQ intensity: 6.7; Δ*0196* = Δ*llmg_0196*. Values in mutants that are significantly different ($p < 0.05$, fold change > 2) from strain MG1363 under the same cultivation conditions are highlighted in bold letters.

Table 5.2. Quantity (Log LFQ intensity) of proteins involved in aerobic respiratory ETC in MG1363 and mutant under different cultivation conditions.

	Protein	Gene	AN				AE				RES			
	Function		MG1363	Δ*menF*	Δ*ispA*	Δ*0196*	MG1363	Δ*menF*	Δ*ispA*	Δ*0196*	MG1363	Δ*menF*	Δ*ispA*	Δ*0196*
Proteins involved in aerobic respiratory ETC	A2RLY0	***noxB***	10.02	10.00	10.01	10.02	10.01	9.97	10.05	10.03	9.93	10.00	10.04	9.97
	NADH dehydrogenase		(0.04)	(0.02)	(0.03)	(0.01)	(0.03)	(0.02)	(0.03)	(0.03)	(0.01)	(0.01)	(0.02)	(0.05)
	A2RLY1	*noxA*	9.70	9.54	9.50	9.56	9.73	9.61	9.61	9.65	9.59	9.61	9.64	9.62
	NADH dehydrogenase		(0.03)	(0.03)	(0.04)	(0.05)	(0.04)	(0.02)	(0.02)	(0.02)	(0.03)	(0.02)	(0.02)	(0.04)
	A2RHR4	*llmg_0195*	9.65	9.63	9.62	9.51	9.58	9.57	9.56	9.49	9.63	9.54	9.54	9.60
	Putative NADH dehydrogenase		(0.03)	(0.02)	(0.03)	(0.08)	(0.03)	(0.02)	(0.04)	(0.03)	(0.02)	(0.02)	(0.04)	(0.04)
	A2RMA6	*cydB*	8.76	8.77	8.65	8.69	8.65	8.58	8.51	8.62	8.47	8.60	8.45	8.69
	Cytochrome d ubiquinol oxidase, subunit II		(0.06)	(0.11)	(0.08)	(0.12)	(0.02)	(0.05)	(0.11)	(0.05)	(0.05)	(0.11)	(0.04)	(0.10)
	A2RMA7	*cydA*	8.71	8.85	8.75	8.86	8.85	8.73	8.62	8.84	8.72	8.79	8.52	8.72
	Cytochrome bd-I ubiquinol oxidase subunit I		(0.14)	(0.09)	(0.05)	(0.02)	(0.09)	(0.01)	(0.08)	(0.02)	(0.07)	(0.01)	(0.03)	(0.06)
	A2RIR7	*hemK*	8.22	8.16	8.27	8.15	7.99	7.83	8.24	7.84	7.81	7.95	**8.29**	7.84
	Release factor glutamine methyltransferase		(0.03)	(0.03)	(0.01)	(0.01)	(0.05)	(0.05)	(0.03)	(0.04)	(0.02)	(0.04)	**(0.05)**	(0.03)
	A2RL35	*hemN*	7.67	7.67	7.67	7.68	ND	**7.44**	**7.50**	**7.44**	7.46	6.93	7.59	7.13
	Coproporphyrinogen III oxidase		(0.05)	(0.06)	(0.07)	(0.04)	-	**(0.14)**	**(0.03)**	**(0.06)**	(0.03)	(0.23)	(0.03)	(0.22)

Values are average from samples collected from 3 independent experiments, SEM values are shown in brackets. Detection limit in Log LFQ intensity: 6.7; Δ*0196* = Δ*llmg_0196*.
Values in mutants that are significantly different ($p < 0.05$, fold change > 2) from strain MG1363 under the same cultivation conditions are highlighted in bold letters.

Table 5.3. Quantity (Log LFQ intensity) of proteins relevant for aerobic growth in general in MG1363 and mutant under different cultivation conditions.

	Protein	Gene	AN				AE				RES			
	Function		MG1363	Δ*menF*	Δ*ispA*	Δ*0196*	MG1363	Δ*menF*	Δ*ispA*	Δ*0196*	MG1363	Δ*menF*	Δ*ispA*	Δ*0196*
Proteins relevant for aerobic growth	A2RIB7	*noxE*	10.09	10.08	10.12	10.13	10.35	10.35	10.36	10.34	9.83	**10.39**	**10.30**	10.12
	NADH oxidase		(0.01)	(0.03)	(0.05)	(0.03)	(0.04)	(0.03)	(0.00)	(0.04)	(0.08)	**(0.03)**	**(0.02)**	(0.02)
	A2RM15	*noxC*	8.53	8.52	8.39	8.63	8.72	8.65	8.73	8.76	8.77	8.80	8.75	8.77
	NADH oxidase		(0.02)	(0.04)	(0.09)	(0.09)	(0.07)	(0.11)	(0.05)	(0.07)	(0.12)	(0.08)	(0.07)	(0.15)
	P0A4J2	*sodA*	9.57	9.59	9.59	9.66	9.68	9.77	9.62	9.73	10.13	**9.74**	**9.68**	9.91
	Superoxide dismutase [Mn]		(0.08)	(0.06)	(0.03)	(0.09)	(0.16)	(0.06)	(0.16)	(0.20)	(0.04)	**(0.10)**	**(0.07)**	(0.14)
	A2RIB5	*trxH*	9.40	9.37	9.30	9.35	9.60	9.54	9.52	9.53	9.72	9.52	9.49	9.52
	Thioredoxin H-type		(0.09)	(0.08)	(0.02)	(0.09)	(0.06)	(0.04)	(0.05)	(0.05)	(0.00)	(0.02)	(0.04)	(0.03)
	A2RJC9	*trxA*	9.94	9.99	9.78	9.91	10.22	10.03	10.18	10.23	10.34	10.19	10.09	10.24
	Thioredoxin		(0.10)	(0.15)	(0.03)	(0.02)	(0.05)	(0.04)	(0.10)	(0.10)	(0.05)	(0.05)	(0.11)	(0.14)
	A2RI31	*tpx*	9.75	9.77	9.72	9.82	10.09	10.06	10.03	10.08	10.19	10.11	10.05	10.14
	Thiol peroxidase		(0.03)	(0.02)	(0.08)	(0.09)	(0.05)	(0.04)	(0.02)	(0.01)	(0.02)	(0.03)	(0.04)	(0.04)
	Q48708	*nrdH*	8.64	8.69	7.97	8.80	9.11	**8.40**	9.09	9.04	9.30	**8.52**	9.07	**8.92**
	Glutaredoxin-like protein		(0.10)	(0.03)	(0.64)	(0.13)	(0.04)	**(0.03)**	(0.04)	(0.08)	(0.04)	**(0.09)**	(0.05)	**(0.04)**
	O32770	*gpo*	9.21	9.19	9.12	9.06	9.45	9.42	9.31	9.39	9.93	**9.38**	**9.35**	**9.61**
	Glutathione peroxidase		(0.01)	(0.04)	(0.09)	(0.04)	(0.07)	(0.02)	(0.03)	(0.06)	(0.03)	**(0.01)**	**(0.09)**	**(0.03)**

Values are average from samples collected from 3 independent experiments, SEM values are shown in brackets. Detection limit in Log LFQ intensity: 6.7; Δ*0196* = Δ*llmg_0196*. Values in mutants that are significantly different ($p < 0.05$, fold change > 2) from strain MG1363 under the same cultivation conditions are highlighted in bold letters.

Table 5.4. Quantity (Log LFQ intensity) of proteins relevant for EET/anaerobic respiration in MG1363 and mutant under different cultivation conditions.

	Protein	Gene	AN				AE				RES			
	Function		MG1363	Δ*menF*	Δ*ispA*	Δ*0196*	MG1363	Δ*menF*	Δ*ispA*	Δ*0196*	MG1363	Δ*menF*	Δ*ispA*	Δ*0196*
Proteins relevant for EET/anaerobic respiration	A2RLE1	*ribD*	9.11	9.11	9.20	9.05	8.43	8.34	**9.00**	8.35	9.06	**8.49**	9.24	8.96
	Riboflavin biosynthesis protein		(0.08)	(0.07)	(0.06)	(0.05)	(0.03)	(0.03)	**(0.02)**	(0.01)	(0.01)	**(0.03)**	(0.03)	(0.02)
	A2RLD9	*ribA*	9.64	9.70	9.82	9.58	9.63	9.71	9.70	9.62	9.61	9.62	9.72	9.65
	Riboflavin biosynthesis protein RibBA		(0.06)	(0.07)	(0.04)	(0.03)	(0.03)	(0.02)	(0.04)	(0.02)	(0.04)	(0.05)	(0.05)	(0.03)
	A2RL46	*ribC*	9.04	9.03	9.17	9.03	9.03	9.03	9.19	8.96	8.95	9.03	9.18	8.99
	Riboflavin biosynthesis protein		(0.02)	(0.01)	(0.04)	(0.03)	(0.08)	(0.02)	(0.03)	(0.02)	(0.02)	(0.01)	(0.03)	(0.01)
	A2RIR6	*llmg_0559*	8.15	8.17	8.11	8.21	8.12	8.29	8.17	8.22	8.18	8.22	8.21	8.22
	NADPH-flavin oxidoreductase		(0.10)	(0.10)	(0.09)	(0.04)	(0.07)	(0.02)	(0.09)	(0.06)	(0.07)	(0.02)	(0.12)	(0.08)
	A2RM04	*llmg_1759*	10.11	10.02	9.97	10.10	10.15	10.17	10.06	10.07	10.27	10.15	10.07	10.17
	Putative NADH-flavin reductase		(0.08)	(0.02)	(0.06)	(0.02)	(0.05)	(0.02)	(0.03)	(0.09)	(0.02)	(0.01)	(0.06)	(0.06)
	A2RL63	*apbE*	8.84	8.76	8.69	8.82	8.79	8.84	8.62	8.75	8.73	8.85	8.81	8.78
	FAD:protein FMN transferase		(0.01)	(0.02)	(0.04)	(0.05)	(0.02)	(0.04)	(0.02)	(0.03)	(0.03)	(0.01)	(0.03)	(0.02)
	A2RL55	*frdC*	10.19	10.15	10.05	10.17	9.84	9.87	9.68	9.79	9.56	**9.87**	9.70	9.76
	Fumarate reductase flavoprotein subunit		(0.04)	(0.04)	(0.03)	(0.04)	(0.06)	(0.03)	(0.02)	(0.10)	(0.05)	**(0.04)**	(0.01)	(0.02)
	A2RIA7	*azpR*	8.37	8.26	8.26	8.23	8.46	8.46	8.47	8.47	8.40	8.45	8.51	8.45
	FMN-dependent NADH-azoreductase		(0.02)	(0.01)	(0.08)	(0.01)	(0.05)	(0.05)	(0.03)	(0.04)	(0.05)	(0.05)	(0.05)	(0.04)

Values are average from samples collected from 3 independent experiments, SEM values are shown in brackets. Detection limit in Log LFQ intensity: 6.7; Δ*0196* = Δ*llmg_0196*. Values in mutants that are significantly different ($p < 0.05$, fold change > 2) from strain MG1363 under the same cultivation conditions are highlighted in bold letters.

Discussion

L. lactis is best-known for its occurrence and applications in dairy fermentations, but its niche extends to a range of natural and food production environments, where *L. lactis* encounters different growth conditions including anaerobic, aerobic and respiration-permissive conditions. *L. lactis* is one of the few LAB species that maintained the ability to produce MKs (vitamin K2), in both short-chain (MK-3) and long-chain forms (MK-9, MK-8). The physiological significance of the short-chain and long-chain MK forms in the lifestyle of *L. lactis* has not been investigated extensively. In this study, we constructed *L. lactis* mutants producing short-chain and long-chain MKs: deletion of genes *menF*, *ispA* and *llmg_0196* resulted in a non-MK producer, a presumed MK-1 producer and a MK-3 producer, respectively. Together with the wildtype MG1363 producing mainly MK-9 and MK-8, these mutants with gene deletions served to further elucidate the functionality of MKs in *L. lactis.* By exposing this set of strains to anaerobic, aerobic and respiration-permissive conditions, functionalities of long-chain and short-chain MKs in *L. lactis* under different environmental conditions could be inferred (Fig. 5.6).

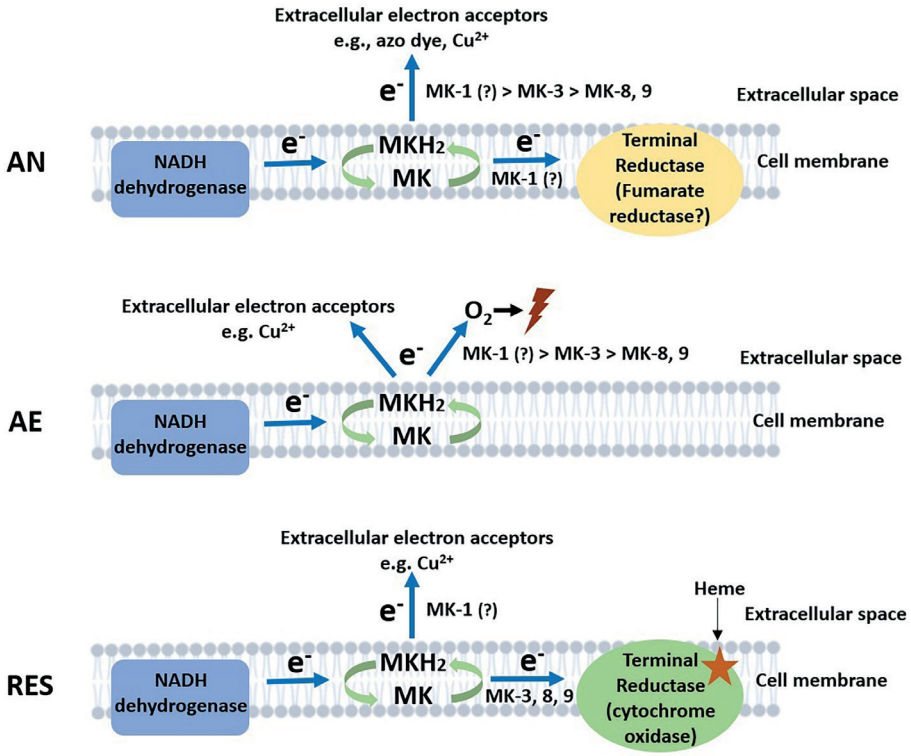

Figure 5.6. Proposed model of electron flows facilitated by MKs under anaerobic, aerobic and respiration-permissive conditions. The predominantly involved MK forms are annotated next to the arrows indicating electron flows, with ">" symbols indicate preferences. Lightning symbol represents loss of viability in the cells. AN: anaerobic; AE: aerobic; RES: respiration-permissive, i.e. heme and aeration. Note that the illustration is only a schematic presentation of proposed electron flow routes, the location of enzymes are not confirmed in this study.

We could confirm that *llmg_0196* indeed encodes a (nona)prenyl diphosphate synthase as the corresponding gene deletion mutant only produced MK-3. The level of MK-3 in Δ*llmg_0196* was lower than the total MK level in MG1363, indicating that there are feedback mechanisms influenced by the intermediate compounds of the MK biosynthetic pathway. Another possible explanation to this is a lower efficiency of the DHNA polyprenyltransferase (MenA) in incorporating the farnesyl diphosphate group (containing 3 isoprene units) to the head group.

Based on the observed MK profiles alone, it can be concluded that strains *ΔmenF* and *ΔispA* hardly produce MKs. The remaining low amount of MK-9 produced in strain *ΔispA* could be a result of additional activity of the prenyl diphosphate synthase encoded by *llmg_0196*. Combining other analyses that demonstrated the role of MKs, we saw distinct phenotypes of *ΔmenF* and *ΔispA*: in *ΔmenF,* phenotypes from all processes including aerobic respiration or copper reduction suggested absence of MK-related functions. In *ΔispA*, clear activities of e.g. azo dye/copper reduction could be observed, suggesting presence of (a) MK form(s) that was not detected in the MK profile analysis. It is most plausible that MK-1 was produced by *ΔispA* but was not revealed in the analysis, because the MK extraction method used in this study is based on hexane extraction of hydrophobic/lipophilic molecules. This method works well for long-chain MKs and lipids, but it is likely that MK-1 is too low in hydrophobicity to be extracted by hexane from the aqueous environment. Notably, this extraction method is commonly adopted for MK analysis in scientific research, which could mean that the presence and role of MK-1, if any, may have been missed so far in MK related studies.

Nevertheless, we could infer the function of MK-1 in the current study from the different phenotypes of the mutants. In this context it is worth mentioning that, we did not analyze the presence of any MK precursors such as demethylmenaquinones DMKs, previously studied in *L. lactis* (Rezaïki et al., 2008) and *Listeria monocytogenes* (Light et al., 2018). Here we focused on the MK forms with various side-chain length, and will therefore not discuss the effect of the methylation (DMK to MK) separately. Moreover, deletion of gene *ispA* as reported for other bacteria is expected to display pleiotropic effects including impaired growth (Krute et al., 2015). This was also observed for strain *ΔispA* in this study since *ΔispA* shows a slightly lower growth rate in comparison to the other strains (supplementary Fig. S5.2B).

Based on existing knowledge on MK roles in bacteria (Duwat et al., 2001; Koebmann et al., 2008; Rezaïki et al., 2008; Light et al., 2018), we examined the phenotypes of mutants in anaerobic, aerobic and respiration-permissive conditions. The common or different functional features of short-chain MKs and long-chain MKs were revealed in the three conditions (Fig. 5.6).

Under anaerobic conditions, the most distinct phenotypes among the strains were the ability to reduce azo dye and copper ions, which are indications of EET. The EET efficiency appeared to be higher in the presumed MK-1 producer *ΔispA* than the MK-3 and long-chain MKs producers, indicating a preference in anaerobic EET for short-chain MKs over long-chain MKs (Fig. 5.6). The same preference

was suggested by the metabolite analysis where succinate was formed by *ΔispA*, plausibly as a result of anaerobic electron transport chain with fumarate serving as the electron acceptor. The role of MKs in anaerobic respiration via reduction of fumarate to succinate has been reported for *E. coli* and *En. faecalis* (Huycke et al., 2001; Brooijmans et al., 2009a). Genome annotation of *L. lactis* strain MG1363 indeed reveals the gene *frdC* encoding a fumarate reductase, homologous to the fumarate reductases reported for *E. coli* and *En. faecalis*. In fact, activity of a fumarate reductase was indeed reported in *L. lactis* a long time ago (Hillier et al., 1979). In agreement with the theory, a fumarate reductase flavoprotein subunit protein (A2RL55) was also identified in this study in the proteome of all strains, with high abundance under anaerobic conditions. In addition, the higher stationary phase survival of *ΔispA* and Δ*llmg_0196* under anaerobic conditions supports the hypothesis that short-chain MKs offer an advantage for *L. lactis* in anaerobic respiration/EET, allowing additional energy generation for maintenance in the stationary phase cells.

Under aerobic conditions, large differences were observed in stationary phase survival of the strains, where non-MK producer *ΔmenF* maintained high viability throughout the incubation period while the presumed MK-1 producer *ΔispA* lost viability fastest followed by the MK-3 producer Δ*llmg_0196*. Under aerobic conditions where the cytochrome oxidase is not functional (no heme supplementation), MKs have been suggested to mediate the reduction of oxygen, promoting ROS formation in *L. lactis* (Rezaïki et al., 2008). The MK-mediated ROS formation could reduce the viability of cells, explaining the observed differences in the tested strains. In the proposed model, we assume MK-mediated ROS formation as an extracellular activity. This model is supported by measurement of extracellular superoxide formation mediated by (D)MKs in *L. lactis* (Rezaïki et al., 2008) and *En. faecalis* (Huycke et al., 2001) under aerobic conditions. However, we do not exclude the possibility that MK-mediated ROS formation also takes place in the cytoplasm, but this intracellular ROS fraction is not expected to pose major damage to the cells due to the activity of an intracellular superoxide dismutase (Huycke et al., 2001; Ballal et al., 2015), which has also been identified in the proteome determined in our study (Table 5.3, protein ID P0A4J2). Therefore, the difference in cell viability observed after prolonged cultivation under aerobic conditions is considered to be mainly a result of the extracellular ROS formation mediated by MKs. Here a preference for short-chain MKs seemed to exist for the reaction with oxygen/ROS formation too (Fig. 5.6).

Furthermore, the copper reduction still took place under aerobic conditions, but to a lesser extent in *Δllmg_0196* as compared to anaerobic conditions. This could mean that, in absence of a functional cytochrome oxidase, the electron flow via MKs towards oxygen and EET can both be active, with possible competition between the two pathways of the electrons (Fig. 5.6).

Under respiration-permissive conditions, it was consistently shown that MG1363 demonstrated all aerobic respiration-related phenotypes: increased biomass yield in comparison to fermentative growth due to more efficient ATP generation, higher oxygen consumption rate than under aerobic conditions, large decrease in lactate production and increase in acetate and acetoin as compared to cultures

in the fermentative growth mode as a result of redox cofactor (NAD/NADH) changes caused by the membrane embedded ETC, etc. (Duwat et al., 2001; Brooijmans et al., 2009c). The MK-3 producer *Δllmg_0196* demonstrated these phenotypical changes, but to a lesser extent than MG1363, which could be explained by the lower content of MKs. The non-MK producer *ΔmenF* as well as presumed MK-1 producer *ΔispA* did not shown these changes. The proteome profiles reflected the same change/difference among the strains. It could be collectively deduced that long-chain MKs (MK-9 and MK-8) and MK-3, but not MK-1, complement the respiratory ETC in *L. lactis*.

As a functional cytochrome oxidase was provided, the copper reduction activity was attenuated in MG1363 and *Δllmg_0196.* This observation agrees with the previous findings: heme-induced respiration of *L. lactis* suppressed copper reduction (Abicht et al., 2013); *L. lactis* could decolorize azo dyes only under anaerobic conditions (Pérez-Díaz and McFeeters, 2009); the EET in *En. faecalis* was attenuated by cytochrome *bd* oxidase activity (Pankratova et al., 2018). The remaining copper reduction activity in *ΔispA* suggest that MK-1 has the highest affinity for EET among all studied electron transfer routes.

The different efficiency of long-chain and short-chain MKs in the various electron transfer pathways is considered to be a result of the hydrophobicity of the MK forms in relation to the location where electron transfer takes place. The respiratory ETC has all components located in the lipid bilayer of the cell membrane, and long-chain MKs are well-embedded in the membrane due to the strong hydrophobicity. In contrast, pathways like EET direct electrons towards the extracellular electron acceptors, and thus the short-chain MKs with higher hydrophilicity demonstrate advantages in transferring electrons to the free flavin shuttles (Light et al., 2018), or even act as soluble electron shuttles themselves (Freguia et al., 2009).

This study examined the functions of short-chain and long-chain MKs in *L. lactis* in lab conditions, but the significance can be inferred for *L. lactis* in natural settings too. For example, the role of MKs in EET allows more options for bacteria to utilize carbon sources that are otherwise not fermentable (Light et al., 2018). Although not investigated extensively in this study, we did identify a putative fumarate reductase flavoprotein (Table 5.4, protein ID A2RL55) that is overproduced under anaerobic conditions in *L. lactis*. This fumarate reductase shows homology to a cell surface-associated fumarate reductase described in *Ls. monocytogenes* (Light et al., 2019). The fumarate reductase in *Ls. monocytogenes* was found to rely on EET to reduce fumarate to succinate, supporting growth of the bacterium via an anaerobic respiration mechanism; an EET mutant showed competitive disadvantage in the gut of mouse (Light et al., 2018). Similarly, competitive advantages offered by EET mediated by MKs can be inferred for *L. lactis*: for its application in cheese production, the ripening process takes place when *L. lactis* faces nutrient limitation/carbon starvation, but metabolic activity is still desired for flavor development in cheese (Smid and Kleerebezem, 2014). EET mediated by MKs, especially the short-chain MKs, are expected to offer advantage to *L. lactis* for additional nutrient source utilization and

maintaining longer survival/metabolic activity period, ideal for successful or even accelerated cheese ripening.

The possible role of MKs in ROS formation and the consequence for stationary phase survival of *L. lactis* suggest disadvantages of MK production in this bacterium, in particular under aerobic conditions when heme is not supplied. This knowledge can be applied for selecting natural variants of *L. lactis* that are extra resistant to the oxidative conditions during starter culture production and initial stages in cheese production, given the improved robustness of the non-MK producer under aerobic conditions. Interestingly, a previous study demonstrated that adaptive laboratory evolution of *L. lactis* under highly aerated conditions resulted in evolved mutants showing elevated vitamin K2 content and enhanced resistance to oxidative stress (Chapter 4 of this thesis - Liu et al., 2021). This supports that natural selection methods, based on the roles of MKs in *L. lactis*, allow us to obtain different types of variants that are of interest for applications.

Nevertheless, as the effect of MKs in *L. lactis* survival is only displayed after prolonged exposure to oxygen (48-72 h), MKs can be considered to be beneficial for *L. lactis* in dairy fermentation, where the bacterium is more exposed to anaerobic conditions. In other natural settings, such as the original niche of *L. lactis*, i.e., plant surfaces, heme and oxygen are often available (Pedersen et al., 2012; Cavanagh et al., 2015). Under such circumstances, maintaining the MK producing ability indeed offers advantage to *L. lactis* as the aerobic respiration promotes the growth and survival of this bacterium (Duwat et al., 2001; Gaudu et al., 2002). The heme-induced respiration has been applied in starter production to obtain higher yield and more robust *L. lactis* for dairy industry (Pedersen et al., 2005; Garrigues et al., 2006).

Notably, MKs are also known as vitamin K2, a fat-soluble vitamin essential to human health (Vermeer and Schurgers, 2000; Beulens et al., 2013). In the human body, vitamin K2 acts as the co-factor for γ-glutamyl carboxylase catalyzing the carboxylation of the glutamate residues in Gla-proteins, thereby ensuring biological functions of Gla-proteins in essential human physiological processes including hemostasis, calcium metabolism and cell growth regulation. Dietary intake of vitamin K2 has been associated with reduced risk of coronary heart disease and improved bone health (Geleijnse et al., 2004; Fujita et al., 2012). In terms of benefits for human health, the interest often goes to the long-chain MKs for the higher bioavailability they demonstrated compared to the short-chain MKs; the association with cardiovascular health was also demonstrated prominently with intake of long-chain MKs (Geleijnse et al., 2004; Sato et al., 2012). The insight in the physiological functions of MKs in *L. lactis* also provides opportunities for vitamin K2 enrichment of fermented food products: suitable conditions can be designed accordingly for natural selection procedures to obtain variants with desired vitamin K2 production profiles.

Taken together, the set of both long-chain and short-chain MKs produced by *L. lactis*, in combination with the different functionality of MK variants in anaerobic, aerobic and respiration-permissive

conditions, points to an efficient strategy to adapt to diverse aeration and nutritional conditions that *L. lactis* strains may encounter in their natural niche or during food fermentation processes. It is highly desirable to extend the inferred significance of MKs in *L. lactis* from lab settings to natural ecological systems with further investigations. As the short-chain MKs are more water soluble and allow possibilities for cross-feeding (Rezaïki et al., 2008), their relevance for interacting not only with the environment, but also with hosts or cohabitating microbes extends the significance to diverse habitats.

Acknowledgements

The authors would like to thank Jeroen Koomen (Food Microbiology, Wageningen University) for his kind help in analyzing proteomics data. The authors also thank Mark Sanders (Food Chemistry, Wageningen University) for his assistance in vitamin K2 analysis.

The work was subsidized by the Netherlands Organization for Scientific Research (NWO) through the Graduate Program on Food Structure, Digestion and Health.

Supplementary materials

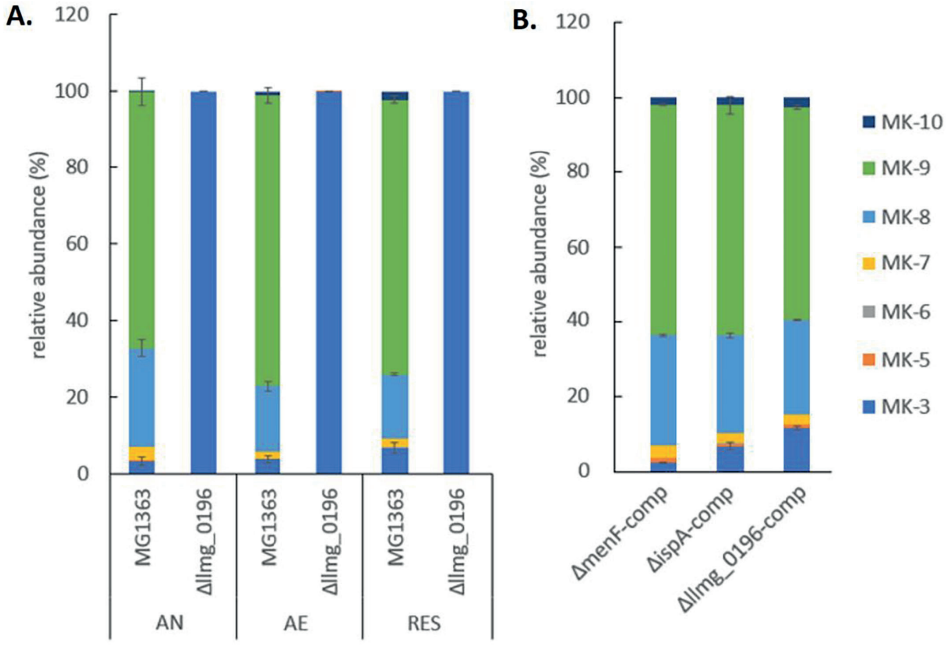

Figure S5.1. MK profile in the biomass of MG1363 and mutants. A) Relative abundance of tested MK forms in MG1363 and mutants with gene deletions. Note that only trace amount of MKs were detected in Δ*menF* and Δ*ispA*, and the relative abundance is therefore not shown. All strains were cultivated in GM17 medium under indicated conditions for 16-18 hours at 30 °C before MKs were extracted from the biomass. AN: anaerobic; AE: aerobic; RES: respiration-permissive, i.e. heme and aeration. Samples for each strain and condition were from three independent experiments. B) Relative abundance of tested MK forms in mutants with respective gene complementation. Strains were cultivated in GM17 medium under anaerobic conditions for 16-18 hours at 30 °C, 5 µg/mL erythromycin was added to the medium, data were from four biological replicates. Error bars show SEM for MK-3, MK-8 and MK-9.

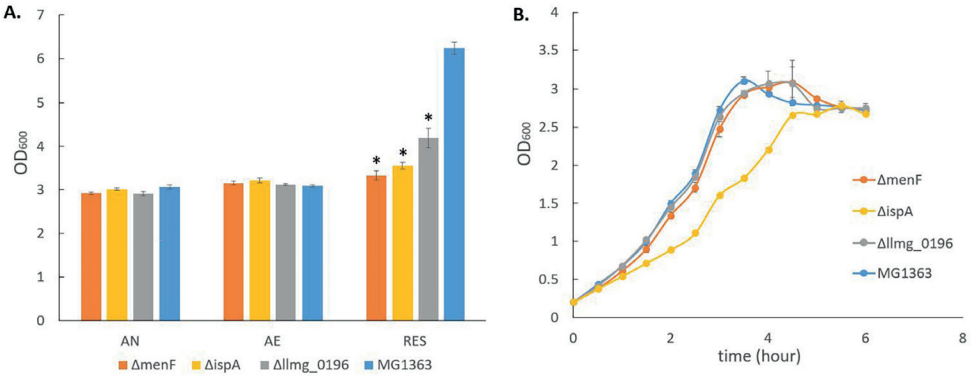

Figure S5.2. Growth performance of MG1363 and mutants. A) Biomass accumulation measured by OD. Data from four independent experiments. AN: anaerobic; AE: aerobic; RES: respiration-permissive, i.e. heme and aeration. *shows significant ($p<0.05$) difference to MG1363. B) growth curves. The growth was monitored under anaerobic conditions. Data from three independent experiments. Error bars show SEM.

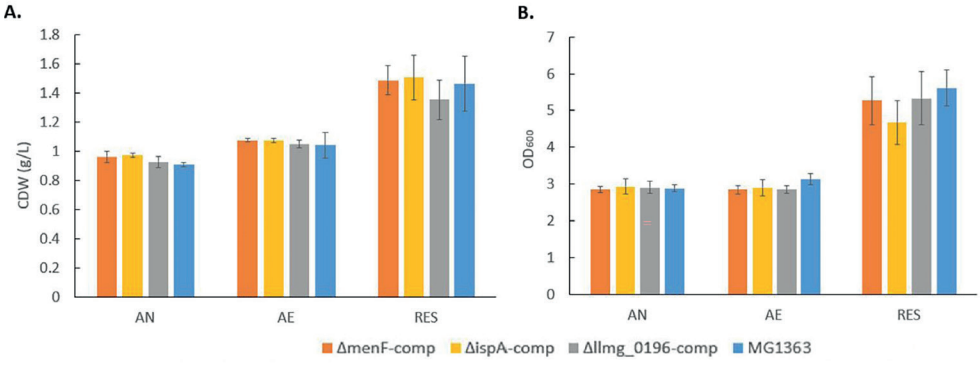

Figure S5.3. Biomass accumulation of MG1363 and mutants with gene complementation. A) Cell dry weight (CDW). Data from four independent experiments. B) OD measurement. Data from three independent experiments. Error bars show SEM. AN: anaerobic; AE: aerobic; RES: respiration-permissive, i.e. heme and aeration.

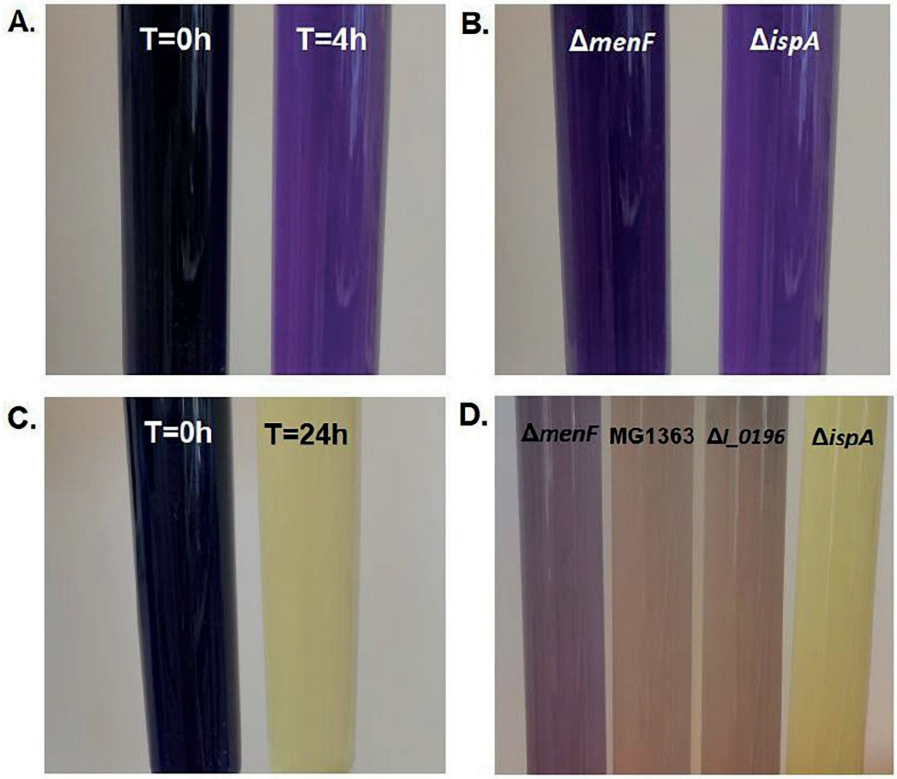

Figure S5.4. Example pictures of azo dye decolorization by *L. lactis*. A) Reaction of *ΔispA* at 0 h and 4 h. B) Reaction of *ΔmenF* and *ΔispA* at 4 h. C) Reaction of *ΔispA* at 0 h and 24 h. D) Reaction of all strains at 24 h. Azo dye reduction was monitored in anaerobic conditions.

Table S5.1. Primers used for PCR amplifying upstream and downstream homologous regions for the target genes.

Name[a]	Primer sequence 5' – 3'[b]
0196_HR1_HindIII_Fw	**AACGTGAAGCTTTACTGACAG**
0196_HR1_PstI_Rv	CGCGCGCTGCAG**CAATGTTTTTCTCTTTCCTCTCG**
0196_HR2_PstI_Fw	AAGAAGCTGCAG**TAAAAGCCTGTCACCGATAGG**
0196_HR2_XbaI_Rv	GGCGGCTCTAGA**ATCACAGGTGTTATTCGCTAAC**
ispA_HR1_HindIII_Fw	CCACCAAAGCTT**CCCTCCTCGACTAACATATCG**
ispA_HR1_PstI_Rv	AAGAAGCTGCAG**GAACAACTGGAAGTGGAATAAATG**
ispA_HR2_PstI_Fw	CGCGCGCTGCAG**TGGCTCTTGAAAGCCTTTGC**
ispA_HR2_XbaI_Rv	CGCGCGTCTAGA**CAACCAGATTGACATGAGCAAC**
menF_HR1_HindIII_Fw	TTGTTGAAGCTT**GCACTATATTGGTTGCTTCC**
menF_HR1_PstI_Rv	ATATATCTGCAG**CATAGAAATTATAACATAGCTCAC**
menF_HR2_PstI_Fw	TATATACTGCAG**GAAGCCTTATGACTTCTATTTAG**
menF_HR2_XbaI_Rv	ATATATTCTAGA**TTCAGAAGAATTGGCTCCTG**

[a]In the primer names, the target gene, up or down stream homologous region (HR 1 or HR2), introduced restriction site, forward (Fw) or reverse (Rv) primer is indicated.

[b]In the primer sequences, the annealing sequences are bold, and introduced restriction sites are underlined.

Table S5.2. Primers used for PCR amplifying the promoter and open reading frame for each target gene.

Name	Primer sequence 5' – 3'[a]
45-menF-Fw	TTGAAAACCGCTACGGATCA**CATATAATTGTTGGCAATCG**
45-menF-Rv	TCAAAGAAAGCTTGAGCTCT**GATATTCTAAATAGAAGTCATAAGG**
45-0196_Fw	TTGAAAACCGCTACGGATCA**AGCGTTCTCGGGAGATTG**
45-0196_Rv	TCAAAGAAAGCTTGAGCTCT**AACCTATCGGTGACAGGC**
45-ispA_Fw	TCAAAGAAAGCTTGAGCTCT**CATTCTCTGTGAGAATTCTAAG**
45-ispA_Rv	TTGAAAACCGCTACGGATCA**GAATTGGTGGCCAACAATATTC**

[a]In the primer sequences, the annealing sequences are bold.

Table S5.3. Primers used for PCR checking mutants with target genes deleted.

Name	Primer sequence 5' – 3'
final check 0196 KO Fw	GCACACAATATTCAAAGTTGGC
final check 0196 KO Rv	CAAAGTCCACCAAATGAGTGC
final check ispA KO FW	GCATCACATCAGTAAATCCTCC
final check ispA KO Rv	GACGAGAAAGGAGAAGAAATTCC
final check menF KO Fw	GCAATCCCACGAACACTGAC
final check menF KO Rv	AGCATCATAGCTGTCCATGAC

Table S5.4. Quantity (Log LFQ intensity) of proteins involved in the primary metabolism in MG1363 and mutant under different cultivation conditions.

Protein	Gene	AN				AE				RES			
Function		MG1363	Δ*menF*	Δ*ispA*	Δ*0196*	MG1363	Δ*menF*	Δ*ispA*	Δ*0196*	MG1363	Δ*menF*	Δ*ispA*	Δ*0196*
A2RMN3	*pflA*	8.71	8.72	8.86	8.79	7.01	ND	7.03	7.04	7.70	6.97	7.37	6.98
Pyruvate formate-lyase-activating enzyme		0.02	0.04	0.07	0.04	0.31	-	0.33	0.34	0.09	0.27	0.34	0.28
O32799	*pfl*	10.26	10.26	10.43	10.25	9.60	9.65	9.86	9.59	9.93	9.69	9.91	**9.56**
Formate acetyltransferase		0.03	0.02	0.02	0.00	0.02	0.02	0.03	0.01	0.04	0.01	0.01	**0.01**
P0CI34	*ldhB*	ND	ND	ND	ND	ND	ND	ND	ND	ND	ND	ND	ND
L-lactate dehydrogenase 2		-	-	-	-	-	-	-	-	-	-	-	-
A2RKA4	*Ldh*	10.71	10.66	10.60	10.68	10.53	10.56	10.37	10.52	10.45	10.55	10.43	10.45
L-lactate dehydrogenase		0.03	0.01	0.02	0.02	0.04	0.01	0.02	0.03	0.01	0.04	0.02	0.02
A2RL45	*ldhX*	8.21	8.34	**8.76**	8.24	7.33	7.69	**8.53**	7.70	7.69	7.86	**8.64**	7.08
L-lactate dehydrogenase		0.13	0.07	**0.04**	0.08	0.32	0.01	**0.03**	0.03	0.01	0.06	**0.02**	0.38
A2RHE1	*pdhD*	10.32	10.39	10.41	10.36	10.55	10.53	10.56	10.56	10.66	10.51	10.54	10.55
Dihydrolipoyl dehydrogenase		0.01	0.02	0.01	0.03	0.01	0.04	0.01	0.01	0.02	0.01	0.00	0.02
A2RHE2	*pdhC*	10.53	10.51	10.49	10.51	10.71	10.64	10.70	10.74	10.80	10.70	10.66	10.72
Dihydrolipoamide acetyltransferase component of pyruvate dehydrogenase complex		0.02	0.04	0.04	0.04	0.02	0.02	0.04	0.03	0.01	0.01	0.02	0.03
A2RHE3	*pdhB*	10.54	10.56	10.56	10.59	10.70	10.70	10.70	10.70	10.84	10.70	10.68	10.71
Pyruvate dehydrogenase E1 component beta subunit		0.02	0.01	0.06	0.02	0.00	0.03	0.02	0.03	0.01	0.03	0.02	0.02
A2RHE4	*pdhA*	10.23	10.19	10.20	10.19	10.37	10.35	10.34	10.37	10.54	10.40	10.36	10.41
Pyruvate dehydrogenase E1 component alpha subunit		0.01	0.02	0.04	0.05	0.06	0.02	0.02	0.03	0.02	0.01	0.03	0.04
A2RMM7	*adhA*	8.45	8.41	8.52	8.39	7.80	7.74	8.06	7.84	8.01	7.74	8.19	8.26
Alcohol dehydrogenase, zinc-containing		0.02	0.04	0.03	0.04	0.02	0.12	0.11	0.04	0.04	0.06	0.03	0.08
A2RNV2	*adhE*	10.66	10.68	10.71	10.67	9.48	9.54	9.42	9.47	8.51	**9.54**	**9.29**	**9.01**
Aldehyde-alcohol dehydrogenase		0.03	0.02	0.02	0.02	0.02	0.03	0.02	0.02	0.03	**0.01**	**0.01**	**0.02**
A2RJB5	*pta*	9.95	10.00	10.01	9.99	10.11	10.08	10.18	10.12	10.15	10.09	10.14	10.15
Phosphate acetyltransferase		0.02	0.01	0.01	0.02	0.02	0.02	0.01	0.02	0.01	0.01	0.02	0.03

Table S5.4. ***Continued***

A2RNG4	*ackA2*	9.69	9.71	9.70	9.69	9.71	9.70	9.75	9.71	9.82	9.74	9.71	9.70
Acetate kinase		0.05	0.01	0.01	0.03	0.04	0.01	0.03	0.04	0.01	0.01	0.02	0.02
A2RNG5	*ackA1*	9.97	9.96	9.95	9.97	9.93	9.96	9.86	9.90	9.82	9.94	9.88	9.87
Acetate kinase		0.05	0.04	0.01	0.00	0.01	0.03	0.02	0.03	0.02	0.01	0.03	0.01
A2RKT5	*als*	9.81	9.82	9.83	9.77	10.18	10.09	10.19	10.13	10.38	10.13	10.21	10.23
Acetolactate synthase large subunit		0.00	0.03	0.01	0.01	0.01	0.02	0.02	0.02	0.03	0.01	0.01	0.02
A2RKQ8	*ilvB*	ND	7.12	7.49	7.11	7.04	7.03	7.81	7.03	7.09	7.72	7.92	7.35
Acetolactate synthase		-	0.42	0.40	0.41	0.34	0.33	0.05	0.33	0.39	0.05	0.06	0.33
P77880	*aldB*	8.83	8.74	8.67	8.70	8.79	8.86	8.95	8.83	8.86	8.87	8.72	8.84
Alpha-acetolactate decarboxylase		0.02	0.03	0.03	0.07	0.03	0.07	0.04	0.11	0.03	0.04	0.09	0.04
A2RLP5	*butA*	9.18	9.18	9.45	9.17	9.21	9.19	9.38	9.26	9.59	**9.21**	9.46	9.47
Acetoin reductase		0.01	0.01	0.02	0.03	0.03	0.01	0.01	0.02	0.01	**0.05**	0.03	0.03

Values are averages from samples collected from 3 independent experiments, SEM values are shown below the average values. Detection limit in Log LFQ intensity: 6.7; Δ*0196* = Δ*llmg_0196*. Values in mutants that are significantly different ($p < 0.05$, fold change > 2) from strain MG1363 under the same cultivation conditions are highlighted in bold letters.

Table S5.5. Quantity (Log LFQ intensity) of proteins that showed significant changes across the strains or cultivation conditions (a non-exhaustive list).

Protein	Gene	AN				AE				RES			
Function		MG1363	Δ*menF*	Δ*ispA*	Δ*0196*	MG1363	Δ*menF*	Δ*ispA*	Δ*0196*	MG1363	Δ*menF*	Δ*ispA*	Δ*0196*
A2RKD8	*pabB*	8.33	7.33	8.48	8.54	ND	7.26	7.69	ND	ND	7.27	7.25	ND
Aminodeoxychorismate synthase		0.03	0.63	0.07	0.05	-	0.56	0.49	-	-	0.57	0.55	-
A2RK13	*llmg_1028*	8.88	8.76	8.98	8.78	8.49	8.37	8.70	8.34	7.58	**8.31**	**8.75**	**8.40**
Putative NAD(P)H nitroreductase		0.03	0.01	0.03	0.07	0.05	0.08	0.05	0.11	0.14	**0.04**	**0.03**	**0.03**
A2RIQ1	*dfpA*	8.87	8.72	8.76	8.68	8.50	8.49	8.29	8.42	8.30	8.28	8.22	7.89
Putative DNA/pantothenate metabolism flavoprotein		0.05	0.07	0.03	0.06	0.04	0.07	0.08	0.07	0.11	0.08	0.09	0.23
A2RLD1	*llmg_1522*	7.92	7.76	7.63	7.75	7.78	7.70	7.77	7.81	7.57	7.75	7.67	7.43
Putative membrane protein		0.10	0.08	0.01	0.04	0.09	0.04	0.03	0.06	0.06	0.02	0.09	0.37
A2RIP8	*yidC*	9.45	9.34	9.29	9.32	9.32	9.26	9.21	9.25	9.10	9.24	9.17	9.23
Membrane protein insertase		0.04	0.06	0.03	0.04	0.04	0.03	0.11	0.10	0.07	0.02	0.01	0.02
A2RNY5	*recX*	8.28	8.10	8.27	8.28	7.82	7.85	**8.17**	7.77	7.95	8.01	8.15	8.04
Regulatory protein		0.08	0.08	0.04	0.05	0.09	0.06	**0.04**	0.06	0.03	0.04	0.10	0.08
A2RHL7	*llmg_0146*	9.24	9.26	9.38	9.30	9.24	9.32	9.36	9.32	9.55	9.32	9.42	9.33
Aryl-alcohol dehydrogenase		0.06	0.01	0.04	0.09	0.04	0.02	0.04	0.07	0.04	0.02	0.03	0.04
Q9S5Z2	*clpE*	10.28	10.25	10.33	10.21	10.29	10.28	10.31	10.27	10.59	10.32	10.28	10.39
ATP-dependent Clp protease ATP-binding subunit		0.02	0.01	0.02	0.01	0.02	0.01	0.03	0.01	0.01	0.02	0.02	0.01
A2RMQ7	*llmg_2023*	10.02	10.08	10.04	10.11	10.10	10.07	10.05	10.13	10.33	10.13	10.09	10.21
Universal stress protein A		0.01	0.03	0.06	0.03	0.04	0.04	0.03	0.01	0.04	0.02	0.02	0.02
A2RLA1	*mntH*	8.53	8.47	8.46	8.53	8.93	8.83	8.69	8.86	8.87	8.88	8.65	8.96
Divalent metal cation transporter		0.05	0.09	0.08	0.09	0.07	0.04	0.09	0.03	0.03	0.06	0.06	0.10
A2RJM2	*llmg_0880*	9.17	9.21	9.20	9.19	9.17	9.15	9.10	9.16	9.52	**9.11**	**9.14**	9.26
Putative oxidoreductase		0.05	0.06	0.04	0.07	0.03	0.02	0.02	0.04	0.03	**0.03**	**0.02**	0.02
A2RM94	*qor*	8.57	8.72	8.54	8.64	8.67	8.68	8.62	8.68	8.92	8.78	**8.55**	8.66
Zinc-type alcohol dehydrogenase-like protein		0.01	0.04	0.01	0.07	0.02	0.10	0.05	0.06	0.03	0.04	**0.02**	0.04
A2RHS0	*msrB*	8.86	8.75	8.82	8.82	8.89	8.89	8.88	8.84	9.21	**8.91**	**8.89**	8.95
Peptide methionine sulfoxide reductase		0.00	0.03	0.04	0.05	0.02	0.01	0.04	0.05	0.02	**0.01**	**0.04**	0.04

Table S5.5. ***Continued***

A2RI61	*fhuD*	8.81	8.73	8.73	8.79	9.30	9.25	9.34	9.31	9.17	9.16	9.33	9.20
Ferrichrome ABC transporter substrate binding protein		0.03	0.04	0.06	0.03	0.01	0.02	0.04	0.04	0.02	0.04	0.02	0.03
A2RJT8	*msrA*	9.11	9.08	9.14	9.05	9.20	9.30	9.16	9.18	9.50	**9.16**	**9.15**	9.32
Peptide methionine sulfoxide reductase		0.07	0.01	0.01	0.06	0.06	0.03	0.02	0.03	0.02	**0.03**	**0.02**	0.05
A2RKC2	*mtsA*	9.40	9.36	9.36	9.44	9.63	9.64	9.50	9.63	9.82	9.62	**9.50**	9.70
Manganese ABC transporter substrate binding protein		0.03	0.03	0.03	0.03	0.05	0.06	0.05	0.05	0.02	0.04	**0.03**	0.03
A2RK08	*fur*	8.30	8.38	8.27	8.44	8.38	8.47	8.30	8.38	8.75	8.52	**8.44**	8.48
Ferric uptake regulation protein		0.12	0.03	0.03	0.06	0.05	0.01	0.15	0.13	0.04	0.03	**0.04**	0.14
A2RM21	*metC*	9.08	9.06	8.92	9.06	9.42	9.36	9.17	9.37	9.56	**9.26**	**9.14**	9.33
Cystathionine beta-lyase		0.02	0.04	0.03	0.04	0.04	0.03	0.04	0.02	0.04	**0.01**	**0.02**	0.00
A2RNK4	*llmg_2331*	9.26	9.18	9.18	9.17	9.32	9.30	9.26	9.30	9.76	**9.27**	**9.23**	**9.44**
Pyridine nucleotide-disulfide oxidoreductase		0.00	0.02	0.04	0.02	0.02	0.01	0.05	0.03	0.01	**0.01**	**0.02**	**0.04**
A2RKC0	*mtsB*	9.12	9.02	9.11	9.18	9.42	9.40	9.39	9.43	9.65	9.43	9.36	9.49
Manganese ABC transporter ATP binding protein		0.03	0.02	0.02	0.02	0.03	0.03	0.02	0.08	0.02	0.04	0.03	0.04
A2RK64	*uspA2*	9.57	9.54	9.69	9.49	9.87	9.76	9.89	9.89	10.12	9.83	9.90	10.09
Universal stress protein A2		0.01	0.04	0.01	0.05	0.01	0.02	0.05	0.04	0.02	0.02	0.01	0.06
A2RJC6	*llmg_0776*	8.59	8.45	8.41	8.59	9.06	8.93	9.01	8.98	9.16	8.98	8.97	9.06
Ferredoxin--NADP reductase		0.05	0.01	0.04	0.03	0.03	0.02	0.02	0.06	0.02	0.02	0.04	0.04
A2RLR6	*uspA*	9.40	9.38	9.49	9.40	9.53	9.54	9.58	9.52	10.02	**9.50**	**9.64**	9.78
Universal stress protein		0.04	0.06	0.03	0.03	0.01	0.02	0.06	0.03	0.04	**0.04**	**0.06**	0.12
A2RHF0	*osmC*	8.93	9.06	8.89	8.97	9.19	9.14	9.14	9.23	9.60	**9.23**	**9.11**	9.28
Osmotically inducible protein		0.14	0.02	0.14	0.04	0.05	0.05	0.06	0.12	0.02	**0.06**	**0.03**	0.12
A2RHZ1	*llmg_0276*	10.44	10.46	10.55	10.47	10.61	10.60	10.58	10.57	11.18	**10.65**	**10.62**	**10.77**
Oxidoreductase, aldo/keto reductase		0.06	0.04	0.03	0.04	0.02	0.03	0.02	0.03	0.03	0.03	0.03	0.02
A2RHG2	*cysD*	8.03	8.28	**8.37**	8.14	8.63	8.53	8.66	8.69	8.81	8.60	8.70	8.51
O-acetylhomoserine sulfhydrylase		0.08	0.10	**0.03**	0.11	0.03	0.03	0.05	0.02	0.03	0.01	0.06	0.06
A2RI58	*fhuC*	7.05	7.80	7.86	7.41	8.04	7.88	**8.41**	8.12	8.11	7.93	8.27	8.05
Ferrichrome ABC transporter		0.35	0.10	0.00	0.35	0.03	0.03	**0.10**	0.08	0.08	0.04	0.04	0.11

A2RNJ4	*poxL*	ND	ND	6.97	ND	ND	ND	ND	ND	8.17	**ND**	**ND**	**ND**
Pyruvate oxidase		-	-	0.27	-	-	-	-	-	0.08	**-**	**-**	**-**
A2RMS9	*nifS*	8.89	8.91	8.95	8.92	8.70	8.64	**9.06**	8.68	9.02	8.93	9.09	8.97
Putative iron-sulfur cofactor synthesis protein		0.10	0.01	0.04	0.05	0.05	0.05	**0.05**	0.08	0.03	0.04	0.01	0.00
P42370	*hrcA*	8.73	8.68	9.01	8.66	8.18	8.19	**8.91**	8.24	8.53	**8.08**	8.80	8.38
Heat-inducible transcription repressor		0.02	0.02	0.04	0.01	0.06	0.02	**0.03**	0.04	0.04	**0.05**	0.01	0.03
A2RLX6	*merP*	7.76	7.76	7.62	7.74	7.16	7.46	**7.87**	7.43	8.09	7.68	7.84	7.80
Mercuric reductase		0.15	0.03	0.21	0.09	0.23	0.15	**0.08**	0.07	0.16	0.05	0.09	0.11
A2RHR8	*feoB*	7.87	7.86	7.80	8.06	6.94	ND	7.50	ND	ND	6.97	**7.68**	6.92
Ferrous iron transport protein B		0.06	0.08	0.04	0.09	0.24	-	0.08	-	-	0.27	**0.04**	0.22
A2RNH7	*dpsA*	9.92	9.87	9.88	9.90	9.08	8.94	9.21	9.11	9.21	9.08	9.25	8.98
Non-heme iron-binding ferritin		0.31	0.31	0.34	0.30	0.07	0.07	0.05	0.05	0.03	0.11	0.18	0.07
A2RMF4	*llmg_1915*	9.32	9.26	9.31	9.24	8.73	8.57	8.88	8.67	8.95	**8.57**	8.87	8.73
Putative Fe-S oxidoreductase		0.06	0.02	0.04	0.04	0.04	0.06	0.05	0.07	0.07	**0.04**	0.03	0.07
A2RHR9	*feoA*	7.07	7.75	7.40	7.71	7.07	7.79	7.36	7.16	7.12	ND	7.72	ND
Ferrous iron transport protein A		0.37	0.01	0.35	0.06	0.37	0.19	0.33	0.46	0.42	-	0.01	-
A2RJ14	*llmg_0661*	7.33	7.53	7.26	7.28	7.60	7.30	7.55	7.59	7.54	**ND**	7.26	7.28
CorA like magnesium and cobalt transport protein		0.32	0.03	0.28	0.29	0.06	0.30	0.03	0.03	0.06	**-**	0.28	0.29
A2RI68	*ahpC*	10.47	10.53	10.42	10.44	10.43	10.40	10.31	10.44	10.18	10.42	10.23	10.29
Alkyl hydroperoxide reductase subunit C		0.04	0.01	0.01	0.05	0.01	0.05	0.04	0.02	0.02	0.03	0.01	0.02
A2RI69	*ahpF*	10.22	10.24	10.19	10.26	10.22	10.17	10.06	10.20	9.94	10.20	10.01	10.07
Alkyl hydroperoxide reductase subunit F		0.02	0.02	0.02	0.01	0.01	0.01	0.03	0.01	0.04	0.02	0.01	0.03
A2RLU6	*copB*	8.64	8.53	8.44	8.59	8.58	8.49	8.52	8.56	8.66	8.47	8.41	8.56
Copper-potassium transporting ATPase B		0.03	0.02	0.05	0.04	0.03	0.04	0.07	0.01	0.03	0.02	0.06	0.03
A2RLX5	*copA*	8.62	8.70	8.53	8.64	8.24	8.29	8.24	8.23	8.25	8.30	**8.60**	8.37
Copper/potassium-transporting ATPase		0.12	0.07	0.08	0.07	0.04	0.01	0.16	0.03	0.06	0.07	**0.09**	0.03
A2RNE6	*cutC*	9.66	9.57	9.54	9.59	9.57	9.52	9.52	9.56	9.58	9.52	9.50	9.56
Copper homeostasis protein		0.01	0.02	0.04	0.04	0.02	0.04	0.06	0.02	0.03	0.03	0.01	0.01

Values are averages from samples collected from 3 independent experiments, SEM values are shown below the average values. Detection limit in Log LFQ intensity: 6.7; Δ*0196* = Δ*llmg_0196*. Values in mutants that are significantly different ($p < 0.05$, fold change > 2) from strain MG1363 under the same cultivation conditions are highlighted in bold letters.

References

Abicht, H. K., Gonskikh, Y., Gerber, S. D., and Solioz, M. (2013). Non-enzymic copper reduction by menaquinone enhances copper toxicity in *Lactococcus lactis* IL1403. *Microbiology* 159, 1190–1197.

Ballal, S. A., Veiga, P., Fenn, K., Michaud, M., Kim, J. H., Gallini, C. A., et al. (2015). Host lysozyme-mediated lysis of *Lactococcus lactis* facilitates delivery of colitis-attenuating superoxide dismutase to inflamed colons. *Proc. Natl. Acad. Sci. U. S. A.* 112, 7803–7808.

Beulens, J. W. J., Booth, S. L., van Den Heuvel, E. G. H. M., Stoecklin, E., Baka, A., and Vermeer, C. (2013). The role of menaquinones (vitamin K2) in human health. *Br. J. Nutr.* 110, 1357–1368.

Brooijmans, R., de Vos, W. M., and Hugenholtz, J. (2009a). Electron transport chains of lactic acid bacteria - walking on crutches is part of their lifestyle. *F1000 Biol. Rep.* 1, 34.

Brooijmans, R. J. W., de Vos, W. M., and Hugenholtz, J. (2009b). *Lactobacillus plantarum* WCFS1 electron transport chains. *Appl. Environ. Microbiol.* 75, 3580–3585.

Brooijmans, R., Smit, B., Santos, F., van Riel, J., de Vos, W. M., and Hugenholtz, J. (2009c). Heme and menaquinone induced electron transport in lactic acid bacteria. *Microb. Cell Fact.* 8, 28.

Bryan, E. M., Bae, T., Kleerebezem, M., and Dunny, G. M. (2000). Improved vectors for nisin-controlled expression in Gram-positive bacteria. *Plasmid* 44, 183–190.

Cavanagh, D., Fitzgerald, G. F., and McAuliffe, O. (2015). From field to fermentation: The origins of *Lactococcus lactis* and its domestication to the dairy environment. *Food Microbiol.* 47, 45–61.

Chen, I. M. A., Chu, K., Palaniappan, K., Pillay, M., Ratner, A., Huang, J., et al. (2019). IMG/M v.5.0: an integrated data management and comparative analysis system for microbial genomes and microbiomes. *Nucleic Acids Res.* 47, D666–D677.

Collins, M. D., and Jones, D. (1981). Distribution of isoprenoid quinone structural types in bacteria and their taxonomic implications. *Microbiol. Rev.* 45, 316–354.

Cretenet, M., Le Gall, G., Wegmann, U., Even, S., Shearman, C., Stentz, R., et al. (2014). Early adaptation to oxygen is key to the industrially important traits of *Lactococcus lactis* ssp. *cremoris* during milk fermentation. *BMC Genomics* 15, 1054.

Daruwala, R., Kwon, O., Meganathan, R., and Hudspeth, M. E. S. (1996). A new isochorismate synthase specifically involved in menaquinone (vitamin K2) biosynthesis encoded by the menF gene. *FEMS Microbiol. Lett.* 140, 159–163.

Duwat, P., Sourice, S., Cesselin, B., Lamberet, G., Vido, K., Gaudu, P., et al. (2001). Respiration capacity of the fermenting bacterium *Lactococcus lactis* and its positive effects on growth and survival. *J. Bacteriol.* 183, 4509–4516.

Fang, Y., Liu, J., Kong, G., Liu, X., Yang, Y., Li, E., et al. (2019). Adaptive responses of *Shewanella decolorationis* to toxic organic extracellular electron acceptor azo dyes in anaerobic respiration. *Appl. Environ. Microbiol.* 85, e00550-19.

Freguia, S., Masuda, M., Tsujimura, S., and Kano, K. (2009). *Lactococcus lactis* catalyses electricity generation at microbial fuel cell anodes via excretion of a soluble quinone. *Bioelectrochemistry* 76, 14–18.

Fujita, Y., Iki, M., Tamaki, J., Kouda, K., Yura, A., Kadowaki, E., et al. (2012). Association between vitamin K intake from fermented soybeans, natto, and bone mineral density in elderly Japanese men: the Fujiwara-kyo Osteoporosis Risk in Men (FORMEN) study. *Osteoporos. Int.* 23, 705–714.

Garrigues, C., Johansen, E., Pedersen, M.B., Mollgaard, H., Sorensen, K.I., Gaudu, P., et al. (2006). Getting high (OD) on heme. *Nat. Rev. Microbiol*. 4, 318.

Gaudu, P., Vido, K., Cesselin, B., Kulakauskas, S., Tremblay, J., Rezaïki, L., et al. (2002). Respiration capacity and consequences in Lactococcus lactis. *Antonie Van Leeuwenhoek* 82, 263–269.

Geleijnse, J. M., Vermeer, C., Grobbee, D. E., Schurgers, L. J., Knapen, M. H. J., van Der Meer, I. M., et al. (2004). Dietary intake of menaquinone is associated with a reduced risk of coronary heart disease: the Rotterdam Study. *J. Nutr.* 134, 3100–3105.

Hillier, A. J., Jericho, R. E., Green, S. M., and Jago, G. R. (1979). Properties and Function of Fumarate Reductase (NADH) in *Streptococcus Lactis*. *Aust. J. Biol. Sci.* 32, 625–635.

Holo, H., and Nes, I. F. (1989). High-Frequency Transformation, by Electroporation, of *Lactococcus lactis* subsp. *cremoris* Grown with Glycine in Osmotically Stabilized Media. *Appl. Environ. Microbiol.* 55, 3119–3123.

Huycke, M. M., Moore, D., Joyce, W., Wise, P., Shepard, L., Kotake, Y., et al. (2001). Extracellular superoxide production by *Enterococcus faecalis* requires demethylmenaquinone and is attenuated by functional terminal quinol oxidases. *Mol. Microbiol.* 42, 729–740.

Jensen, P. R., and Hammer, K. (1993). Minimal Requirements for Exponential Growth of Lactococcus lactis. *Appl. Environ. Microbiol.* 59, 4363–4366.

Johnston, J. M., and Bulloch, E. M. (2020). Advances in menaquinone biosynthesis: sublocalisation and allosteric regulation. *Curr. Opin. Struct. Biol.* 65, 33–41.

Kanehisa, M., and Goto, S. (2000). KEGG: Kyoto Encyclopedia of Genes and Genomes. *Nucleic Acids Res.* 28, 27–30.

Kleerebezem, M., Bachmann, H., van Pelt-KleinJan, E., Douwenga, S., Smid, E. J., Teusink, B., et al. (2020). Lifestyle, metabolism and environmental adaptation in *Lactococcus lactis*. *FEMS Microbiol. Rev.* 44, 804–820.

Kobayashi, K., Ehrlich, S. D., Albertini, A., Amati, G., Andersen, K. K., Arnaud, M., et al. (2003). Essential *Bacillus subtilis* genes. *Proc. Natl. Acad. Sci. U. S. A.* 100, 4678–4683.

Koebmann, B., Blank, L. M., Solem, C., Petranovic, D., Nielsen, L. K., and Jensen, P. R. (2008). Increased biomass yield of *Lactococcus lactis* during energetically limited growth and respiratory conditions. *Biotechnol. Appl. Biochem.* 50, 25–33.

Krute, C. N., Carroll, R. K., Rivera, F. E., Weiss, A., Young, R. M., Shilling, A., et al. (2015). The disruption of prenylation leads to pleiotropic rearrangements in cellular behavior in *Staphylococcus aureus. Mol. Microbiol.* 95, 819–832.

Kurosu, M., and Begari, E. (2010). Vitamin K2 in electron transport system: are enzymes involved in vitamin K2 biosynthesis promising drug targets? *Molecules* 15, 1531–1553.

Lenaz, G., and Genova, M. L. (2013). "Quinones," in *Encyclopedia of Biological Chemistry*, eds. W. Lennarz and M. Lane (Academic Press), 722–729.

Light, S. H., Méheust, R., Ferrell, J. L., Cho, J., Deng, D., Agostoni, M., et al. (2019). Extracellular electron transfer powers flavinylated extracellular reductases in Gram-positive bacteria. *Proc. Natl. Acad. Sci. U. S. A.* 116, 26892–26899.

Light, S. H., Su, L., Rivera-Lugo, R., Cornejo, J. A., Louie, A., Iavarone, A. T., et al. (2018). A flavin-based extracellular electron transfer mechanism in diverse Gram-positive bacteria. *Nature* 562, 140–144.

Liu, Y., de Groot, A., Boeren, S., Abee, T., and Smid, E. J. (2021). *Lactococcus lactis* Mutants Obtained From Laboratory Evolution Showed Elevated Vitamin K2 Content and Enhanced Resistance to Oxidative Stress. *Front. Microbiol.* 12, 746770.

Liu, Y., van Bennekom, E. O., Zhang, Y., Abee, T., and Smid, E. J. (2019). Long-chain vitamin K2 production in *Lactococcus lactis* is influenced by temperature, carbon source, aeration and mode of energy metabolism. *Microb. Cell Fact.* 18, 129.

Love, J., Selker, R., Marsman, M., Jamil, T., Dropmann, D., Verhagen, J., et al. (2019). JASP: Graphical statistical software for common statistical designs. *J. Stat. Softw.* 88, 2.

Nagel, R., Thomas, J. A., Adekunle, F. A., Mann, F. M., and Peters, R. J. (2018). Arginine in the FARM and SARM: a role in chain-length determination for arginine in the aspartate-rich motifs of isoprenyl diphosphate synthases from *Mycobacterium tuberculosis. Molecules* 23, 2546.

Pankratova, G., Leech, D., Gorton, L., and Hederstedt, L. (2018). Extracellular electron transfer by the Gram-positive bacterium *Enterococcus faecalis. Biochemistry* 57, 4597–4603.

Pedersen, M. B., Gaudu, P., Lechardeur, D., Petit, M. A., and Gruss, A. (2012). Aerobic respiration metabolism in lactic acid bacteria and uses in biotechnology. *Annu. Rev. Food Sci. Technol.* 3, 37–58.

Pedersen, M. B., Iversen, S.L., Sorensen, K.I., and Johansen, E. (2005). The long and winding road from the research laboratory to industrial applications of lactic acid bacteria. *FEMS Microbiol. Rev*. 29, 611-624.

Pérez-Díaz, I. M., and McFeeters, R. F. (2009). Modification of azo dyes by lactic acid bacteria. *J. Appl. Microbiol.* 107, 584–589.

Rezaïki, L., Lamberet, G., Derré, A., Gruss, A., and Gaudu, P. (2008). *Lactococcus lactis* produces short-chain quinones that cross-feed Group B Streptococcus to activate respiration growth. *Mol. Microbiol.* 67, 947–957.

Sato, T., Schurgers, L. J., and Uenishi, K. (2012). Comparison of menaquinone-4 and menaquinone-7 bioavailability in healthy women. *Nutr. J.* 11, 93.

Smid, E. J., and M. Kleerebezem. (2014). Production of aroma compounds in lactic fermentations. *Annu. rev. food sci. technol.* 5, 313-326.

Solem, C., Defoor, E., Jensen, P. R., and Martinussen, J. (2008). Plasmid pCS1966, a new selection/counterselection tool for lactic acid bacterium strain construction based on the *oroP* gene, encoding an orotate transporter from *Lactococcus lactis*. *Appl. Environ. Microbiol.* 74, 4772–4775.

Vermeer, C., and Schurgers, L. J. (2000). A comprehensive review of vitamin K and vitamin K antagonists. *Hematol. Oncol. Clin. North Am.* 14, 339–353.

Walther, B., Karl, J. P., Booth, S. L., and Boyaval, P. (2013). Menaquinones, bacteria, and the food supply: the relevance of dairy and fermented food products to vitamin K requirements. *Adv. Nutr.* 4, 463–473.

Wegmann, U., O'Connell-Motherway, M., Zomer, A., Buist, G., Shearman, C., Canchaya, C., et al. (2007). Complete genome sequence of the prototype lactic acid bacterium *Lactococcus lactis* subsp. *cremoris* MG1363. *J. Bacteriol.* 189, 3256–3270.

Zheng, J., Wittouck, S., Salvetti, E., Franz, C. M. A. P., Harris, H. M. B., Mattarelli, P., et al. (2020). A taxonomic note on the genus *Lactobacillus*: Description of 23 novel genera, emended description of the genus *Lactobacillus* Beijerinck 1901, and union of *Lactobacillaceae* and *Leuconostocaceae*. *Int. J. Syst. Evol. Microbiol.* 70, 2782–2858.

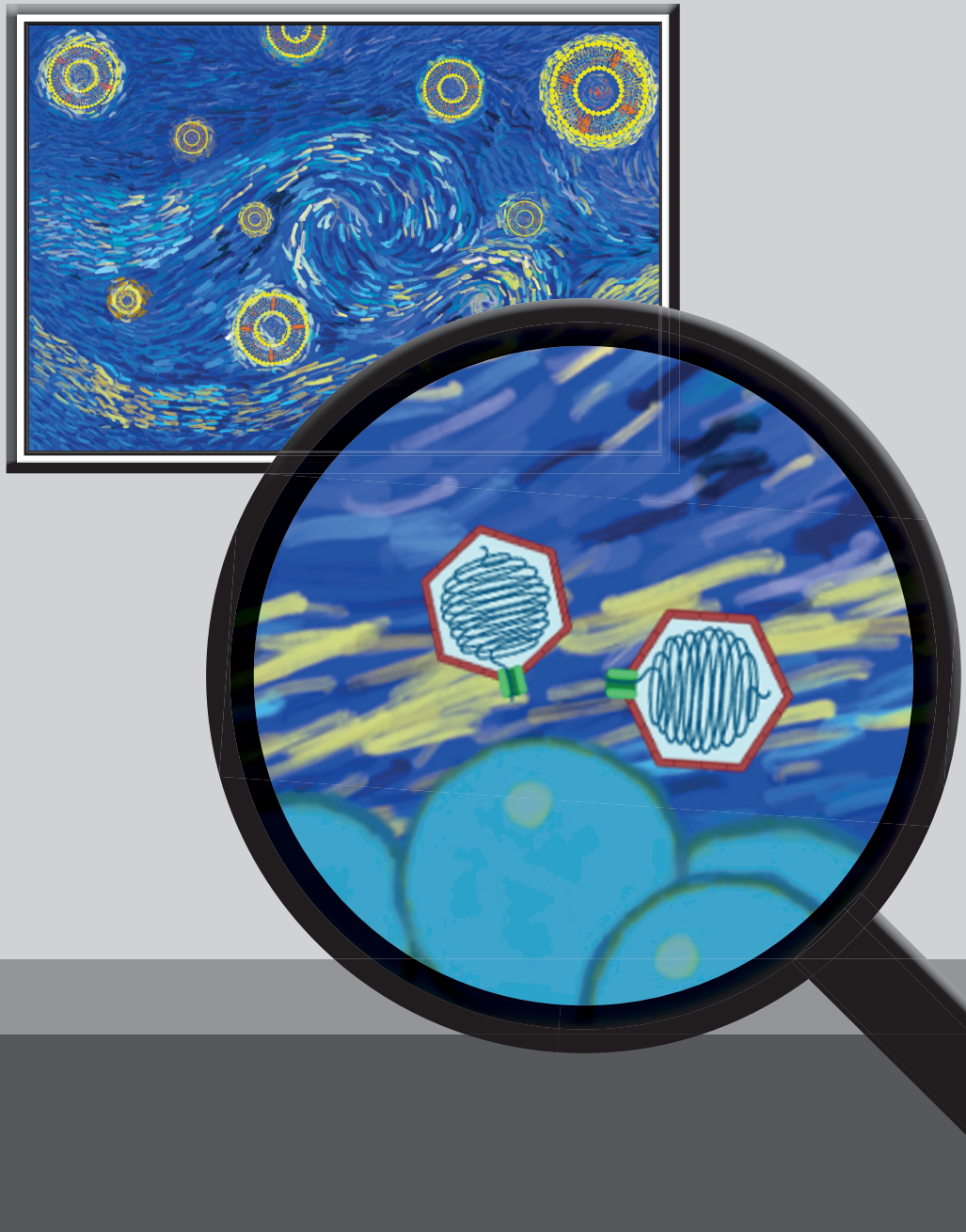

Chapter 6

Genomics of tailless bacteriophages in a complex lactic acid bacteria starter culture

Svetlana Alexeeva[1], Yue Liu[1], Jingjie Zhu, Joanna Kaczorowska,
Thijs R. H. M. Kouwen, Tjakko Abee & Eddy J. Smid

[1] Equal contributions.

Published in

International Dairy Journal, 2021, 114:104900

Abstract

Our previous study on a model microbial community originating from an artisanal cheese fermentation starter revealed that bacteriophages not only co-exist with bacteria but also are highly abundant. Here we describe the genomic content of phage particles released by 6 different strains in the starter culture. The identified prophages belong to three different subgroups of the *Siphoviridae* P335 phage group. Remarkably, most analyzed prophages show disruptions in different tail encoding genes, explaining the common tailless phenotype. Furthermore, a number of potentially beneficial features for the host carried by prophages were identified. The prophages carry up to 3 different phage defense systems per genome that are potentially functional in protecting the host from foreign phage infection. We suggest that the presumably defective prophages are a result of bacteria-phage coevolution and could convey advantages to host bacteria.

Introduction

Cells from all domains of life are susceptible to viral infections. As prokaryotes outnumber eukaryotes, their viruses (bacteriophages or simply phages), are estimated to be the most abundant biological entities on Earth. Total number of bacteriophages is estimated to be 10^{31} in the biosphere (Comeau et al., 2008). Phages are ubiquitously distributed in nature and play an important role in the ecology of their bacterial hosts. In complex microbial consortia such as those found in a marine environment, the gastrointestinal tract and in complex food fermentations, bacteriophages can alter the dynamics and diversity of microbial communities (Stern and Sorek, 2011; Erkus et al., 2013; Smid et al., 2014; Spus et al., 2015). Additionally, bacteriophages help to drive microbial evolution through phage-mediated gene transfer (Canchaya et al., 2003; Penadés et al., 2015).

Bacteriophages can also occur naturally in food. Lactic acid bacteria have been used for centuries in the production of fermented food products, with for instance *Lactococcus lactis* as an important player in various dairy fermentations. Bacteriophages infecting *L. lactis* strains are mostly studied because of their detrimental impact on industrial milk fermentation processes (Mahony and van Sinderen, 2015).

All described *L. lactis* phages are members of the *Caudovirales* order and possess a double-stranded DNA genome and a non-contractile tail. The vast majority of lactococcal phages belong to one of the three main groups within *Siphoviridae* family: 936, c2, or P335 (Mahony et al., 2017). Groups 936 and c2 consist of only virulent phages, while the P335 group consists of both temperate and virulent phages (Chmielewska-Jeznach et al., 2018). P335 phages resemble lambdoid phages, are genetically heterogeneous and have a mosaic genome structure with functional modules exchangeable through homologous recombination (Moineau et al., 1994; Chopin et al., 2001; Desiere et al., 2002). Maintenance of a temperate bacteriophage inside a bacterial chromosome in the form of a prophage, also referred to as lysogeny, is a common phenomenon in *L. lactis* strains (Brøndsted and Hammer, 2006; Kelleher et al., 2018). Lysogenic bacterial strains, carrying inducible prophages in the chromosome, usually do not find their way into commercial fermentation practice when it concerns a defined starter composition (Garneau and Moineau, 2011). Nevertheless, lysogenic bacteria are often found in undefined mixed starter cultures. It was discovered that a naturally evolved complex starter culture (named Ur), featured by stable composition and robustness, is composed of mainly lysogenic strains (Alexeeva et al., 2018). Remarkably, all released bacteriophages from the complex starter culture Ur were found essentially tailless. Up to 10^{10} tailless phage particles per mL of culture are spontaneously produced by cultures of the individual strains without the occurrence of clear signs of lysis of the lysogenic strain. In this study, we subjected phage particles released from 6 representative strains to DNA sequencing followed by annotation and attribution of functions based on *in silico* approaches, with the objective to understand the unusual phage phenotype and explain the evolutionary relevance of such case.

Materials and Methods

L. lactis strains and bacteriophages

Representative strains of *Lactococcus lactis* TIFN1-TIFN7 were used throughout this study. These strains represent isolates from different genetic lineages originally isolated from single colonies from a complex starter culture Ur and the genome sequence has been determined (Erkus et al., 2013). *L. lactis* TI1c is a phage cured derivative of TIFN1 described earlier (Alexeeva et al., 2018). The strains were maintained as 15% glycerol stocks at -80 °C and routinely grown in M17 broth (OXOID) with 0.5% (wt/vol) glucose or lactose addition (OXOID). Bacteriophages used in the phage sensitivity screen are listed in supplementary Table S6.1.

Phage preparation and DNA isolation

Induction of the prophages was performed using mitomycin C (the stock 0.5 mg/mL solution in 0.1M $MgSO_4$ was stored at 4 °C). Overnight cultures were grown in M17 supplemented with 0.5% glucose at 30°C. The cells were diluted in fresh medium to OD_{600} = 0.2 and incubated 1-2 hours, until middle/late exponential phase was reached (OD_{600} = 0.4 - 0.5). At this point mitomycin C solution was added to final concentration 1 µg/mL. The cultures were further incubated for 6 hours, as OD_{600} was monitored hourly. Cultures were centrifuged for 15 minutes at 6000 x *g* at 4 °C and the supernatant was filter-sterilized using 0.2 µm polyethersulfone (PES) filters. The phage particles in the filtrate were precipitated using 1 volume of 20% polyethylene glycol 8000 and 2.5 M NaCl to 4 volumes crude bacteriophage suspension. The samples were incubated overnight at 4 °C and then centrifuged at 11000 x *g* for 60 min at 4 °C. Supernatants were discarded and the pellets were left to dry on clean absorbent paper.

The pellets were directly used for DNA extraction using Promega Wizard® Genomic DNA Purification Kit. The phage pellets were re-suspended in 600 µL of Nuclei Lysis Solution and transferred into clean 1.5 mL micro-centrifuge tubes. The suspension was incubated at 80 °C for 5 min and then cooled to room temperature. Three µL of RNase solution (provided with the kit) was added to each sample. The samples were mixed by inversion and incubated at 37 °C for about 50 min. Proteinase K (20 mg/mL) was added to a final concentration 200 mg/L and then samples were incubated at 50 °C for 30 min. The samples were cooled to room temperature and 200 µL of Protein Precipitation Solution was added to the tubes. The tubes were vortexed vigorously for 20 seconds and incubated on ice for 5 min. After this step the samples were centrifuged (17000 x *g*, 3 min, room temperature). The supernatant was transferred in a new 1.5 mL micro-centrifuge tube containing 600 µL of isopropanol kept at room temperature. Next the samples were mixed by inversion until strands of DNA were visible, centrifuged (17000 x *g*, 2 min, room temperature) and the supernatant was poured off. Six hundred µL of 70% ethanol (kept at room temperature) was added to the tubes. Tubes were inverted several times to wash the DNA pellet and then centrifuged (17000 x *g*, 2 min, room temperature). Ethanol was allowed to evaporate and the tubes were dried on clean absorbent paper. The tubes were left open for 15 min

to air dry the pellet, then 100 µL of DNA Rehydration Solution was added and DNA was rehydrated at 65 °C for 1 h. Alternatively, the DNA was rehydrated by incubating the solution overnight at 4 °C.

The isolated and rehydrated DNA was additionally purified from low molecular weight DNA species using Amicon® Ultracel 100 K columns (cut-off 100 kDa or double-stranded nucleotide cut-off > 600 bp). DNA solution was brought to 0.5 mL using 5 mM Tris buffer (pH = 8) and added to the column. The samples were centrifuged at 14000 x *g* and washed 3 times with 0.5 mL buffer. The quality of DNA before and after micro-column purification was examined by agarose gel electrophoresis.

Sequencing and assembly of sequences

Library preparation using TruSeq DNA sample kit and genome sequencing was performed by BaseClear BV (Leiden, The Netherlands). A paired-end DNA library with a mean gap length size between 230 and 360 bp was constructed and the sequencing was performed using HiSeq 2500 Illumina technology (Illumina Inc, Hayward, CA) using a 50-cycle or 100-cycle (proPhi7) paired-end protocol. The sequencing yielded on average 1350000 reads (135 MB, for 50-cycle) and 800000 reads (155 MB, for 100-cycle).

Next-generation assembly was performed using SeqMan NGen *de novo* algorithm (v12, DNAStar, USA). In 4 of 6 cases 68 - 88% of all reads assembled in a single contig (see Table 6.1 for assembly statistics). The assemblies were also checked with host genome data.

Table 6.1. Phage genome assembly statistics.

Phage	N reads	Number of contigs	Contig length raw	Contig coverage	Background average coverage	% reads in contig	x covarage above background
proPhi1	5,815,949	1	41886	7211	59	68	121
proPhi2	3,336,448	1	37935	3175	27	75	119
proPhi4	2,927,954	1	38129	3106	28	88	112
proPhi5	2,288,894	3	41186	2292	40	88	58
proPhi6	2,248,210	1	38549	2189	38	82	58
proPhi7	1,547,972	15	40045	1146	47	29	24

The sequences were initially subjected to automated annotation using MyRAST (Rapid Annotation Subsystem Technology (RAST) server (Aziz et al., 2008). All predicted protein-coding genes were screened using BLASTP and Psi-BLAST algorithms against the non-redundant protein database at NCBI and for conserved motifs using InterProScan 5 (Jones et al., 2014). Where applicable, nucleotide BLAST was performed at NCBI and gene ontology (GO) annotations on the gene products were performed by UniProt “QuickGO” (The UniProt Consortium, 2019).

All contigs > 600 nt long with high coverage or > 25000 nt long obtained from SeqMan NGen analyses were annotated using MyRAST server (Aziz et al., 2008) and screened for phage-related features.

The genome extremities of the prophages were determined by identifying the attachment sites, followed by conformation by PCR analysis [Fig. 8 in (Alexeeva et al., 2018)]. The sequence assembly was checked for correctness by comparison with restriction data obtained by using restriction enzymes ScaI and AvaII. The data indicated that the assembly was correct.

Phylogenetic analysis and classification

Alignment of sequences was run on MAFFT server. The evolutionary history was inferred by using the Maximum Likelihood method based on the Tamura-Nei model (Tamura and Nei, 1993). The percentage of trees in which the associated taxa clustered together is shown next to the branches. Initial tree(s) for the heuristic search were obtained automatically by applying Neighbor-Joining and BioNJ algorithms to a matrix of pairwise distances estimated using the Maximum Composite Likelihood (MCL) approach, and then selecting the topology with superior log likelihood value. The tree is drawn to scale, with branch lengths measured in the number of substitutions per site (next to the branches). The analysis involved 10 and 22 nucleotide sequences. All positions containing gaps and missing data were eliminated. Evolutionary analyses were conducted in MEGA6 (Tamura et al., 2013).

Nucleotide and protein sequences accession numbers

The sequence data reported in the present study have been deposited in GenBank database under accession no. MN534315 - MN534320. The complete genomic sequences of the P335 group phages analyzed in this study are available under the following GenBank accession numbers: phage name (accession number): (P335 (DQ838728), 4268 (AF489521), bIL285 (AF323668), bIL286 (AF323669), bIL309 (AF323670), BK5-T (AF176025), phiLC3 (AF242738), r1t (U38906), TP901-1 (AF304433), Tuc2009 (AF109874), and µl36 (AF349457). Prophage sequences of *L. lactis* SK11 (SK11-1, SK11-2, SK11-3, SK11-4 and SK11-5) were derived from (NC_008527) (Ventura et al., 2007).

Bacteriophage sensitivity tests

Plaque assays were conducted to quantify the phage sensitivities of wild type strains and their cured derivatives. One hundred µL of phage suspensions in 3 - 4 dilution series were mixed with 100 µL overnight culture of the target bacterium. The mixtures were incubated for 10 min prior to adding to tubes containing 2.8 mL soft agar. After 24 h incubation at 30 °C, plaques were counted and plaque-forming units per mL values were calculated.

Results

Genomic organization and annotation

Whole phage genome sequences were obtained for phage particles released by *L. lactis* strains TIFN1, TIFN2, TIFN4, TIFN5, TIFN6 and TIFN7 upon mitomycin C (MitC) induction. The host strains are representative isolates from different genetic lineages and the genome sequence has been determined (Erkus et al., 2013). With whole genome sequencing, two prophages were predicted for all host strains

mentioned above, but one of the predicted prophages in TIFN1, TIFN5 and TIFN6 and both prophages in TIFN7 have questionable completeness (Alexeeva et al., 2018). In this study only one phage genome per strain was assembled in a single scaffold of high coverage (above 1100x). We cannot exclude the possibility that more than one prophage from each strain was induced, but we confirmed that only one phage from each strain was released in great abundance. The bacteriophages released by TIFN1, TIFN2, TIFN4, TIFN5, TIFN6 and TIFN7 strains were named proPhi1, proPhi2, proPhi4, proPhi5, proPhi6 and proPhi7 respectively. The genome sequence of proPhi1 was found to be identical to proPhi5, and the sequence of proPhi2 was found to be identical to proPhi4. The sequence assembly was checked for correctness by comparison with restriction analysis data obtained by using two restriction enzymes (ScaI and AvaII). The data indicated that the assembly was correct and no additional fragments were detectable, confirming that only the described prophages were released from each host in high abundance (data not shown). All prophage genome sequences with annotations have been deposited in GenBank database under accession no. MN534315 - MN534320.

General characteristics of the released phages such as the genome size, the GC content and the number of open reading frames (ORFs) are summarized in Table 6.2. The initiation codon AUG is present in most protein-coding genes, but GUG and UUG are also found in all phage genomes albeit with lower frequency (Table 6.2).

Table 6.2. General characteristics of the 6 phage genomes.

Phage	Genome size (bp)	% GC	ORFs total	The frequency of initiation codon usage, % AUG/GUG/UUG
proPhi1 & proPhi5[a]	41249	35.92	62	89/5/6
proPhi2 & proPhi4[a]	36976	35.61	49	90/4/6
proPhi6	37410	35.4	55	89/7/4
proPhi7	38158	35.24	56	95/2/4

[a] Genome sequences of proPhi1 and proPhi5 are identical to each other, proPhi2 and proPhi4 are identical to each other.

Analysis of phage genomes revealed that all released phage genomes have mosaic structure, organized in two clusters of divergently transcribed genes, typical for temperate lactococcal phages. The cluster transcribed leftwards mainly comprises genes encoding functions for integration and maintenance of lysogeny. Genes encoding proteins involved in DNA replication, transcriptional regulation, packaging, structural proteins and phage release are mostly transcribed rightwards.

Taxonomy and comparative genomics

To establish the degree of diversity between the newly described phages and their relatedness to other lactococcal phages, a comparative genome analysis was carried out. In total, 16 published P335 phage genomes (Ventura et al., 2007; Kelly et al., 2013), along with proPhi1 & proPhi5 (sequence identical), proPhi2 & proPhi4 (sequence identical), proPhi6 and proPhi7 were used to construct a

phylogenetic tree (Fig. 6.1). The 16 phages of the lactococcal P335 group of temperate bacteriophages were selected based on earlier studies describing 4 subgroups of the P355 group lactococcal phages (Ventura et al., 2007): SK11-1 and SK11-5 belong to subgroup 1; Tuc2009, TP901-1, SK11-2, SK11-3, ul36 and bIL285 belong to subgroup 2; P335, bIL309, BK5-T and bIL286 belong to subgroup 3; r1t and LC3 belong to subgroup 4; SK11-4 and 4268 were not classified.

The phages proPhi1 & proPhi5 are most closely related to Tuc2009, TP901-1 and SK11-2. The genome sequence of proPhi6 showed most similarity to that of prophage SK11-3 and phage µl36. All of these phages fall into subgroup 2 P335 bacteriophages, all of which seem to share *pac*-type packaging mechanism (Labrie et al., 2008).

The sequences of proPhi2 & proPhi4 clustered into subgroup 3 and proPhi7 is found among subgroup 4 bacteriophages, with bIL286 and r1t as most closely related bacteriophages respectively. The members of these subgroups share, in contrast to the subgroup 2 members, *cos*-type packaging mechanism (Labrie et al., 2008).

Tail disruptions

Thorough sequence analysis of genes encoding structural tail elements (Fig. 6.2) provided an explanation for the tailless phenotype of the released phage particles [(Alexeeva et al., 2018); additional EM pictures in supplementary Fig. S6.1]. In proPhi1/proPhi5, ORF48 and ORF51 resemble most the N- and C terminal parts of a structural tail protein in prophage SK11-2 (98 and 94% amino acid (aa) identity, respectively) (Fig. 6.2A). ORF51 is 90% identical to 475 aa C terminal part of tail length tape measure protein (TMP, ORF45) of phage TP901-1, a tail protein determining tail length (Pedersen et al., 2000; Vegge et al., 2005). ORF48 shares 36% identity to N terminal part of TMP (ORF45) of phage TP901-1. Whereas SK11-2 and TP901-1 both encode a complete protein of 874 and 937 amino acids long respectively, in proPhi1/proPhi5 the two open reading frames are separated by insertion of two mobile elements (transposase/integrase) encoded on the opposite strand (Fig. 6.2A). These observations suggest that ORF48 and ORF51 of proPhi1/proPhi5 encode the putative TMP that is disrupted by insertions, resulting in the tailless phenotype of the released phages.

In proPhi6 a different tail element is the target of disruption. ORF39 of proPhi6, 75 aa, is 97% identical to first 75 aa of ORF40 in Tuc2009 (102 aa) and 95% to ORF39 in TP901-1 (103 aa). This protein seems to be highly conserved, identical proteins are also present and intact in phages µl36, P335 and in proPhi1/proPhi5 (Fig. 6.2B). It functions at head-tail interface and has been described earlier as putative head to tail joining protein (Brøndsted et al., 2001). In proPhi6, however, the C-terminal sequence is separated from its N-terminus by insertion of a mobile element (transposase, ORF40) encoded on the opposite strand. This fits with the observed phenotype of proPhi6: TIFN6 is the only strain that released separated tails next to the phage heads [(Alexeeva et al., 2018); additional EM pictures in supplementary Fig. S6.1c] indicating that the head to tail joining function is indeed impaired.

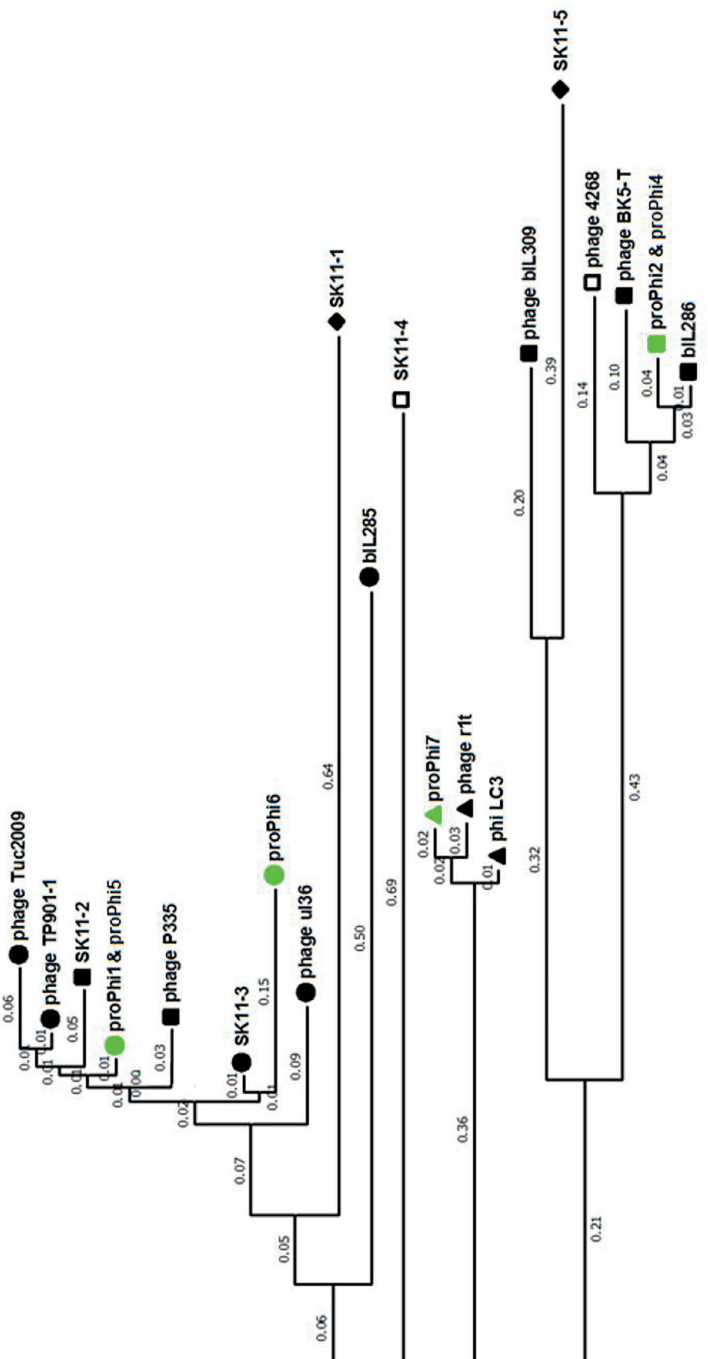

Figure 6.1. The phylogenetic tree of lactococcal phages including the bacteriophages described in this study (prophages). The tree is drawn to scale, with branch lengths measured in the number of substitutions per site (next to the branches). The analysis involved 20 nucleotide sequences. All positions containing gaps and missing data were eliminated. There were a total of 917 positions in the final dataset. Evolutionary analyses were conducted in MEGA6 (Tamura et al., 2013). Black filled symbols: P335 group, circles - subgroup 2, squares – subgroup 3, triangles – subgroup 4, diamonds – subgroup 1 as classified based on proteomic analysis earlier (Ventura et al., 2007; Kelly et al., 2013). Open symbols – phage 4268 was not analyzed in (Ventura et al., 2007; Kelly et al., 2013); phage SK11-4 was unclassified. Green filled symbols – newly classified Ur phages. The numbers indicate branch length.

Figure 6.2. **Alignment of structural tail elements encoding regions of prophages, disrupted by insertions of mobile elements.** The tail elements are aligned to their homologous counterparts of earlier described bacteriophages using MUSCLE (Madeira et al., 2019). Green bar represent homology regions, similarity profile height represents the level of conservation, regions in grey lack detectable homology. Corresponding scale (in base pair) and encoded features are shown under each sequence. The alignments are shown for **A)** putative TMP of proPhi1/proPhi5; **B)** putative head-tail joining protein of proPhi6; **C)** putative TMP of proPhi7. No disruption in the tail elements was identified in proPhi2/proPhi4 and therefore no information of these phages are shown in this figure.

The 3450 bp-region encompassing ORFs 44, 45, 46 of proPhi7 shares 90% nucleotide identity to ORF40, 41 and 42 of phage r1t (Fig. 6.2C). ORF 44 and 46 in proPhi7 and ORF 40 and 42 in phage r1t encode the N and C-terminus of a TMP. It has been suggested that r1t ORF41, identical to proPhi7 ORF45 and separating N and C-terminus of the TMP, belongs to HNH homing endonuclease or a group I introns (van Sinderen et al., 1996; McGrath et al., 2006). However, r1t has been shown to possess a tail (Lowrie, 1974). On the other hand, phage phiLC3 encodes 843 aa long TMP, identical to r1t and proPhi7, but not interrupted by an insertion (Fig. 6.2C). It is therefore unclear, whether or not the insertion between N and C-terminus of proPhi7 TMP results in the tailless phenotype of proPhi7. In addition, no obvious disruptive elements could be identified in the tail module of proPhi2/proPhi4 despite the observed tailless phage morphology.

Potentially beneficial prophage encoded features

Next to the obvious phage-related features, e.g. integration, the regulation of lytic/lysogenic conversion and structural proteins, the prophages also encode proteins with potential benefits to the host. Phage-defense protein encoding genes are among the most frequently observed ones (Table 6.3). ORF2 in proPhi1/proPhi5 is 98% identical to the gene encoding Sie family SieIL409 protein of *Lactococcus* phage 409, and SieIL409 has been shown to mediate phage resistance by a DNA injection blocking mechanism (McGrath et al., 2002; Mahony et al., 2008). The terminal ORF62 in proPhi1/proPhi5 is also assigned to have methyltransferase activity by GO annotation and is possibly part of an restriction-modification system. ORF61 of proPhi1/proPhi5 codes for an abortive infection AbiD/AbiF-like protein, showing conserved domain of Abi_2 protein superfamily and about 50% identity to the amino acid sequences of abortive infection bacteriophage resistance proteins in several *Streptococcus* phages. The Abi system is another feature potentially involved in a phage defense mechanism: it allows phage absorption and phage DNA injection but interfere with further phage development, so that the death of infected cells occurs but no viral progeny is released (Labrie et al., 2010). Also proPhi7 carries two genes (ORF55 & ORF56) encoding Abi-like proteins near the attR terminus: ORF55 shows conserved domain of AAA_21 protein superfamily (AbiEii proteins) and 30% - 50% identity to the amino acid sequences of abortive phage resistance proteins in several *Lactobacillus* phages; ORF56 shows conserved domain of RloB protein superfamily (AbiLii proteins) and up to 40% identity to the amino acid sequences of RloB domain-containing protein in plenty members of Firmicutes bacteria.

Furthermore, proPhi6 carries a gene for a membrane protein related to a metallopeptidase (ORF49, with 80% identity to ORF53 in proPhi1/proPhi5). The product of ORF33 in proPhi2/proPhi4 is a putative protease (ATP-dependent serine endopeptidase, ClpP) and finally proPhi6 possesses prepillin peptidase (ORF13) encoding gene. Whether products of these genes could offer competitive advantages to the hosts in a microbial community by inhibiting other species remains to be elucidated.

Table 6.3. Phage-defence protein encoding genes identified in Ur prophages.

Prophage	ORF	Putative product	Defence mechanism
proPhi1/proPhi5	ORF2	Sie protein	superinfection-exclusion
	ORF61	Abi-like protein	abortive infection
	ORF62	N-4/N-6 DNA methylase	restriction modification
proPhi7	ORF55	abortive phage resistance protein	abortive infection
	ORF56	abortive phage resistance protein	abortive infection

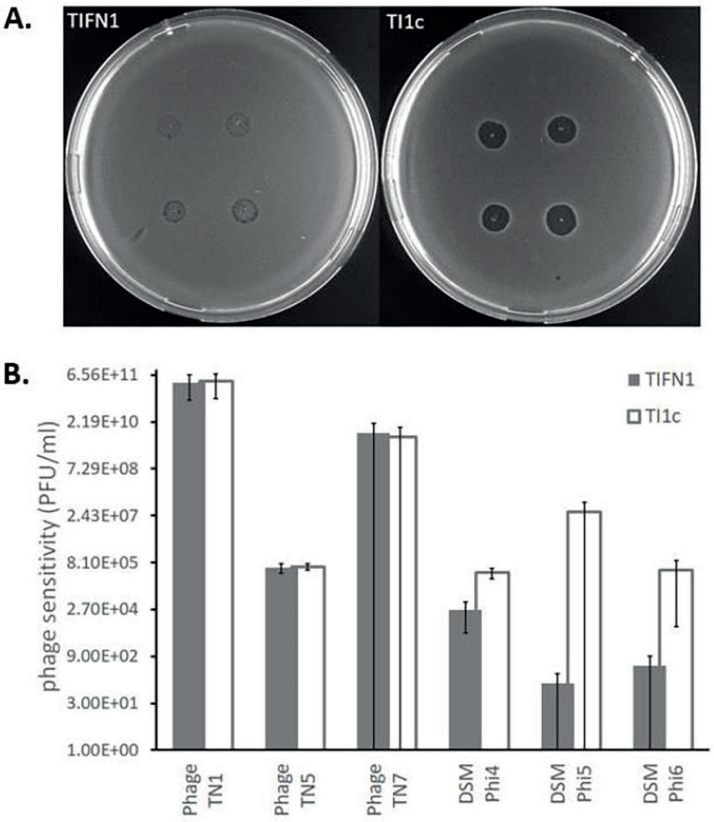

Figure 6.3. Phage sensitivity in TIFN1 and TI1c. A) Spot clearance and morphology produced on the lawns of TIFN1 (left) and TI1c (right) by DSM Phi5 (upper spots) and DSM Phi6 (lower spots), in duplicate. **B)** Quantification of phage sensitivity by plaque assay. Data from two to seven experimental replicates, error bars represent standard errors. * indicates $p < 0.1$; **indicates $P < 0.05$; *** indicates $p < 0.01$.

The variety of phage resistance genes carried by prophage genomes suggests that the prophages likely contribute to host's ability to counteract superinfections. To assess this contribution we challenged lysogenic wild-type strains TIFN1 in parallel with its phage-cured derivative TI1c with 16 lactococcal phages (supplementary Table S6.1).

Six phages (phage TN1, TN5, TN7, DSMPhi4, DSMPhi5 and DSMPhi6) from the phage collection were lysis-positive for TIFN1 and TI1c as revealed by spot tests, and clear differences in sensitivity of the two strains were already visualized towards some of the phages (example Fig. 6.3A). Further, phage sensitivity towards the 6 lysis-positive phages was quantified for the two strains (Fig. 6.3B). TIFN1 showed significantly ($p < 0.1$) lower phage sensitivity towards phages DSMPhi4, DSMPhi5 and DSMPhi6 compared to TI1c. Moreover, it was also noticed that the plaques were smaller and more opaque on TIFN1 than TI1c for these 3 phages (supplementary Fig. S6.2).

Discussion

In our previous study we described morphologically tailless bacteriophages, abundantly and continuously released by all analyzed *L. lactis* strains originating from a complex dairy starter culture Ur without showing obvious cell lysis (Alexeeva et al., 2018). Because of their distinct morphology, behavior and no apparent impact on host cell integrity, we hypothesized that these bacteriophages belong to a separate (novel) group of temperate lactococcal phages. However, detailed genome analysis of the released phages presented here, revealed that the bacteriophages possess a typical lactococcal P335 group *Siphoviridae* family genome structure, and that the phages fall under three different known subgroups of P335 phages (Ventura et al., 2007).

Temperate lactococcal phages of *Siphoviridae* family, belonging to the P335 group, are usually characterized by a long non-contractile tail - a structure responsible for host recognition, adsorption and the initiation of phage infection by envelope penetration and DNA ejection (McGrath et al., 2006). Despite the fact that all inducible prophages found in strains from the complex starter culture Ur so far are essentially tailless, phage sequencing revealed the presence of genes encoding most of the tail structural elements: head-tail connector, major tail protein (MTP), tail length tape-measure protein (TMP), distal tail protein, tail associated lysin, upper and lower base plate protein (Vegge et al., 2005; Veesler and Cambillau, 2011; Veesler et al., 2012; Stockdale et al., 2015). Detailed sequence analysis identified the presence of insertions of mobile genetic elements in the tail module in most of the phage genomes analyzed in this study. Furthermore, the insertions occurred at different sites of the tail module: proPhi1, proPhi5 and proPhi7 contained (different) insertions in the TMP while proPhi6 in the head-tail joining protein. TMP determines the length of the phage tail (Katsura, 1987; Pedersen et al., 2000) and serves as a component of the precursor complex, involved in the initiation of polymerization of MTP. It has been shown for λ phage that in the absence of TMP, MTP polymerization may be initiated but the formation of tail-tube related structure is abolished (Katsura, 1976). The

tailless morphology of proPhi2/proPhi4 could not be explained by this sequence analysis as no obvious disruptive elements could be identified in the tail modules. It is postulated that the absence of tails for the phage proPhi2/proPhi4 belonging to these particular *L. lactis* strains is caused by modifications at transcriptional and translational level of the phage genes, or minor mutations in gene sequence.

Bacteria-phage coevolution has been regarded as an important driver of evolutionary processes and an essential player in shaping of microbial communities (Koskella and Brockhurst, 2014). This is also reflected in the results of the phage genomics analysis performed in this study. In the Ur strains, most of the inducible prophages have mutational insertions in different tail encoding genes, resulting in tailless phage particles that are likely to be defective to infect their hosts as the tail is required for adhesion and subsequent injection of phage DNA, which is possibly a host strategy to minimize the phage impact. In fact, defective prophages are commonly observed in bacterial genomes. Out of more than 200 prophages from 83 bacterial genomes analyzed in a study (Casjens, 2003), only 9 prophages were experimentally shown to be fully functional. All other prophages were found to have experienced different levels of mutational decay. Moreover, it is also acknowledged that many genes in the defective prophages remain functional and contribute to various traits of the hosts, and that the prophage functions are a result of purifying selection in the bacterial chromosome (Bobay et al., 2014; Kelleher et al., 2018). Prophage genes encoding core phage-related functions, e.g. tail and lysis proteins, were found to be under stronger purifying selections (Bobay et al., 2014), presumably due to the critical functions in phage spreading or host integrity carried by these genes. This finding coincides with our observation that prophages in bacterial community members of the dairy starter culture Ur, showed disruptions in the tail protein encoding genes. This could be explained, as the loss of the key structure to re-infect the same bacterial species was likely advantageous for the species to be maintained in the microbial community. In addition, the current genetic analysis also predicted prophage-encoding phage resistance systems in some of the Ur prophages, which could be linked to the phage resistance phenotype of the host; this could be also a result of purifying selection.

Another uncommon phenotype of the studied Ur phages was the spontaneous, continuous release of phage particles, even when no stress or prophage-inducing condition was applied (Alexeeva et al., 2018). For lambda phage the spontaneous excision rates are approximately 10^{-6} per cell division (Gottesman and Yarmolinsky, 1968; Bobay et al., 2014) while another study (Muhammed et al., 2018) observed up to 10^{7} mL^{-1} spontaneous release of P335 phages. It is remarkable that up to 10^{10} mL^{-1} phage particles are released by Ur strains spontaneously (Alexeeva et al., 2018). Attempts to explain this phenotype were made by examining the repressor sequences in the prophages. In all the prophages, a repressor has been identified: orf3 in proPhi1 & proPhi5, orf2 in proPhi2 & proPhi4, orf3 in proPhi7 and orf4 in proPhi7. All identified repressors showed homology to full-length repressor genes in other phages and we did not identify obvious disrupting elements or mutations leading to premature stop codons. However, as described by (Kot et al., 2016), even single point mutations in the CI repressor of phage TP901-1 were enough to affect the maintenance of the lysogenic state. It is therefore plausible that the phage-host coevolution has resulted in (minor) mutations in sequence,

or modifications in the transcriptional or translational levels in the regulatory elements, that allow continuous assembly of these phage particles. Notably, the fitness of the host does not seem to be compromised by the continuous phage release, when comparing the growth performance of TIFN1 to its proPhi1-cured derivative TI1c based on OD measurement (supplementary Fig. S6.3).

It should be noted that although prophage-encoded phage-resistance elements were predicted and TIFN1 showed higher phage resistance than its phage-cured derivative, this study does not intend to provide direct conclusions on the functionality of the phage-resistance elements but to provide possible explanations based on the genome data available. The phage-resistance phenotype in the prophage-harboring strain could also be a result of self-immunity mediated by repressors, or the continuous phage producing phenotype inhibits successful infection of other incoming phages by competing and interfering with the assembly process.

All these could serve as the explanation of the phenomenon that in the bacterial community of the dairy starter Ur, presumably after a long-term selection, predominantly strains with a prophage sequence were maintained. In conclusion, the analysis of the genomic content of phage particles released by 6 different strains in the starter culture Ur provided insights for bacteria-phage coevolution, and this may also provide new leads in for future research and implications in practice, for example in defining strain selection criteria in (dairy) industry, where traits like phage resistance are desired.

Acknowledgements

This work was supported by Top Institute Food and Nutrition (TIFN) in Wageningen, the Netherlands through contract FF001. In addition, Yue Liu was subsidized by the Netherlands Organization for Scientific Research (NWO) through the Graduate Program on Food Structure, Digestion and Health.

The authors are grateful to Laurens Hanemaaijer of DSM for technical support in phage sensitivity tests, acquiring and sharing of phages DSM Phi1-DSM Phi10 suspension stocks, Michiel Wels for support with sequence assemblies and Anne de Jong for support with sequence annotations. We also thank students of Wageningen University for their contribution: Venera Proneva for purification of proPhi4, and proPhi5, and proPhi6 DNA; Yixin Ge for purification of proPhi7 DNA. We thank Dr Jennifer Mahony of University College Cork, Cork, Ireland for kindly providing us bacteriophages sk1, p2 and jj50. We also gratefully acknowledge Jan van Lent (Wageningen Electron Microscopy Centre (WEMC)) for his help with electron microscopy.

Supplementary materials

Table S6.1. Bacteriophages used in phage sensitivity screen.

Phage/code	Relevant features	Source or reference
sk1	936-type lytic isometric-headed phage	Chandry et al., 1997
jj50	936-type lytic isometric-headed phage	Josephsen et al., 1989
p2	936-type lytic isometric-headed phage	Higgins et al., 1988
Phage TN1	P335-type temperate phage	=FTIFN1 in Erkus et al., 2013
Phage TN5	936-type lytic	=FTIFN5 in Erkus et al., 2013
Phage TN7	P335-type temperate phage	=FTIFN7 in Erkus et al., 2013
DSM Phi1	c2-type lytic	DSM Food Specialities B.V.
DSM Phi2	c2-type lytic	DSM Food Specialities B.V.
DSM Phi3	P335-type temperate phage	DSM Food Specialities B.V.
DSM Phi4	936-type lytic	DSM Food Specialities B.V.
DSM Phi5	936-type lytic	DSM Food Specialities B.V.
DSM Phi6	936-type lytic	DSM Food Specialities B.V.
DSM Phi7	936-type lytic	DSM Food Specialities B.V.
DSM Phi8	not typed	DSM Food Specialities B.V.
DSM Phi9	not typed	DSM Food Specialities B.V.
DSM Phi10	c2-type lytic	DSM Food Specialities B.V.

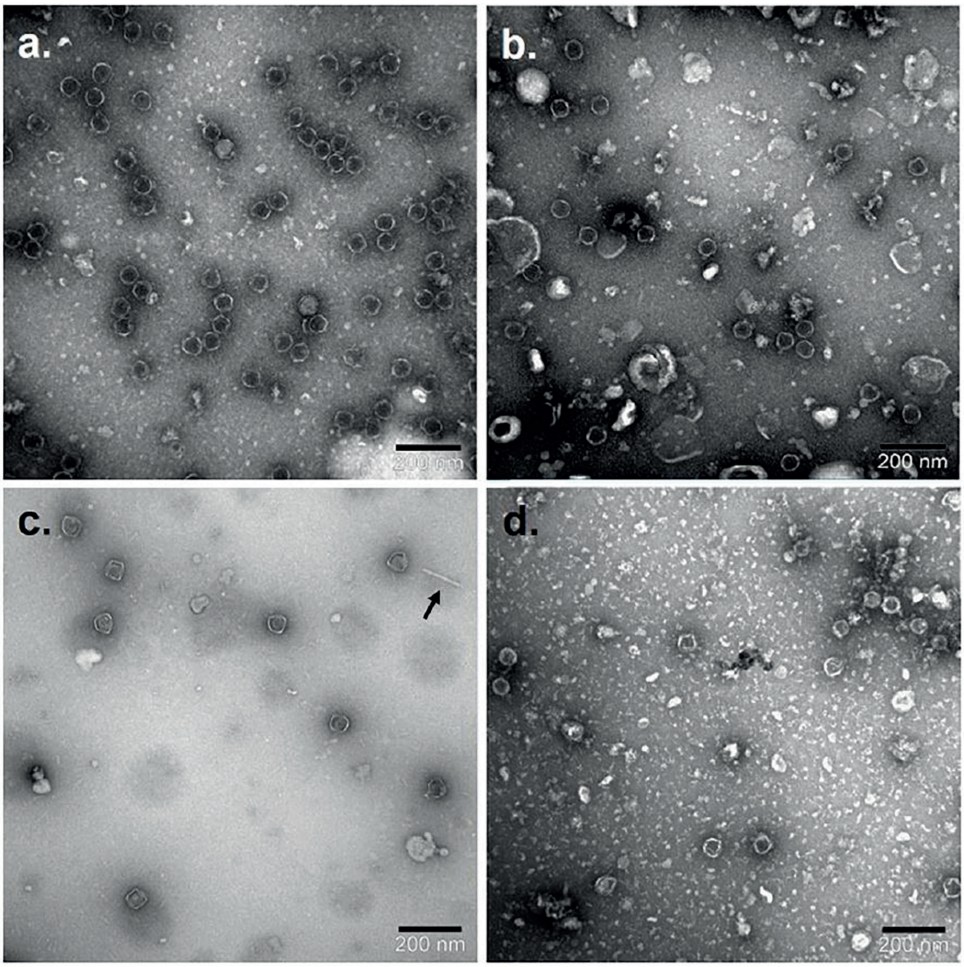

Figure S6.1. Transmission electron microscopic (TEM) pictures of Ur phages. a) proPhi1; b) proPhi2; c) proPhi6, arrow shows a phage tail separated from the head; d) proPhi7. Samples for proPhi1, proPhi6 and proPhi7 were treated with chloroform before TEM imaging, the sample for proPhi2 was not treated with chloroform.

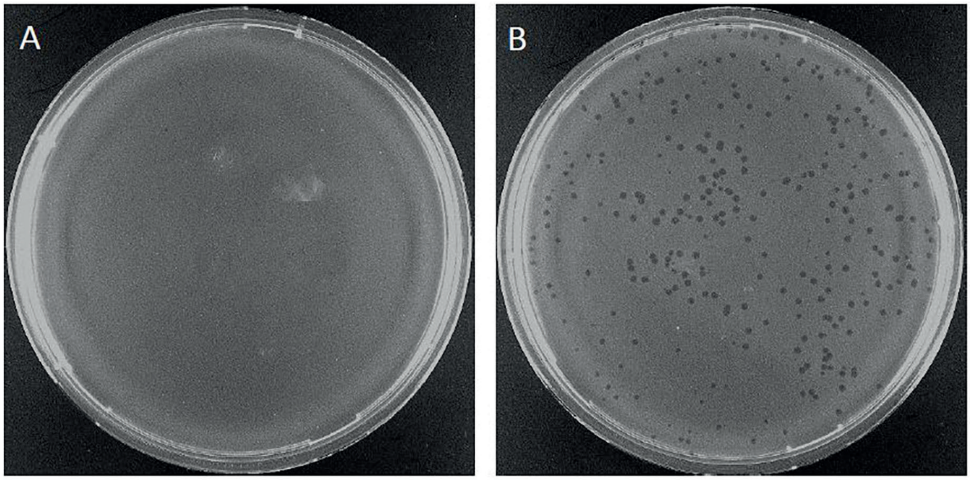

Figure S6.2. Example of plaque morphology on TIFN1 and TI1c. DSM Phi4 plaque appearance on the lawns of A. WT TIFN1, B. cured TI1c.

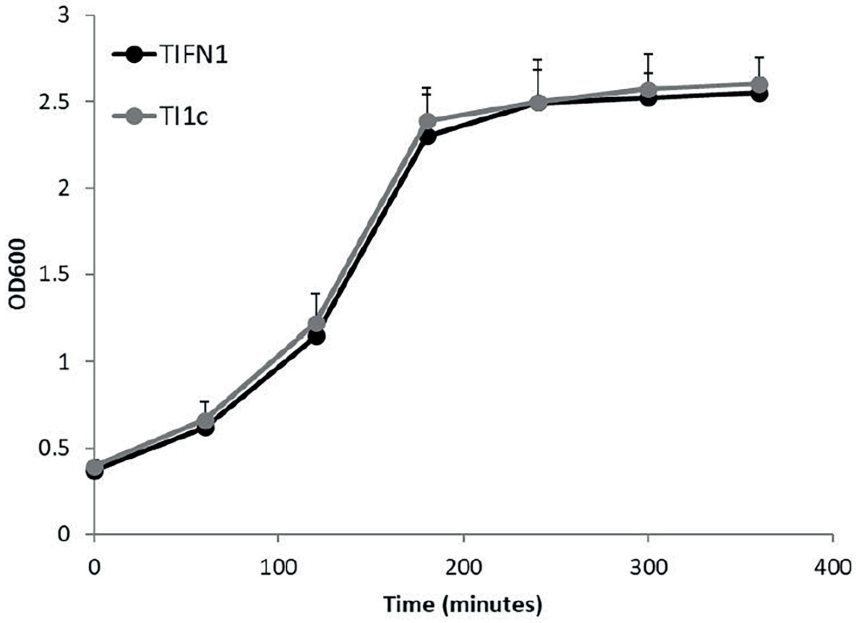

Figure S6.3. Growth performance of TIFN1 and TI1c based on OD measurement. TIFN1 is represented by black symbol and TI1c grey. Data from six independent experimental replicates, error bars represent standard errors.

References

Alexeeva, S., Guerra Martínez, J. A., Spus, M., and Smid, E. J. (2018). Spontaneously induced prophages are abundant in a naturally evolved bacterial starter culture and deliver competitive advantage to the host. *BMC Microbiol.* 18, 120.

Aziz, R. K., Bartels, D., Best, A., DeJongh, M., Disz, T., Edwards, R. A., et al. (2008). The RAST Server: rapid annotations using subsystems technology. *BMC Genomics* 9, 75.

Bobay, L. M., Touchon, M., and Rocha, E. P. C. (2014). Pervasive domestication of defective prophages by bacteria. *Proc. Natl. Acad. Sci. U. S. A.* 111, 12127–12132.

Brøndsted, L., and Hammer, K. (2006). "Phages of *Lactococcus lactis*," in *The Bacteriophages*, ed. R. L. Calendar (Oxford University Press), 572–592.

Brøndsted, L., Østergaard, S., Pedersen, M., Hammer, K., and Vogensen, F. K. (2001). Analysis of the complete DNA sequence of the temperate bacteriophage TP901-1: evolution, structure, and genome organization of lactococcal bacteriophages. *Virology* 283, 93–109.

Canchaya, C., Fournous, G., Chibani-Chennoufi, S., Dillmann, M. L., and Brüssow, H. (2003). Phage as agents of lateral gene transfer. *Curr. Opin. Microbiol.* 6, 417–424.

Casjens, S. (2003). Prophages and bacterial genomics: what have we learned so far? *Mol. Microbiol.* 49, 277–300.

Chmielewska-Jeznach, M., Bardowski, J. K., and Szczepankowska, A. K. (2018). Molecular, physiological and phylogenetic traits of Lactococcus 936-type phages from distinct dairy environments. *Sci. Rep.* 8, 12540.

Chopin, A., Bolotin, A., Sorokin, A., Ehrlich, S. D., and Chopin, M.-C. (2001). Analysis of six prophages in *Lactococcus lactis* IL1403: different genetic structure of temperate and virulent phage populations. *Nucleic Acids Res.* 29, 644–651.

Comeau, A. M., Hatfull, G. F., Krisch, H. M., Lindell, D., Mann, N. H., and Prangishvili, D. (2008). Exploring the prokaryotic virosphere. *Res. Microbiol.* 159, 306–313.

Desiere, F., Lucchini, S., Canchaya, C., Ventura, M., and Brüssow, H. (2002). Comparative genomics of phages and prophages in lactic acid bacteria. *Antonie Van Leeuwenhoek* 82, 73–91.

Erkus, O., de Jager, V. C. L., Spus, M., van Alen-Boerrigter, I. J., van Rijswijck, I. M. H., Hazelwood, L., et al. (2013). Multifactorial diversity sustains microbial community stability. *ISME J.* 7, 2126–2136.

Garneau, J. E., and Moineau, S. (2011). Bacteriophages of lactic acid bacteria and their impact on milk fermentations. *Microb. Cell Fact.* 10, S20.

Gottesman, M. E., and Yarmolinsky, M. B. (1968). Integration-negative mutants of bacteriophage lambda. *J. Mol. Biol.* 31, 487–492.

Jones, P., Binns, D., Chang, H. Y., Fraser, M., Li, W., McAnulla, C., et al. (2014). InterProScan 5: genome-scale protein function classification. *Bioinformatics* 30, 1236–1240.

Katsura, I. (1976). Isolation of λ prophage mutants defective in structural genes: their use for the study of bacteriophage morphogenesis. *Mol. Gen. Genet.* 148, 31–42.

Katsura, I. (1987). Determination of bacteriophage λ tail length by a protein ruler. *Nature* 327, 73–75.

Kelleher, P., Mahony, J., Schweinlin, K., Neve, H., Franz, C. M., and van Sinderen, D. (2018). Assessing the functionality and genetic diversity of lactococcal prophages. *Int. J. Food Microbiol.* 272, 29–40.

Kelly, W. J., Altermann, E., Lambie, S. C., and Leahy, S. C. (2013). Interaction between the genomes of *Lactococcus lactis* and phages of the P335 species. *Front. Microbiol.* 4, 257.

Koskella, B., and Brockhurst, M. A. (2014). Bacteria-phage coevolution as a driver of ecological and evolutionary processes in microbial communities. *FEMS Microbiol. Rev.* 38, 916–931.

Kot, W., Kilstrup, M., Vogensen, F. K., and Hammer, K. (2016). Clear plaque mutants of lactococcal phage TP901-1. *PLoS One* 11, e0155233.

Labrie, S. J., Josephsen, J., Neve, H., Vogensen, F. K., and Moineau, S. (2008). Morphology, genome sequence, and structural proteome of type phage P335 from *Lactococcus lactis*. *Appl. Environ. Microbiol.* 74, 4636–4644.

Labrie, S. J., Samson, J. E., and Moineau, S. (2010). Bacteriophage resistance mechanisms. *Nat. Rev. Microbiol.* 8, 317–327.

Lowrie, R. J. (1974). Lysogenic strains of group N lactic streptococci. *Appl. Microbiol.* 27, 210–217.

Madeira, F., Park, Y. M., Lee, J., Buso, N., Gur, T., Madhusoodanan, N., et al. (2019). The EMBL-EBI search and sequence analysis tools APIs in 2019. *Nucleic Acids Res.* 47, W636–W641.

Mahony, J., McGrath, S., Fitzgerald, G. F., and van Sinderen, D. (2008). Identification and characterization of lactococcal-prophage-carried superinfection exclusion genes. *Appl. Environ. Microbiol.* 74, 6206–6215.

Mahony, J., Oliveira, J., Collins, B., Hanemaaijer, L., Lugli, G. A., Neve, H., et al. (2017). Genetic and functional characterisation of the lactococcal P335 phage-host interactions. *BMC Genomics* 18, 146.

Mahony, J., and van Sinderen, D. (2015). Novel strategies to prevent or exploit phages in fermentations, insights from phage-host interactions. *Curr. Opin. Biotechnol.* 32, 8–13.

McGrath, S., Fitzgerald, G. F., and van Sinderen, D. (2002). Identification and characterization of phage-resistance genes in temperate lactococcal bacteriophages. *Mol. Microbiol.* 43, 509–520.

McGrath, S., Neve, H., Seegers, J. F. M. L., Eijlander, R., Vegge, C. S., Brøndsted, L., et al. (2006). Anatomy of a lactococcal phage tail. *J. Bacteriol.* 188, 3972–3982.

Moineau, S., Pandian, S., and Klaenhammer, T. R. (1994). Evolution of a lytic bacteriophage via DNA acquisition from the *Lactococcus lactis* chromosome. *Appl. Environ. Microbiol.* 60, 1832–1841.

Muhammed, M. K., Olsen, M. L., Kot, W., Neve, H., Castro-Mejía, J. L., Janzen, T., et al. (2018). Investigation of the bacteriophage community in induced lysates of undefined mesophilic mixed-strain DL-cultures using classical and metagenomic approaches. *Int. J. Food Microbiol.* 272, 61–72.

Pedersen, M., Østergaard, S., Bresciani, J., and Vogensen, F. K. (2000). Mutational analysis of two structural genes of the temperate lactococcal bacteriophage TP901-1 involved in tail length determination and baseplate assembly. *Virology* 276, 315–328.

Penadés, J. R., Chen, J., Quiles-Puchalt, N., Carpena, N., and Novick, R. P. (2015). Bacteriophage-mediated spread of bacterial virulence genes. *Curr. Opin. Microbiol.* 23, 171–178.

Smid, E. J., Erkus, O., Spus, M., Wolkers-Rooijackers, J. C. M., Alexeeva, S., and Kleerebezem, M. (2014). Functional implications of the microbial community structure of undefined mesophilic starter cultures. *Microb. Cell Fact.* 13, S2.

Spus, M., Li, M., Alexeeva, S., Wolkers-Rooijackers, J. C. M., Zwietering, M. H., Abee, T., et al. (2015). Strain diversity and phage resistance in complex dairy starter cultures. *J. Dairy Sci.* 98, 5173–5182.

Stern, A., and Sorek, R. (2011). The phage-host arms race: shaping the evolution of microbes. *BioEssays* 33, 43–51.

Stockdale, S. R., Collins, B., Spinelli, S., Douillard, F. P., Mahony, J., Cambillau, C., et al. (2015). Structure and assembly of TP901-1 virion unveiled by mutagenesis. *PLoS One* 10, e0131676.

Tamura, K., and Nei, M. (1993). Estimation of the number of nucleotide substitutions in the control region of mitochondrial DNA in humans and chimpanzees. *Mol. Biol. Evol.* 10, 512–526.

Tamura, K., Stecher, G., Peterson, D., Filipski, A., and Kumar, S. (2013). MEGA6: Molecular evolutionary genetics analysis version 6.0. *Mol. Biol. Evol.* 30, 2725–2729.

The UniProt Consortium (2019). UniProt: a worldwide hub of protein knowledge. *Nucleic Acids Res.* 47, D506–D515.

van Sinderen, D., Karsens, H., Kok, J., Terpstra, P., Ruiters, M. H. J., Venema, G., et al. (1996). Sequence analysis and molecular characterization of the temperate lactococcal bacteriophage r1t. *Mol. Microbiol.* 19, 1343–1355.

Veesler, D., and Cambillau, C. (2011). A common evolutionary origin for tailed-bacteriophage functional modules and bacterial machineries. *Microbiol. Mol. Biol. Rev.* 75, 423–433.

Veesler, D., Spinelli, S., Mahony, J., Lichière, J., Blangy, S., Bricogne, G., et al. (2012). Structure of the phage TP901-1 1.8 MDa baseplate suggests an alternative host adhesion mechanism. *Proc. Natl. Acad. Sci. U. S. A.* 109, 8954–8958.

Vegge, C. S., Brøndsted, L., Neve, H., McGrath, S., van Sinderen, D., and Vogensen, F. K. (2005). Structural characterization and assembly of the distal tail structure of the temperate lactococcal bacteriophage TP901-1. *J. Bacteriol.* 187, 4187–4197.

Ventura, M., Zomer, A., Canchaya, C., O'Connell-Motherway, M., Kuipers, O., Turroni, F., et al. (2007). Comparative analyses of prophage-like elements present in two *Lactococcus lactis* strains. *Appl. Environ. Microbiol.* 73, 7771–7780.

Chapter 7

Chronic release of tailless phage particles from *Lactococcus lactis*

Yue Liu[1], Svetlana Alexeeva[1], Herwig Bachmann, Jesús Adrián Guerra Martínez, Nataliya Yeremenko, Tjakko Abee & Eddy J. Smid

[1]Equal contributions.

Published in

Applied and Environmental Microbiology, 2022, 88:e01483-21

Abstract

Lactococcus lactis strains residing in the microbial community of a complex dairy starter culture named "Ur" are hosts to prophages belonging to the family *Siphoviridae*. *L. lactis* strains (TIFN1 to TIFN7) showed detectable spontaneous phage production and release (10^9-10^{10} phage particles/mL) and up to 10-fold increases upon prophage induction, while in both cases we observed no obvious cell lysis, typically described for the lytic life cycle of *Siphoviridae* phages. Intrigued by this phenomenon, we investigated the host-phage interaction using strain TIFN1 (harboring prophage proPhi1) as a representative. We confirmed that during the massive phage release, all bacterial cells remain viable. Further, by monitoring phage replication *in vivo*, using a green fluorescence protein reporter combined with flow cytometry, we demonstrated that the majority of the bacterial population (over 80%) is actively producing phage particles when induced with mitomycin C. The released tailless phage particles were found to be engulfed in lipid membranes, as evidenced by electron microscopy and lipid staining combined with chemical lipid analysis. Based on the collective observations, we propose a model of phage-host interaction in *Lactococcus lactis* TIFN1, where the phage particles are engulfed in membranes upon release, thereby leaving the producing host intact. Moreover, we discuss possible mechanisms of chronic, or non-lytic release of LAB *Siphoviridae* phages and its impact on the bacterial host.

Introduction

Bacteriophages, viruses that infect bacteria, are highly diverse in shape, structure and composition. They can be icosahedral, spherical, pleomorphic, filamentous, droplet-, bottle- and spindle-shaped; some are with a long or short tail, some are tailless, engulfed in a lipid bilayer or containing lipids beneath the protein capsid; the genetic material can be double-stranded or single-stranded, DNA or RNA (Clokie et al., 2011; Hatfull and Hendrix, 2011). The broad accessibility of high-throughput sequencing technologies also revealed a high degree of genetic diversity in bacteriophages; mosaic genomes and numerous novel sequences of unknown function have been reported (Ackermann, 2009; Krupovic et al., 2011; Parmar et al., 2017; Chapter 6 of this thesis - Alexeeva et al., 2021). Over 90% of reported phages are tailed double-stranded DNA phages belonging to the order *Caudovirales* (Ackermann, 2007). Tailed phages primarily interact with their host cell by using tail fibers and baseplate structures, and use the tail for penetrating the bacterial cell surface and viral DNA injection (McGrath et al., 2006; Legrand et al., 2016). At the end of infection cycle, virulent tailed phage particles are released from the cells by holin-lysin induced lysis of the host. So called temperate bacteriophages undergo an alternative, lysogenic cycle in which the bacteriophage DNA integrates into the chromosome of the host becoming a prophage (Howard-Varona et al., 2017; Pleška et al., 2018). In this dormant state the prophage can replicate its genome as a part of the bacterial chromosome. Under conditions insulting its host's DNA integrity the prophage can enter the lytic cycle meaning that it excises from the bacterial chromosome, replicates its genome, assembles into mature phage particles and escapes the host following phage holin-lysin induced cell burst (Erez et al., 2017; Dou et al., 2018).

About 4% of the described bacteriophages lack genes encoding tail proteins and they represent polyhedral, filamentous or pleomorphic phages (Ackermann, 2007, 2009). Some members of this group also apply alternative strategies to release their progeny from infected bacteria. Filamentous phages of the *Inoviridae* family are assembled at the cell surface and excreted from infected cells continuously by extrusion, a process mediated by membrane translocation and channel proteins and that leaves the host cells fully viable (Russel, 1991; Marvin et al., 2014). Another distinct mechanism of progeny release is budding, a delicate mechanism typical for animal viruses. During budding these viruses are encapsulated by the cell membrane and released, without killing the host. So far, budding has been suggested only for the family of *Plasmaviridae*, tailless phages infecting wall-less bacteria *Acholeplasma* species via membrane fusion (Putzrath and Maniloff, 1977; Krupovic and ICTV Report Consortium, 2018). In contrast to lytic phage release that kills the host, the non-lytic release is also referred to as chronic release (Hobbs and Abedon, 2016). The group of tailless phages includes bacteriophages that have, in addition to nucleic acid and proteins, internal or external lipid constituents - a property originally associated with viruses infecting multicellular eukaryotes. Currently, the lipid-containing bacteriophages are classified into four families, *Corticoviridae*, *Cystoviridae*, *Plasmaviridae* and *Tectiviridae* (Oksanen et al., 2010).

In complex microbial communities, for instance the ones from the marine environment, the gastrointestinal tract and in complex food fermentations, bacteriophages have impacts on the dynamics and diversity of microbial communities, and the bacterium-phage interactions play a key role in the evolution of both partners in the interaction (Erkus et al., 2013; Smid et al., 2014). Lactic acid bacteria (LAB) have been historically used in food fermentation, among which *Lactococcus lactis* plays important roles in various dairy fermentations. Phages infecting lactic acid bacteria (LAB), and in particular *L. lactis*, are among the mostly studied, for their detrimental impact on industrial (dairy) fermentation processes - phage activities may result in low/inconsistent quality of products and even failure of the whole fermentation (Mahony and van Sinderen, 2015). However, recent insights have revealed that the impacts of phages on the bacterial hosts are not all negative (Erkus et al., 2013; Alexeeva et al., 2018).

Earlier, we described (pro)phages abundantly released and co-existing within a naturally evolved microbial community - mixed (originally undefined) complex starter culture of LAB used in dairy fermentations (Alexeeva et al., 2018). These cultures represent an interesting model ecosystem because it was established through long term propagation by back-slopping. Practicing back-slopping creates the boundaries for natural selection which drives adaptive evolution of the culture and its constituent microbial strains. Although (pro)phages are not desired in industrial fermentations with defined starter compositions, the common presence of prophages in the naturally evolved, stable and robust starter cultures like Ur suggests an evolutionary success (Alexeeva et al., 2018, Chapter 6 of this thesis - Alexeeva et al., 2021). Investigating the behavior of phages and bacteria in such a model system contributes to the understanding of bacterium-phage interactions, as well as its ecological and evolutional significance.

Based on analysis of the genomic content the isolated (pro)phages belong to P335 group lactococcal phages of *Siphoviridae* family, order *Caudovirales*. In fact, all currently known phages infecting LAB are members of the *Caudovirales* order (Ackermann, 2007), or tailed phages. However, they possess some peculiar features: phage particles are abundantly released spontaneously and further stimulated by mitomycin C induction (Alexeeva et al., 2018). They appear to be tailless due to disruptions in tail-protein encoding genes (Chapter 6 of this thesis - Alexeeva et al., 2021). Moreover, the release of the (pro)phages from the host cells was not accompanied by detectable cell lysis, a phenomenon which is typical for release of *Siphoviridae* bacteriophages (Lavigne et al., 2012; Hertel et al., 2015; Zhu et al., 2015; Fu et al., 2019). We set out to investigate this phenomenon in this study. Here we demonstrate that the tailless *Siphoviridae* phage particles are enclosed in lipid membrane and are released from the cells by a non-lytic mechanism, a phenomenon not described before in LAB phages.

Materials and methods

Strains and media

Lactococcus lactis strains used in this study, including the wildtype strain TIFN1 isolated from a complex dairy starter culture named Ur (Erkus et al., 2013), the prophage-cured derivative named TI1c (Alexeeva et al., 2018), and the mutants created from strain TIFN1 in this study namely TIFN1::*cat* and TIFN1::*gfp,* were all statically cultivated in M17 broth (OXOID) with 0.5% (wt/vol) lactose addition (OXOID) at 30 °C, unless specified otherwise. All *Escherichia coli* strains harboring plasmids used in this study were cultivated at 37 °C, in LB broth (BD Difco) supplemented with 150 µg/mL erythromycin, incubated at 37 °C with aeration (shaking) at 150 x *g* in a shaker incubator.

Cell growth, prophage induction, phage purification and quantification

Overnight cultures in M17 broth supplemented with 0.5% lactose (LM17) were diluted up to OD_{600} = 0.2 and allowed to grow for 1 hour at 30 °C before Mitomycin C (MitC) was added (final concentrations of 1 µg/mL). For control purposes, the same diluted cultures without MitC were used. Incubation proceeded for 6 hours unless specified otherwise, and the turbidity (OD_{600}) was monitored at 1 hour intervals. At the end of induction the total cell number was determined by direct counting in a hemocytometer chamber and the viable count was made by a standard spread plating on M17 agar supplemented with 0.5% lactose. Released phage particles were concentrated from the culture supernatants by PEG/NaCl precipitation as previously described (Chapter 6 of this thesis - Alexeeva et al., 2021), and the quantity was estimated based on phage DNA content in culture supernatants or in PEG/NaCl concentrated phage suspensions using agarose gel electrophoresis as previously described (Alexeeva et al., 2018).

Construction of plasmids for chromosomal integration into prophage sites

Plasmid pSA114 is a derivative of plasmid pCS1966 (Solem et al., 2008) - the chromosomal integration vector, allowing positive selection of cells in which the plasmid had been excised from the genome, resulting in unmarked integrations in the chromosome of *L. lactis*.

Two DNA fragments 671 and 941bp of adjacent loci of prophage (proPhi1) were amplified from *L. lactis* TIFN1 chromosome using 1M_HR1_Fw+/1M_HR1_Rv and 1M_HR2_Fw/1M_HR2_1Rv+ primer pairs respectively (see Table 7.1). The two fragments were interconnected by multiple cloning site (MCS) introduced by PCR overlap extension mutagenesis in order to allow further insertions between the homology arms. The resulting 1.7 Kb-PCR fragment was digested with KpnI and NcoI and ligated into corresponding sites of pSEUDO-GFP (Pinto et al., 2011) resulting in plasmid pSA114. The 34 bp MCS between the amplified prophage sequences of pSA114 was used for further cloning. pSA116, the vector for integration of CmR (chloramphenicol resistance cassette, *cat*) into prophage was made by inserting CmR between the prophage homology regions of pSA114. Chloramphenicol cassette (*cat*) was amplified by PCR using pGhCAM2_Fw/pGhCAM_Rv primers (Table 7.1) and pVE6007 (pGhost7, (Maguin et al., 1992)) as a template. The fragment was digested with EcoRI and BamHI and sub cloned

into corresponding sites of pSA114, yielding pSA116. Plasmid pSA120, the vector for integration of *gfp* [the gene of the superfolder variant of GFP, (Pédelacq et al., 2006)] into prophage was made as follows. The *gfp* flanked by CP25 artificial promoter (Jensen and Hammer, 1998) and two terminator sequences was excised from pIL-JK2 using EcoRI and BamHI and inserted into the same site (between the prophage homology regions) of pSA114, yielding pSA120.

Table 7.1. Primers used in this study. Restriction enzyme (RE) sites are underlined.

Name	RE	Nucleotide sequence (5'–3')
1M_HR1_Fw+	MCS	GAATTCCCGGGTCGACAAGCTTAGATCTGGATCCTTGTTGGTTTTGGGCCCATCACTTTA
1M_HR1_Rv	NcoI	TTCCATGGGCGCTCCTTCAGGAAAGACGATTA
1M_HR2_Fw	KpnI	TTGGTACCGGCGCTTGGTTATTCTGCTTCTGA
1M_HR2_1Rv+	MCS	GGATCCAGATCTAAGCTTGTCGACCCGGGAATTCTTTGGGTGGCCCATTTCCTACA
pGhCAM2_fw	EcoRI	AAGAATTCAAGGGGATTTTATGCGTGAGAATG
pGhCAM_rv	BglII/ XhoI/ BamHI	ATGGATCCTCGAGATCTGAAAACCCTGGCGTTACCC

Modification of the chromosomal integration strategy for industrial strains and construction of new integration vectors

The designed vectors are derivatives of pCS1966 and unable to replicate in *L. lactis*. The original strategy (Solem et al., 2008) includes both transformation and chromosomal integration by homologous recombination for the successful acquisition of such vectors by *L. lactis* cells. Therefore, the plasmid acquisition is drastically dependent on the efficiency of transformation. Industrial "wild" strains are usually featured by poor transformability compared to "domesticated" laboratory *L. lactis* strains. Therefore, a new strategy has been designed by splitting plasmid transformation and its homologous recombination events. We constructed vectors that combine *L. lactis* thermosensitive (Ts) replication origin $repA^{Ts}$ and *oroP* gene. Ts replication origin allows the plasmid replication under permissive temperature after the transformation event, followed by integration through homologous recombination at elevated temperature. Gene *oroP* enables counterselection for loss of the plasmid backbone, leaving unmarked integrations in the chromosome of *L. lactis* at specific target sites.

New vectors, pSA130-YL and pSA132-YL were constructed as follows. *E. coli* strain EC1000 (Leenhouts et al., 1998) was used for cloning and plasmid propagation. pG^{+}host9 (Maguin et al., 1992) was used to provide the backbone with $repA^{Ts}$ and *ermAM*. The plasmids pSA116 and pSA120 were used to provide the cassettes of DNA labels (CmR or *sf-gfp*) flanked by proPhi1 homology regions (MHR) and *oroP*. The KpnI/FspI fragment of pSA116, was ligated into KpnI/EcoRV digested pG^{+}host9, resulting in pSA130-YL. pSA132-YL was constructed in two steps: first KpnI/SalI fragment of pSA120 was ligated into the corresponding site of pG^{+}host9, then SalI/FspI fragment of pSA120 was ligated into SalI/EcoRV site, yielding pSA132-YL.

Plasmid integration and backbone elimination

L. lactis transformation was performed using a modified protocol as we described earlier (Alexeeva et al., 2018). The confirmed transformants were propagated at the permissive temperature, 28 °C in M17 broth (0.5% glucose or lactose) with 3 µg/mL erythromycin, and stored in 15% glycerol at -80 °C until further use. For the integration step, *L. lactis* cells transformed with constructed plasmids were incubated at 37 °C overnight, the OD_{600} of cultures was measured, cells were plated in proper dilutions (depending on OD_{600} values) on selection plates (L/GM17, 1.5% agar, 0.5 M sucrose and 3 µg/mL erythromycin), and incubated at 37 °C till colonies emerged. The presence and orientation of the whole plasmid inserts were checked with PCR, and correct validated clones were maintained as 15% glycerol stocks at -80 °C.

For the backbone elimination step, the validated clones with integrated plasmids were inoculated in 2 mL SA medium (Jensen and Hammer, 1993) containing 1% lactose or glucose and incubated at 30 °C overnight. Then they were diluted 10x in SA (1% lactose or glucose) medium and incubated 30 °C for 6 h. Thereafter 10 µL of the culture was streaked on SA (1% lactose or glucose) agar plate supplemented with 10 µg/mL 5-fluoroorotate (Sigma). Plates were incubated at 30 °C until 5-fluoroorotate resistant colonies emerged. For resulting labelled strains, TIFN1::*cat* and TIFN1::*gfp* (inserted genes from corresponding plasmid-donors, pSA130-YL and pSA132-YL), correct inserts and their location on TIFN1 chromosome were confirmed by PCR, sequencing the PCR products and phenotypic analysis: either green fluorescence or chloramphenicol resistance.

Phage lipid and DNA labelling

The dyes used for labelling of lipids and DNA are shown in Table 7.2. To stain DNA, PEG precipitated phage particles were incubated with Sybr Green (Invitrogen, Molecular probes Cat. no. S7563) at 80 °C for 10 minutes in 10^{-4} final dilution of commercial stock as described earlier (Brussaard, 2009) or with GelRed nucleic acid gel stain (Biotium,10^{-4} final dilution of commercial stock) under the same conditions.

Table 7.2. Corresponding labelling of lipid and DNA dyes.

Label used in text	Name of the dye
Lipophilic dye 1	FM 4-64
Lipophilic dye 2	MitoTracker Green FM
Lipophilic dye 3	CellMask Deep Red
DNA dye 1	Sybr Green
DNA dye 2	GelRed Nucleic Acid Gel stain

For membrane detection CellMask DeepRed (Life Technologies GmbH) was used in final dilution 10^{-3} of commercial stock and phages were incubated for 5 minutes at 37 °C; FM4-64 (Molecular Probes) was used in a final concentration 20 µg/mL, incubation proceeded 15 minutes at room temperature;

and MitoTracker Green FM (Molecular Probes Cat. no. M7514) was used at final concentration of 20 nM and phages were incubated with the dye for 15 minutes at 37 °C. For double staining of DNA and membrane, MitoTracker was added to the phages stained with GelRed, the samples were vortexed and measured immediately by flow cytometry. In control experiment the membranes were first extracted by adding to the phage suspension equal volumes of chloroform, the samples were vortexed, centrifuged during 3 minutes at 14000 × *g*, aqueous phase containing the phage particles was collected and the staining was performed as described above.

When phages were not added, no detectable fluorescent particles were present in the control samples. To exclude contamination of phage suspension by bacterial cells, bacteria were added to phage suspension prior to staining of either DNA or lipids. In these control samples an additional population of particles with much higher fluorescence intensity was detected (not shown), as anticipated, given a bacterial cell contains much higher amounts of lipids and DNA per particle compared to phages.

Flow Cytometry

Prior to flow cytometry analysis 2 µL of fluorescent microspheres ($1x10^{-3}$ of the stock Fluoresbrite® YG Microspheres 0.75 µm, Polysciences) was added and the volume was adjusted to 500 µL by adding FACSFlow solution (10 mM phosphate-buffered saline, 150 mM NaCl, pH 7.4; Becton-Dickinson).

Samples were analyzed by using a BD FACSAria™ III flow cytometer (BD Biosciences, San Jose, CA). The cytometer was set up using an 85 µm nozzle and was calibrated daily using BD FACSDiva Cytometer Setup and Tracking (CS&T) software and CS&T Beads (BD Biosciences). An 488 nm, air-cooled argon-ion laser and the photomultipliers with 488/10 band pass filter for forward and side scatter and with filter 530/30 nm (with 502 LP filter) was used for the detection of GFP, Sybr Green and MitoTracker. GelRed was excited with a yellow-green 561nm laser and detected using a 610/20 nm with LP 600 nm filter. CellMask DeepRed was excited with 633 nm laser and detected with 660/20 nm filter. FM4-64 dye was excited with 561 nm laser and detected with a 780/60 nm with LP 735 nm filter. FSC and SSC voltages of 300 and 350, respectively, and a threshold of 1200 on FSC was applied to gate on the bacteriophages and bacterial cells population.

Chemical lipid analysis

Normal phase high performance liquid chromatography (NP-HPLC) with evaporative light scattering detection (ELSD) was used for the quantitative analysis of phospholipids (Christie et al., 1987).

The analyses were performed with a 600E System Controller (Waters), vacuum degasser (Knauer), 231 XL sampling injector (Gilson) and a 3300 (ELSD) evaporative light scattering detector (Alltech). Extraction of the phospholipids from a freeze dried sample was done with a mixture of chloroform, methanol and ammonia (NH_3) in water. After centrifugation of the sample 10 min at 4500 x *g*, 10.0 mL of the supernatant was evaporated under vacuum at 40 °C in a heating block. When the sample was dried, 1 mL absolute ethanol was added and again evaporated to dryness. The dried sample was

dissolved in 1.0 mL of the phospholipid solvent containing iso-octane, chloroform and methanol in the ratio 20:55:25 respectively.

Fifty milliliter of the sample solution was injected on an Xbridge amide analytical column, 3.5 µm, 4.6 x 250 mm (Waters). The components were eluted at a flow rate of 1.0 mL/min with a gradient of eluent A (iso-octane and acetone) and eluent B (2-propanol and ethyl acetate) to eluent C (2-propanol, water, ammonia and acetic acid) in 50 minutes.

1,2-dipalmitoyl-sn-glycero-3-phosphoryl ethanolamine (PE, Matreya), 1,2-dipalmitoyl-sn-glycero-3-phosphoryl glycerol (PG, Matreya), 3-sn-lyso phosphatidyl ethanolamine (LPE, Sigma), DL-α-phosphatidyl choline (dipalmitoyl, C16:0) (PC, Sigma), Sphingomyelin (SM, Sigma), phosphatidyl serine (oleoyl) (PS, Matreya), lyso-phosphatidylcholine (palmitoyl) (LPC, Matreya) and phosphatydyl inositol (linoleoyl) (PI, Matreya) were used as calibration standards for quantitative analysis. A reference sample (buttermilk powder) with known amounts of phospholipids was analyzed and recovery of spiked phospholipids was performed to control for accuracy and precision of the method.

Scanning/transmission electron microscopy

For scanning electron microscopy, *L. lactis* TIFN1 and TI1c cultures were subjected to 1 µg/mL MitC induction as described above. After 5h of induction the samples were fixed with 2.5% glutaraldehyde in PBS buffer for 1 hour at room temperature. A droplet of the fixed cell suspension was placed onto poly-L-lysine coated coverslips (Corning BioCoat, USA) and allowed to stand for 1 hour at room temperature. After rinsing in PBS the samples were post stained in 1% osmium tetroxide in PBS. Subsequently the samples were dehydrated in a graded series of ethanol followed by critical point drying with CO_2 (Leica EM CPD300, Leica Microsystems). The coverslips were fitted onto sample stubs using carbon adhesive tabs and sputter coated with 6 nm Iridium (Leica SCD500). Samples were imaged at 2 KV, 6 pA, at room temperature in a field emission scanning electron microscope (Magellan 400, FEI Company, Oregon, USA).

For transmission electron microscopy, purified phage particles were subjected to negative staining and examined exactly as descried previously (Alexeeva et al., 2018).

Data analysis

The flow cytometry data were acquired by using BD FACSDiva™ software and analyzed by using FlowJo flow cytometry analysis software (Tree Star, Ashland, OR).

Lipid analysis (HPLC) data was analyzed with Chromeleon software version 7.2 (Thermo Fisher Scientific). The non-linear response of the ELSD was converted to a more linear signal in order to increase the accuracy of the quantification of phospholipids differing in fatty acid composition compared to those of the standard.

Results

No detectable cell lysis during phage release

A previous study on *Lactococcus lactis* strains TIFN1-7 originating from the mixed cheese starter culture indicated no obvious drop in the optical density of the bacterial cultures following prophage activation (Alexeeva et al., 2018). We were triggered by this observation and therefore we further examined this phenomenon using strain TIFN1 as a model. We first analyzed the cell viability in prophage induced cultures supplemented with Mitomycin C (MitC) and control cultures without MitC induction. The total cell counts determined using a hemocytometer and the number of culturable cells, i.e., colony forming units, revealed not significantly different, albeit slightly lower average cell counts in the prophage induced cultures (supplementary Fig. S7.1), indicating that at least the vast majority of TIFN1 cells present in the tested conditions remained viable. Both cell counting methods showed no obvious differences in cell numbers from the prophage-induced cultures and non-induced control cultures, further confirming that in the *L. lactis* strains, represented by lysogen TIFN1, there was no detectable cell lysis in spite of the abundant phage release upon phage induction.

The major part of the culture actively produces phages

To elucidate whether phage production is a population-wide activity in a clonal culture of strain TIFN1, we monitored *in vivo* phage replication using a reporter strain, in which a *gfp* reporter was inserted within the prophage. In cells actively replicating the phage particles, green fluorescence intensity was expected to increase. As mentioned, we used *L. lactis* TIFN1 as the model strain, which harbors the genome of prophage proPhi1 (Chapter 6 of this thesis - Alexeeva et al., 2021). The insertion site was selected within the prophage sequence between stop codons of open reading frames (ORFs) 48 and 49 encoded on opposite DNA strands (Fig. 7.1A), resulting in strain TIFN1::*gfp*. In parallel, a fluorescence-negative control strain was constructed in which the chloramphenicol resistance gene *cat* was inserted at the same site, yielding strain TIFN1::*cat*.

The derived strain TIFN1::*gfp* showed similar growth behavior (Fig. 7.1B) to the wild-type TIFN1 (data see Alexeeva et al., 2018), where prophage induction by MitC led to a merely slight inhibition in growth instead of a decay in biomass, as indicated by monitoring culture turbidity. TIFN1::*gfp* also produced phage particles (Fig. 7.1C) to a similar amount as the wild-type (data see Alexeeva et al., 2018): 10^{10} phage particles/mL were found in cultures without added MitC and phage numbers increased to ~10^{11}/mL upon MitC induction in 6 h, as estimated by quantifying phage DNA content.

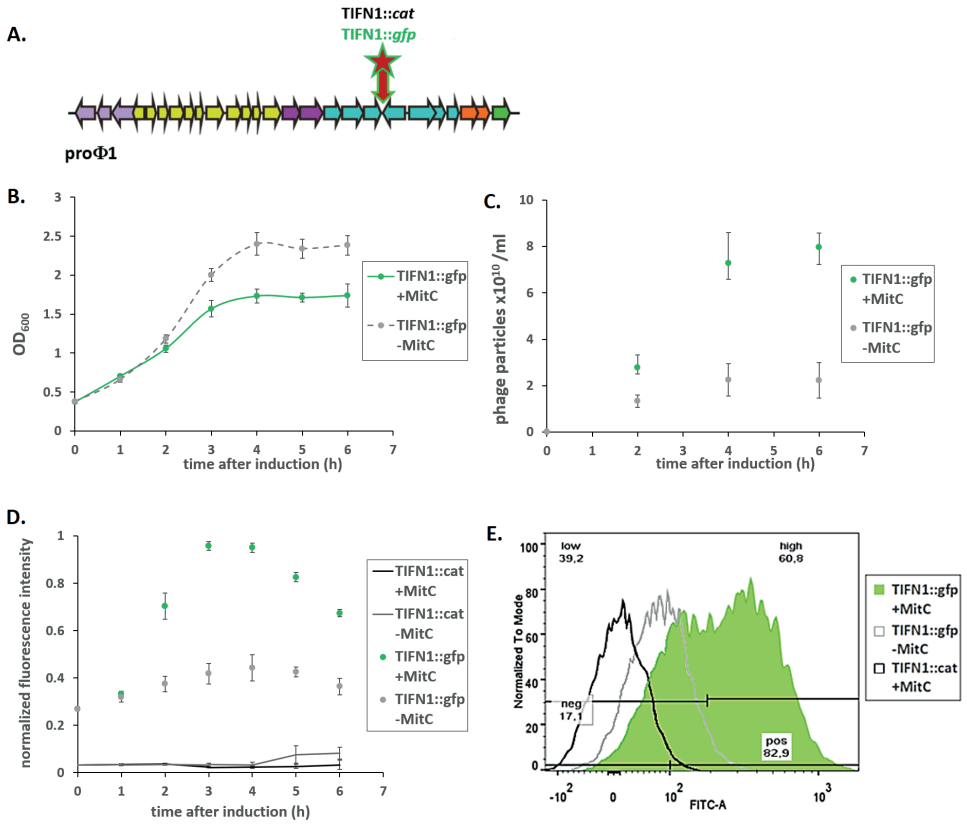

Figure 7.1. Phage labelling and examination of phage replication. (A) Schematic drawing of the prophage genome with marked *gfp* and *cat* insertion sites. Arrows represent ORFs and indicate the direction of gene transcription. The number of arrows does not reflect the real ORF numbers but is only a schematic presentation. The insertion was made in between two convergent ORFs. Colors in arrows schematically represent different phage gene clusters. **(B)** Growth response of TIFN1::*gfp* to MitC treatment. **(C)** Phage release by TIFN1::*gfp* during MitC induction. Green symbols represent MitC treated cultures, grey symbols represent control cultures without MitC. **(D)** Dynamics of phage replication (as derived from average cell fluorescence intensity) during MitC induction (green symbols) and in uninduced samples (grey symbols) in reporter strain (TIFN1::*gfp*) compared to base-line fluorescence of non-*gfp* cultures (TIFN1::*cat,* black and grey lines for induced and uninduced conditions respectively). **(E)** Fluorescence distribution in the population at 3 hours of induction in non-*gfp* TIFN1::*cat* (black unfilled), uninduced TIFN1::*gfp* (grey unfilled), and MitC induced TIFN1::*gfp* (green filled) cultures. The statistics in (e) is shown for induced TIFN1::*gfp*: 82.9% of the population was positive for green fluorescence (pos 82.9), 17.1% was fluorescence-negative (neg 17.1); 60.8% was highly fluorescent (high 60.8) and 39.2% was low in fluorescence (low 39.2).

To study the *in vivo* dynamics of prophage induction in *L. lactis* TIFN1 we used strain TIFN1::*gfp* and followed in time the fluorescence intensity of the cells by flow cytometry in MitC-induced and un-induced cultures. As a fluorescence-negative control we used TIFN1::*cat*. TIFN1::*cat* exhibited very low background fluorescence, not changing in time and not affected by MitC addition (Fig. 7.1D). The un-induced culture of TIFN1::*gfp* showed moderate fluorescence (time point 0 h), and the fluorescence increased slightly in time. This is in line with the observed constitutive phage induction

and replication taking place even without MitC induction (Fig. 7.1C and Fig. 7.1D). The induced culture of TIFN1::*gfp* showed a clear increase in fluorescence intensity till the 4th hour post-induction, and then the fluorescence intensity declined slightly. The increase in fluorescence intensity of the cells was 2.5 - 3 fold and correlated with the increase in the number of released phage particles (Fig. 7.1C and Fig. 7.1D).

To examine whether the major fraction of the bacterial population actively produces phage particles, the distribution of fluorescence in individual cells was measured by flow cytometry. The fluorescence distribution per particle in the negative control (TIFN1::*cat*, black unfilled) as well as in un-induced cultures of TIFN1::*gfp* (grey unfilled) and MitC induced TIFN1::*gfp* (green filled) at time point 3 hours post-induction was measured (Fig. 7.1E). In the MitC induced TIFN1::*gfp* culture more than 80% of the cells are green fluorescent and more than 60% are highly fluorescent, which is a distinct population (second green peak in Fig. 7.1E). This indicates that the majority of the cells in the population actively replicate phage DNA and produce phage proteins. When relating this observation to the cell count results (supplementary Fig. S7.1), where the phage inducing condition only led to slight growth inhibition rather than drastic decay in optical density, the hypothesis of non-lytic phage release is supported.

Phages are enclosed in lipid bilayers

Non-lytic, chronic phage release has been previously described to occur via budding (*Plasmaviridae*) or extrusion (*Inoviridae*) (Putzrath and Maniloff, 1977; Russel, 1991; Marvin et al., 2014; Krupovic and ICTV Report Consortium, 2018). In case the budding mechanism of cell exit is recruited by the phage particles, it is expected to be enveloped by cellular lipids upon release. Therefore, first of all, we analyzed the presence of a lipid bilayer in/engulfing the phage particles. We employed three lipophilic dyes staining cellular membranes/lipid bilayers, but all essentially non-fluorescent in aqueous media. All three lipophilic dyes were efficiently staining the phage particles (Fig. 7.2A - C), confirming presence of lipid membranes. Moreover, when the phage particles were treated with chloroform prior to staining with lipophilic dye 3, the fluorescence was largely abolished (Fig. 7.2C, blue line). The chloroform treated particles were visualized by EM and showed typical morphology of phage heads (see Fig. 1A & B from Alexeeva et al., 2018). We further confirmed that the lipid enclosed particles are indeed bacteriophages containing DNA: the phage particles were readily stained with the two DNA dyes (Fig. 7.2D & E). Moreover, double staining with DNA dye 2 (red fluorescence) in combination with lipophilic dye 2 (membrane stain, green fluorescence) resulted in double stained particles, confirming that the phage particles indeed contain DNA and are enclosed by membranes (Fig. 7.2F). This conclusion is also supported by the previous study where the tailless phage particles were isolated with the same method and subjected to DNA sequencing, and full phage genomes were recovered with more than 100-fold higher coverage than background (Chapter 6 - Alexeeva et al., 2021).

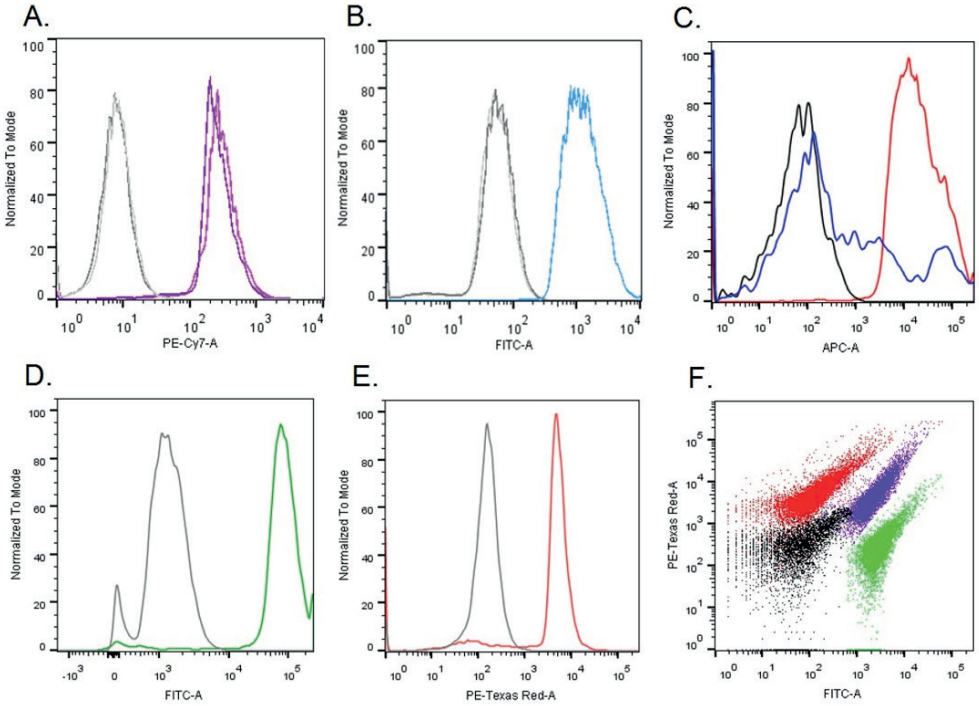

Figure 7.2. Staining proPhi1 particles with various lipophilic (A, B, C, F) and DNA binding (D, E, F) dyes followed by flow cytometry analysis. Grey/black - unstained phage particles. **(A)** Lipophilic dye 1; **(B)** Lipophilic dye 2; **(C)** Lipophilic dye 3, the blue line represents the sample stained after chloroform treatment; **(D)** DNA dye 1; **(E)** DNA dye 2; **(F)** superimposed dot plot of proPhi1 particle samples with different staining: unstained (black), lipophilic dye 2 (green), DNA dye 2 (red), and double stained lipophilic dye 2 and DNA dye 2 (purple-blue).

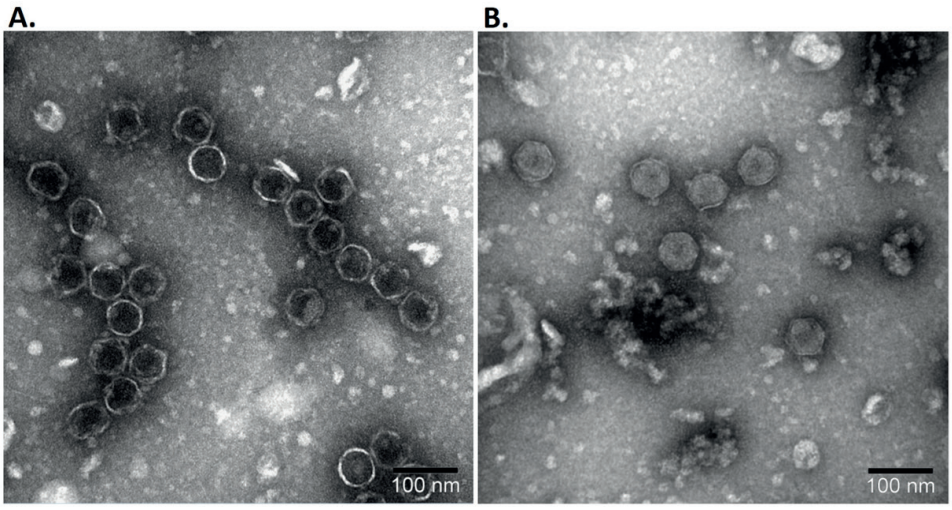

Figure 7.3. Transmission electron micrograph of proPhi1 with (A) and without (B) chloroform treatment.

Since the hypothesis of phage particles being enclosed in lipid bilayer is now supported by experimental evidence, we continued to find additional support by studying the phage particles with transmission electron microscopy (TEM). In this case, phage particles were not pre-treated with chloroform to retain the lipid membrane, and we compared the particle morphology and size to chloroform-treated phage particles. It was observed that the morphology of untreated (Fig. 7.3A) and chloroform-treated (Fig. 7.3B) particles was similar, although they did show different electron-densities as reflected by the different darkness of particles, possibly indicating differences in compositions as chloroform will disintegrate lipid bilayers and dissolve lipids. We also noticed a difference in particle sizes caused by chloroform treatment. When measuring the particle diameters (defined as the distance between two opposite corners of the hexagon shape, measured by ObjectJ), untreated particles showed diameters of 65.4 ± 4.1 nm (n = 54), significantly ($p < 0.00001$, 2-tailed, unequal variance) larger than chloroform-treated particles with diameters 58.0 ± 2.0 nm (n = 27). The difference in average diameters, 7.4 ± 4.6 nm, coincides with the thickness of two lipid bilayers (Mitra et al., 2004). This analysis also supports the hypothesis that the released phage particles of *L. lactis* TIFN1 are enclosed in lipid bilayers.

Lipid composition of phage particles differs from host cells

Next, we extracted the lipids from phage crops produced by strain TIFN1 and also from whole cell-derived protoplasts and subjected them to chemical lipid analysis using liquid chromatography coupled with mass spectrometry (LS-MS). As a phage-free control, phage-cured strain TI1c (Alexeeva et al., 2018) was subjected to the same procedure of prophage induction and purification from the culture supernatant. The TIFN1 phage specimen lipid signals were well above the background level of the phage-free control from TI1c (supplementary Fig. S7.2). Phosphatidyl glycerol (PG) and cardiolipin (CA) were detected in phage samples as well as in cellular lipid samples, however, the ratio between the two major lipid species differed between the phage and the cell membrane lipid samples (Fig. 7.4).

The major lipid in the *L. lactis* cell membrane is cardiolipin and a CA/PG ratio of about 2.2 has been determined for *L. lactis* membrane earlier (Driessen et al., 1988). We found the CA/PG ratio value of 1.5 for cellular lipids extracted from TIFN1 (Fig. 7.4B). Remarkably, lipids of the phage crops were enriched in phosphatidyl glycerol with a CA/PG ratio of 0.4 (Fig. 7.4A). This suggests that the released phage particles are possibly enclosed by phospholipids derived from distinct regions of lipid rafts/ domains in the *L. lactis* cell membrane (Matsumoto et al., 2006; Epand and Epand, 2009).

To further characterize the phage release from the cells we employed scanning electron microscopy to observe MitC induced cells of wild-type strain TIFN1 and its prophage cured derivative strain TI1c (Fig. 7.5). The MitC treated TI1c had the usual morphology and smooth surface of a Gram-positive coccus without any detectable alteration (Fig. 7.5C & D). Strain TIFN1 however, showed a ruffled cell surface and accumulated numerous budlike, small spherical structures, typically near the cell division septum (Fig. 7.5A & B). The phage cured strain TI1c lacked these extracellular structures.

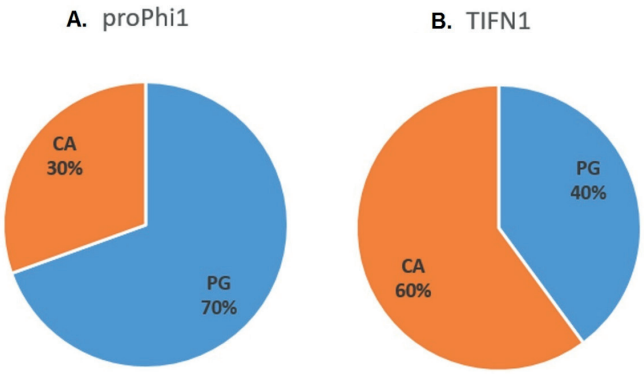

Figure 7.4. Phage and cell lipid composition. Composition of lipids extracted from A) isolated proPhi1 phage particles and **(B)** TIFN1 whole cell-derived protoplast. PG, phosphatidyl glycerol; CA, cardiolipin.

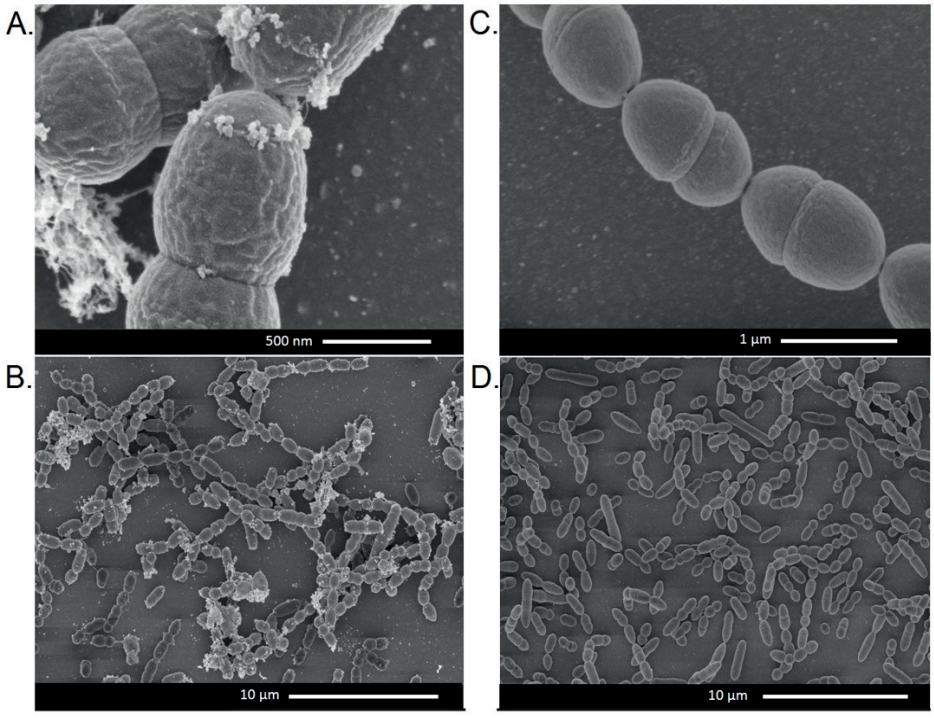

Figure 7.5. Scanning electron micrograph of cells subjected to 6h MitC treatment. (A) and **(B)** TIFN1, **(C)** and **(D)** TI1c.

From our observation that the lipid compositions differed between the released phages and the host cells, we speculated that the process of phage engulfing and release could be specific for defined regions of the cell membrane - this speculation is further supported by the electron microscopic observation, where the phage particles are accumulated near the cell division planes upon release.

Discussion

Bacteriophages are thought to be the most abundant biological entities on Earth and adopted a striking variety of forms and mechanisms of interaction with their host cells (Keen, 2015). Combining observations from this study, we propose a novel mechanism of interaction for lactococcal phages and their hosts, where the tailless *Siphoviridae* phage particles are enclosed in a lipid membrane and are released from the cells by a non-lytic mechanism (Fig. 7.6). This chronic, non-lytic phage release mechanism has not been previously described for LAB phages or *Siphoviridae* phages.

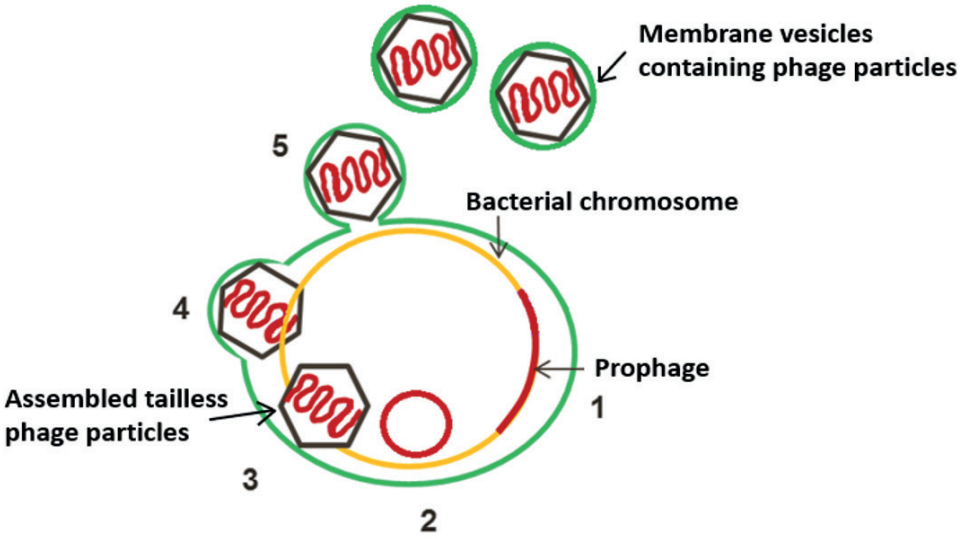

Figure 7.6. Schematic presentation of the proposed mechanism (step 1-5) of phage release from *Lactococcus lactis* TIFN1. Activation of proPhi1 (step 1 and 2) results in production of tailless *Siphoviridae* phage particles (3), enclosed in lipid membrane derived from the cytoplasmic membrane (green) (4), and released from the cells by a budding-like, non-lytic mechanism (5).

The prophage found in *L. lactis* TIFN1, referred to as proPhi1, is classified in the family of *Siphoviridae,* which members are by definition tailed bacteriophages. Genomic analysis also revealed that genes encoding tail structures are present in these prophages, but due to disruptions in some of the tail genes, the assembled phage particles show a tailless phenotype (Chapter 6 - Alexeeva et al., 2021). Interestingly, the lipid-containing phages discovered so far, mostly assigned to families of *Corticoviridae*, *Cystoviridae*, *Plasmaviridae* and *Tectiviridae,* are exclusively tailless phages (Mäntynen et al., 2019).

Plausibly, the reason that the membrane-containing feature was not found in any tailed phages is that they already achieve successful infection with the help of the tail device that efficiently penetrates the cell envelop, and no alternative infection mechanism was required (Mäntynen et al., 2019). Tailless phages, on the other hand, are evolved to utilize the membrane to infect or interact with their hosts (Gowen et al., 2003; Mäntynen et al., 2019). For example, enveloped phages use a membrane fusion mechanism to interact with the host and deliver their genetic materials (Bamford et al., 1987; Poranen and Bamford, 2008; Harrison, 2015). Therefore, it was part of the hypothesis that the tailless proPhi1 being enclosed in a lipid membrane could serve as an alternative infection strategy as the tail device is not available anymore, but we did not obtain evidence demonstrating the (re)infection of host by the membrane-enclosed tailless phage particles (data not shown). It remains to be investigated whether the hurdle was for membrane-enclosed phage particles to attach and enter the host, or rather for the tailless phage particles to inject their genetic material into the bacterial cytoplasm to complete the life cycle.

In previously described membrane-enclosed phages, the mechanism of incorporation of lipids to form virus-specific vesicles has been subjected to investigation, and hypothesis concerning underlying mechanisms have been proposed (Mäntynen et al., 2019). For one, phage encoded membrane proteins trigger cytoplasmic membrane formation in the host, and enclose the phages during assembly in the cell. For example, *Cystoviridae* phage phi6 applies a mechanism, in which the protein P9 was found to facilitate cytoplasmic membrane formation in bacteria (Lyytinen et al., 2019). In this case, phage-encoded membrane proteins are incorporated into the host membrane, providing a scaffold for phage assembly, and the assembled phage particles are released upon lysis of the host (Rydman and Bamford, 2003; Krupovič et al., 2007). Examples are *Tectiviridae* phage PRD1 employing membrane protein P10 (Mindich et al., 1982), and *Corticoviridae* phage PM2 employing membrane proteins P3 and P6 to interact with phage-specific areas on the cell membrane (Abrescia et al., 2008; Mäntynen et al., 2019). For all above mentioned phage-encoded proteins, we did not find homology to any of the proteins encoded on proPhi1 or any of the other prophages found in lactococci isolated from the starter culture Ur (Chapter 6 of this thesis - Alexeeva et al., 2021). However, it should be noted that other membrane-associated protein coding sequences were indeed predicted in the Ur prophages, namely ORF42 in proPhi1&5, ORF08 in proPhi2&4 and ORF49 in proPhi6 (Chapter 6 of this thesis - Alexeeva et al., 2021). Targeting phage particles to special areas of cell membrane by membrane-associated proteins could potentially be an explanation for the distinct lipid composition associated with released phage particles. Nevertheless, non-lytic release via a mechanism of budding is still not confirmed in other phages but suggested for plasmavirus (Putzrath and Maniloff, 1977) and is considered a very delicate life cycle of viruses, as it leaves the host alive while phages get to spread the progeny (Mäntynen et al., 2019). Whether the non-lytic release of membrane-enclosed phages in *L. lactis* TIFN1 and other lactococcal strains found in the starter culture Ur is a result of long-term phage-host co-evolution thus becomes an even more interesting hypothesis, especially as we observed similar growth behavior during phage release in other Ur strains (Alexeeva et al., 2018).

Another intriguing question is how the membrane-enclosed phage particles escape from the bacterial host without lysis, especially given the fact that *L. lactis* is Gram-positive, possessing thick cell wall outside the cell membrane. A similar question has been raised for extracellular membrane vesicles (MVs or EVs) produced by Gram-positive bacteria ever since the discovery of such phenomenon. It has already been known for a long time that Archaea, Gram-negative bacteria, and mammalian cells actively secrete the nano-sized, lipid bilayer-enclosed particles named EVs, harboring various nucleotide and protein cargos as a mechanism for cell-free intercellular interactions (Mashburn-Warren and Whiteley, 2006; Deatherage and Cookson, 2012; Schwechheimer and Kuehn, 2015). Only recently, evidence was provided that EVs are also released by organisms with thick cell walls like Gram-positive bacteria, mycobacteria and fungi (Marsollier et al., 2007; Rodrigues et al., 2007; Lee et al., 2009; Brown et al., 2015), but the mechanistic insights are still lacking. Brown et al. (2015) proposed several non-mutually exclusive mechanisms on the formation and release of EVs through thick cell walls, including the actions of turgor pressure, cell wall-modifying enzymes and protein channels. The most evidence-supported mechanism is via cell-wall modifying enzymes, namely autolysin (Wang et al., 2018) and prophage-encoded holin-endolysin (Toyofuku et al., 2017; Andreoni et al., 2019). Notably, phage particles have also been identified as part of the cargos in EVs produced by Bacillus subtilis (Toyofuku et al., 2017). Further studies dedicated to elucidating the roles of autolysin and/or phage-encoded holin-endolysin in *L. lactis* TIFN1 would serve to reveal the release mechanism in this case.

Moreover, the effect of turgor pressure could also play a role in addition (Brown et al., 2015). It is plausible that upon prophage induction, the defective proPhi1 particles are abundantly assembled and accumulated in the cells, causing cytoplasmic crowding that results in elevated turgor pressure. The cell division site is often the target site of autolysins (Vermassen et al., 2019), in combination with induced phage-encoded endolysins, forming the weakest spot on the cell and giving opportunities for the phage particles to release under turgor pressure, which could explain our observation that the membrane-enclosed particles are mostly observed near the cell division sites, and have a distinct lipid profile comparing the whole cell samples. Therefore, we propose that the phenomenon of non-lytic membrane engulfed phage release observed in *L. lactis* TIFN1 could be driven by the concerted action of enzymatic activity and turgor pressure on the cell envelope, in combination with phage-encoded proteins to achieve phage-specific engulfment and release.

Although this is the first study to demonstrate non-lytic release of membrane-engulfed phages in LAB, we would like to point out that this could be a more common but up to now overlooked phenomenon in other microbial communities for two reasons. Firstly, studies focused on the detection of inducible prophages, use cell lysis/plaque formation as a benchmark for phage activation. Obviously, when (tailless) phage particles are released via membrane envelops or other non-lytic ways, no apparent phenotype will be observed thus discouraging further investigation. Secondly, it is a common practice in phage isolation protocol to employ chloroform to remove contaminating materials derived from bacterial cells (Mäntynen et al., 2019), however, this treatment demolishes the membrane structures

and therefore the lipid-containing phenotype is conceivably not retrieved in further analysis of phage particles. We hope that our findings will inspire further studies, not only in elucidating the detailed mechanism of this case, but also in awareness and discovery of similar phenomena in other microbial species, and further shedding light on bacteria-phage interaction and co-evolution.

Conclusions

In this study, we focused on a lysogenic *L. lactis* strain TIFN1 isolated from a complex dairy starter culture as the model to examine phage-bacteria interactions. Employing a green fluorescent protein reporter, we monitored phage replication and release *in vivo* using flow cytometry. From this result, in combination with data on bacterial growth and phage particle quantification, we demonstrated that the majority of the bacterial population is actively producing phage particles when induced with mitomycin C while all bacterial cells remain viable. Evidence from electron microscopy, lipid staining and chemical lipid analysis collectively suggest that the released tailless phage particles are engulfed in lipid membranes upon release, thereby leaving the bacterial host intact. Findings from this study provide additional insights into the diverse manners of phage-bacteria interactions, which is essential for understanding the population dynamics in complex microbial communities like fermentation starters and the co-evolution of phages and bacteria.

Acknowledgments

This study was financed by Top Institute Food and Nutrition (TIFN) in Wageningen, the Netherlands. In addition, Yue Liu was subsidized by the Netherlands Organization for Scientific Research (NWO) through the Graduate Program on Food Structure, Digestion and Health.

We thank Lieke Gijtenbeek and Jan Kok (RUG) for providing plasmids pCS1966, pVE6007, and pSEUDO-GFP. Emmanuelle Maguin (INRA, France) is acknowledged for providing pG$^+$host9. The authors cordially thank Guido Staring (NIZO food research, Ede, the Netherlands) for performing LC-MS/ESI lipid analysis. The electron microscopy images were obtained with the help of Marcel Giesbers at the Wageningen Electron Microscopy Centre (WEMC) of Wageningen University (Wageningen, The Netherlands).

Supplementary materials

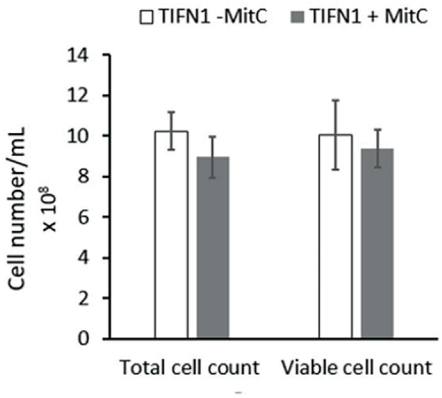

Figure S7.1. Cell count of *Lactococcus lactis* strain TIFN1 under phage induction conditions. Total cell count (obtained by counting cells using a hemocytometer) and viable cell count (determined by plating and colony count) in TIFN1 cultures induced with MitC at 7 hours and control cultures without induction.

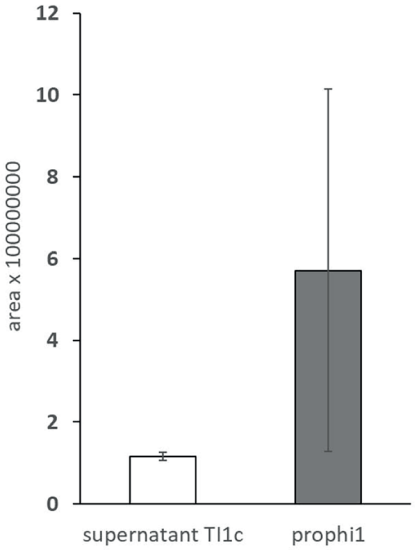

Figure S7.2. Lipid (sum of phosphatidyl glycerol and cardiolipin) signal detected in culture supernatant of phage-free control TI1c and proPhi1 collected from culture supernatant of TIFN1.

References

Abrescia, N. G. A., Grimes, J. M., Kivelä, H. M., Assenberg, R., Sutton, G. C., Butcher, S. J., et al. (2008). Insights into virus evolution and membrane biogenesis from the structure of the marine lipid-containing bacteriophage PM2. *Mol. Cell* 31, 749–761.

Ackermann, H.-W. (2007). 5500 Phages examined in the electron microscope. *Arch. Virol.* 152, 227–243.

Ackermann, H.-W. (2009). Phage classification and characterization. *Methods Mol. Biol.* 501, 127–140.

Alexeeva, S., Guerra Martínez, J. A., Spus, M., and Smid, E. J. (2018). Spontaneously induced prophages are abundant in a naturally evolved bacterial starter culture and deliver competitive advantage to the host. *BMC Microbiol.* 18, 120.

Alexeeva, S., Liu, Y., Zhu, J., Kaczorowska, J., Kouwen, T. R. H. M., Abee, T., et al. (2021). Genomics of tailless bacteriophages in a complex lactic acid bacteria starter culture. *Int. Dairy J.* 114, 104900.

Andreoni, F., Toyofuku, M., Menzi, C., Kalawong, R., Shambat, S. M., François, P., et al. (2019). Antibiotics stimulate formation of vesicles in *Staphylococcus aureus* in both phage-dependent and -independent fashions and via different routes. *Antimicrob. Agents Chemother.* 63.

Bamford, D. H., Romantschuk, M., and Somerharju, P. J. (1987). Membrane fusion in prokaryotes: bacteriophage phi 6 membrane fuses with the *Pseudomonas syringae* outer membrane. *EMBO J.* 6, 1467–1473.

Brown, L., Wolf, J. M., Prados-Rosales, R., and Casadevall, A. (2015). Through the wall: extracellular vesicles in Gram-positive bacteria, mycobacteria and fungi. *Nat Rev Microbiol.* 13, 620–630.

Brussaard, C. P. D. (2009). Enumeration of bacteriophages using flow cytometry. *Methods Mol. Biol.* 501, 97–111.

Christie, W. W., Noble, R. C., and Davies, G. (1987). Phospholipids in milk and dairy products. *Int. J. Dairy Technol.* 40, 10–12.

Clokie, M. R. J., Millard, A. D., Letarov, A. V., and Heaphy, S. (2011). Phages in nature. *Bacteriophage* 1, 31–45.

Deatherage, B. L., and Cookson, B. T. (2012). Membrane vesicle release in bacteria, eukaryotes, and archaea: A conserved yet underappreciated aspect of microbial life. *Infect. Immun.* 80, 1948–1957.

Dou, C., Xiong, J., Gu, Y., Yin, K., Wang, J., Hu, Y., et al. (2018). Structural and functional insights into the regulation of the lysis–lysogeny decision in viral communities. *Nat. Microbiol.* 3, 1285–1294.

Driessen, A. J. M., Zheng, T., In't Veld, G., Op den Kamp, J. A. F., and Konings, W. N. (1988). Lipid requirement of the branched-chain amino acid transport system of *Streptococcus cremoris*. *Biochemistry* 27, 865–872.

Epand, R. M., and Epand, R. F. (2009). Domains in bacterial membranes and the action of antimicrobial agents. *Mol. Biosyst.* 5, 580–587.

Erez, Z., Steinberger-Levy, I., Shamir, M., Doron, S., Stokar-Avihail, A., Peleg, Y., et al. (2017). Communication between viruses guides lysis-lysogeny decisions. *Nature* 541, 488–493.

Erkus, O., de Jager, V. C. L., Spus, M., van Alen-Boerrigter, I. J., van Rijswijck, I. M. H., Hazelwood, L., et al. (2013). Multifactorial diversity sustains microbial community stability. *ISME J.* 7, 2126–2136. doi:10.1038/ismej.2013.108.

Fu, Y., Wu, Y., Yuan, Y., and Gao, M. (2019). Prevalence and diversity analysis of candidate prophages to provide an understanding on their roles in *Bacillus thuringiensis*. *Viruses* 11, 388.

Gowen, B., Bamford, J. K. H., Bamford, D. H., and Fuller, S. D. (2003). The tailless icosahedral membrane virus PRD1 localizes the proteins involved in genome packaging and injection at a unique vertex. *J. Virol.* 77, 7863–71.

Harrison, S. C. (2015). Viral membrane fusion. *Virology* 479–480, 498–507.

Hatfull, G. F., and Hendrix, R. W. (2011). Bacteriophages and their genomes. *Curr. Opin. Virol.* 1, 298–303.

Hertel, R., Rodríguez, D. P., Hollensteiner, J., Dietrich, S., Leimbach, A., Hoppert, M., et al. (2015). Genome-based identification of active prophage regions by next generation sequencing in *Bacillus licheniformis* DSM13. *PLoS One* 10, e0120759.

Hobbs, Z., and Abedon, S. T. (2016). Diversity of phage infection types and associated terminology: the problem with 'Lytic or lysogenic.' *FEMS Microbiol. Lett.* 363, fnw047.

Howard-Varona, C., Hargreaves, K. R., Abedon, S. T., and Sullivan, M. B. (2017). Lysogeny in nature: mechanisms, impact and ecology of temperate phages. *ISME J.* 11, 1511–1520.

Jensen, P. R., and Hammer, K. (1993). Minimal requirements for exponential growth of *Lactococcus lactis*. *Appl. Environ. Microbiol.* 59, 4363–6.

Jensen, P. R., and Hammer, K. (1998). The sequence of spacers between the consensus sequences modulates the strength of prokaryotic promoters. *Appl. Environ. Microbiol.* 64, 82–87.

Keen, E. C. (2015). A century of phage research: bacteriophages and the shaping of modern biology. *BioEssays* 37, 6–9.

Krupovič, M., Daugelavičius, R., and Bamford, D. H. (2007). A novel lysis system in PM2, a lipid-containing marine double-stranded DNA bacteriophage. *Mol. Microbiol.* 64, 1635–1648.

Krupovic, M., and ICTV Report Consortium (2018). ICTV virus taxonomy profile: *Plasmaviridae*. *J. Gen. Virol.* 99, 617–618.

Krupovic, M., Prangishvili, D., Hendrix, R. W., and Bamford, D. H. (2011). Genomics of bacterial and archaeal viruses: dynamics within the prokaryotic virosphere. *Microbiol. Mol. Biol. Rev.* 75, 610–35.

Lavigne, R., Molineux, I. J., and Kropinski, A. M. (2012). "Order - *Caudovirales*," in *Virus Taxonomy: Ninth Report of the International Committee on Taxonomy of Viruses*, eds. A. M. Q. King, M. J. Adams, E. B. Carstens, and E. J. Lefkowitz (Elsevier), 39–45.

Lee, E.-Y., Choi, D.-Y., Kim, D.-K., Kim, J.-W., Park, J. O., Kim, S., et al. (2009). Gram-positive bacteria produce membrane vesicles: proteomics-based characterization of *Staphylococcus aureus*-derived membrane vesicles. *Proteomics* 9, 5425–5436.

Leenhouts, K., Venema, G., and Kok, J. (1998). A lactococcal pWV01-based integration toolbox for bacteria. *Methods Cell Sci.* 20, 35–50.

Legrand, P., Collins, B., Blangy, S., Murphy, J., Spinelli, S., Gutierrez, C., et al. (2016). The atomic structure of the phage Tuc2009 baseplate tripod suggests that host recognition involves two different carbohydrate binding modules. *MBio* 7, e01781-15.

Lyytinen, O. L., Starkova, D., and Poranen, M. M. (2019). Microbial production of lipid-protein vesicles using enveloped bacteriophage phi6. *Microb. Cell Fact.* 18, 29.

Maguin, E., Duwat, P., Hege, T., Ehrlich, D., and Gruss, A. (1992). New thermosensitive plasmid for Gram-positive bacteria. *J. Bacteriol.* 174, 5633–8.

Mahony, J., and van Sinderen, D. (2015). Novel strategies to prevent or exploit phages in fermentations, insights from phage-host interactions. *Curr. Opin. Biotechnol.* 32, 8–13.

Mäntynen, S., Sundberg, L. R., Oksanen, H. M., and Poranen, M. M. (2019). Half a century of research on membrane-containing bacteriophages: bringing new concepts to modern virology. *Viruses* 11, 76.

Marsollier, L., Brodin, P., Jackson, M., Korduláková, J., Tafelmeyer, P., Carbonnelle, E., et al. (2007). Impact of *Mycobacterium ulcerans* biofilm on transmissibility to ecological niches and Buruli ulcer pathogenesis. *PLoS Pathog.* 3, e62.

Marvin, D. A., Symmons, M. F., and Straus, S. K. (2014). Structure and assembly of filamentous bacteriophages. *Prog. Biophys. Mol. Biol.* 114, 80–122.

Mashburn-Warren, L. M., and Whiteley, M. (2006). Special delivery: vesicle trafficking in prokaryotes. *Mol. Microbiol.* 61, 839–846.

Matsumoto, K., Kusaka, J., Nishibori, A., and Hara, H. (2006). Lipid domains in bacterial membranes. *Mol. Microbiol.* 61, 1110–1117.

McGrath, S., Neve, H., Seegers, J. F. M. L., Eijlander, R., Vegge, C. S., Brøndsted, L., et al. (2006). Anatomy of a Lactococcal phage tail. *J. Bacteriol.* 188, 3972–82.

Mindich, L., Bamford, D., McGraw, T., and Mackenzie, G. (1982). Assembly of bacteriophage PRD1: particle formation with wild-type and mutant viruses. *J. Virol.* 44, 1021–1030.

Mitra, K., Ubarretxena-Belandia, I., Taguchi, T., Warren, G., and Engelman, D. M. (2004). Modulation of the bilayer thickness of exocytic pathway membranes by membrane proteins rather than cholesterol. *Proc. Natl. Acad. Sci. U. S. A.* 101, 4083–4088.

Oksanen, H. M., Poranen, M. M., and Bamford, D. H. (2010). "Bacteriophages: Lipid-containing," in *Encyclopedia of Life Sciences* (Chichester, UK: John Wiley & Sons, Ltd).

Parmar, K. M., Gaikwad, S. L., Dhakephalkar, P. K., Kothari, R., and Singh, R. P. (2017). Intriguing interaction of bacteriophage-host association: an understanding in the era of omics. *Front. Microbiol.* 8, 559.

Pédelacq, J.-D., Cabantous, S., Tran, T., Terwilliger, T. C., and Waldo, G. S. (2006). Engineering and characterization of a superfolder green fluorescent protein. *Nat. Biotechnol.* 24, 79–88.

Pinto, J. P. C., Zeyniyev, A., Karsens, H., Trip, H., Lolkema, J. S., Kuipers, O. P., et al. (2011). pSEUDO, a genetic integration standard for *Lactococcus lactis*. *Appl. Environ. Microbiol.* 77, 6687–6690.

Pleška, M., Lang, M., Refardt, D., Levin, B. R., and Guet, C. C. (2018). Phage-host population dynamics promotes prophage acquisition in bacteria with innate immunity. *Nat. Ecol. Evol.* 2, 359–366.

Poranen, M. M., and Bamford, D. H. (2008). "Entry of a segmented dsRNA virus into the bacterial cell," in *Segmented Double-stranded RNA Viruses: Structure and Molecular Biology*, ed. J. T. Patton (Norfolk, UK: Caister Academic Press), 215–226.

Putzrath, R. M., and Maniloff, J. (1977). Growth of an enveloped mycoplasmavirus and establishment of a carrier state. *J. Virol.* 22, 308–314.

Rodrigues, M. L., Nimrichter, L., Oliveira, D. L., Frases, S., Miranda, K., Zaragoza, O., et al. (2007). Vesicular polysaccharide export in *Cryptococcus neoformans* is a eukaryotic solution to the problem of fungal trans-cell wall transport. *Eukaryot. Cell* 6, 48–59.

Russel, M. (1991). Filamentous phage assembly. *Mol. Microbiol.* 5, 1607–13.

Rydman, P. S., and Bamford, D. H. (2003). Identification and mutational analysis of bacteriophage PRD1 holin protein P35. *J. Bacteriol.* 185, 3795–3803.

Schwechheimer, C., and Kuehn, M. J. (2015). Outer-membrane vesicles from Gram-negative bacteria: biogenesis and functions. *Nat. Rev. Microbiol.* 13, 605–619.

Smid, E. J., Erkus, O., Spus, M., Wolkers-Rooijackers, J. C. M., Alexeeva, S., and Kleerebezem, M. (2014). Functional implications of the microbial community structure of undefined mesophilic starter cultures. *Microb. Cell Fact.* 13, S2. doi:10.1186/1475-2859-13-S1-S2.

Solem, C., Defoor, E., Jensen, P. R., and Martinussen, J. (2008). Plasmid pCS1966, a new selection/counterselection tool for lactic acid bacterium strain construction based on the oroP gene, encoding an orotate transporter from *Lactococcus lactis*. *Appl. Environ. Microbiol.* 74, 4772–4775.

Toyofuku, M., Cárcamo-Oyarce, G., Yamamoto, T., Eisenstein, F., Hsiao, C. C., Kurosawa, M., et al. (2017). Prophage-triggered membrane vesicle formation through peptidoglycan damage in *Bacillus subtilis*. *Nat. Commun.* 8, 481.

Vermassen, A., Leroy, S., Talon, R., Provot, C., Popowska, M., and Desvaux, M. (2019). Cell wall hydrolases in bacteria: Insight on the diversity of cell wall amidases, glycosidases and peptidases toward peptidoglycan. *Front. Microbiol.* 10, 331.

Wang, X., Thompson, C. D., Weidenmaier, C., and Lee, J. C. (2018). Release of *Staphylococcus aureus* extracellular vesicles and their application as a vaccine platform. *Nat. Commun.* 9, 1–13.

Zhu, W., Wang, J., Zhu, Y., Tang, B., Zhang, Y., He, P., et al. (2015). Identification of three extra-chromosomal replicons in Leptospira pathogenic strain and development of new shuttle vectors. *BMC Genomics* 16, 90.

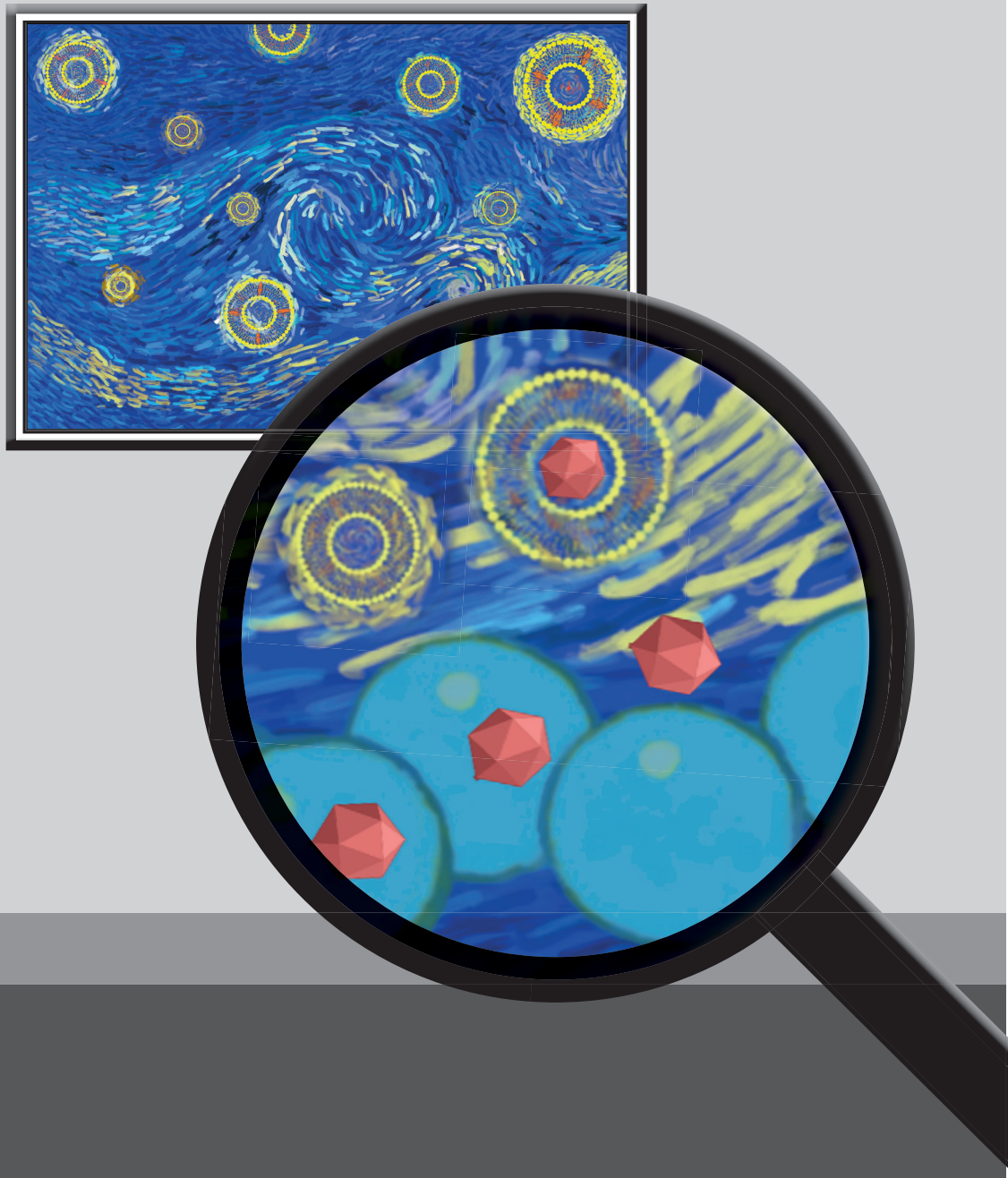

Chapter 8

Extracellular vesicle formation in *Lactococcus lactis* is stimulated by prophage-encoded holin-lysin system

Yue Liu, Marcel H. Tempelaars, Sjef Boeren, Svetlana Alexeeva,
Eddy J. Smid & Tjakko Abee

Accepted for publication in
Microbial Biotechnology

Abstract

Although discovered 30 years later than their Gram-negative counterparts, Gram-positive bacterial extracellular membrane vesicles (EVs) have been drawing more attention in recent years. However, mechanistic insights are still lacking on how EVs are released through the cell walls in Gram-positive bacteria, as the peptidoglycan layer had been historically presumed to be a strong physical barrier preventing such event. In this study, we characterized underlying mechanisms of EV production and provide evidence for a role of prophage activation in EV release using the Gram-positive bacterium *Lactococcus lactis* as a model.

By applying a standard EV isolation procedure, we observed the presence of EVs in the culture supernatant of a lysogenic *L. lactis* strain FM-YL11, for which the prophage-inducing condition (addition of mitomycin C) led to an over 10-fold increase in EV production in comparison to the non-inducing condition. In contrast, the prophage-encoded holin-lysin knock-out mutant YL11ΔHLH and the prophage-cured mutant FM-YL12, produced constantly low levels of EVs, under both prophage-inducing and non-inducing conditions. Under the prophage-inducing condition, FM-YL11 did not show massive cell lysis. Defective phage particles were found to be released in and associated with holin-lysin induced EVs from FM-YL11, as demonstrated by transmission electron microscopic images, flow cytometry and proteomics analysis.

Findings from this study further generalized the EV producing phenotype to Gram-positive *L. lactis*, and provide additional insights into the EV production mechanism involving prophage-encoded holin-lysin system. The knowledge on bacterial EV production can be applied to all Gram-positive bacteria and other lactic acid bacteria with important roles in fermentations and probiotic formulations, to enable desired release and delivery of cellular components with nutritional values or probiotic effects.

Introduction

Cells from all domains of life produce extracellular membrane vesicles (EVs or MVs). These membrane-enclosed, nano-sized vesicles have been found to carry a variety of biomolecules and demonstrate various physiological and ecological functions (György et al., 2011; Gill et al., 2019). In the domain of bacteria, observations and studies of EVs started to appear several decades ago with the Gram-negative bacteria, while studies of Gram-positive bacterial EVs are catching up in recent years (Brown et al., 2015; Kim et al., 2015; Toyofuku et al., 2018).

EV-producing Gram-positive bacterial species have been revealed gradually, including a wide range of pathogens, probiotics and fermentation starters (Chapter 2 of this thesis - Liu et al., 2018; Bose et al., 2020; Briaud and Carroll, 2020). Nucleic acids, viral particles, enzymes, receptors and many other effector molecules have been found to be the cargos of Gram-positive EVs, associating EVs with roles in bacterial survival and competition in a microbial community, as well as in microbe-host interactions.

The delay in discovery of Gram-positive bacterial EV production was largely due to the historical presumption that the cell wall of Gram-positive bacteria, consisting of a thick peptidoglycan layer, would act as a strong physical barrier preventing the release of EVs generated from the cell membrane (Brown et al., 2015). Hence, the mechanism of Gram-positive EV production has not been fully elucidated. A limited number of studies examining the production mechanism of Gram-positive EVs so far contributed to theories on two steps: (i) budding of the cytoplasmic membrane and (ii) passage through the cell wall. Driving forces like turgor pressure and factors improving membrane fluidity were shown to facilitate the formation of membrane vesicles and cell-wall modifications leading to compromised integrity were shown to be the key of EV release (Briaud and Carroll, 2020). To explain the latter, factors such as antibiotics that reduce the peptidoglycan cross-linking, and cell-wall degrading enzymes like autolysins and prophage-derived endolysins, have been demonstrated to promote EV release in *Staphylococcus aureus* and *Bacillus subtilis* (Toyofuku et al., 2017; Andreoni et al., 2019).

Lactic acid bacteria (LAB) are an important group of Gram-positive bacteria, with many species recognized for their probiotic effects as well as key players in food fermentation (Pasolli et al., 2020). EV production has been described for a number of LAB species including *Lactiplantibacillus plantarum* [previously referred to as *Lactobacillus plantarum* (Zheng et al., 2020)] (Li et al., 2017) and *Lacticaseibacillus casei* [previously referred to as *Lactobacillus casei* (Zheng et al., 2020)] (Domínguez Rubio et al., 2017), and *Lactococcus lactis* (Chapter 7 of this thesis – Liu et al., 2021a).

L. lactis is extensively used for the production of fermented dairy products (Cavanagh et al., 2015). In the cases of artisanal cheese production, undefined complex starter cultures containing *L. lactis* strains are commonly used. Such complex cultures are usually shaped by historical use through sequential propagation of starters that lead to successful fermentation (back-slopping), which eventually delivered a stable and robust microbial community (Erkus et al., 2013; Smid et al., 2014). Complex bacterial

communities like undefined starter cultures, often show diverse interactions between co-existing microorganisms and viruses, resulting in co-evolution between for instance bacteriophages (phages) and bacteria and between different bacterial species and strains. Previous studies of an undefined complex cheese starter culture (named Ur) revealed many intriguing properties of members in such a microbial community: in this stable, robust culture, most *L. lactis* strains appeared to be lysogenic and to release defective tailless phage particles continuously in a chronic, non-lytic manner, where the phage particles were enclosed in a lipid membrane layer (Alexeeva et al., 2018; Chapter 6 of this thesis - Alexeeva et al., 2021; Chapter 7 of this thesis - Liu et al., 2021a).

Given the abundance of prophages and intriguing phage-bacteria interactions of lysogenic *L. lactis* strains resident in complex dairy cultures (Alexeeva et al., 2018; Chapter 6 of this thesis - Alexeeva et al., 2021; Chapter 7 of this thesis – Liu et al., 2021a), as well as earlier findings on the prophage roles in Gram-positive bacterial EV release (Toyofuku et al., 2017; Andreoni et al., 2019), we decided to investigate the role of prophages in EV release in *L. lactis*.

We isolated a *L. lactis* ssp. *cremoris* strain FM-YL11 from an artisanal cheese (typically made from complex starter cultures), which shows similar growth behavior as the previously described Ur culture strain TIFN1 (Alexeeva et al., 2018; Chapter 7 of this thesis – Liu et al., 2021a) under prophage inducing conditions. Whole genome sequencing also revealed a prophage sequence in FM-YL11 that is identical to proPhi1 and proPhi5 (Chapter 6 of this thesis - Alexeeva et al., 2021) harbored by strains TIFN1 and TIFN5 in Ur, confirming that this strain is an ideal model to study the role of prophage in EV release. We demonstrated that *L. lactis* strain FM-YL11 produces EV, provided evidence for a role of phage holin-lysin in EV release, and characterized the cargos and compositions of the EVs.

Materials and methods

Strains and conditions

L. lactis ssp. *cremoris* strain FM-YL11 is an isolate from artisanal cheese, and strain FM-YL12 is a prophage-cured derivative from strain FM-YL11 obtained in the same manner as described by Alexeeva et al. (2018). Strains wildtype FM-YL11, prophage-cured derivative FM-YL12 and holin-lysin knockout mutant FM-YL11ΔHLH were cultivated in M17 medium (Difco, BD Biosciences) supplemented with 0.5% (w/v) lactose (LM17) and statically incubated at 30 °C, unless specified differently. The strain with gene complementation, containing pNisA-HLH and the control strain containing pNisA were cultivated in LM17 media supplemented with 3 μg/mL erythromycin.

Escherichia coli strains used as plasmid hosts in this study were cultivated in LB broth (BD Difco) supplemented with 150 μg/mL erythromycin, in Erlenmeyer flasks shaken at 120 rpm at 37 °C.

Genome sequencing

The original strain *L. lactis* FM-YL11 and its prophage-cured derivative strain FM-YL12 were subjected to genome sequencing. The genomic DNA was isolated from 1mL overnight culture (cultivated in GM17 media) by using the DNeasy Blood & Tissue Kit (Qiagen, Germany) according to the manufacture's instruction. DNA was sequenced using the PacBio RSII technology and sequences were assembled by Hierarchical Genome Assembly Process (HGAP, v.3) (GATC Biotech, Germany). The genome coverages for strain FM-YL11 and FM-YL12 were 382 x and 257 x, respectively.

The genome sequences of strain FM-YL11 and FM-YL12 can be accessed in GenBank under accession numbers CP071729 and CP071728, respectively. The genome annotation was performed using the NCBI Prokaryotic Genome Annotation Pipeline (PGAP).

Mutant construction

Plasmid construction

Gene knockout in *L. lactis* FM-YL11 was performed by homologous recombination. Based on 100% sequence identity of prophage sequence in FM-YL11 to proPhi1 (Chapter 6 of this thesis - Alexeeva et al., 2021), bases 1990275-1990499 of FM-YL11 were annotated as a prophage holin gene, while bases 1986322 - 1987874 were annotated as a second holin next to a lysin encoding gene. All three genes were the targets for gene knockout.

To construct the plasmids for gene knockout, 600 - 800 bp upstream and downstream regions of the single holin gene as well as the holin-lysin genes were amplified by PCR, during which the restriction sites were introduced using primers listed in supplementary Table S8.1. Phusion High-fidelity PCR kit (Thermo Fisher Scientific) was used according to manufacturer's instruction. The upstream and downstream homologous regions of the single holin gene and the holin-lysin gene cluster were inserted in plasmid pG$^+$host9 (Maguin et al., 1992) by restriction digestion and ligation following enzyme product manuals from Thermo Fisher Scientific. In brief, restriction site PstI was used to connect the upstream and downstream homologous regions of the single holin gene, and the XhoI and EagI restriction sites were employed to insert the two homologous regions into pG$^+$host9, yielding pYL006. Restriction site HindIII was used to connect the upstream and downstream homologous regions of the holin-lysin cluster, and the XhoI and PstI sites were employed to insert the two homologous regions into pG$^+$host9, yielding pYL002.

For gene complementation, the coding regions of the holin-lysin cluster and the single holin gene were amplified by PCR using primers listed in supplementary Table S8.2. The two PCR products were inserted into the backbone (the 8515 bp XbaI - PstI fragment) of plasmid pMSP3545 [gift from Gary Dunny (Bryan et al., 2000), Addgene plasmid # 46888]. NEBuilder HiFi DNA assembly cloning kit (New England Biolabs) was employed for assembly the three DNA fragments in one step according to manufacturer's instruction. This delivered plasmid pNisA-HLH, in which the holin-lysin cluster as

well as the single holin gene were inserted under the control of a nisin-inducible promoter coming in pMSP3545.

Transformation

For construction of the plasmids for gene knockout, *E. coli* strain EC1000 (Leenhouts et al., 1998) was used for cloning and plasmid propagation. Treatment to obtain competent cells and heat-shock transformation of EC1000 was performed as described by (Chang et al., 2017) with the following modifications: prior to the two washing steps with 0.1 M $CaCl_2$, the cells were washed with 1x volume of 0.1 M $MgCl_2$. The heat-shock at 42 °C was for 90 sec, followed by immediate addition of LB broth and incubation at 37 °C statically for 1 hour before plating on selection plates.

For constructing the plasmid for gene complementation, assembled plasmids were used to transform *E. coli* competent cells Mix & Go Zymo 5α (Zymo research) according to manufacturer's instructions.

Plasmids pYL002 and pYL006 were introduced into *L. lactis* FM-YL11 to knockout the holin-lysin cluster and the single holin successively. Transformation of strain FM-YL11 with plasmids pYL002 and pYL006 was performed as described previously (Alexeeva et al., 2018), except that transformed cells were selected and incubated at 28 °C, which was the temperature that allows the replication of pG^+host9-derived plasmids (containing thermosensitive replication origin). Then, the plasmid integration and backbone elimination steps were performed as described in Chapter 7 of this thesis (Liu et al., 2021a), with lactose as the carbon source throughout. The only change was that the mutants propagated in SA medium were streaked on SA agar plates without 5-fluoroorotate, and the selection of the correct knockout mutants was performed by colony screening using PCR.

Plasmid pNisA-HLH for gene complementation was used to transform the knockout mutant FM-YL11ΔHLH, exactly as described previously (Alexeeva et al., 2018). The empty vector pMSP3545, renamed as pNisA, was used to transform strain FM-YL11ΔHLH to obtain a negative control strain for gene complementation.

EV production and isolation

For EV production in strains FM-YL11, FM-YL12 and FM-YL11ΔHLH, an overnight culture of *L. lactis* in LM17 was diluted to OD_{600} of 0.2 (light path 1 cm) in fresh LM17 medium and incubated for 1 hour at 30 °C. Then 1 μg/mL mitomycin C was added, which was referred to as the "prophage inducing condition"; where no mitomycin C was added, we refer to the "non-inducing condition". The OD_{600} of cultures was monitored every 30 min. After 6 hours treatment at prophage inducing condition or non-inducing condition, EVs were harvested from the culture supernatant.

For EV production in strains with gene complementation (FM-YL11ΔHLH containing pNisA-HLH and control strain containing pNisA), 1 mL overnight culture was diluted with 50 mL fresh LM17 media

supplemented with 3 µg/mL erythromycin, and 10 ng/mL nisin (Sigma-Aldrich) was added. After 20 hours incubation, EVs were harvested from the culture supernatant.

To harvest EVs, the cell culture was centrifuged at 5000 x *g* for 15 minutes at 4 °C (low spin), and the supernatant was collected. The pH value of the supernatant was adjusted to 7.0 with 1 N NaOH. The supernatant was filtered through a polyethersulfone (PES) membrane filter (Minisart) with a pore size of 0.45 µm. The filtered supernatant was added to Beckman Coulter centrifuge tubes and centrifuged at 160000 x *g* for 1 hour in a Beckman L60 Ultracentrifuge (high spin). The supernatant was discarded and the pellets were then re-suspended in phosphate-buffered saline (PBS) and aliquots were stored at -80 °C until further use. Repeated freezing and thawing was avoided by using new aliquots in the different experiments.

EV quantification

Fifty milliliters PBS with EVs in suspension was mixed with 50 µL 10 µg/mL FM4-64 dye (Invitrogen) solution dissolved in PBS. PBS was mixed with the dye in the same manner as the control for background signal. The sample-dye mixtures were added to a black polystyrene 96-wells plate, and incubated for 15 min at room temperature while protected from light. The results were measured in a spectrophotometer at an excitation and emission wavelength of 515 and 640 nm respectively. After removing the background signals from all samples, a relative comparison was made between samples measured in the same assay.

Transmission electron microscopy (TEM)

Negative staining was performed on EV samples prior to TEM imaging, where 2 µL EV suspension was applied to a 400 mesh copper grid supplied with a formvar/carbon film. After 30 sec incubation, the grid was washed with 2 µL milliQ water. Then the grid was stained with 2% uranyl acetate for 30 sec, and dried with filter paper. Samples were analyzed with a Jeol JEM-1400 plus TEM equipment (Jeol, Japan) with an accelerating voltage of 120 kV.

Flow cytometry analysis

Prior to staining and flow cytometry analysis, the EV suspensions were treated with 1 mg/mL DNase I (Roche) in a reaction buffer containing 10 mM tris-HCl (pH 7.5), 2.5 mM $MgCl_2$ and 0.1 M $CaCl_2$, at 30 °C for 1 hour. EVs were stained for flow cytometry with 10 µg/mL FM4-64 membrane dye and/or 16 µg/mL DAPI DNA dye for 15 min at room temperature while protected from light. A BD-FACS Aria III flow cytometer was used for flow cytometry analysis. Particles from the EV suspension were gated and differentiated based on forward scatter (FSC), side scatter (SSC), DAPI and FM4-64 parameters. A 405 nm laser with a 502 LP filter (510/50 nm) was used to detect DAPI signals and a 561 nm laser with 780/60 nm filter for detection FM4-64 signals. For each sample, 50,000 (non-background) events were analyzed.

BD FACSDiva™ software was used for data acquisition and FlowJo flow cytometry analysis software (version 10, Tree Star, Ashland, OR) was applied for data analysis.

Proteomics analysis

The EV samples were sonicated with a sonication probe 2 times for 30 sec. Protein concentrations in EV and cytoplasmic membrane samples were determined by the bicinchoninic acid (BCA) assay. The protein aggregation capture (PAC) method (Batth et al., 2019) was used in a slightly modified way for preparation for proteomics analysis. In brief, in each sample 60 µg protein was reduced with 15 mM DTT at 45 °C for 30 min, unfolded in 6 M Urea, and alkylated with 20 mM acrylamide at room temperature for 30 min. The pH of the protein solution was adjusted to 7 using 10% (v/v) trifluoro-acetic acid (TFA). SpeedBeads (magnetic carboxylate modified particles, GE Healthcare) of product 45152105050250 and 65152105050250 were mixed with 1:1 ratio at 50 µg/uL, and 8 µL SpeedBeads was added to each protein sample. Acetonitrile was added up to 71% (v/v) to the protein-beads mixture, incubated at room temperature with gentle shaking for 20 min. A magnet was used to separate the SpeedBeads from the supernatant for 30 sec, and the supernatant was removed. The SpeedBeads were then washed with 1 mL 70% ethanol and 1 mL 100% acetonitrile successively, resuspended in 100 ul 5 ng/µL trypsin solution and incubated overnight at room temperature with gentle shaking. The pH of SpeedBeads suspension was adjusted to 3 using 10% TFA, and the SpeedBeads were separated from the supernatant by using a magnet. The supernatant was filtered using C8 Empore disk filters. To improve yield, 0.1% formic acid was used to wash the beads and a 1:1 mixture of acetonitrile and 0.1% formic acid was used to wash the filter. All eluents were combined and dried to 10 - 15 µL, then topped up to 50 µL with 0.1% formic acid.

For the LC-MS/MS analysis, 1.5 µL prepared sample was injected into the system, and the analysis protocol was essentially as described in Chapter 4 of this thesis (Liu et al., 2021b). The MaxQuant quantitative proteomics software package was used to analyze LC-MS data with all MS/MS spectra as described previously (Cox et al., 2014), and the proteome of *L. lactis* ssp. *cremoris* TIFN1 (UniProt ID UP000015849) was used as the protein database. We used Perseus for filtering and further bioinformatics and statistical analysis of the MaxQuant ProteinGroups files (Tyanova et al., 2016). Reverse hits were removed; identified protein groups contained minimally two peptides, of which at least one is unique and one unmodified. The values of intensity based absolute quantitation (iBAQ) was calculated by MaxQuant, in which the protein intensities are corrected for the number of measurable peptides.

Bioinformatics analysis

For detecting DNA sequence similarities, the NCBI Blast-n tool was used. For gene ontology (GO) annotation, the UniProt Retrieve/ID mapping tool was used in combination with manual curation.

Results

The genome of strain *L. lactis* ssp. *cremoris* FM-YL11

L. lactis ssp. *cremoris* FM-YL11 was isolated from an artisanal cheese, and its genome was sequenced (GenBank No. CP071729). In the 2406538 bp chromosome of strain FM-YL11, bases 1984716 – 2025964 were shown to share 100% sequence coverage and identity with prophage proPhi1 (GenBank No. MN534315) in *L. lactis* ssp. *cremoris* strain TIFN1 and proPhi5 (MN534318) from strain TIFN5 (Chapter 6 of this thesis - Alexeeva et al., 2021), and 99.99% identity to corresponding chromosomal regions in *L. lactis* ssp. *cremoris* strain 3107 (GenBank No. CP031538) and JM4 (GenBank No. AP015909).

Sequencing of the prophage-cured derivative FM-YL12 (GenBank No. CP071728) confirmed that the prophage sequence in strain FM-YL11 (bases 1984716 – 2025964) is absent in strain FM-YL12, and this difference is the only gap when comparing sequences of the two strains. Except for the absence of the described prophage sequence, strain FM-YL12 showed 99% sequences identity to strain FM-YL11 with no rearrangement of the genome.

L. lactis strain produces 10-fold more EVs under a prophage-inducing condition

To investigate the role of prophage in *L. lactis* EV production, as reported previously for *B. subtilis* (Toyofuku, 2017), two derivatives of strain FM-YL11 were employed: strain FM-YL12 is a prophage-cured derivative of FM-YL11, and FM-YL11ΔHLH is a mutant in which the two holin genes and one endolysin gene encoded by the prophage have been knocked out. (Fig. 8.1A). Prophage was induced by supplementing mitomycin C (MitC), an antibiotic causing DNA damage, which triggers prophage to enter the active lytic cycle in the lysogenic bacteria (Oliveira *et al.*, 2017; Filipiak *et al.*, 2020), where prophage-encoded genes are expressed, proteins synthesized and new phage particles formed. Typically in the lytic cycle, the prophage-encoded holin-lysin system degrades the cell envelope, leading to cell lysis and liberation of phage progenies.

Growth under non-inducing and prophage inducing (by addition of 1 µg/mL MitC) conditions of the wildtype strain FM-YL11 and the two derived mutants was compared (Fig. 8.1B - D). The prophage inducing condition did not result in massive cell lysis in the FM-YL11 culture but only lead to a slight inhibition of growth (Fig. 8.1B). In addition, growth of strains FM-YL12 (Fig. 8.1C) and FM-YL11ΔHLH (Fig. 8.1D) was not and only slightly inhibited by the prophage inducing condition, respectively, as reflected by the growth curves of all strains with and without prophage induction. The growth behavior of strain FM-YL11 under both tested conditions was comparable to that reported for the lysogenic *L. lactis* ssp. *cremoris* strain TIFN1 (Alexeeva et al., 2018).

Analysis of EV production under the tested conditions of strain FM-YL11 and mutants at the early stationary phase, showed the presence of structures with typical size and morphology of EVs in the recovered supernatant fractions (supplementary Fig. S8.1). In non-inducing conditions, supernatant fraction of strain FM-YL11 showed besides EV-like structures, particles with typical size and morphology

of phage heads (supplementary Fig. S8.1A & B). Under prophage-inducing condition, the quantity of EVs recovered from FM-YL11 culture supernatant was 10-fold higher than in the culture without prophage induction, as reflected by fluorescent signals of membrane-specific fluorescent dye (Fig. 8.2A). Again, EV-like structures were observed in the fraction recovered from culture supernatant under the prophage-induced condition, together with abundant phage head-like particles (supplementary Fig. S8.1C & D). The sizes of EV-like structures ranged from 50 nm to 300 nm in diameter, while the phage head-like structures were around 50 nm in diameter.

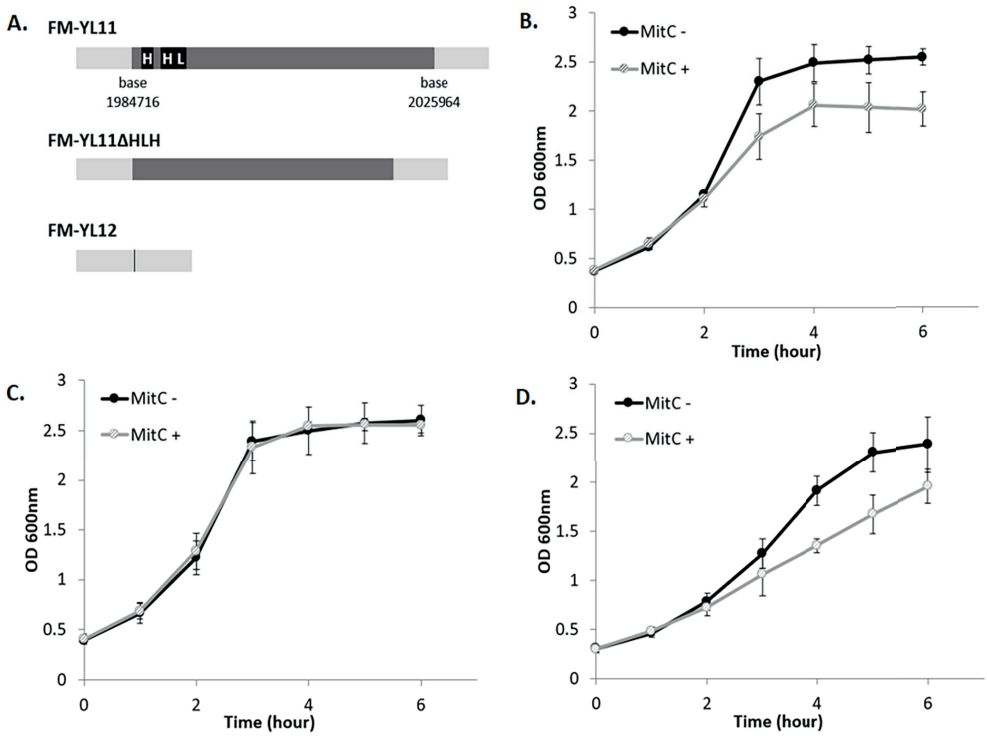

Figure 8.1. Strains of study and optical density-based growth curves. A) Schematic presentation of the various strains used in this study. The bacterial chromosome (non-prophage sequence) is shown in light grey, prophage shown in dark grey except for prophage holin and lysin genes shown in black. The insertion site of the prophage is shown as a black line for prophage-cured strain FM-YL12. Growth curves of B) FM-YL11; C) FM-YL12; D) FM-YL11ΔHLH under prophage inducing condition and non-inducing condition based on OD_{600} values. For prophage-inducing condition, 1 µg/mL mitomycin C was added to bacterial cultures in early exponential phase. For non-inducing condition, no mitomycin C was added to the cultures. Mitomycin C was added at time 0 hour indicated by the graph. Data from 6 independent experiments. Error bars show standard deviations.

Prophage-encoded holin-lysin system stimulates EV formation

When the strains FM-YL12 and FM-YL11ΔHLH were exposed to the prophage-inducing condition, we did not observe an increase of the EV quantities recovered from culture supernatant, as compared to the non-inducing condition (Fig. 8.2A). The EV quantities of both derivatives under both conditions

were slightly lower than that from strain FM-YL11 without prophage induction. EV-like structures were observed in the EV fraction of both FM-YL12 and FM-YL11ΔHLH, and the phage head-like structures could be spotted in the sample from YL11ΔHLH but no longer in FM-YL12 (supplementary Fig. S8.1E - H). The EV-like structures recovered from FM-YL12 were in general smaller than 150 nm in diameter.

To verify the role of prophage encoded holin-lysin system in EV production of *L. lactis*, we constructed a mutant with holin and lysin gene complementation. Mutant FM-YL11ΔHLH was transformed with a plasmid containing the prophage encoded two holins and one endolysin gene, using a nisin-inducible promoter (pNisA-HLH) to drive expression. Addition of nisin resulted in 10-fold increase of EV production in the mutant with holin-lysin gene complementation but not in the control strain where only an empty vector (pNisA) was introduced (Fig. 8.2B).

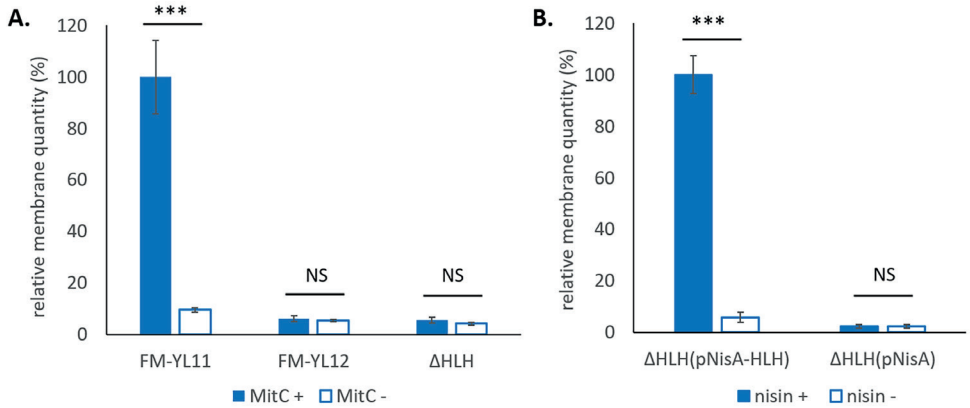

Figure 8.2. EV quantification by staining with membrane-specific fluorescent dye FM4-64. A) Relative membrane quantity of EVs isolated from the culture supernatant of strain FM-YL11, FM-YL12 and FM-YL11ΔHLH (shown as ΔHLH) under prophage inducing condition and non-inducing condition. The quantity (as reflected by the fluorescent signal intensity of dye FM4-64) of EVs from FM-YL11 under prophage inducing condition was regarded as 100%. For prophage-inducing condition, 1 µg/mL mitomycin C was added to bacterial cultures in early exponential phase, and EVs were collected from the supernatant by ultracentrifugation after 6 hours treatment. For non-inducing condition, all treatment were the same except that no mitomycin C was added to the cultures. Samples were from 4-6 independent experiments. B) Relative membrane quantity of EVs isolated from the culture supernatant of FM-YL11ΔHLH with holin-lysin gene complementation (pNisA-HLH) and control plasmid (pNisA) under holin-lysin inducing condition and non-inducing condition. The quantity (as reflected by the fluorescent signal intensity of dye FM4-64) of EVs from FM-YL11ΔHLH (pNisA-HLH) under nisin inducing condition was regarded as 100%. For holin-lysin inducing condition, 10 ng/mL nisin was added to bacterial cultures in early exponential phase, and EVs were collected from the supernatant by ultracentrifugation after 20 hours treatment. For non-inducing condition, all treatment were the same except that no nisin was added to the cultures. Samples were from 3 - 4 independent experiments. Error bars show standard errors of the mean. ***, $p < 0.001$; NS, $p > 0.05$ in t-tests.

A subpopulation of holin-lysin induced EVs enclose tailless phage particles

We examined the composition and cargo of the isolated EV fractions from strain FM-YL11 under the prophage-inducing condition. The EV fractions were first treated with DNase to remove any extra-vesicular DNA, and then stained with fluorescent dyes for flow cytometry analysis. EVs from FM-YL12 treated under the same condition served as the phage-free control.

The EVs from strain FM-YL11, stained with the DNA dye DAPI showed clear positive signals for all analyzed particles compared to the unstained samples (Fig. 8.3A), while the majority of FM-YL12 EVs showed no signal upon DNA staining except for a very small population showing a low DNA signal (Fig. 8.3D). We identified two distinct populations varying in signal intensity in the EV fraction of strain FM-YL11 (Fig. 8.3A). The population with relatively low DNA signal intensity, but not the population with very high signal intensity, was observed in the EV fraction from the prophage cured derivative FM-YL12 (Fig. 8.3D). Based on EM pictures, phage head-like particles were spotted in the EV fraction from FM-YL11 (supplementary Fig. S8.1C & D). It is plausible that the very high DNA signal was achieved by the tight packing of the phage genome. Therefore, we deduced that the population with very high DNA signal intensity consisted of the phage heads.

When stained with the membrane-specific dye FM4-64, EVs from FM-YL12 all showed positive signals compared to the unstained sample (Fig. 8.3E). A small population of FM-YL11 EVs showed negative signals for the membrane staining, while the majority of the EVs were positive (Fig. 8.3B). The average signal intensity in FM-YL12 sample was lower than the membrane-positive population of FM-YL11. This could be caused by the difference in EV sizes in the two samples, as also observed by electron microscopy (supplementary Fig. S8.1).

When the EV fraction from strain FM-YL11 was stained with the DNA and membrane dye simultaneously, the majority of the population with low DNA signals showed positive signals for the membrane dye (Fig. 8.3C, lower orange cloud in Q2), indicating a population of EVs enclosing free DNA molecules. This was hardly observed from FM-YL12, where the majority EVs showed positive membrane signal but low/negative for DNA signal with the double staining (Fig. 8.3F).

The population with very high DNA signals in FM-YL11 was divided further into a subpopulation that is high in membrane signal (Fig. 8.3C, higher orange cloud in Q2) and a subpopulation low/negative in membrane signal (Fig. 8.3C, orange cloud in Q1). The subpopulation high in DNA signal but low/negative in membrane signal likely consisted of the free, unenveloped phage heads, while the subpopulation high in both DNA and membrane signal likely pointed to EVs that enclosed tailless phage particles. Structures that conceivably represent the subpopulation of EVs enclosing phage heads were also observed under electron microscope (Fig. 8.4).

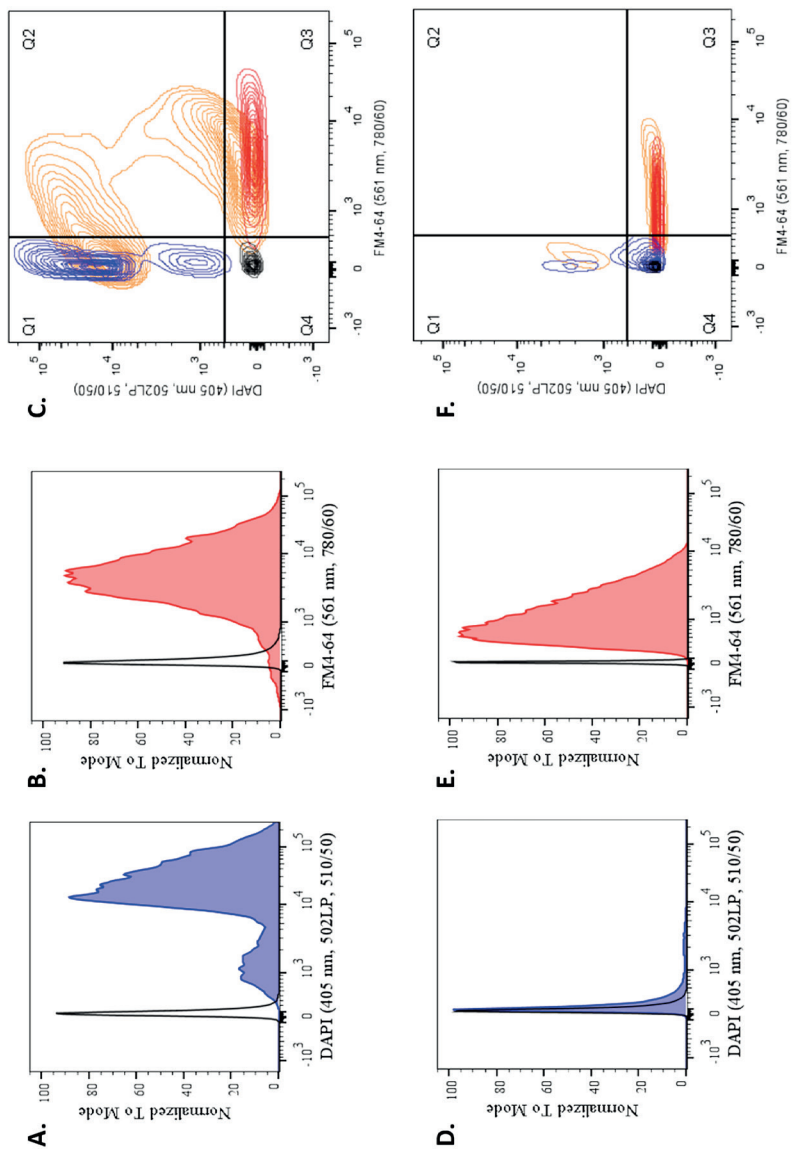

Figure 8.3. Flow cytometry analysis of EVs stained by DNA and membrane-specific fluorescent dyes. A) - C) are analysis of EVs from FM-YL11 under prophage-inducing condition, while D) - F) are analysis of EVs from FM-YL12 under prophage-inducing condition. A) and D), fluorescence distribution in the population of EVs stained by DNA dye DAPI (blue filled) comparing to unstained EVs (black unfilled). B) and E), fluorescence distribution in the population of EVs stained by membrane-specific dye FM4-64 (red filled) comparing to unstained EVs (black unfilled). C) and F), superimposed signal distribution of EVs that are unstained (black), stained only with DAPI (blue), stained only with FM4-64 (red), and stained with DAPI and FM4-64 simultaneously (orange).

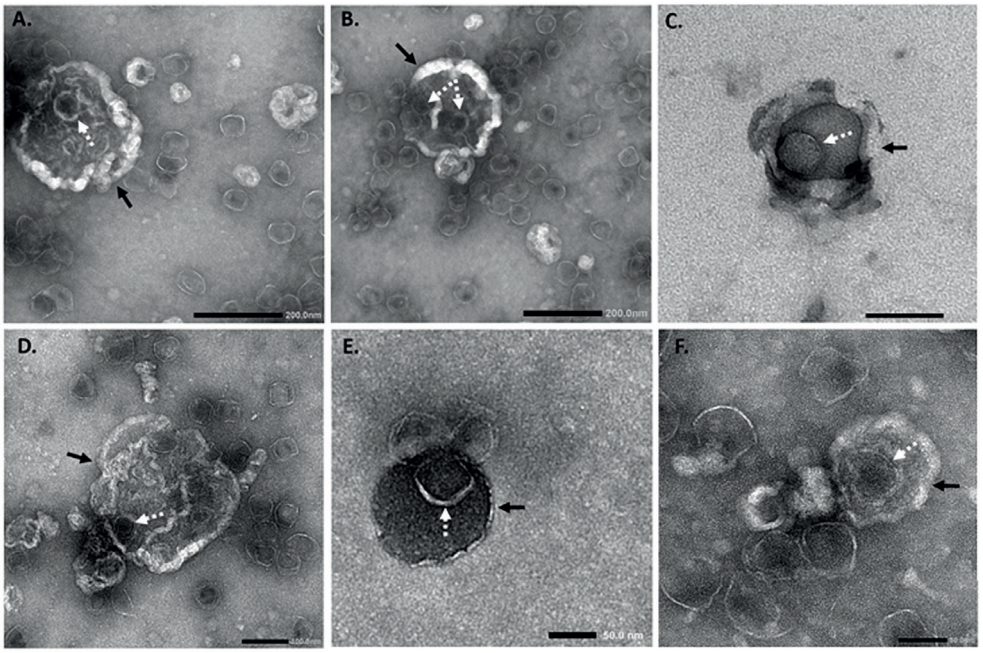

Figure 8.4. TEM pictures of EVs isolated from FM-YL11 supernatant under prophage-inducing condition. Cases are shown where phage particles seemed to be enclosed in EVs. Arrows with solid lines point at EV-like structures, and arrows with dashed lines point at phage head-like particles. Scale bars in A) and B) represent 200 nm, in C) and D) represent 100 nm and in E) and F) 50 nm.

Proteome of holin-lysin included EVs

The proteome of the EV fraction collected from the culture supernatant of strain FM-YL11 under prophage-inducing condition was examined. The reference genome used for FM-YL11 contained 2670 predicted proteins, and 1283 proteins were detected in the EV samples. Average iBAQ (intensity-based absolute quantification) values of samples from two independent experiments were examined. Due to very high sensitivity of the detection method as well as limitations in the EV purification method, here we only focus on the top 600 proteins in abundance (supplementary Table S8.3) to describe the main proteome profile, which counted up to 98% of the total protein quantity.

Phage head protein and scaffolding protein were among the most abundant proteins revealed from the FM-YL11 EV fraction, counting up to 11% signal intensity of the total top 600 proteins, further confirming the identity of the phage head-like structures observed next to EVs. Phage tail proteins were also detected in the top 600 protein list in the EV fraction from FM-YL11, although we did not observe any phage tail-like structures in TEM analysis. In total about 40 proteins encoded by the prophage in FM-YL11, including holin and lysin were also among the top 600 most abundant proteins found in the EV fraction of FM-YL11.

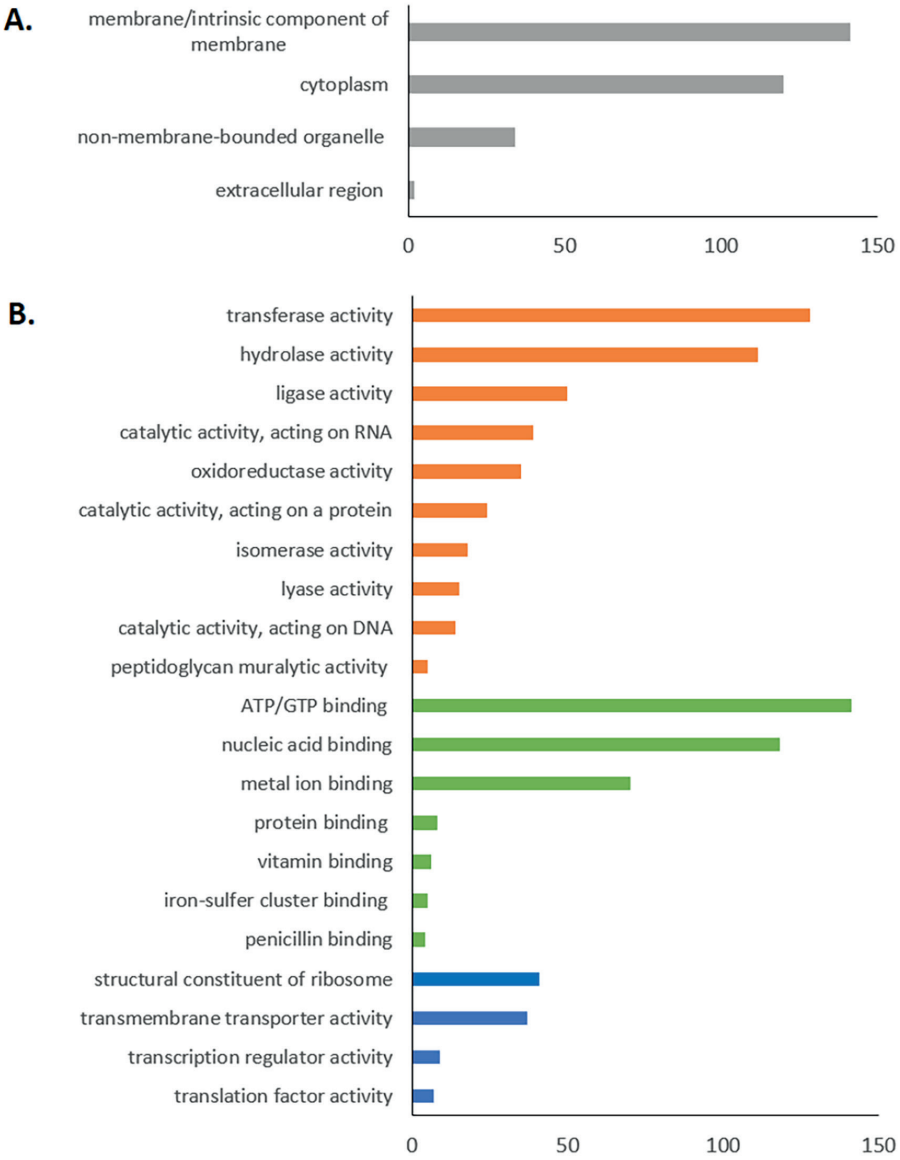

Figure 8.5. Distribution of top 500 proteins from *L. lactis* FM-YL11 prophage holin-lysin induced EVs based on their GO annotations in A) subcellular locations and B) molecular functions. In B), orange bars represent subcategories under category "catalytic activity", green bars represent subcategories under "binding", and blue bars for other categories under the domain of molecular functions. Some proteins are assigned to more than one category.

When examining the gene ontology (GO) annotations of the top 600 proteins detected in the EV fraction of FM-YL11, more than 300 proteins were assigned a GO term as cellular anatomical entity under the cellular component domain, from which more than 140 proteins were assigned a GO term of membrane, and 120 proteins were assigned to be in the cytoplasm (Fig. 8.5A). Nearly 40 ribosomal

proteins also made a significant category. For molecular function, more than 320 proteins were assigned a GO term of catalytic activity, 280 proteins with binding activity and about 40 proteins with transmembrane transporter activity. Note that it is possible for one protein to get multiple GO terms (Fig. 8.5B). Among the proteins with catalytic activity, transferase and hydrolase activities were the most abundant with more than 100 hits. Among the proteins with binding activity, ATP/GTP binding, nucleic acid binding and metal ion binding (magnesium, zinc, iron and potassium binding) were the subcategories with the most hits. The proteins in FM-YL11 EVs are predicted to be involved in a variety of biological processes according to the GO annotation, including translation, localization, cell division, lipid biosynthesis, peptidoglycan biosynthesis, stress/stimulus response, etc (supplementary Table S8.3).

Discussion

Recent insight in variety in cargos carried by Gram-positive EVs and the diverse roles they play in bacterial physiology, ecology and microbe-host interactions, highlighted the importance of this research field. Gram-positive bacterial species cover a wide range including beneficial commensal bacteria and pathogens. Hence, knowledge on the biogenesis, composition and functions of Gram-positive EVs contributes not only to fundamental research in microbiology, but also to understanding the implications of Gram-positive EV in human health and disease, and to diverse potential biotechnological or medical applications (Chapter 2 of this thesis - Liu et al., 2018; Briaud and Carroll, 2020).

In this study, we provide further evidence for EV production by the Gram-positive bacterium *Lactococcus lactis*, using an artisanal cheese isolate FM-YL11 as a model. We showed that *L. lactis* FM-YL11 EV production was largely stimulated by prophage activity, and more specifically, by the prophage-encoded holin-lysin system. Defective phage particles were found to be released along with and enclosed by EVs.

Prophage-dependent EV release mechanism has also been demonstrated in other Gram-positive bacteria namely *Bacillus subtilis* and *Staphylococcus aureus* (Toyofuku et al., 2017; Andreoni et al., 2019). The prophage-triggered EV release in *B. subtilis* was not found to cause immediate cell death and explosive cell lysis: the cells remained in shape during EV extrusion, although eventually cell death took place as the integrity of the cytoplasmic membrane was heavily compromised. Phage particles (with tails) were found to be enclosed by the *B. subtilis* EVs. In *S. aureus* the prophage-dependent mechanism of EV release was found to be associated with cell lysis upon prophage activation, as indicated by ghost cells and (tailed) phage particles released along with the EVs. Observed differences in lysis of *B. subtilis* and *S. aureus* producer cells may be explained by extend of prophage induction and differences in activity of prophage-encoded cell envelop degrading enzymes.

Combining all information, we propose a new model for EV production in *L. lactis* that is a mixed scenario of the gradual extrusion/non-lytic release and cell lysis as a result of prophage holin-lysin activity (Fig. 8.6). Under prophage inducing condition, the growth of FM-YL11 appeared to be only slightly inhibited in comparison to the non-inducing condition. The same effect of slight growth inhibition was observed for FM-YL11ΔHLH under the prophage inducing condition but not for FM-YL12, indicating that this growth inhibition was most likely a result of the metabolic burden for producing intracellularly accumulating phage particles instead of cell lysis during EV production. Other than the growth inhibition, it is likely that the majority of FM-YL11 cells remained intact throughout the 6 hours following exposure to mitomycin C, in spite of substantial release of EVs. The presence of phage particles in the culture supernatant may point to cell lysis of a small subpopulation. In the presented model, the gradual extrusion of EVs and cell lysis formed EVs were due to the action of prophage-encoded holin and lysin. Differences in EV production routes may be explained by heterogeneity in prophage gene expression and production of phage proteins in the population upon prophage induction, with the subpopulation of lysed cells representing cells with high level holin-lysin production (Fig. 8.6B), while the majority of cells are considered to have a moderate level of production that allows for gradual, non-lytic release of EVs (Fig. 8.6A).

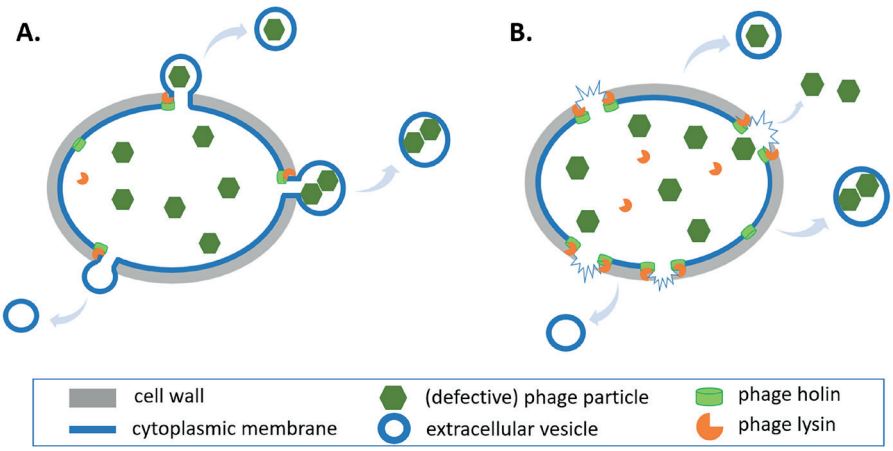

Figure 8.6. Schematic presentation of the proposed model for prophage holin-lysin induced EV production mechanism in *L. lactis*. A) When prophage-encoded holin and lysin are produced at moderate levels in *L. lactis* under the tested prophage inducing condition, EVs are produced by gradual extrusion of the cytoplasmic membrane without immediate cell lysis. This is expected to be the case for the major bacterial population in the culture of strain FM-YL11. The (defective) phage particles accumulated in the cytoplasm may be enclosed by EVs upon release. B) When prophage encoded holin and lysin are produced at high levels in *L. lactis* under the tested prophage-inducing condition, EVs are produced by cell lysis. This scenario is expected to be among a small subpopulation in the culture of strain FM-YL11. Phage particles are released freely into the extracellular environment or enclosed by the membrane upon forming EVs. Note that not all illustrated components are drawn at the same scale.

Although EV production was clearly stimulated by prophage encoded holin-lysin system in *L. lactis*, prophage-independent EV production can also occur. This is reflected by the presence of EVs in the culture supernatants from both the non-inducing and prophage-inducing conditions of strains FM-YL12 and YL11 ΔHLH, albeit in low quantity. Prophage-independent triggers have also been described for EV production in *S. aureus*, for example antibiotics that weaken the peptidoglycan layer and production of cell wall degrading autolysins (Wang et al., 2018; Andreoni et al., 2019). *L. lactis* is known to produce autolysins (N-acetylglucosaminidases) too. The four lactococcal autolysins, namely AcmA, AcmB, AcmC and AcmD, have been experimentally confirmed for their functionality in cell separation and autolysis in the model strain *L. lactis* ssp. *cremoris* MG1363 (Buist et al., 1997; Visweswaran et al., 2013, 2017). In the genome of strain FM-YL11, we identified homologous sequences of all four autolysin-encoding genes to strain MG1363 (GenBank No. AM406671) with 97% - 98% sequences identity. A possible role of putative autolysins in EV production in *L. lactis* remains to be confirmed.

In comparison to the EVs produced by strain FM-YL12, the prophage-encoded holin-lysin induced EVs in strain FM-YL11 seem to be larger in size, as reflected by both electron microscopy and flow cytometry of membrane-stained particles. Besides the subpopulation of EVs from strain FM-YL11 that enclosed phage particles with uniquely high DNA content, most likely there is also an EV subpopulation that entrapped a substantial amount of other DNA molecules. Prophage holin-lysin induced EVs generally show a high DNA content in comparison to EVs produced by a prophage independent route. Similar observations were reported in the study of *S. aureus* EV production via phage-dependent and -independent routes, conceivably as a result of fragmentation of the bacterial chromosome caused by prophage activation (Andreoni et al., 2019). Proteomics analysis in our study also revealed a number of nucleic acid binding proteins in EVs released by strain FM-YL11. Our finding of nucleic acid cargos in *L. lactis* EVs adds to the limited evidence that Gram-positive EVs contain nucleotides as the cargo (Klieve et al., 2005; Resch et al., 2016; Rodriguez and Kuehn, 2020). DNA containing EVs potentially facilitate the exchange of genetic material between bacterial cells in a microbial community.

Moreover, the substantial population of holin-lysin induced EVs that contain phage head-like particles is intriguing. This deduction was supported by EM pictures and flow cytometry. In the latter, a population with positive membrane signals and distinctly high DNA signals was identified. Notably, in the study of the lysogenic strain TIFN1, when phage particles were collected from similar prophage induction conditions, the complete proPhi1 genome was identified with high DNA sequencing coverage in the phage particles (Chapter 6 of this thesis - Alexeeva et al., 2021). In addition, the prophage sequence in strain FM-YL11 showed 100% sequence identity to the *Siphoviridae* phage proPhi1 (Chapter 6 of this thesis - Alexeeva et al., 2021), where the tail tape measurement gene was found to be truncated by a mobile element, explaining the tailless phenotype of the phages. Interestingly, viral particles or complete viral genomes have been previously observed in *B. subtilis* and *Thermococcus nautilus* EVs and roles in exchange of genetic material have been suggested (Gaudin et al. 2014; Toyofuku et al. 2017; Y. Kim, Edwards, and Fenselau 2016). In addition, Tzipilevich et al. have demonstrated that *B. subtilis* EVs may contribute to phage infection by spreading phage receptors to non-sensitive strains

and making them susceptible to phage infection (Tzipilevich et al., 2017). Similarly, proteomics analysis also revealed phage infection protein (T0UL74) in FM-YL11 EVs (supplementary Table S8.3), which may potentially enable EVs to act as decoy for phage targeting or spread phage sensitivity to other cells. Whether the EVs enclosing phage particles offer a novel route in lactococcal phage infection remains to be studied.

Proteomic analysis of holin-lysin induced EVs showed high abundance of membrane proteins and cytoplasmic proteins, the latter indicating enclosure of cytoplasmic content by EVs, in line with previous studies of other Gram-positive EVs (Lee et al., 2009; Kim et al., 2016). This is considered a unique feature for Gram-positive EVs, in contrast to Gram-negative EVs, since EVs from Gram-positive bacteria are generated from the cytoplasmic membrane allowing direct encapsulation of cytoplasmic content, while Gram-negative EVs are mostly generated from the outer membrane, and tend to encapsulate periplasmic components (Kim et al., 2015). It remains to be elucidated whether the proteins in EVs were loaded randomly or by specific sorting mechanisms generated by specific cellular domains in the cytoplasmic membrane of *L. lactis* strain FM-YL11. Protein, lipid and nucleic acid analysis of bacterial EVs from *Streptococcus pyogenes*, *Streptococcus mutans*, *S. aureus* and *Lactiplantibacillus plantarum* also revealed compositional differences compared to the respective cell membranes (Lee et al., 2009; Liao et al., 2014; Biagini et al., 2015; Kim et al., 2020a), suggesting that active EV production involves dedicated sorting mechanisms. In this study, the over-representation of proteins involved in translation, lipid and peptidoglycan biosynthesis, and cell division in FM-YL11 EVs (supplementary Table S8.3), may point to hotspots for EV production such as the cell division site. Similarly, in the previous study of membrane-enclosed phage release by *L. lactis* isolates from the starter culture Ur, EV release was most prominent at the cell division site, and had a lipid profile that differed from that of the cytoplasmic membrane (Chapter 7 of this thesis – Liu et al., 2021a).

Protein cargos detected in the holin-lysin induced *L. lactis* EVs also included metal ion (e.g. iron) binding proteins and penicillin binding proteins (supplementary Table S8.3). Similarly, EVs from *Mycobacterium tuberculosis*, *Streptomyces coelicolor* and *S. aureus* were shown to contain iron-binding factors, which contributed to bacterial survival under iron-limited conditions (Lee et al., 2009, 2015; Schrempf et al., 2011). The penicillin binding proteins are involved in peptidoglycan synthesis and cell division (David et al., 2018), but also offer binding sites to penicillin and β-lactam antibiotics. This observation supports previous findings where EVs have been considered to contribute to bacterial survival by removing the antibiotics from the extracellular environment, acting as the decoy of antibiotic targeting or containing antibiotic-degrading enzymes (Lee et al., 2009; Chattopadhyay and Jaganandham, 2015; Kim et al., 2018, 2020b; Sabnis et al., 2018; Bose et al., 2020).

Besides the solid evidence on the roles of prophage holin-lysin in *L. lactis* EV production, this study also highlights the interest for further investigations to answer the remaining important questions: firstly, comparative analysis of the nucleic acid and protein content in EVs and producer cells, will support validation of the hypothesized model of EV release (Fig. 8.6), and the occurrence of subpopulations

of EVs, as well as to providing insights on the possible physiological and ecological significance of EV production. Secondly, mechanisms underlying prophage induction and hence EV production can be further investigated in relation to possible DNA damage and RecA-mediated damage repair as described for *B. subtilis* (Toyofuku et al. 2017). Last but not least, it is of high interest to examine the effect of prophage activation and EV release on colonization capacity and competitive fitness of respective producer(s) in selected environments.

To conclude, this study adds *L. lactis* to the list of EV producing Gram-positive bacteria species. Evidence is provided for an important role of phage holin-lysin in EV release. As prophages or prophage-encoded elements are extremely widespread and common in bacterial genomes, the role of prophage activation, especially the holin-lysin system, in EV production can be generalized to more Gram-positive bacteria. Considering the important roles of *L. lactis* and other LAB in a range of fermentations and probiotic formulations, knowledge of the EV production mechanisms can be exploited to achieve desired traits and functionalities in fermentation processes, such as efficient release and delivery of intracellular/membrane embedded effector molecules or nutritional compounds, and in probiotic applications. Moreover, findings from this study can also pave the way for exploiting bacterial EVs for biotechnological applications, such as for delivery of genome editing tools (Liu *et al.*, 2019).

Acknowledgements

The authors would like to thank Eline van Ophem, Alexios Voloch and Alisha Geraldine Lewis (Food Microbiology, Wageningen University) for their contributions in mutant construction, and Dennis van den Berg (Food Microbiology, Wageningen University) for the advice in selection of vectors. The electron microscopy images were obtained with the help of Jelmer Vroom at the Wageningen Electron Microscopy Centre (WEMC) of Wageningen University.

This work was subsidized by the Netherlands Organization for Scientific Research (NWO) through the Graduate Program on Food Structure, Digestion and Health.

Supplementary materials

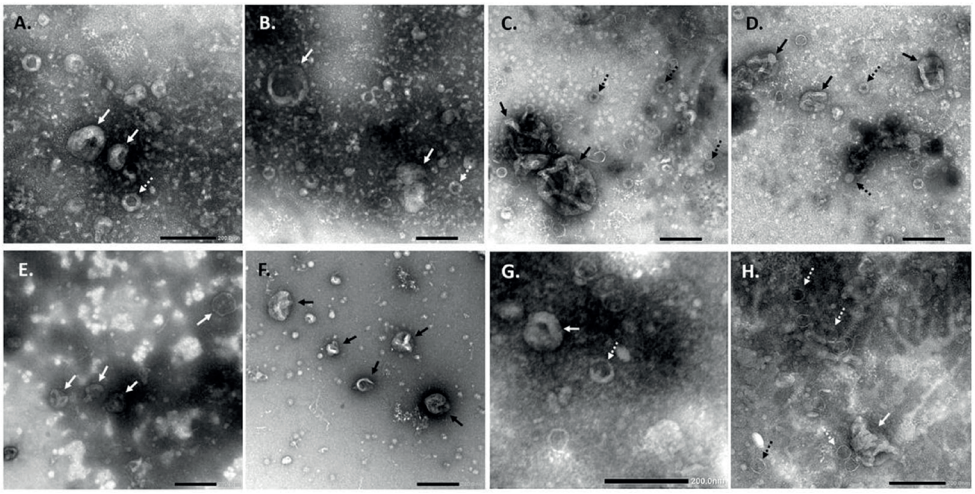

Figure S8.1. TEM pictures of lactococcal EVs. A) and B) are EVs collected from the culture supernatant of strain FM-YL11, under non-inducing condition. C) and D) are EVs from the culture supernatant of strain FM-YL11, under prophage-inducing condition. E) and F) are EVs from strain FM-YL12 supernatant under prophage-inducing condition. G) and H) are from strain FM-YL11ΔHLH, under prophage-inducing condition. For prophage-inducing condition, 1 µg/mL mitomycin C was added to bacterial cultures in early exponential phase, and EVs were collected from the supernatant by ultracentrifugation after 6 hours treatment. For non-inducing condition, all treatments were the same except that no mitomycin C was added to the cultures. Arrows with solid lines point at EV-like structures, and arrows with dashed lines point at phage head-like particles. All scale bars represent 200 nm.

Table S8.1 Primers used for constructing plasmids used for holin and lysin gene knockout in strain FM-YL11.

Name	Sequence (5'-3')
HL_up_XhoI Fw	GGTGGTCTCGAG**ACGGTTTCACGACTGTTTATCCG**
HL_up_HindIII Rv	CCTCCTAAGCTT**ATGTTTTTATGCAGTCCGTTGCC**
HL_dn_HindIII Fw	CTCCTCAAGCTT**AGAAATACCCTTGGCATATTCGC**
HL_dn_PstI Rv	CCACCACTGCAG**CCAAAAGCTCCATATTGTTCACC**
Holin_up PstI Rv	CCGCCGCTGCAG**GATCCCTACTTTCTTAATCTATTG**
Holin_up_XhoI-Fw	ATATATCTCGAG**CTCAAGCAAGTACGATTGGG**
holin1-dn HR_PstI Fw	GAGGAGCTGCAG**AAGGAGTTCCCAATGAGTTTAG**
holin1_dn HR_EagI Rv	CCTCCTCGGCCG**GTCTGTCATTGCACTTTGTAAGC**

Table S8.2 Primers used for constructing plasmids used for holin and lysin gene complementation in strain FM-YL11ΔHLH.

Name	Sequence (5'-3')
45-holin-lysin_fwd	CACTCACCATGGGTACTGCAG**TAGGAGAGTAAAATGAATCAAATC**
45/35-holin-lysin_rev	TCCCTACTTT**GCCAAGGGTATTTCTTTAATAAAC**
45/35-holin2_fwd	TACCCTTGGC**AAAGTAGGGATCATGGAGG**
45-holin2_rev	TCAAAGAAAGCTTGAGCTCT**GGGAACTCCTTTTAAAGTATTTTAG**

Table S8.3. Top 600 protein hits with greatest abundance from the EV fraction of strain FM-YL11 under the prophage-inducing condition.

UniProt IDs	Protein names	iBAQ signal	GO categories						
			1	2	3	4	5	6	7
T0UW71	Head protein	6.29E+09							
T0URE1	Elongation factor Tu	3.45E+09							
T0UW80	Scaffolding protein	2.59E+09							
T0W8S4	50S ribosomal protein L4	2.55E+09							
T0W8S8	30S ribosomal protein S3	1.65E+09							
T0UZ71	30S ribosomal protein S11	1.57E+09							
T0UIU4	30S ribosomal protein S4	1.4E+09							
T0VMR3	30S ribosomal protein S7	1.3E+09							
T0V5G7	30S ribosomal protein S2	1.22E+09							
T0W643	50S ribosomal protein L5	1.21E+09							
T0UYK9	50S ribosomal protein L3	1.2E+09							
T0UT97	50S ribosomal protein L2	1.16E+09							
T0VXP0	50S ribosomal protein L19	1.13E+09							
T0VSC0	30S ribosomal protein S12	1.1E+09							
T0W645	30S ribosomal protein S5	1.08E+09							
T0UZG8	Universal stress protein UspA	1.01E+09							
T0VRD6	Peptide-binding protein	1.01E+09							
T0UZC3	Preprotein translocase subunit YajC	1E+09							
T0URV5	Foldase protein PrsA	1E+09							
T0UTB9	30S ribosomal protein S13	9.17E+08							
T0W5P3	UPF0154 protein LLT1_9680	9.05E+08							
T0UQ99	50S ribosomal protein L21	8.86E+08							
T0URM1	50S ribosomal protein L20	7.28E+08							
T0UM40	30S ribosomal protein S1	6.62E+08							
T0VRG6	Galactose-6-phosphate isomerase subunit LacB	6.22E+08							
T0VR76	Membrane protein	6.16E+08							
T0W1W8	ATP synthase subunit beta	5.97E+08							
T0UPF6	CTP synthase	5.87E+08							
T0URD6	Uncharacterized protein	5.7E+08							

Table S8.3. ***Continued***

T0VVL7	Dihydrolipoamide acetyltransferase component of pyruvate dehydrogenase complex	5.62E+08								
T0W2N8	Portal protein	5.32E+08								
T0W640	50S ribosomal protein L16	5.32E+08								
T0W4T5	UTP--glucose-1-phosphate uridylyltransferase	5.28E+08								
T0W8U7	50S ribosomal protein L17	5.14E+08								
T0UKQ3	Uncharacterized protein	5.14E+08								
T0URG4	50S ribosomal protein L35	5.12E+08								
T0W5S1	[neck passage]BppU_N domain-containing protein	4.69E+08								
T0UZ62	30S ribosomal protein S8	4.47E+08								
T0W275	Methionine ABC transporter ATP-binding protein	4.43E+08								
T0URE6	30S ribosomal protein S15	4.23E+08								
T0UYM1	50S ribosomal protein L6	3.97E+08								
T0UA69	EIICB-Lac	3.97E+08								
T0VS84	30S ribosomal protein S9	3.87E+08								
T0UZ53	30S ribosomal protein S10	3.64E+08								
T0UKP1	ATP synthase subunit alpha	3.61E+08								
T0VTL1	Enoyl-[acyl-carrier-protein] reductase [NADH]	3.58E+08								
T0W2V1	PTS fructose transporter subunit IIC	3.55E+08								
T0UYS4	GTP-binding protein	3.51E+08								
T0USD3	PTS mannose transporter subunit IID	3.44E+08								
T0W2P1	[tail length tape-measure protein] Uncharacterized protein	3.37E+08								
T0UZ58	30S ribosomal protein S17	3.37E+08								
T0UVN1	Uncharacterized protein	3.3E+08								
T0UI30	Protease	3.24E+08								
T0UY81	50S ribosomal protein L1	3.13E+08								
T0VRU5	Peptide ABC transporter ATP-binding protein	3.08E+08								
T0UQG3	ATP-dependent zinc metalloprotease FtsH	3.02E+08								
T0URA1	Uncharacterized protein	2.98E+08								
T0UWL2	S-adenosylmethionine synthase	2.97E+08								
T0USJ1	Catabolite control protein A	2.96E+08								
T0W634	Uncharacterized protein	2.9E+08								
T0UVM5	[head-tail connector]Uncharacterized protein	2.86E+08								
T0V5R4	Glutamine synthetase	2.81E+08								

T0URR4	ATP synthase subunit b	2.76E+08							
T0ULH7	Translation initiation factor IF-2	2.75E+08							
T0URZ7	Amino acid ABC transporter permease	2.71E+08							
T0UH11	50S ribosomal protein L13	2.67E+08							
T0ULX2	Nitrogen regulatory protein P-II	2.63E+08							
T0VMA2;T0UKD9	Peptide ABC transporter ATPase	2.54E+08							
T0UC37	Serine hydroxymethyltransferase	2.5E+08							
T0UT82	Large-conductance mechanosensitive channel	2.33E+08							
T0VSD6	Flotillin	2.29E+08							
T0VRF8	Uncharacterized protein	2.27E+08							
T0UK13	Uncharacterized protein	2.24E+08							
T0V5G0	Crp/Fnr family transcriptional regulator	2.17E+08							
T0UZ67	50S ribosomal protein L15	2.12E+08							
T0UIJ0	DEAD-box ATP-dependent RNA helicase CshA	2.11E+08							
T0WF61	Septation ring formation regulator EzrA	1.98E+08							
T0UYF1	NADH dehydrogenase	1.97E+08							
T0UYM6	DNA-directed RNA polymerase subunit alpha	1.96E+08							
T0VVB4	GntR family transcriptional regulator	1.94E+08							
T0VQ31	Uncharacterized protein	1.91E+08							
T0UPB9	Tyrosine--tRNA ligase	1.89E+08							
T0VTZ2	dTDP-glucose 4,6-dehydratase	1.86E+08							
T0UA32;T0UCB7	Alpha-acetolactate decarboxylase	1.82E+08							
T0UV91	50S ribosomal protein L10	1.77E+08							
T0USW8	DNA primase	1.76E+08							
T0UVT0	Ribonucleoside-diphosphate reductase	1.71E+08							
T0UQJ7	Amino acid ABC transporter substrate-binding protein	1.67E+08							
T0UKC2	Cell division protein FtsZ	1.65E+08							
T0UMT9	Uncharacterized protein	1.64E+08							
T0VYQ0	EIIAB-Man	1.63E+08							
T0UQ31	Fumarate reductase	1.61E+08							
T0VWP4	30S ribosomal protein S21	1.59E+08							
T0W625	Uncharacterized protein	1.59E+08							
T0UTJ0	Proline--tRNA ligase	1.57E+08							

Table S8.3. ***Continued***

T0W635	50S ribosomal protein L23	1.57E+08								
T0UT09	Phosphoribosylaminoimidazole-succinocarboxamide synthase	1.56E+08								
T0VX48;T0VSK8	Site-specific DNA-methyltransferase (adenine-specific) (Fragment)	1.55E+08								
T0UQF2	Cell division protein FtsX	1.52E+08								
T0WD50	DUF536 domain-containing protein	1.52E+08								
T0VT45	Enolase	1.51E+08								
T0UDZ9	Uncharacterized protein	1.49E+08								
T0VYA5	ATP synthase gamma chain	1.48E+08								
T0VW51	Lysine--tRNA ligase	1.47E+08								
T0UZ49	Preprotein translocase subunit SecE	1.47E+08								
T0UT31	UDP-N-acetylmuramate--L-alanine ligase	1.47E+08								
T0VXY4	Aspartyl/glutamyl-tRNA(Asn/Gln) amidotransferase subunit B	1.43E+08								
T0UPR3	Lipoprotein	1.42E+08								
T0V5I9	30S ribosomal protein S18	1.41E+08								
T0UL96	Biotin carboxylase	1.39E+08								
T0UW75	Tail protein	1.39E+08								
T0W628	Uncharacterized protein	1.38E+08								
T0UI20	2-oxoisovalerate dehydrogenase subunit beta	1.37E+08								
T0UJS0	Uncharacterized protein	1.35E+08								
T0W8T6	50S ribosomal protein L18	1.35E+08								
T0UPM3	Asparagine synthase (glutamine-hydrolyzing)	1.35E+08								
T0UK73	BRO-like protein (antirepressor)	1.31E+08								
T0W1R9	DNA-directed RNA polymerase subunit beta	1.28E+08								
T0US03	ATP synthase subunit delta	1.28E+08								
T0USW5	Uncharacterized protein	1.27E+08								
T0W1M0	Cell division protein SepF	1.25E+08								
T0UBX9	Endolytic murein transglycosylase	1.24E+08								
T0VVI3	[mobile element protein] Uncharacterized protein	1.24E+08								
T0W8W3	Phenylalanine--tRNA ligase alpha subunit	1.23E+08								
T0V5G9	Peptidase C51 domain-containing protein	1.23E+08								
T0VZW4	Protein RecA	1.23E+08								
T0UBZ3	General stress protein	1.21E+08								
T0UYA6	Histidine--tRNA ligase	1.19E+08								

T0USU2	Adenylosuccinate synthetase	1.19E+08							
T0UDT1	SHOCT domain-containing protein	1.19E+08							
T0UMT0	Glucose-1-phosphate thymidylyltransferase	1.17E+08							
T0UP82	DNA-binding protein HU	1.17E+08							
T0UQB8	Phage_Mu_F domain-containing protein	1.16E+08							
T0UKD2	Asparagine--tRNA ligase	1.14E+08							
T0VVB1	Phospho-2-dehydro-3-deoxyheptonate aldolase	1.14E+08							
T0UHX1	Pyruvate carboxylase	1.14E+08							
T0VW85	Peptidylprolyl isomerase	1.13E+08							
T0W5P7	50S ribosomal protein L7/L12	1.13E+08							
T0V5Q2	Chaperone protein DnaJ	1.12E+08							
T0VR16	Exopolysaccharide biosynthesis protein	1.12E+08							
T0W8Q6	ABC transporter substrate-binding protein	1.11E+08							
T0UZA0	Threonine--tRNA ligase	1.11E+08							
T0UR35;T0UM78	Foldase protein PrsA	1.09E+08							
T0UHW1	Ribosome hibernation promoting factor	1.09E+08							
T0UT00	Uncharacterized protein	1.08E+08							
T0UZF9	Glyceraldehyde-3-phosphate dehydrogenase	1.06E+08							
T0VR37	LytR family transcriptional regulator	1.06E+08							
T0UIP9	Ferrichrome ABC transporter substrate-binding protein	1.05E+08							
T0US50	Phosphate ABC transporter substrate-binding protein	1.04E+08							
T0UVU3	Holin	1.04E+08							
T0W060	Ribonucleoside triphosphate reductase	1.04E+08							
T0UP19	Heme ABC transporter ATP-binding protein	1.03E+08							
T0W6H8	Ribonuclease Y	1.02E+08							
T0VP90	Membrane protein insertase YidC	1.01E+08							
T0W1N8	Translation initiation factor IF-3	1.01E+08							
T0UK77	Histidine kinase	99177000							
T0USY8	GTPase Obg	96919500							
T0VXX9	Glycosyltransferase	96913000							
T0VW56	Gamma-aminobutyrate permease	96398500							
T0W6L5	Uncharacterized protein	96312000							
T0UAZ8	Elongation factor G	96160500							

Table S8.3. ***Continued***

T0UNP6	Tellurite resistance protein TelA	95810500							
T0UJ77	Ribosome-binding ATPase YchF	94270500							
T0UPK8	2,3-bisphosphoglycerate-dependent phosphoglycerate mutase	91378500							
T0W359	NADH dehydrogenase	90689000							
T0UK98	Cell division protein FtsZ (Fragment)	90191000							
T0W2R5	Cell division ATP-binding protein FtsE	90062000							
T0VZ42	Protein translocase subunit SecA	89197500							
T0URK2	DNA-directed RNA polymerase subunit beta	89058500							
T0UER7	Transcriptional repressor NrdR	88485650							
T0VVD6	Short-chain dehydrogenase	88236500							
T0USZ0	Ammonium transporter	86084000							
T0V5H3	HAD family hydrolase	85857700							
T0UTB1	30S ribosomal protein S14 type Z	85536000							
T0UW92	Redox-sensing transcriptional repressor Rex	84880500							
T0VVD0	[transcriptional regulation protein] Uncharacterized protein	84427500							
T0W0B1	GTPase	84245500							
T0UPT1	GTPase Era	84055500							
T0UK07	Uncharacterized protein	83717500							
T0UDY2	Methyltransferase	83416500							
T0W1P9	Pyrophosphate phospho-hydrolase	82597050							
T0W680	Uracil phosphoribosyltransferase	82039600							
T0UPZ4	UDP-N-acetylglucosamine 1-carboxyvinyltransferase	80494500							
T0UQ28	Inosine-5-monophosphate dehydrogenase	79515500							
T0UYS8	Uridylate kinase	79507500							
T0VU22	Uncharacterized protein	78692350							
T0UES5	Aspartokinase	78412500							
T0UKX8	tRNA (guanine-N(7)-)-methyltransferase	78076000							
T0UPC1	Pyruvate dehydrogenase E1 component subunit alpha	77815000							
T0UQT9	DNA-directed RNA polymerase subunit omega	77753000							
T0VRF3	Uncharacterized protein	76442000							
T0UZV7	Site-specific DNA-methyltransferase (adenine-specific) (Fragment)	75885500							
T0UMX9	Membrane protein insertase YidC	74790000							
T0UYL4	50S ribosomal protein L22	74064260							

T0UVI1	Glycine--tRNA ligase alpha subunit	73207500							
T0VZC9	Thymidylate synthase	72678000							
T0W8H7	tRNA-dihydrouridine synthase	72651000							
T0UTU9	Uncharacterized protein	71466600							
T0UPY7	L-lactate dehydrogenase	71454000							
T0URV9	HAD hydrolase	70586250							
T0UKY5	Chorismate synthase	69618000							
T0UM65	P-type Ca(2+) transporter	69543500							
T0UFR2	Tagatose 1,6-diphosphate aldolase	69432500							
T0W4S5	Heme ABC transporter ATP-binding protein	69039500							
T0W2M8	Signal recognition particle protein	68820650							
T0UVB9	Uncharacterized protein	68756500							
T0UVA7;T0UR10	Holin	68505000							
T0UW47;T0UI22	Sugar phosphate phosphatase	68105000							
T0UHK2	Uncharacterized protein	67600500							
T0VU18	Glycosyl transferase	67484000							
T0UPJ1	DEAD-box ATP-dependent RNA helicase CshB	67343500							
T0W379	Carbamoyl-phosphate synthase large chain	66892500							
T0W5V2	Niacin transporter NiaX	66149850							
T0URR1	ATP synthase epsilon chain	65427000							
T0VTV5	Aminotransferase AlaT	65200500							
T0VTW5	Uncharacterized protein	64529400							
T0WD54	Uncharacterized protein	63934500							
T0UVE1	Homoserine kinase	63921915							
T0UHB9	ATP-dependent Clp protease ATP-binding protein	63783000							
T0UER5	GTPase Der	62793500							
T0UK87	[DNA binding protein]Uncharacterized protein	62480650							
T0W5X7	FAD:protein FMN transferase	62022400							
T0UNX4	(p)ppGpp synthase	61826000							
T0W679	Protein GrpE	61610000							
T0UQ10	Spermidine/putrescine import ATP-binding protein PotA	61380500							
T0USN1	Carbamoyl-phosphate synthase small chain	61108000							
T0UVB2	[receptor binding protein]Uncharacterized protein	60767350							

Table S8.3. ***Continued***

T0UIK8	ABC transporter ATPase	60445600	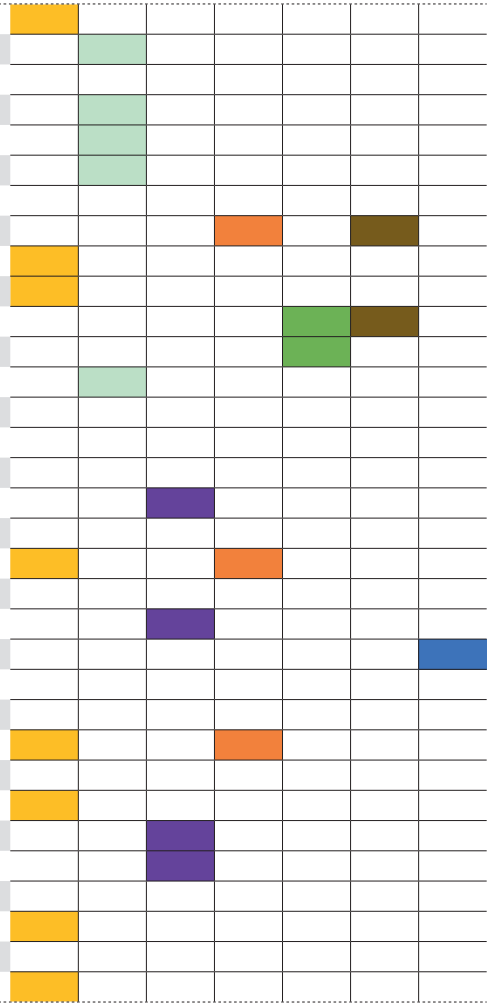
T0UKD4	Uncharacterized protein	60371000	
T0UQS6	Fructose-bisphosphate aldolase	60329500	
T0UJY2	dUTP diphosphatase	60233000	
T0VVK9	Uncharacterized protein	59810000	
T0W2A3;T0VXJ2;T0ULM6	1,4-beta-N-acetylmuramidase (Fragment)	59445850	
T0UJ83	Hypoxanthine phosphoribosyltransferase	59352900	
T0VVJ0	UDP-N-acetylglucosamine 1-carboxyvinyltransferase	59332500	
T0UZI3	Uncharacterized protein	59084000	
T0UYM4	Protein translocase subunit SecY	59080000	
T0VXU3	Bifunctional protein GlmU	57849100	
T0ULH3	3-hydroxyacyl-[acyl-carrier-protein] dehydratase FabZ	57158000	
T0UQC2	LACLC[capsid and scaffolding protein] Uncharacterized protein	57077950	
T0W2G0	ATP-dependent DNA helicase	56707500	
T0VYZ3	Bifunctional protein PyrR	56666000	
T0W5V6	Spermidine/putrescine ABC transporter substrate-binding protein	56265000	
T0UMN7	Glutamyl-tRNA(Gln) amidotransferase subunit A	56036000	
T0W2P9	Glutamine--fructose-6-phosphate aminotransferase [isomerizing]	55745800	
T0URB6	Cell division protein FtsA	55595050	
T0UGK4	Pur operon repressor	54386500	
T0W673	Phenylalanine--tRNA ligase beta subunit	53763950	
T0VXX8	UvrABC system protein A	53728500	
T0WFB9	Asparagine synthase	53324900	
T0UQ33	2,3,4,5-tetrahydropyridine-2,6-dicarboxylate N-acetyltransferase	52994150	
T0W2I2	Mid-cell-anchored protein Z	52317450	
T0VXW2	Universal stress protein	52215795	
T0URU6	Phosphate import ATP-binding protein PstB	52112900	
T0W8H5	Aspartate--tRNA ligase	51642750	
T0VV94	50S ribosomal protein L33	51281000	
T0VZG8	Uncharacterized protein	51065500	
T0W225	Phosphate import ATP-binding protein PstB	50084500	
T0UV12	TPR_REGION domain-containing protein	49008800	
T0W6A8	Zinc metalloprotease	48960500	

T0UUJ7	Glycerol-3-phosphate dehydrogenase [NAD(P)+]	48665050							
T0WF59	MFS transporter	48654230							
T0UPX4	[upper base plate protein]Uncharacterized protein	48337500							
T0UKB9	Cell division protein DivIVA	48094000							
T0UR70	Non-specific serine/threonine protein kinase	47429500							
T0W6E3	3-dehydroquinate dehydratase	47422400							
T0UZH2	Cell shape-determining protein MreC	47414950							
T0W2C9	Probable GTP-binding protein EngB	47141850							
T0UMQ9	Major cold shock protein	46264500							
T0UY72	DNA methyltransferase	46165150							
T0USA3	Dipeptidase	46071400							
T0W2L7	Uracil transporter	45965000							
T0UPH9;T0UGS1	60 kDa chaperonin	45949500							
T0UJR5	Cation transporter	45948800							
T0VZ02	Ribonuclease J	45806500							
T0URS8	DNA repair protein RecN	45804400							
T0W1X2	ATP synthase subunit a	45698500							
T0VZD8	Ribose-phosphate pyrophosphokinase	45338150							
T0UYY6	Uncharacterized protein	45272000							
T0UPS4	XRE family transcriptional regulator	45206000							
T0W5U4	ATP-dependent Clp protease ATP-binding subunit ClpX	44886050							
T0UPX0	Energy-coupling factor transporter ATP-binding protein EcfA	44846935							
T0UPJ8	Pyruvate-flavodoxin oxidoreductase	44730950							
T0VTU6	RNA polymerase sigma factor SigA	44726850							
T0UJ20	Uncharacterized protein (Fragment)	44481500							
T0W2A0	[tail element protein] Uncharacterized protein	44059050							
T0VP60	2-oxoglutarate reductase	44026800							
T0UVK6	Methylenetetrahydrofolate--tRNA-(uracil-5-)-methyltransferase TrmFO	43866900							
T0VWJ1	Ribonuclease J	43653450							
T0UKD7	Universal stress protein UspA	43595400							
T0VZA2	UDP-N-acetylmuramoylalanine--D-glutamate ligase	43554500							
T0UPB6	Probable tRNA sulfurtransferase	43285150							
T0W8E0	Acetate kinase	43212850							

Table S8.3. ***Continued***

T0VWV0	Hydrolase	42989650							
T0VT73	Probable potassium transport system protein kup	42928250							
T0UGP8	UDP-galactopuranose mutase	42857000							
T0UVU9	Heat-inducible transcription repressor HrcA	42637000							
T0ULR8	Dihydroorotate dehydrogenase	42252250							
T0UPW1	Ribosome biogenesis GTPase A	42072650							
T0UKY4	Cyclic-di-AMP phosphodiesterase	41823400							
T0W8F7	HTH_11 domain-containing protein	41275000							
T0WD64	Carboxylate--amine ligase	41129350							
T0UJY6	DNA replication protein	40892050							
T0UHY3	Uncharacterized protein	40840500							
T0UMU6	Glycos_transf_1 domain-containing protein	40144950							
T0UYT2	1,2-diacylglycerol 3-glucosyltransferase	39767100							
T0W078	Cation transporter	39416000							
T0VZI2	FMN-dependent NADH-azoreductase	39284600							
T0VZ56	Uncharacterized protein	38925500							
T0WF88	Endopeptidase La	38576050							
T0UMR0	Dihydroxyacetone kinase	38515000							
T0UGL7	Uncharacterized protein	37893250							
T0UUX1	5-bromo-4-chloroindolyl phosphate hydrolysis protein	37836100							
T0VWX6	N5-carboxyaminoimidazole ribonucleotide synthase	37816800							
T0UVW7	UPF0145 protein LLT1_7225	37722500							
T0VW65	NADH dehydrogenase	36004150							
T0UPA1	LytR family transcriptional regulator	35904800							
T0V5E6	Uncharacterized protein	35721950							
T0UPW8	Peptidoglycan hydrolase	35060000							
T0UCQ3	Glycine/betaine ABC transporter permease	34974000							
T0WFD0	Glucose-6-phosphate 1-dehydrogenase	34969250							
T0UP98	Trigger factor	34848000							
T0VSV9	Bifunctional purine biosynthesis protein PurH	34104500							
T0UKG2	Uncharacterized protein	34055050							
T0UVP2	Pseudouridine synthase	34027800							
T0W2N0	Terminase	33803050							

T0USR6	30S ribosomal protein S16	33650200								
T0VZ39	Uncharacterized protein	33556000								
T0W5R2	Protease	33373950								
T0UID7	Uncharacterized protein	33273500								
T0VWV5	Chromosomal replication initiator protein DnaA	33187050								
T0ULA0	Malonyl CoA-acyl carrier protein transacylase	33179400								
T0VYI4	3-phosphoshikimate 1-carboxyvinyltransferase	33128150								
T0UYL8	50S ribosomal protein L14	33064200								
T0UI46	Isochorismatase	32554050								
T0UPR8	Methionine import ATP-binding protein MetN	32359900								
T0W2W9	UDP-N-acetylglucosamine--N-acetylmuramyl-(pentapeptide) pyrophosphoryl-undecaprenol N-acetylglucosamine transferase	32238050								
T0VRD3	Crossover junction endodeoxyribonuclease RusA	32129000								
T0UQE0	Dihydroorotase	32067650								
T0US48	Peptidoglycan-binding protein LysM	31964850								
T0W2B1	Riboflavin biosynthesis protein	31883650								
T0VY29	Uncharacterized protein	31365950								
T0UMV4	Glycosyl transferase	31351100								
T0W5Z2	Glycine--tRNA ligase beta subunit	30914550								
T0VTZ7	ABC transporter ATP-binding protein	30853450								
T0UGP3	Lipopolysaccharide biosynthesis protein	30701250								
T0UQ32	Probable nicotinate-nucleotide adenylyltransferase	30553700								
T0UKL3	Ribosomal RNA small subunit methyltransferase A	30406600								
T0UZA7	Zinc ABC transporter substrate-binding protein	30332150								
T0UFD1	Hypoxanthine phosphoribosyltransferase	30185950								
T0UYX4	ABC transporter ATP-binding protein	30037500								
T0UPD4	Ribosomal RNA small subunit methyltransferase I	29764750								
T0UNQ7	Dihydroorotate dehydrogenase B (NAD(+)), electron transfer subunit	29722750								
T0UT77	Acyltransferase	29244300								
T0VXZ6	Uncharacterized protein	29046000								
T0UVU7	Uncharacterized protein	29025750								
T0UZE5	RNA methyltransferase	28826000								
T0UVN6	HeH domain-containing protein	28769150								

Table S8.3. ***Continued***

T0UPI7	Diphosphomevalonate decarboxylase	28756750	
T0VZA0	DD-transpeptidase	28753750	
T0VZV2	UDP-N-acetylmuramoyl-tripeptide--D-alanyl-D-alanine ligase	28691300	
T0UUJ2	Pyruvate kinase	28617650	
T0UL57	Serine--tRNA ligase	28508650	
T0W6A3	Serine protease	28177850	
T0US52	Regulator	27538450	
T0UZ56	30S ribosomal protein S19	27496200	
T0UVR2	Pseudouridine synthase	27390000	
T0W2G9	Sortase	27384450	
T0UBU6	Acetate--CoA ligase	27254850	
T0W2B5	Triosephosphate isomerase	26624900	
T0W5U0	Repressor	26574500	
T0UVI5	UPF0176 protein LLT1_10055	26241350	
T0UP24	Polysaccharide deacetylase	26126300	
T0UKM0	Sodium ABC transporter ATP-binding protein	25782300	
T0VZC1	Phosphoribosylformylglycinamidine synthase subunit PurQ	25555000	
T0USB7	Uridine kinase	25477300	
T0VTX5	Probable dual-specificity RNA methyltransferase RlmN	25339450	
T0UP92	Diadenylate cyclase	25317650	
T0UFS7	DeoR family transcriptional regulator	25116150	
T0W676	3-5 exoribonuclease	25017405	
T0W065	Energy-coupling factor transporter ATP-binding protein EcfA	24982650	
T0UQW8;T0W381	[CAAX protease]Uncharacterized protein	24880250	
T0UQ86	Uncharacterized protein	24855900	
T0URX0	DeoR family transcriptional regulator	24734600	
T0W2H6	Oxidoreductase	24709500	
T0VXV3	rRNA methyltransferase	24607650	
T0UTG5	Ribonucleotide reductase	24540900	
T0VWE5	Uncharacterized protein	24521500	
T0UMU9	Uncharacterized protein (Fragment)	24509950	
T0W604	Twitching motility protein pilT	24183750	
T0VW64	Transcription antitermination protein NusB	24134050	

T0VZI7	DD-transpeptidase	24039500							
T0UT30	L-serine dehydratase	23999600							
T0VW76	Amino acid transporter	23926750							
T0VSC8	Oligoribonuclease	23864750							
T0W2Y8	Exodeoxyribonuclease 7 large subunit	23843200							
T0UVX5	Cobalt ABC transporter ATP-binding protein	23787300							
T0UKE3	Uncharacterized protein	23605850							
T0UQ37	S1 RNA-binding protein	23283450							
T0UIY9	GTPase HflX	22935500							
T0URS9	Penicillin-binding protein 2X	22802350							
T0VZ29	Recombinase RarA	22714150							
T0UHU3	Ribosomal RNA small subunit methyltransferase E	22503050							
T0UGG3	Chromosome partitioning protein ParA	22478750							
T0UP15	Phosphate acyltransferase	22442100							
T0W151	Branched-chain amino acid ABC transporter permease	22237400							
T0UVG4	DNA gyrase subunit A	22229450							
T0UR37	Universal stress protein	22180600							
T0W8X2	RmuC family endonuclease	22074550							
T0UPC5	tRNA-binding protein	21901500							
T0UYW3	S4 RNA-binding domain-containing protein	21888500							
T0ULN4	GMP synthase [glutamine-hydrolyzing]	21832250							
T0US54	Alanine--tRNA ligase	21643900							
T0UVV3	Lactose transport regulator	21635100							
T0UQP4	DUF4767 domain-containing protein	21473850							
T0W2I7	NH(3)-dependent NAD(+) synthetase	21433450							
T0W2L5	Phosphate starvation-inducible protein PhoH	21355750							
T0VYR5	Demethylmenaquinone methyltransferase	21264350							
T0UVS1	Nucleotide-binding protein LLT1_7985	21242300							
T0US23	Cell division protein FtsL	21138450							
T0UPD5	RNA methyltransferase	21130500							
T0VW71	Peptide chain release factor 3	21104550							
T0UT74	tRNA-specific 2-thiouridylase MnmA	20928250							
T0UGI3	DNAse	20901600							

Table S8.3. ***Continued***

T0URJ3	Fe-S cluster assembly protein SufB	20825700							
T0UGK9	Nitroreductase	20622650							
T0UKS1	Ribosomal RNA small subunit methyltransferase H	20580500							
T0W1K6	Putative ribose-phosphate pyrophosphokinase	20580150							
T0W5T9	Xanthine phosphoribosyltransferase	20507200							
T0UHU7	1-acyl-sn-glycerol-3-phosphate acyltransferase	20422150							
T0USU7	Bifunctional protein FolD	20366400							
T0W6G4	Hydrolase	20359350							
T0VSW2	Chaperone protein ClpB	20257450							
T0VSL7	Acetyl-CoA carboxytransferase	20077650							
T0W4T8	Orotidine 5-phosphate decarboxylase	20031200							
T0W2P5	Glycosyltransferase	19813100							
T0W1Q1	Macrolide ABC transporter ATP-binding protein	19722300							
T0W338	LuxR family transcriptional regulator	19638250							
T0USY9	Membrane protein	19549215							
T0W4U7	GntR family transcriptional regulator	19471350							
T0VT54	AAA_31 domain-containing protein	19233800							
T0UIG0	3-hydroxyacyl-[acyl-carrier-protein] dehydratase FabZ	19115500							
T0USY0	Haloacid dehalogenase	18963300							
T0UQU5	Methionyl-tRNA formyltransferase	18933800							
T0V5L7	Valine--tRNA ligase	18925400							
T0UVY6	Homoserine dehydrogenase	18669200							
T0UI54	UvrABC system protein B	18506050							
T0UYZ3;T0VR83	Uncharacterized protein	18378850							
T0VT82	Adenine phosphoribosyltransferase	18143175							
T0VS82	Signal peptidase I	18142800							
T0UL94	Haloacid dehalogenase	18051500							
T0UIZ2	Ribosomal silencing factor RsfS	18024500							
T0W1N2	DUF5590 domain-containing protein	17976350							
T0UGM6	Glycosyl transferase family 2	17917350							
T0UII0	Penicillin-binding protein 2B	17866900							
T0VP67	Sua5/YciO/YrdC/YwlC family RNA-binding protein	17818200							
T0UI24	Uncharacterized protein	17789500							

T0VZG3	tRNA pseudouridine synthase A	17611600								
T0VRG0	[DNA topoisomerase] Uncharacterized protein	17500300								
T0UVX9	GTP cyclohydrolase 1	17480250								
T0UQB2	Uncharacterized protein	17473000								
T0VVX9	Uncharacterized protein	17469950								
T0V5G3	Chromosome partitioning protein ParB	17266600								
T0W957	Uncharacterized protein	17266300								
T0UM12	Uncharacterized protein	17258250								
T0UL48	Transcriptional regulator	17240900								
T0VVA4	Ribosomal protein L11 methyltransferase	17172850								
T0UNJ2	TPM_phosphatase domain-containing protein	16959600								
T0UL90	HAD family hydrolase	16903050								
T0ULS1	Membrane protein	16882950								
T0UMX2	RNA-binding protein	16624850								
T0W0B7	Probable transcriptional regulatory protein LLT1_5485	16590700								
T0UJ02	Uracil-DNA glycosylase	16367300								
T0UES9	Uncharacterized protein	16340650								
T0VYC5	Transporter	16211200								
T0W651	DNA repair protein RadA	16132900								
T0US59	Guanine permease	15993550								
T0VZL6	DNA ligase	15908600								
T0URS3	Iron ABC transporter ATP-binding protein	15876400								
T0UQF8	Septum formation initiator	15738400								
T0UW97	Cardiolipin synthase	15594250								
T0W4M9	Virion core protein	15531100								
T0VNY5	Phosphatidylglycerol--prolipoprotein diacylglyceryl transferase	15490000								
T0VLW1	6-phospho-beta-galactosidase	15391000								
T0UFG6	Phosphoribosylamine--glycine ligase	15357550								
T0W160	Dihydroorotate dehydrogenase	15331940								
T0ULX3	Anthranilate phosphoribosyltransferase	15308250								
T0V5B1	Aldehyde-alcohol dehydrogenase	15122750								
T0W2C0	Acyl-ACP thioesterase	15075750								
T0UHH3	Oxidoreductase	15065100								

Table S8.3. ***Continued***

T0UW91;T0UI89;T0W148	Aminoglycoside N(3)-acetyltransferase	15058150							
T0W6B2	DNA-directed DNA polymerase (Fragment)	15057300							
T0W5U3	Uncharacterized protein	15020500							
T0W2U7	Chaperone protein DnaK	14941100							
T0W6F6	Sensor histidine kinase	14830350							
T0UPH5	Thioredoxin	14782860							
T0W074	tRNA N6-adenosine threonylcarbamoyltransferase	14752800							
T0W1R2	Uncharacterized protein	14702950							
T0UUW9	L-lactate dehydrogenase	14660700							
T0UVI4	Nicotinate phosphoribosyltransferase	14580300							
T0V5R1	DNA mismatch repair protein MutL	14577650							
T0W312	SAM-dependent methyltransferase	14576600							
T0USY4	UPF0109 protein LLT1_11195	14511100							
T0W5N9	Potassium transporter KefA	14505500							
T0UZJ6	30S ribosomal protein S6	14442200							
T0W2N3	Aspartate-semialdehyde dehydrogenase	14427300							
T0UHW5	Formate acetyltransferase	14328700							
T0UMS7	Alpha-L-Rha alpha-1,3-L-rhamnosyltransferase	14197150							
T0VZ90	4-hydroxy-tetrahydrodipicolinate reductase	14102950							
T0UG73	Oligopeptidase PepB	14027800							
T0W5Y3	Elongation factor 4	14004200							
T0UTQ4;T0UZQ2;T0UFZ4	Uncharacterized protein	13862500							
T0UQC5	[head protein]Uncharacterized protein	13858750							
T0ULA9	Cell division protein	13733360							
T0VXT2	Aminopeptidase	13687100							
T0VYU8	Hydrolase	13578650							
T0ULB3	CoA-disulfide reductase	13486500							
T0UI77	Uncharacterized protein	13285065							
T0VLT1	Peptide ABC transporter permease	13281650							
T0UKF0	Membrane protein	13240150							
T0VWB0	Lipoprotein	13159050							
T0UW58	6-phosphogluconolactonase	13157350							
T0V032;T0UZH9;T0UHA4	Uncharacterized protein (Fragment)	13122500							

T0UI65	6-phosphogluconate dehydrogenase, decarboxylating	13058900							
T0UKJ4	ArsR family transcriptional regulator	12857850							
T0W1R6	Adapter protein mecA	12854250							
T0VWE3	Primosomal protein DnaI	12778850							
T0W005	Lipoprotein	12773200							
T0VTT1	Rrf2 family transcriptional regulator	12718300							
T0UVC6	Peptidoglycan hydrolase	12538700							
T0W8Z8	DNA polymerase I	12528550							
T0UC47	Phosphomannomutase	12492000							
T0UL74	Phage infection protein	12448850							
T0UFQ7	Methylase	12421650							
T0UYT3	50S ribosomal protein L11	12411650							
T0USS3	Cell division protein DivIB	12372150							
T0VZ88	GDSL family lipase	12309650							
T0UIR9	GTPase	12288050							
T0VSM1	3-oxoacyl-[acyl-carrier-protein] synthase 2	12272300							
T0VTY0	Ferrous iron transport protein B	12224300							
T0W1J5	Uncharacterized protein	12198560							
T0W6D8	DNA gyrase subunit B	12172900							
T0UPC0	Glycine/betaine ABC transporter permease	12165950							
T0UBV1	Uncharacterized protein	12035550							
T0UVA9	Acetolactate synthase	12028200							
T0VZ46	Alpha/beta hydrolase	11859750							
T0W5Q9	Uncharacterized protein	11641600							
T0W8N0	Glucokinase	11541000							
T0UQ40	Peptidase M22	11495900							
T0UUW6	Uncharacterized protein	11495650							
T0VXV5	Uncharacterized protein	11395550							
T0UHG9	Uncharacterized protein	11365950							
T0USG4	Aspartate carbamoyltransferase	11359190							
T0V5F4	ATP-dependent DNA helicase RecG	11255400							
T0UF21	3-oxoacyl-[acyl-carrier-protein] reductase	11202000							
T0W5B0	Membrane protein	11198250							

Table S8.3. ***Continued***

T0VWF5	2-succinyl-5-enolpyruvyl-6-hydroxy-3-cyclohexene-1-carboxylate synthase	11192370							
T0W376	Stress response regulator Gls24	11182700							
T0UKR8	Cell division protein FtsJ	11156050							
T0US64	Phosphoglycerate mutase	11135400							
T0UPU3	GTP pyrophosphokinase	10999050							
T0W2W7	Thioredoxin reductase	10961000							
T0UEG8	Cytochrome D ubiquinol oxidase subunit I	10955950							
T0UFC5	Uncharacterized protein	10931100							
T0W6H3	Stress-responsive transcriptional regulator, PspC family	10930250							
T0WFB5	Ribose-5-phosphate isomerase A	10757250							
T0VWG4	Anaerobic ribonucleoside-triphosphate reductase-activating protein	10693900							
T0W2I0	UDP-N-acetylmuramyl peptide synthase	10691200							
T0U9L4;T0VTG3	RepB family protein (Fragment) T0VTG3; RepB family protein	10658350							
T0UIW6	Alanine acetyltransferase	10607810							
T0UP71	Lipoate--protein ligase	10591850							
T0URJ1	Polyribonucleotide nucleotidyltransferase	10423650							
T0VR80	Pantothenate kinase	10418480							
T0W2W5	S-adenosylmethionine:tRNA ribosyltransferase-isomerase	10381965							
T0UF18	Acetyl-coenzyme A carboxylase carboxyl transferase subunit beta	10332300							
T0VNX4	23S rRNA methyltransferase	10331150							
T0W5N8	S1 RNA-binding protein	10307850							
T0UI90	Mevalonate kinase	10223700							
T0VVE6	Tryptophan--tRNA ligase	10221900							
T0VZU8	Alkyl hydroperoxide reductase C	10196950							
T0UIU9	Uncharacterized protein	10173350							
T0UZI0	Probable membrane transporter protein	10169800							
T0UKV1	Phosphate transport system permease protein	10145250							
T0ULN1	Phosphoribosylglycinamide formyltransferase	10121275							
T0VY24	Uncharacterized protein	10006050							
T0UPV3	Glutamate racemase	10005750							
T0VSN0	Transcription termination/antitermination protein NusA	9998000							
T0UQ50	Multidrug ABC transporter permease	9993800							
T0VYX6	Replication protein	9858650							

T0W1Z8	Phospho-N-acetylmuramoyl-pentapeptide-transferase	9794685							
T0UQA7	SAM-dependent methyltransferase	9775700							
T0UPX3	Lipoprotein	9764490							
T0VWH7	Energy-coupling factor transporter transmembrane protein EcfT	9693750							
T0UJ60	GntR family transcriptional regulator	9651050							
T0UH18	Uncharacterized protein	9620100							
T0VWL2	Peptidase_M22 domain-containing protein	9581250							
T0W909	Phosphatidate cytidylyltransferase	9566500							
T0UIV6	Multidrug ABC transporter ATP-binding protein	9565950							
T0UQH7	Phosphoglycerate mutase	9510300							
T0VVM0	Uncharacterized protein	9454650							

Samples were from two independent experiments. Seven GO categories were selected to be presented here: 1 - membrane (associated) protein, 2 – prophage encoded protein, 3 – translation, 4 – cell division, 5 – lipid biosynthesis, 6 – peptidoglycan biosynthesis, 7 – stress/stimulus response.

References

Alexeeva, S., Guerra Martínez, J. A., Spus, M., and Smid, E. J. (2018). Spontaneously induced prophages are abundant in a naturally evolved bacterial starter culture and deliver competitive advantage to the host. *BMC Microbiol.* 18, 120.

Alexeeva, S., Liu, Y., Zhu, J., Kaczorowska, J., Kouwen, T. R. H. M., Abee, T., et al. (2021). Genomics of tailless bacteriophages in a complex lactic acid bacteria starter culture. *Int. Dairy J.* 114, 104900.

Andreoni, F., Toyofuku, M., Menzi, C., Kalawong, R., Shambat, S. M., François, P., et al. (2019). Antibiotics stimulate formation of vesicles in *Staphylococcus aureus* in both phage-dependent and -independent fashions and via different routes. *Antimicrob. Agents Chemother.* 63, e01439-18.

Batth, T. S., Tollenaere, M. A. X., Rüther, P., Gonzalez-Franquesa, A., Prabhakar, B. S., Bekker-Jensen, S., et al. (2019). Protein aggregation capture on microparticles enables multipurpose proteomics sample preparation. *Mol. Cell. Proteomics* 18, 1027–1035.

Biagini, M., Garibaldi, M., Aprea, S., Pezzicoli, A., Doro, F., Becherelli, M., et al. (2015). The human pathogen *Streptococcus pyogenes* releases lipoproteins as lipoprotein-rich membrane vesicles. *Mol. Cell. Proteomics* 14, 2138–2149.

Bose, S., Aggarwal, S., Singh, D. V., and Acharya, N. (2020). Extracellular vesicles: An emerging platform in Gram-positive bacteria. *Microb. Cell* 7, 312–322.

Briaud, P., and Carroll, R. K. (2020). Extracellular vesicle biogenesis and functions in Gram-positive bacteria. *Infect. Immun.* 88, e00433-20.

Brown, L., Wolf, J. M., Prados-Rosales, R., and Casadevall, A. (2015). Through the wall: extracellular vesicles in Gram-positive bacteria, mycobacteria and fungi. *Nat. Rev. Microbiol.* 13, 620–630.

Bryan, E. M., Bae, T., Kleerebezem, M., and Dunny, G. M. (2000). Improved vectors for nisin-controlled expression in Gram-positive bacteria. *Plasmid* 44, 183–190.

Buist, G., Karsens, H., Nauta, A., van Sinderen, D., Venema, G., and Kok, J. (1997). Autolysis of *Lactococcus lactis* caused by induced overproduction of its major autolysin, AcmA. *Appl. Environ. Microbiol.* 63, 2722–2728.

Cavanagh, D., Fitzgerald, G. F., and McAuliffe, O. (2015). From field to fermentation: the origins of *Lactococcus lactis* and its domestication to the dairy environment. *Food Microbiol.* 47, 45–61.

Chang, A. Y., Chau, V. W., Landas, J. A., and Pang, Y. (2017). Preparation of calcium competent *Escherichia coli* and heat-shock transformation. *JEMI methods* 1, 22–25.

Chattopadhyay, M. K., and Jaganandham, M. V. (2015). Vesicles-mediated resistance to antibiotics in bacteria. *Front. Microbiol.* 6, 758.

Cox, J., Hein, M. Y., Luber, C. A., Paron, I., Nagaraj, N., and Mann, M. (2014). Accurate proteome-wide label-free quantification by delayed normalization and maximal peptide ratio extraction, termed MaxLFQ. *Mol. Cell. Proteomics* 13, 2513–2526.

David, B., Duchêne, M.-C., Haustenne, G. L., Pérez-Núñez, D., Chapot-Chartier, M.-P., De Bolle, X., et al. (2018). PBP2b plays a key role in both peripheral growth and septum positioning in *Lactococcus lactis*. *PLoS One* 13, e0198014.

Domínguez Rubio, A. P., Martínez, J. H., Martínez Casillas, D. C., Coluccio Leskow, F., Piuri, M., and Pérez, O. E. (2017). *Lactobacillus casei* BL23 produces microvesicles carrying proteins that have been associated with its probiotic effect. *Front. Microbiol.* 8, 1783.

Erkus, O., de Jager, V. C. L., Spus, M., van Alen-Boerrigter, I. J., van Rijswijck, I. M. H., Hazelwood, L., et al. (2013). Multifactorial diversity sustains microbial community stability. *ISME J.* 7, 2126–2136.

Filipiak, M., Łoś, J. M., and Łoś, M. (2020). Efficiency of induction of Shiga-toxin lambdoid prophages in *Escherichia coli* due to oxidative and antibiotic stress depends on the combination of prophage and the bacterial strain. *J. Appl. Genet.* 61, 131–140.

Gaudin, M., Krupovic, M., Marguet, E., Gauliard, E., Cvirkaite-Krupovic, V., Le Cam, E., et al. (2014). Extracellular membrane vesicles harbouring viral genomes. *Environ. Microbiol.* 16, 1167–1175.

Gill, S., Catchpole, R., and Forterre, P. (2019). Extracellular membrane vesicles in the three domains of life and beyond. *FEMS Microbiol. Rev.* 43, 273–303.

György, B., Szabó, T. G., Pásztói, M., Pál, Z., Misják, P., Aradi, B., et al. (2011). Membrane vesicles, current state-of-the-art: emerging role of extracellular vesicles. *Cell. Mol. Life Sci.* 68, 2667–2688.

Kim, H., Kim, M., Myoung, K., Kim, W., Ko, J., Kim, K. P., et al. (2020a). Comparative lipidomic analysis of extracellular vesicles derived from *Lactobacillus plantarum* APsulloc 331261 living in green tea leaves using liquid chromatography-mass spectrometry. *Int. J. Mol. Sci.* 21, 8076.

Kim, J. H., Lee, J., Park, J., and Gho, Y. S. (2015). Gram-negative and Gram-positive bacterial extracellular vesicles. *Semin. Cell Dev. Biol.* 40, 97–104.

Kim, S. W., Park, S. Bin, Im, S. P., Lee, J. S., Jung, J. W., Gong, T. W., et al. (2018). Outer membrane vesicles from β-lactam-resistant *Escherichia coli* enable the survival of β-lactam-susceptible *E. coli* in the presence of β-lactam antibiotics. *Sci. Rep.* 8, 5402.

Kim, S. W., Seo, J. S., Park, S. Bin, Lee, A. R., Lee, J. S., Jung, J. W., et al. (2020b). Significant increase in the secretion of extracellular vesicles and antibiotics resistance from methicillin-resistant *Staphylococcus aureus* induced by ampicillin stress. *Sci. Rep.* 10, 21066.

Kim, Y., Edwards, N., and Fenselau, C. (2016). Extracellular vesicle proteomes reflect developmental phases of *Bacillus subtilis*. *Clin. Proteomics* 13, 6.

Klieve, A. V., Yokoyama, M. T., Forster, R. J., Ouwerkerk, D., Bain, P. A., and Mawhinney, E. L. (2005). Naturally occurring DNA transfer system associated with membrane vesicles in cellulolytic *Ruminococcus* spp. of ruminal origin. *Appl. Environ. Microbiol.* 71, 4248–4253.

Lee, E. Y., Choi, D. Y., Kim, D. K., Kim, J. W., Park, J. O., Kim, S., et al. (2009). Gram-positive bacteria produce membrane vesicles: proteomics-based characterization of *Staphylococcus aureus*-derived membrane vesicles. *Proteomics* 9, 5425–5436.

Lee, J., Kim, S. H., Choi, D. S., Lee, J. S., Kim, D. K., Go, G., et al. (2015). Proteomic analysis of extracellular vesicles derived from *Mycobacterium tuberculosis*. *Proteomics* 15, 3331–3337.

Leenhouts, K., Venema, G., and Kok, J. (1998). A lactococcal pWV01-based integration toolbox for bacteria. *Methods Cell Sci.* 20, 35–50.

Li, M., Lee, K., Hsu, M., Nau, G., Mylonakis, E., and Ramratnam, B. (2017). *Lactobacillus*-derived extracellular vesicles enhance host immune responses against vancomycin-resistant enterococci. *BMC Microbiol.* 17, 66.

Liao, S., Klein, M. I., Heim, K. P., Fan, Y., Bitoun, J. P., Ahn, S. J., et al. (2014). *Streptococcus mutans* extracellular DNA is upregulated during growth in biofilms, actively released via membrane vesicles, and influenced by components of the protein secretion machinery. *J. Bacteriol.* 196, 2355–2366.

Liu, Y., Alexeeva, S., Bachmann, H., Guerra Martínez, J.A., Yeremenko, N., Abee, T., and Smid, E.J. (2021a) Chronic release of tailless phage particles from *Lactococcus lactis*. Accepted in *Appl. Environ. Microbiol.*

Liu, Y., Defourny, K. A. Y., Smid, E. J., and Abee, T. (2018). Gram-positive bacterial extracellular vesicles and their impact on health and disease. *Front. Microbiol.* 9, 1502.

Liu, Y., de Groot, A., Boeren, S., Abee, T., and Smid, E.J. (2021b) *Lactococcus lactis* mutants obtained from laboratory evolution showed enhanced vitamin K2 production and resistance to oxidative stress. *Front. Microbiol.* 12:746770.

Liu, Y., Smid, E. J., Abee, T., and Notebaart, R. A. (2019). Delivery of genome editing tools by bacterial extracellular vesicles. *Microb. Biotechnol.* 12, 71–73.

Maguin, E., Duwat, P., Hege, T., Ehrlich, D., and Gruss, A. (1992). New thermosensitive plasmid for Gram-positive bacteria. *J. Bacteriol.* 174, 5633–5638.

Oliveira, J., Mahony, J., Hanemaaijer, L., Kouwen, T. R. H. M., Neve, H., MacSharry, J., et al. (2017). Detecting *Lactococcus lactis* prophages by mitomycin C-mediated induction coupled to flow cytometry analysis. *Front. Microbiol.* 8, 1343.

Pasolli, E., De Filippis, F., Mauriello, I. E., Cumbo, F., Walsh, A. M., Leech, J., et al. (2020). Large-scale genome-wide analysis links lactic acid bacteria from food with the gut microbiome. *Nat. Commun.* 11, 1–12.

Resch, U., Tsatsaronis, J. A., Le Rhun, A., Stübiger, G., Rohde, M., Kasvandik, S., et al. (2016). A two-component regulatory system impacts extracellular membrane-derived vesicle production in group A streptococcus. *MBio* 7, e00207-16.

Rodriguez, B. V., and Kuehn, M. J. (2020). *Staphylococcus aureus* secretes immunomodulatory RNA and DNA via membrane vesicles. *Sci. Rep.* 10, 18293.

Sabnis, A., Ledger, E. V. K., Pader, V., and Edwards, A. M. (2018). Antibiotic interceptors: Creating safe spaces for bacteria. *PLoS Pathog.* 14, e1006924.

Schrempf, H., Koebsch, I., Walter, S., Engelhardt, H., and Meschke, H. (2011). Extracellular *Streptomyces* vesicles: amphorae for survival and defence. *Microb. Biotechnol.* 4, 286–299.

Smid, E. J., Erkus, O., Spus, M., Wolkers-Rooijackers, J. C. M., Alexeeva, S., and Kleerebezem, M. (2014). Functional implications of the microbial community structure of undefined mesophilic starter cultures. *Microb. Cell Fact.* 13, S2.

Toyofuku, M., Cárcamo-Oyarce, G., Yamamoto, T., Eisenstein, F., Hsiao, C. C., Kurosawa, M., et al. (2017). Prophage-triggered membrane vesicle formation through peptidoglycan damage in *Bacillus subtilis*. *Nat. Commun.* 8, 481.

Toyofuku, M., Nomura, N., and Eberl, L. (2018). Types and origins of bacterial membrane vesicles. *Nat. Rev. Microbiol.* 17, 13–24.

Tyanova, S., Temu, T., Sinitcyn, P., Carlson, A., Hein, M. Y., Geiger, T., et al. (2016). The Perseus computational platform for comprehensive analysis of (prote)omics data. *Nat. Methods* 13, 731–740.

Tzipilevich, E., Habusha, M., and Ben-Yehuda, S. (2017). Acquisition of phage sensitivity by bacteria through exchange of phage receptors. *Cell* 168, 186-199.e12.

Visweswaran, G. R. R., Kurek, D., Szeliga, M., Pastrana, F. R., Kuipers, O. P., Kok, J., et al. (2017). Expression of prophage-encoded endolysins contributes to autolysis of *Lactococcus lactis*. *Appl. Microbiol. Biotechnol.* 101, 1099–1110.

Visweswaran, G. R. R., Steen, A., Leenhouts, K., Szeliga, M., Ruban, B., Hesseling-Meinders, A., et al. (2013). AcmD, a homolog of the major autolysin AcmA of *Lactococcus lactis*, binds to the cell wall and contributes to cell separation and autolysis. *PLoS One* 8, e72167.

Wang, X., Thompson, C. D., Weidenmaier, C., and Lee, J. C. (2018). Release of *Staphylococcus aureus* extracellular vesicles and their application as a vaccine platform. *Nat. Commun.* 9, 1379.

Zheng, J., Wittouck, S., Salvetti, E., Franz, C. M. A. P., Harris, H. M. B., Mattarelli, P., et al. (2020). A taxonomic note on the genus *Lactobacillus*: Description of 23 novel genera, emended description of the genus *Lactobacillus* Beijerinck 1901, and union of *Lactobacillaceae* and *Leuconostocaceae*. *Int. J. Syst. Evol. Microbiol.* 70, 2782–2858.

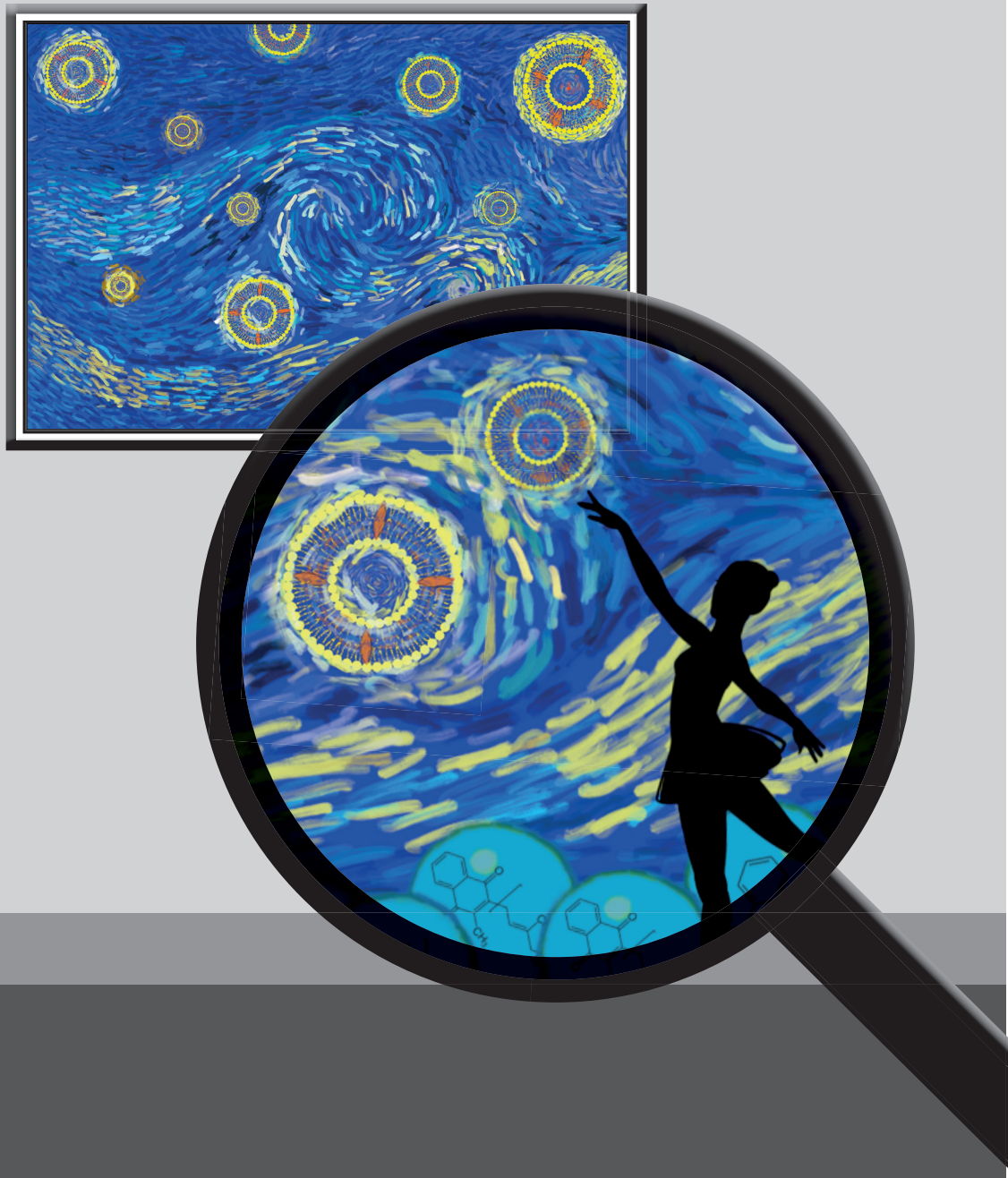

Chapter 9

Lactococcal extracellular membrane vesicles deliver bioactive vitamin K2 to human cells

Yue Liu, Eline van Ophem, Eddy J. Smid & Tjakko Abee

Manuscript in preparation.

Abstract

Vitamin K2 (menaquinone, MK-n) is a lipophilic vitamin located in bacterial cell membranes and essential for human health as a carboxylation co-factor. The long-chain forms of vitamin K2 show a better retention in the serum and have a better bioavailability for target tissues in the human body compared to the short-chain forms. However, the strong lipophilicity of long-chain vitamin K2 forms poses challenges to their uptake by target cells of the human host to achieve desired biological function. In this study, bacterial extracellular membrane vesicles (EVs) produced by *Lactococcus lactis* were shown to carry mainly long-chain vitamin K2 (MK-8 and MK-9). When these EVs were applied to *in vitro* grown osteosarcoma cells, the ratio of carboxylated over non-carboxylated osteocalcin increased, indicating functional delivery of bioactive vitamin K2 by bacterial EVs. The efficiency of vitamin K2 delivery by EVs was higher than adding solvent-dissolved pure compounds at similar concentrations. Therefore, this study provides proof of principle that bacterial EVs are ideal vehicles to deliver lipophilic compounds like vitamin K2 to the human host.

Introduction

Vitamin K is a fat-soluble vitamin that is essential for human health. It functions in the human body as a co-factor for the integral membrane protein γ-glutamyl carboxylase located on the endoplasmic reticulum (ER), that functions in post-translational carboxylation of proteins in which the glutamate (Glu) residues are converted into γ-carboxyglutamate (Gla) – during which redox cycling of vitamin K provides the driving force (Uotila, 1997; Berkner, 2005). The vitamin K-dependent carboxylation is essential for the maturation and the calcium-binding functionality of Gla-proteins, including blood coagulation factors and osteocalcin. The latter protein is produced by osteoblast cells and associated with bone assembly and turnover, matrix Gla protein and Gla-rich protein which are strong tissue/cardiovascular calcification inhibitors, and growth-arrest-specific gene 6 protein (Gas6) (Cranenburg et al., 2007; Schurgers et al., 2013; Willems et al., 2014). The wide range of vitamin K-dependent Gla-proteins highlights the essential role of vitamin K in physiological processes including hemostasis, bone metabolism, cardiovascular mineralization and cell growth regulation (Booth, 2009; Xiao et al., 2021).

Vitamin K2 is also referred to as menaquinones (MK-n), and constitutes a group of compounds that share a naphthoquinone ring but differ in the number of the isoprene side chain units (depicted by n) (Beulens et al., 2013). Vitamin K2 is primarily synthesized by bacteria, with the only exception of MK-4 which is formed in animal tissues by converting vitamin K1 – the counterpart of plant origin (Walther et al., 2013; Halder et al., 2019). In the producing bacteria, menaquinones accumulate in the cytoplasmic membrane and function as electron carriers, forming an essential component of the respiratory electron transport chain (Walther et al., 2013). The side chain length of vitamin K2 is variable and depends on the species of producing bacteria. In addition, the vitamin K form has impact on its delivery to the human host as well as the bioavailability (Schurgers and Vermeer, 2002; Halder et al., 2019). The long-chain vitamin K2 variants, represented by MK-7 to MK-9, were found to have longer half-life in the serum after absorption comparing to the short-chain forms represented by MK-4 or vitamin K1, and therefore the long-chain vitamin K2 variants have greater contribution to vitamin K status and greater bioavailability in the human body (Schurgers and Vermeer, 2002; Beulens et al., 2013). In contrast to vitamin K1 which is retained in the liver after absorption, vitamin K2 is transported to tissues in the whole body by lipoproteins (Schurgers and Vermeer, 2002). In addition, dietary intake of vitamin K2 has been uniquely associated with a reduced risk of coronary heart disease and improved bone health (Geleijnse et al., 2004; Cockayne et al., 2006; Beulens et al., 2009). However, as the side chain length increases, the lipophilicity of vitamin K2 increases, and the difficulty in absorption by the human body increases. This was indeed observed for MK-9, compared to MK-4 and MK-7 (Schurgers and Vermeer, 2002).

Vitamin K2 absorption in the human body is thought to proceed as follows. The lipophilic vitamins mixes with lipids present in the ingested food. Next micelle formation takes place by the action of bile salts, and subsequently, these micelles are taken up by the intestinal epithelium (Meydani and Martin,

2001; Kiela and Ghishan, 2016). Thereafter, vitamin K2 is transported in the blood by lipoproteins to reach target tissues, for instance the osteoblasts (Schurgers and Vermeer, 2002; Simes et al., 2020). The efficiency of vitamin K2 solubilization and absorption depends largely on the (food) matrix it is embedded. Fermented foods are the dietary source of long-chain vitamin K2 (Walther et al., 2013; Halder et al., 2019), where vitamin K2 producing bacteria, e.g. *Lactococcus lactis* (MK-8 and MK-9) (Chapter 3 of this thesis - Liu et al., 2019), *Bacillus subtilis* "natto" (MK-7) (Taber et al., 1981), and propionibacteria (MK-9(4H)) (Hojo et al., 2007), are key players. All these examples of food-grade vitamin K2 producers have a Gram-positive cell wall. Given that vitamin K2 is accumulated in the cell membrane of producing bacteria (Bentley and Meganathan, 1982; Walther et al., 2013), the thick cell wall conceivably acts as a strong physical barrier for the membrane-embedded vitamin K2 to be accessible for the human body. This fact, together with the lipophilicity of vitamin K2 present as long chain variants in fortified foods and food supplements, may result in suboptimal absorption and utilization of vitamin K2.

Some efforts have been made to improve the oral delivery of fat-soluble vitamins like vitamin K2 and many other pharmaceutical compounds using liposomes (Mirafzali et al., 2014; Sercombe et al., 2015; Emami et al., 2016). Advantages in solubility, chemical stability, epithelium permeability and bioavailability have been demonstrated with the liposomes. Liposomes are artificially made, but in nature, similar lipid particles exist, namely extracellular membrane vesicles (EVs or MVs). EVs are produced by organisms found in all domains of life, including Bacteria (Kim et al., 2015; Chapter 2 of this thesis - Liu et al., 2018b; Gill et al., 2019). These nano-sized spheres enclosed by lipid-bilayers have been identified to deliver a wide range of biological molecules, from nucleic acids to proteins, to interact with other microorganisms, the environment, and the host. Depending on the producer and the cargos, bacterial EVs play various roles in host health and disease. Besides natural secretion of EVs by bacteria, artificial generation of EVs is also possible by mechanical fragmentation of cell membranes (García-Manrique et al., 2018; Liu et al., 2018a).

EV secretion has been identified for the vitamin K2 producing *L. lactis* (Chapter 8 of this thesis). As vitamin K2 accumulates in the cell membrane, the lactococcal EVs conceivably contain vitamin K2. We propose that the vitamin K2-containing *L. lactis* EVs can act as a delivery system, similar to the already proposed liposomes, for the human host to absorb and utilize vitamin K2, especially the long-chain forms. In this study, we used *L. lactis* to produce naturally secreted or artificial bacterial EVs, examined the vitamin K2 profile in the vesicles, and demonstrated vitamin K2 delivery to human cells using an *in vitro* model. As osteoblasts are one of the targets where vitamin K2 functions as the carboxylation co-factor, the osteosarcoma MG-63 cell line was used for the *in vitro* model, and the carboxylation status of vitamin K-dependent protein osteocalcin produced by the cell line was used as the marker for vitamin K2 delivery and bioactivity in the host cells.

Materials and methods

Bacterial strains

Lactococcus lactis ssp. *cremoris* strain FM-YL11 was reported to secrete EVs (Chapter 8 of this thesis), and was used to produce EVs in this study. Strain FM-YL11 was cultivated in M17 broth (BD Difco) supplemented with 0.5% (w/v) lactose in 50 mL centrifuge tubes filled with 50 mL medium with closed caps, incubated at 30 °C statically.

L. lactis ssp. *cremoris* strain MG1363 and its mutants were used to produce artificial EVs. As reported previously (Chapter 5 of this thesis), strain MG1363Δ*menF* produces near-zero amounts of vitamin K2 under aerobic condition and strain MG1363Δ*llmg_0196* produces only short-chain vitamin K2. Strain MG1363 and its mutants were cultivated in M17 broth supplemented with 0.5% (w/v) glucose; fifty milliliters of culture medium was filled in 500 mL flasks, incubated at 30 °C, shaking at 180 rpm.

Bacterial EV production and collection

EV production by strain FM-YL11 was induced with mitomycin C for 6 hours exactly as described previously (Chapter 8 of this thesis). Bacterial cells were collected by centrifugation at 6000 x *g* for 20 min. The supernatant was filtered through 0.45 µm filter and then ultra-centrifuged at 160000 x *g* for 1 h. The pellet containing EVs was suspended in phosphate-buffered saline (PBS) and stored at -80 °C until further use.

Overnight cultures of strain MG1363 and its mutants were used for the production of artificial EVs. Bacterial cells from 50 mL culture were collected by centrifugation at 6000 x *g* for 20 min, and washed twice with 50 mL PBS. Then the cells were re-suspended in 20 mL PBS containing 0.5 M sucrose and 1 mg/mL lysozyme (from chicken egg white, Sigma). The cell suspensions were incubated at 37 °C for 1.5 h with gentle mixing at 0.5 h and 1 h, and then centrifuged at 3000 x *g* to collect protoplasts. The pellets were washed twice in 20 mL PBS containing 0.5 M sucrose, and eventually re-suspended in 5 mL PBS. Then the suspensions were sonicated with a sonication probe (Soniprep 150, MSE) for 10 rounds of 30 sec, with 30 sec cooling on ice between the sonication rounds. The cell lysates were centrifuged at 11000 x *g*, and the supernatants were filtered through 0.45 µm filter and then ultra-centrifuged at 160000 x *g* for 1 h, and the pellet containing EVs was suspended in phosphate-buffered saline (PBS) and stored at -80 °C until further use.

EVs were quantified by membrane-specific fluorescent dye FM 4-64 (Invitrogen) as described previously (Chapter 8 of this thesis).

Vitamin K2 extraction and analysis

Vitamin K2 was extracted from bacterial cells exactly as described previously (Chapter 3 of this thesis - Liu et al., 2019) Vitamin K2 was extracted from EVs by mixing the EV suspension with 1x volume iso-propanol and 2x volume hexane, vigorously vortexed, and centrifuged at 3000 x *g* for layer separation.

The hexane layer was collected. Another 2x volume hexane was added to the remaining mix to repeat the extraction, and the hexane layer was combined with the first extract. The hexane was evaporated in a fume hood overnight, and then iso-propanol was added to dissolve vitamin K2.

Iso-propanol dissolved vitamin K2 extracts were diluted in methanol before subjecting to ultra-performance liquid chromatography-mass spectrometry (UPLC-MS) analysis exactly as described previously (Chapter 4 of this thesis).

Transmission electron microscopy

Transmission electron microscopy was applied to examine the morphology and sizes of EVs from *L. lactis*. The procedure was as described previously (Chapter 8 of this thesis).

Cultivation of MG-63 cell line

The human osteosarcoma cell line MG-63 (obtained from European Collection of Authenticated Cell Cultures, ECACC) was routinely maintained in Dulbecco's modified eagle medium (DMEM, Corning) with 4.5 g/L glucose, L-glutamine and pyruvate. DMEM was supplemented with 10% fetal bovine serum (FBS, non-USA origin, Sigma) and 100 U/mL penicillin-streptomycin (Gibco) solution. This medium is referred to as "original medium". Cell cultures were incubated in rectangular canted neck cell culture flasks with vent caps (Corning) placed in a HERAcell 150 CO_2 incubator (Heraeus), at 37 °C with 5% CO_2, 95% air and 95% humidity. For passing, the cells were detached by TrypLE Express (Gibco).

For our vitamin K2 delivery assay, the cell line was first adapted to serum-free medium. Cells at 90%-100% confluency in the original medium were passed onto serum-reduced media in a stepwise manner. The original medium was mixed with 50%, 75%, 90%, 92.5%, 95%, 97.5% and 99% Opti-MEM reduced serum medium (Gibco) at each step of adaptation, with an additional 5 U/mL penicillin-streptomycin to the media in the last two steps. At each step of adaptation, a passage with 1:8 dilution was made when cells reach 90%-100% confluency. At the last step, where 99% Opti-MEM was mixed with the original medium, the FBS concentration was reduced to 0.1%.

Vitamin K2 delivery *in vitro* assay

Vitamin K2 delivery *in vitro* assay was performed in 6-well plates (Greiner CELLSTAR). The 6-well plates were coated by adding 1 mL collagen coating solution (Sigma) to each well, which were then incubated at 37 °C for 30 minutes. Then the collagen solution was removed and the wells were washed one time with 3 mL PBS.

MG-63 cells adapted to Opti-MEM with 0.1% FBS were seeded into the collagen-coated 6-well plates at about 10^6 cells/well. Each well contained 3 mL medium. Cell from passage 24, 26 and 28 were used for the assay. When cells reach 95%-100% confluency in all wells, media was removed from the wells and cells were washed with 2 mL PBS/well. Then 3 mL/well 100% Opti-MEM supplemented with 5 U/mL penicillin-streptomycin (referred to as assay medium) was added to the cells, incubated for 24 hours.

The assay medium was then refreshed (3 mL/well), and vitamin solutions or EV suspensions were added to different wells to initiate the treatment. After 48 h treatment, the supernatant from each well was collected, centrifuged at 10000 x *g* for 5 min to remove insoluble particles. The supernatants were stored at -20 °C until further analysis.

Vitamin D_3 (1α,25-dihydroxyvitamin D_3, Sigma) was added to induce osteocalcin production at a concentration of 20 nM. Vitamin K2 variants MK-4 (sigma) and MK-9 (Santa Cruz Biotechnology) were added at 0.1 nM, 1 nM and 5 nM. Both vitamin D_3 and vitamin K2 were dissolved in pure ethanol. After adding the vitamin solutions, the ethanol content in each well was 6 µL in total. In controls where no vitamin D_3 or vitamin K2 was not added, pure ethanol was added to each well to 6 µL.

Vitamin K2 concentrations of all EV suspensions were made equal based on membrane-dye quantifications. Vitamin K2 quantity in each EV suspension was measured. To achieve desired vitamin K2 concentrations, 10 µL - 100 µL EV suspensions were applied to each well. EVs made from strain MG1363Δ*menF* were used as the vitamin K2-negative control, and 100 µL/well of these was applied.

Cell culture supernatants were exposed to ELISA assays to examine the quantity and carboxylation status of osteocalcin. Two ELISA kits (MK111 and MK118, Takara) were used to quantify carboxylated (Gla-OC) and undercarboxylated (Glu-OC) osteocalcin according to the manufacture's instruction. Where applicable, the culture supernatant was concentrated with 3K centrifugal ultrafilters (Amicon, Merck).

Data analysis

Calculation of vitamin K2 content was performed as described previously (Chapter 4 of this thesis). Calculations of Gla-OC and Glu-OC quantities were performed according to instructions from manufactures of ELISA kits (MK111 and MK118, Takara). Box plots were made in Excel for Microsoft 365, with option "inclusive median" for quartile calculation.

To compare the effect of vitamin K2 delivery with negative controls, statistical significance analysis was performed in IBM SPSS Statistics (version 25) using one-way analysis of variance (ANOVA). Passage number of the cell line was set as a random factor. Homogeneity of variance was examined using Levene's test ($\alpha = 0.05$). The post hoc multiple comparisons were conducted using Dunnett test (> control, $^*p \leq 0.05$). To compare the carboxylation effect of solvent-dissolved and EV-delivered vitamin K2, t-tests were performed (paired, one-tailed, $^*p \leq 0.05$).

Results

EVs produced by *Lactococcus lactis* contain vitamin K2

We collected lactococcal EVs in two manners: from *L. lactis* ssp. *cremoris* strain FM-YL11, the EVs were naturally secreted by the cells by the action of prophage-encoded holin-lysin system (Chapter 8 of this thesis); from *L. lactis* ssp. *cremoris* strain MG1363 and derived mutants Δ*llmg_0196* and Δ*menF*, EVs were artificially produced by fragmenting the cell membranes. Transmission electron microscopy confirmed that the EVs produced by the two methods all showed typical EV morphology with diameters of 50-300 nm (supplementary Fig. S9.1).

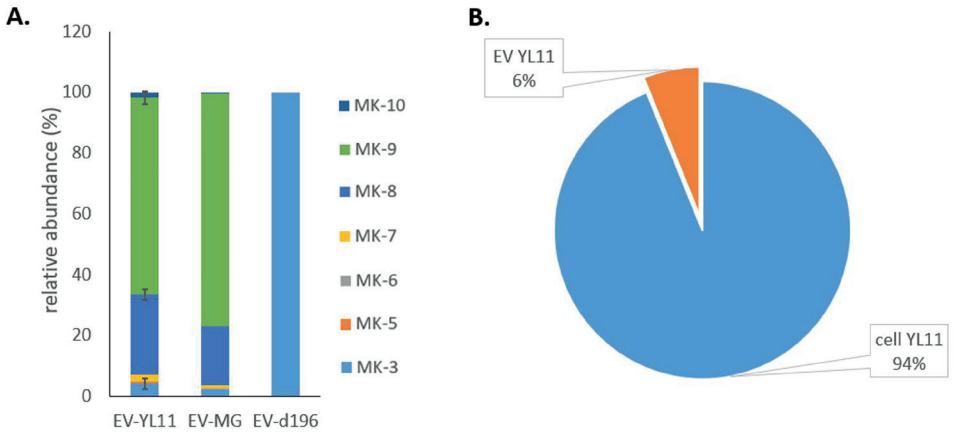

Figure 9.1. Vitamin K2 in *L. lactis* EVs. A) Vitamin K2 profile in *L. lactis* EVs. EV-YL11 are EVs secreted by strain FM-YL11; EV-MG are EVs artificially generated from strain MG1363; EV-d196 are EVs artificially generated from strain MG1363Δ*llmg_0196*. B) Percentage of vitamin K2 present in naturally secreted lactococcal EVs and in bacterial cells from the culture of strain FM-YL11. Data from three independent experiments for strain YL11 cells and EVs, error bars represent standard deviations.

We examined the vitamin K2 presence and profile in both the cells and EVs. We found that vitamin K2 was present in the EVs with a similar profile as the producing bacteria: EVs from strain FM-YL11 and MG1363 contained MK-8 and MK-9 as the major forms, which amounted up to 80 - 90% of all the forms, followed by minor amounts of other forms including MK-3, MK-7, MK-10, MK-5 and MK-6 (Fig. 9.1A). EVs from MG1363Δ*llmg_0196* (a mutant that produces MK-3 as the only form) only contained MK-3; from MG1363Δ*menF* (a mutant that produces near zero level of MKs), trace amount of MK-9 was measured just above the detection limit, of which the concentration was 200 times lower than in MG1363 EVs. From the naturally produced EVs, the vitamin K2 amount was found to be 6% of the total vitamin K2 recovered from the whole bacterial culture of strain FM-YL11 (102 ± 22 nmol/L). This amount in EVs is considerable, but also highlights the need for an artificial EV producing system to allow use of the whole-cell biomass containing majority of the vitamin K2.

All EVs described here with known vitamin K2 profiles were applied to test the delivery of vitamin K2 in the osteosarcoma cell line *in vitro* assay: EVs from strain FM-YL11 and MG1363 were applied to demonstrate delivery of (mainly) long-chain forms MK-8 and MK-9; MG1363Δ*llmg_0196* EVs were used to demonstrate delivery of short-chain form MK-3; MG1363Δ*menF* EVs were used as negative controls.

Lactococcal EVs delivered bioactive vitamin K2 to human osteosarcoma cell line MG-63

We applied solvent-dissolved pure vitamin K2 as well as vitamin K2 containing EVs to the osteosarcoma cell line MG-63, and then measured the quantity (Supplementary Fig. S9.2) and carboxylation status (Fig. 9.2) of osteocalcin (OC) produced by the cell line. The carboxylation status, indicated as the ratio of Gla-OC/Glu-OC, was mainly used as the marker for vitamin K2 delivery and bioactivity.

To induce OC production, vitamin D_3 was added to all test conditions except for the negative control of OC production ("no vitamin"), where no vitamin D_3 nor K2 was given to the cells. Indeed, from this control, OC was hardly detected (Supplementary Fig. S9.2). A negative control for vitamin K2 effect was included, where vitamin D_3 but not vitamin K2 was applied ("no VK"). Detectable OC was found in this control, but with an extremely low ratio of Gla-OC to Glu/OC (Fig. 9.2A), indicating negative carboxylation. This negative control was used to distinguish the delivery of vitamin K2 where the solvent-dissolved compounds were applied to cells. We used pure MK-4 and MK-9 as the representative for short-chain and long-chain vitamin K2, respectively, at concentrations 0.1 nM, 1 nM and 5 nM. All conditions, except for MK-9 at 0.1 nM, showed a positive effect of vitamin K2 delivery, demonstrated by significantly higher Gla-OC/Glu-OC ratios comparing to the negative control. The delivery of MK-9 was less than MK-4 when applied at the same concentration, but the carboxylation effect improved as the concentrations increased to 5 nM. For MK-4, the effect appeared to be already saturated at 1 nM.

Significant effects of vitamin K2 delivery on carboxylation status were observed for EVs containing mainly long-chain MK-8 and MK-9 (EV-YL11, EV-MG) and short-chain MK-3 (EV-d196) in all tested concentrations, in comparison to the negative control (EV-NC) (Fig. 9.2B). When solvent-dissolved MKs were added to the negative control sample, effect of MK-4 but not MK-9 was observed.

Noticeably, when long-chain vitamin K2 was delivered by EVs, the carboxylation effects were often more obvious, comparing to solvent-dissolved vitamin K2 added at the same concentration: EV-MG or EV-YL11 containing 0.1 nM and 1 nM long-chain MK-8 and MK-9, showed significantly higher Gla-OC/Glu-OC ratio than pure MK-9 given at the same concentrations (Fig. 9.2C).

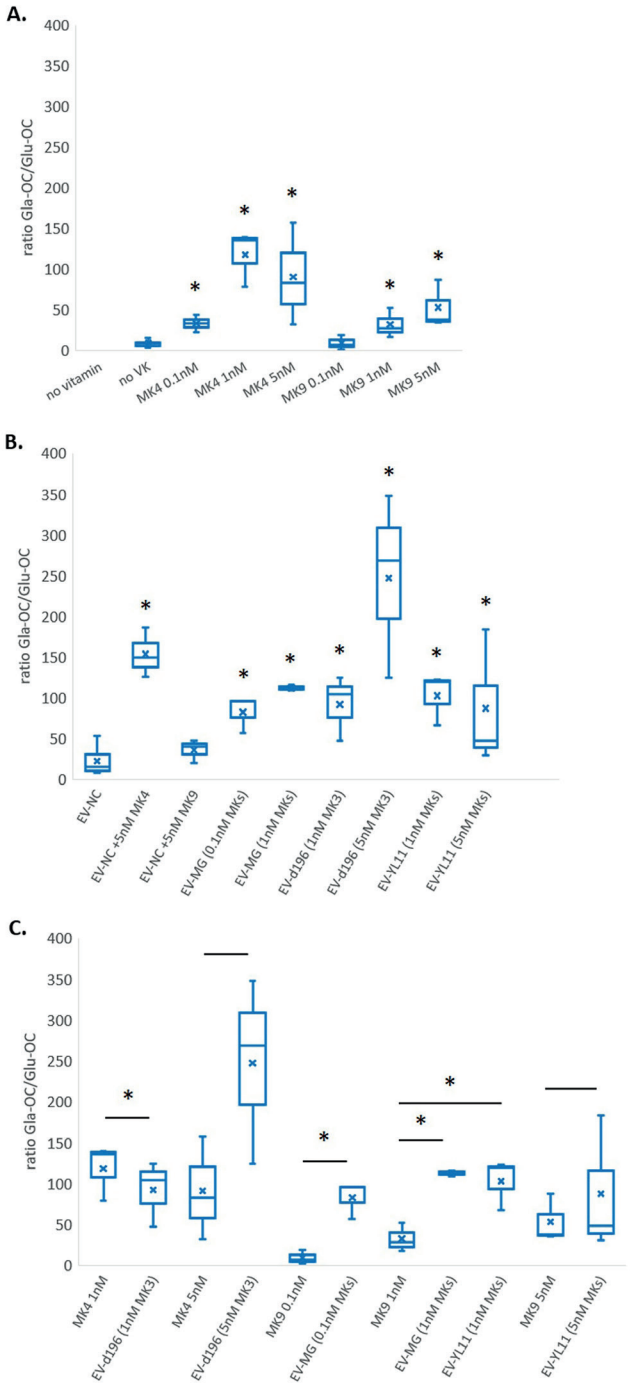

Figure 9.2. Carboxylation status of osteocalcin produced in cell line MG-63 . A) Carboxylation status of OC indicated by the ratio of Gla-OC/Glu-OC when solvent-dissolved pure vitamin K2 were applied to cells. In the "no vitamin" control, neither vitamin D_3 nor vitamin K2 was added. For all other conditions, 20 nM vitamin D_3 was

added to induce OC production. In the "no VK" control, no vitamin K2 was added; this was the control for the effect of adding solvent-dissolved pure vitamin K2 (MK-4 and MK-9) in various concentrations (Dunnett test, one-sided, *p ≤ 0.05). B) Carboxylation status of OC when EVs containing vitamin K2 were applied to cells. For all conditions, 20 nM vitamin D_3 was added to induce OC production. MK (main) forms and quantity carried by EVs are indicated in brackets. In the "EV-NC" sample, EVs made from MG1363Δ*menF* was added, and was used as the vitamin K2-negative control for the other conditions with EV treatment (Dunnett test, one-sided, *p≤0.05). In "EV-MG", "EV-d196" and "EV-YL11", EVs from strains MG1363,MG1363Δ*llmg_0196* and FM-YL12 were added respectively. C) Carboxylation status of OC when comparing solvent-dissolved and EV-carried vitamin K2 at the same concentrations (paired t-test, one-tail, *p≤0.05). Data were from three independent experiments.

Discussion

Vitamin K2 is valuable for various aspects of human health. The long-chain vitamin K2 forms increase in lipophilicity, resulting in less efficient absorption by the human host after oral intake. However, the long-chain vitamin K2 forms are also found to have longer half-life once in the blood circulation and therefore more available to be utilized by the target tissue (Schurgers and Vermeer, 2002). Moreover, intake of long-chain vitamin K2 is associated with additional health benefits that are not associated with the short-chain forms (Halder et al., 2019). These features highlight the importance of improving vitamin K2 delivery to the host, especially for the long-chain forms.

As vitamin K2 is accumulated in the membrane of various food-grade bacteria, the nano sized EVs produced by these bacteria potentially serve as ideal vehicles for (long-chain) vitamin K2 delivery. Using *L. lactis* as an example, in this study we demonstrated first that vitamin K2 is indeed carried by the EVs secreted by bacterial cells. We also demonstrated a convenient approach to generate artificial EVs composed of vitamin K2-containing membranes derived from *L. lactis* cells (Fig. 9.3).

To the best of our knowledge, this is also the first report demonstrating functional delivery of bioactive vitamin K2 to host cells using bacterial EVs. Not only did we observe that lactococcal EVs carrying vitamin K2 lead to improved carboxylation status of OC *in vitro* in a dose-dependent manner, most intriguingly, it was demonstrated that the carboxylation was more efficient when the same concentration of vitamin K2 was delivered in EVs comparing to the solvent-dissolved form, possibly due to improved uptake of EV-carried vitamin K2 by the cells.

Existing evidence on the interaction between EVs and mammalian cells support that bacterial EVs can be taken up by the host cells via endocytosis and membrane fusion (Kesty et al., 2004; Nagakubo et al., 2020), and the same mechanism could be used by osteosarcoma cells to take up lactococcal EVs. Thereafter, vitamin K2 carried by lactococcal EVs can be brought to the γ-glutamyl carboxylase located on the ER membrane via the membrane vesicle trafficking processes in the cells (Howell et al., 2006), where the communication and material exchange between the cell membrane and organelles like ER, are realized. Then, vitamin K2 is able to perform the co-factor function on the γ-glutamyl carboxylase and initiate the carboxylation process, enabling the transformation of Glu-OC into mature, functional Gla-OC (Fig. 9.3).

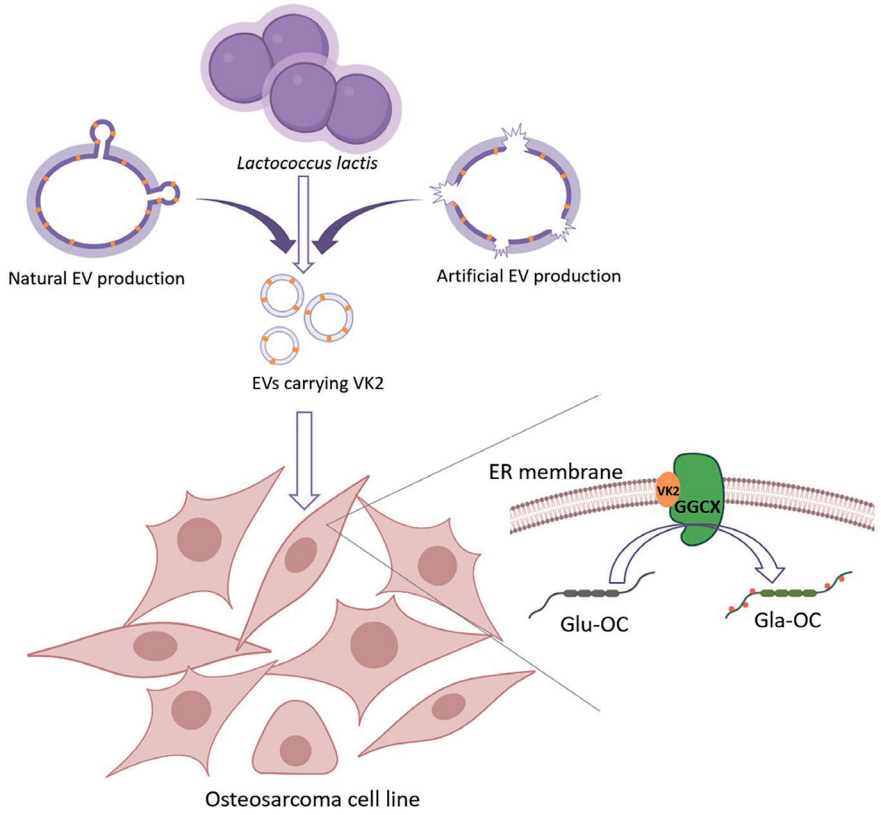

Figure 9.3. Concept scheme of lactococcal membrane vesicles delivering vitamin K2 to the human osteosarcoma cell line. In this study, EVs were naturally secreted or artificially made from *Lactococcus lactis* cells, and were shown to carry vitamin K2 with similar profile as the producing bacteria. When the vitamin K2-containing EVs were administered to MG-63 osteosarcoma cells, the changes in carboxylation status of osteocalcin protein produced by the cell line indicated functional delivery of bioactive vitamin K2 by bacterial EVs. Vitamin K2 is represented by the orange ovals, bacterial cell membrane as dark purple line and cell wall as light purple line. Note that bacterial cells, EVs and osteosarcoma cells are not drawn at the same scale. VK2, vitamin K2; GGCX, γ-glutamyl carboxylase; ER, endoplasmic reticulum. This figure was created with BioRender.com.

Although this study shows direct delivery of vitamin K2 by EVs to the cells from the target tissue *in vitro*, we can only speculate about the *in vivo* digestion and transportation of vitamin K2-loaded EVs following oral ingestion. It has been suggested that liposome digestion follows the conventional lipid digestion route where the liposomes are solubilized by bile salts and pancreatic enzymes, components absorbed by the intestinal cells as micelles and carried to the whole body by lipoproteins to reach the target tissues (Liu et al., 2020). The same route can indeed be expected to be followed by EVs. Most interestingly, an alternative route has been shown for bacterial EVs, where they pass through the intestinal barrier and enter the bloodstream directly, and interact with host cells in their native forms (Stentz et al., 2018; Haas-Neill and Forsythe, 2020). In this alternative route, a similar interaction between EVs and host cells can be expected as demonstrated in the *in vitro* assay.

In conclusion, this study provides evidence that bacterial EVs are ideal vehicles to deliver lipophilic vitamin K2 to human cells. Not only does this finding contribute to the fundamental understanding of bacteria-host interaction via EVs, but also to applications for improved human nutrition and conceivable health benefits. Bacterial EVs are currently receiving increased attention as their roles in human health and disease are gradually revealed. Finally, the application of bacterial EVs as delivery systems can be extended to other nutritional/pharmaceutical compounds, such as probiotic factors, antimicrobial compounds, and vaccines.

Acknowledgements

The authors would also to thank Mark Sanders (Food Chemistry, Wageningen University) for his assistance in vitamin K2 analysis. The electron microscopy images were obtained with the help of Jelmer Vroom at the Wageningen Electron Microscopy Centre (WEMC) of Wageningen University.

The work was subsidized by the Netherlands Organization for Scientific Research (NWO) through the Graduate Program on Food Structure, Digestion and Health.

Supplementary materials

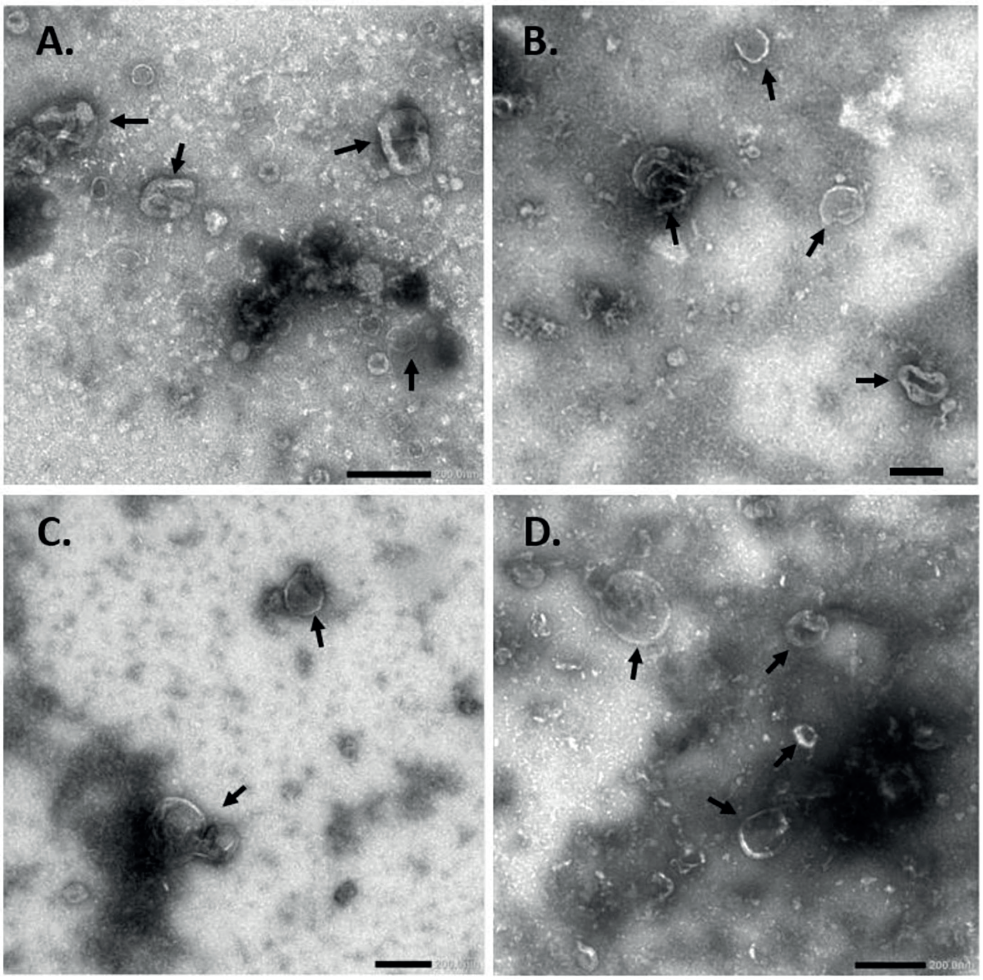

Figure S9.1. Transmission electron microscopic pictures of EVs. A) Naturally secreted EVs (induced by prophage-encoded holin-lysin system) from *L. lactis* FM-YL11. B) Artificial EVs made from *L. lactis* MG1363. C) Artificial EVs made from MG1363Δ*llmg_0196*. D) Artificial EVs made from MG1363Δ*menF*. Structures with typical EV morphology are indicated with black arrows. Scale bars are 200 nm.

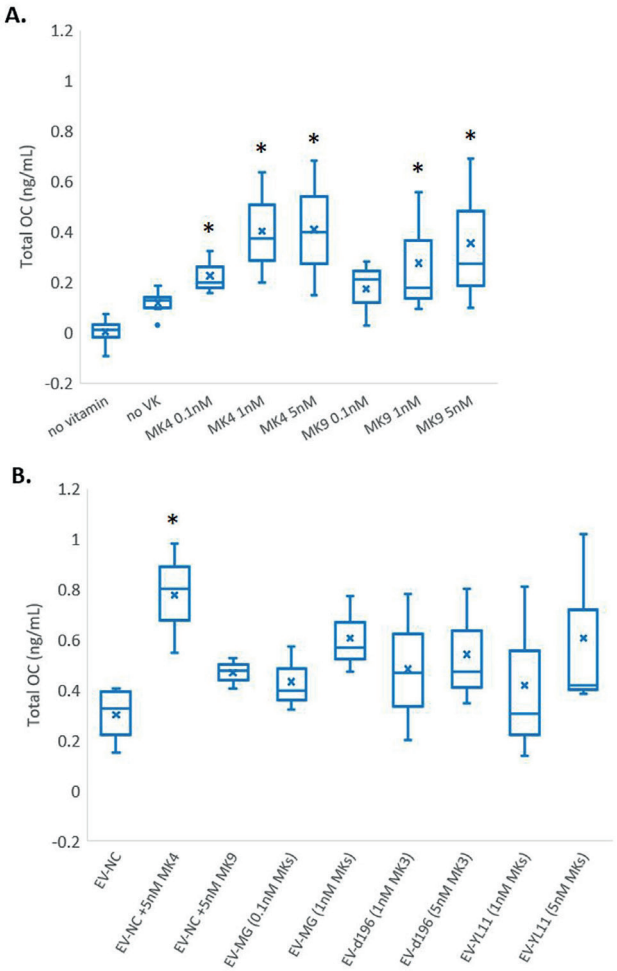

Figure S9.2. Quantity of osteocalcin produced in cell line MG-63 . A) Total OC concentration calculated by adding Glu-OC and Glu-OC concentrations, when solvent-dissolved pure vitamin K2 were applied to cells. In the "no vitamin" control, neither vitamin D_3 nor vitamin K2 was added. For all other conditions, 20 nM vitamin D_3 was added to induce OC production. In the "no VK" control, no vitamin K2 was added; this was the control for the effect of adding solvent-dissolved pure vitamin K2 (MK-4 and MK-9) in various concentrations (Dunnett test, one-sided, *$p \leq 0.05$). B) Total OC concentration OC when EVs containing vitamin K2 were applied to cells. For all conditions, 20 nM vitamin D_3 was added to induce OC production. MK (main) forms and quantity carried by EVs are indicated in brackets. In the "EV-NC" sample, EVs made from MG1363Δ*menF* was added, and was used as the vitamin K2-negative control for the other conditions with EV treatment (Dunnett test, one-sided, *$p \leq 0.05$). In "EV-MG", "EV-d196" and "EV-YL11", EVs from strains MG1363,MG1363Δ*llmg_0196* and FM-YL12 were added respectively.

References

Bentley, R., and Meganathan, R. (1982). Biosynthesis of vitamin K (menaquinone) in bacteria. *Microbiol. Rev.* 46, 241–280.

Berkner, K. L. (2005). The vitamin K-dependent carboxylase. *Annu. Rev. Nutr.* 25, 127–149.

Beulens, J. W. J., Booth, S. L., van den Heuvel, E. G. H. M., Stoecklin, E., Baka, A., and Vermeer, C. (2013). The role of menaquinones (vitamin K2) in human health. *Br. J. Nutr.* 110, 1357–1368.

Beulens, J. W. J., Bots, M. L., Atsma, F., Bartelink, M.-L. EL, Prokop, M., Geleijnse, J. M., et al. (2009). High dietary menaquinone intake is associated with reduced coronary calcification. *Atherosclerosis* 203, 489–93.

Booth, S. L. (2009). Roles for vitamin K beyond coagulation. *Annu. Rev. Nutr.* 29, 89–110.

Cockayne, S., Adamson, J., Lanham-New, S., Shearer, M. J., Gilbody, S., and Torgerson, D. J. (2006). Vitamin K and the prevention of fractures: systematic review and meta-analysis of randomized controlled trials. *Arch. Intern. Med.* 166, 1256–61.

Cranenburg, E. C. M., Schurgers, L. J., and Vermeer, C. (2007). Vitamin K: the coagulation vitamin that became omnipotent. *Thromb. Haemost.* 98, 120–125.

Emami, S., Azadmard-Damirchi, S., Peighambardoust, S. H., Valizadeh, H., and Hesari, J. (2016). Liposomes as carrier vehicles for functional compounds in food sector. *J. Exp. Nanosci.* 11, 737–759.

García-Manrique, P., Matos, M., Gutiérrez, G., Pazos, C., and Blanco-López, M. C. (2018). Therapeutic biomaterials based on extracellular vesicles: classification of bio-engineering and mimetic preparation routes. *J. Extracell. Vesicles* 7, 1422676.

Geleijnse, J. M., Vermeer, C., Grobbee, D. E., Schurgers, L. J., Knapen, M. H. J., van Der Meer, I. M., et al. (2004). Dietary intake of menaquinone is associated with a reduced risk of coronary heart disease: the Rotterdam Study. *J. Nutr.* 134, 3100–3105.

Gill, S., Catchpole, R., and Forterre, P. (2019). Extracellular membrane vesicles in the three domains of life and beyond. *FEMS Microbiol. Rev.* 43, 273–303.

Haas-Neill, S., and Forsythe, P. (2020). A budding relationship: bacterial extracellular vesicles in the microbiota–gut–brain axis. *Int. J. Mol. Sci.* 21, 8899.

Halder, M., Petsophonsakul, P., Akbulut, A. C., Pavlic, A., Bohan, F., Anderson, E., et al. (2019). Vitamin K: Double bonds beyond coagulation insights into differences between vitamin K1 and K2 in health and disease. *Int. J. Mol. Sci.* 20, 896.

Hojo, K., Watanabe, R., Mori, T., and Taketomo, N. (2007). Quantitative measurement of tetrahydromenaquinone-9 in cheese fermented by propionibacteria. *J. Dairy Sci.* 90, 4078–4083.

Howell, G. J., Holloway, Z. G., Cobbold, C., Monaco, A. P., and Ponnambalam, S. (2006). Cell biology of membrane trafficking in human disease. *Int. Rev. Cytol.* 252, 1–69.

Kesty, N. C., Mason, K. M., Reedy, M., Miller, S. E., and Kuehn, M. J. (2004). Enterotoxigenic Escherichia coli vesicles target toxin delivery into mammalian cells. *EMBO J.* 23, 4538–4549.

Kiela, P. R., and Ghishan, F. K. (2016). Physiology of intestinal absorption and secretion. *Best Pract. Res. Clin. Gastroenterol.* 30, 145–159.

Kim, J. H., Lee, J., Park, J., and Gho, Y. S. (2015). Gram-negative and Gram-positive bacterial extracellular vesicles. *Semin. Cell Dev. Biol.* 40, 97–104.

Liu, W., Hou, Y., Jin, Y., Wang, Y., Xu, X., and Han, J. (2020). Research progress on liposomes: Application in food, digestion behavior and absorption mechanism. *Trends Food Sci. Technol.* 104, 177–189.

Liu, Y., Alexeeva, S., Defourny, K. A., Smid, E. J., and Abee, T. (2018a). Tiny but mighty: bacterial membrane vesicles in food biotechnological applications. *Curr. Opin. Biotechnol.* 49, 179–184.

Liu, Y., Defourny, K. A. Y., Smid, E. J., and Abee, T. (2018b). Gram-positive bacterial extracellular vesicles and their impact on health and disease. *Front. Microbiol.* 9, 1502.

Liu, Y., van Bennekom, E. O., Zhang, Y., Abee, T., and Smid, E. J. (2019). Long-chain vitamin K2 production in *Lactococcus lactis* is influenced by temperature, carbon source, aeration and mode of energy metabolism. *Microb. Cell Fact.* 18, 129.

Meydani, M., and Martin, K. R. (2001). "Intestinal absorption of fat-soluble vitamins," in *Intestinal Lipid Metabolism*, eds. C. M. Mansbach, P. Tso, and A. Kuksis (Boston, MA: Springer), 367–368.

Mirafzali, Z., Thompson, C. S., and Tallua, K. (2014). "Application of liposomes in the food industry," in *Microencapsulation in the Food Industry*, eds. A. G. Gaonkar, N. Vasisht, A. R. Khare, and R. Sobel (Elsevier), 139–150.

Nagakubo, T., Nomura, N., and Toyofuku, M. (2020). Cracking Open Bacterial Membrane Vesicles. *Front. Microbiol.* 10, 3026.

Schurgers, L. J., Uitto, J., and Reutelingsperger, C. P. (2013). Vitamin K-dependent carboxylation of matrix Gla-protein: a crucial switch to control ectopic mineralization. *Trends Mol. Med.* 19, 217–226.

Schurgers, L. J., and Vermeer, C. (2002). Differential lipoprotein transport pathways of K-vitamins in healthy subjects. *Biochim. Biophys. Acta* 1570, 27–32.

Sercombe, L., Veerati, T., Moheimani, F., Wu, S. Y., Sood, A. K., and Hua, S. (2015). Advances and challenges of liposome assisted drug delivery. *Front. Pharmacol.* 6, 286.

Simes, D. C., Viegas, C. S. B., Araújo, N., and Marreiros, C. (2020). Vitamin K as a diet supplement with impact in human health: current evidence in age-related diseases. *Nutrients* 12, 138.

Stentz, R., Carvalho, A. L., Jones, E. J., and Carding, S. R. (2018). Fantastic voyage: the journey of intestinal microbiota-derived microvesicles through the body. *Biochem. Soc. Trans.* 46, 1021–1027.

Taber, H. W., Dellers, E. A., and Lombardo, L. R. (1981). Menaquinone biosynthesis in *Bacillus subtilis*: isolation of men mutants and evidence for clustering of men genes. *J. Bacteriol.* 145, 321–327.

Uotila, L. (1997). "Vitamin K: Metabolic functions, mechanism of action, and human requirements," in *Principles of Medical Biology, Volume 8, Molecular and Cellular Pharmacology*, eds. E. E. Bittar and N. Bittar (Elsevier), 965–984.

Walther, B., Karl, J. P., Booth, S. L., and Boyaval, P. (2013). Menaquinones, bacteria, and the food supply: the relevance of dairy and fermented food products to vitamin K requirements. *Adv. Nutr.* 4, 463–73.

Willems, B. A. G., Vermeer, C., Reutelingsperger, C. P. M., and Schurgers, L. J. (2014). The realm of vitamin K dependent proteins: Shifting from coagulation toward calcification. *Mol. Nutr. Food Res.* 58, 1620–1635.

Xiao, H., Chen, J., Duan, L., and Li, S. (2021). Role of emerging vitamin K-dependent proteins: Growth arrest-specific protein 6, Gla-rich protein and periostin (Review). *Int. J. Mol. Med.* 47, 2.

Chapter 10

General discussion

Yue Liu

The fat-soluble vitamin K is essential for human health for its function as a co-factor for maturation of proteins that play important roles in hemostasis, calcium and bone metabolism, as well as cell growth regulation (Cranenburg et al., 2007; Schurgers et al., 2013; Willems et al., 2014). Among the different forms of vitamin K, long-chain vitamin K2 (menaquinone, MK-n) demonstrated higher bioavailability and efficacy in the human body (Schurgers and Vermeer, 2000; Schurgers et al., 2007). Additionally, dietary intake of long-chain forms of vitamin K2 has been associated with reduced risk of coronary heart disease (Geleijnse et al., 2004; Gast et al., 2009). Therefore, vitamin K2 enrichment in the diet is of high interest for human health. As long-chain vitamin K2 (MK-5 to MK-10) is exclusively produced by bacteria, vitamin K2 producing bacteria that are commonly used in food fermentations provide unique opportunities for dietary vitamin K2 enrichment. *Lactococcus lactis* has a long history of safe use in fermented foods including multiple types of cheeses, buttermilk and sour cream, and produce vitamin K2 mainly in the forms of MK-9 and MK-8 (Walther et al., 2013; Chollet et al., 2017). Knowledge on the influence of cultivation conditions, biosynthesis pathway and physiological mechanism of vitamin K2 production in *L. lactis* is important for improved vitamin K2 content in diet.

While it is of interest to improve the content of vitamin K2 in fermentation workhorses like *L. lactis* and eventually in the diet, the actual efficiency for delivering this vitamin to the human body is important as well. Vitamin K2 may not be readily and thoroughly absorbed by the human body due to the lipophilicity, especially for the long-chain forms like MK-9 (Schurgers and Vermeer, 2002). The thick cell wall of Gram-positive bacteria like *L. lactis* could add an additional barrier for accessing vitamin K2, which is accumulated in the bacterial cell membrane. Efforts to improve the delivery of bacterial membrane-bound vitamin K2 into the human host are desired, yet not made previously.

Opportunities for bacterial membrane-bound vitamin K2 delivery are expected with extracellular membrane vesicles (EVs or MVs), which are produced by organisms found in all three phylogenetic domains of life, including Bacteria, both Gram-positive and Gram-negative (Kim et al., 2015; Toyofuku et al., 2019). These vesicles are derived from the cell membrane, forming membrane-enclosed spheres carrying various types of cargos in the lumen and the membrane (DNA, RNA, proteins, metabolites, etc.) supporting exchange between cells (Nagakubo et al., 2020). Since vitamin K2 is present in the bacterial cell membrane, EVs are potentially ideal vehicles for efficient delivery of this vitamin to the human host with a similar principle as liposomes, which improves the solubility and absorption of fat-soluble compounds (Simão et al., 2015; Emami et al., 2016; Yang et al., 2016).

In this study, the possibility of improving vitamin K2 content, as well as the physiological roles of MKs in *L. lactis* were investigated (Part I, Chapter 3 - 5). In parallel, the production of EVs in relation to prophage activity in *L. lactis* was examined (Part II, Chapter 6 - 8). Finally, the first two research themes join into the ultimate goal of this study: the delivery of vitamin K2 by *L. lactis* EVs to human cells (Part III, Chapter 9). In the current chapter, each part of this research will be discussed from phenotypical observations to mechanistic insights, from current findings to future perspectives.

Improved vitamin K2 content in *L. lactis*: *how* and *why*

Possibilities to improve vitamin K2 content in *L. lactis* were explored by means of optimizing cultivation conditions (Chapter 3) and laboratory evolution (Chapter 4), resolving the ***how*** question. As for ***why*** some of the strategies could successfully enhance the vitamin K2 content, attempts to understand the mechanisms behind the changes of vitamin K2 content in *L. lactis* were also made by characterizing evolved strains (Chapter 4) and mutants (Chapter 5) with altered MK content and profiles.

How – optimization of cultivation conditions, strain screening and improvement

Within the limited set of *L. lactis* strains tested, up to 10-fold differences in vitamin K2 titers were already observed (Chapter 3). All tested parameters of the cultivation conditions, namely temperature, carbon source, aeration and mode of metabolism, were shown to solely and in synergism affect the vitamin K2 specific concentration and titer of *L. lactis* ssp. *cremoris* MG1363 in M17 medium with a maximally observed fold-change of 5. When tested for quark fermentation, the pre-cultivation conditions of the starter, especially the aeration conditions, also had impact on vitamin K2 content in the final product. The diversity and complexity of influencing factors on vitamin K2 content in *L. lactis* could not only explain the extreme diversity of vitamin K2 content in various cheese types and products (Vermeer et al., 2018; Walther et al., 2021), but also highlight the potential of vitamin K2 natural enrichment.

For biotechnological production of vitamin K2 as food supplement, most studies so far focused on *Bacillus subtilis* for MK-7 production (Ren et al., 2020). The study described in Chapter 3 obviously extended the opportunities to *L. lactis* for MK-9 and MK-8 production. Although only tested as batch fermentation in this study, it would be highly interesting to apply the optimized cultivation conditions in controlled bioreactors with biomass retention. Moreover, the possibility of utilizing low-value substrates such as agricultural byproducts can also be explored for microbial production of vitamin K2, as demonstrated with the utilization of various carbon sources.

For food fermentations with well-established procedures such as cheese or quark production, changing conditions during the fermentation is not always desired or possible, but opportunities of vitamin K2 enrichment are seen with strain selection and pre-cultivation of the starters. Moreover, the possibility of utilizing various carbon sources such as fructose by *L. lactis* to achieve high vitamin K2 content is inspiring for vitamin K2 enrichment in (novel) fermented foods based on for instance vegetables/plants. These developments can contribute to more widespread dietary sources of vitamin K2 besides cheeses, which is currently the main source of vitamin K2 in typical western diets. It has often been in dispute whether cheeses, especially hard cheese, should be recommended for a healthy diet due to the high fat content despite the benefits from the rich vitamin K2 content (Vermeer et al., 2018); the increasing popularity of vegan lifestyle also puts forward the requirement for non-animal or dairy-based products as the vitamin K2 source.

Besides screening for ideal strains and conditions, strain improvement offers an effective approach for enriched vitamin K2 in both biotechnological production and *in situ* fermentation. Triggered by the observation in the study described in Chapter 3, where aerated conditions consistently resulted in higher vitamin K2 content in *L. lactis* in comparison to static cultivation, a laboratory evolution experiment was performed on *L. lactis* ssp. *cremoris* MG1363 under aerated condition for a prolonged cultivation period (Chapter 4). Evolved strains were selected for stationary phase survival under the aerated condition, and showed considerable increase (50% - 110%) of total vitamin K2 content. So far, most strain improvement studies aiming for optimized vitamin K2 production have been focused on *Bacillus subtilis*, and effective approaches included mutagenesis, selection of vitamin K2 analog-resistant variants and targeted genetic modification by suppressing competing reactions or overexpressing vitamin K2 synthesis genes (Ren et al., 2020). Only one recent study focused on *L. lactis*, showing that over-expressing key genes in the vitamin K2 biosynthesis pathway successfully improved the content of this vitamin (Bøe and Holo, 2020). Although genetic modification has also been shown to be an effective approach, the stringent regulations in Europe and low acceptance for genetically modified organisms (GMOs) greatly limit the applications. The non-GM approach of laboratory evolution provided promising leads for strain improvement that finds wide applications in food fermentations. To this end, finding the proper condition of laboratory evolution and setting the selection criteria are key for obtaining the ideal variants effectively. Besides observations on the influencing factors, understanding of the physiological role of vitamin K2 in *L. lactis* could also contribute to accurate definition of the evolution directions: this will be discussed in the next section.

For selection of strains with outstanding vitamin K2 content, a cost-efficient, high-throughput screening method is of great interest. The HPLC-MS analysis adopted in this thesis study provided accurate identification and quantification of the various MK forms in the extracts, but in practice requires dedicated equipment and an analytical method to be setup, and could be costly and time consuming when large collections of strains are to be screened. Bioassays based on microbial growth stimulation of non-producers upon receiving cell extracts obtained from potential vitamin K2 producers, could provide opportunities for a quick, initial screening: for non-vitamin K2 producers such as *Lactiplantibacillus plantarum* [previously referred to as *Lactobacillus plantarum* (Zheng et al., 2020)], supplementation of MKs and heme has been shown to complete a simple electron transport chain and induce functional respiration when oxygen is present (Brooijmans et al., 2009). As a result of aerobic respiration, an increased biomass is obtained. In a preliminary trial we observed a linear correlation of supplemented (solvent-dissolved) MK-4 and the biomass accumulation reflected by optical density of *La. plantarum* under respiration permissive condition, and the linear range covered 0 - 20 µg/mL MK-4 in both 12- and 24- well plate format (Fig. 10.1). Although the correlation of biomass and other MK-forms remains to be established with such bioassays, it provides a proof of principle for a fast, initial screening of outstanding vitamin K2 producers.

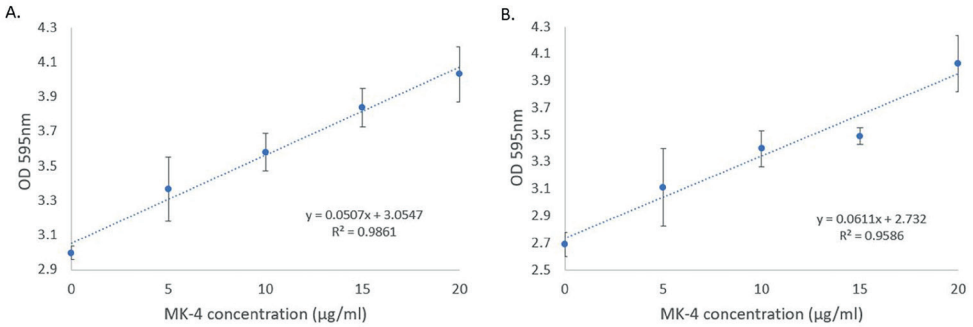

Figure 10.1. The linear correlation of supplemented (solvent-dissolved) MK-4 and the optical density of *Lactiplantibacillus plantarum* cultures under respiration permissive condition in A) 12- and B) 24- well plate format. *La. plantarum* WCFS1 was cultivated in MRS medium supplemented with 2 µg/mL heme, shaking at 180 rpm, 37 °C for 24 hours before the optical density was measured. Cheese cloth was used to cover the well plates. The data were collected by MSc students from Advanced Fermentation Science course 2017: Lewis, Huijboom, Huang, Jing, Hoang and Wang.

Why – vitamin K2 content is the result of complex factors

It was intriguing to observe that the aerated conditions consistently resulted in higher vitamin K2 content and higher abundance of long-chain MKs in *L. lactis* in comparison to static cultivation (Chapter 3), and that strains evolved from aerated conditions showed enhanced vitamin K2 content and oxidative stress resistance (Chapter 4). The role of MKs in *L. lactis* has been somewhat mysterious: the most well-known role of MKs in bacteria is as electron carriers in the respiratory electron transport chain (ETC), but *L. lactis* has been historically classified as a non-respiring, facultative anaerobic bacterium, hence the role of MKs in aerobic respiratory electron transport seems not of evident significance for such a lifestyle. Previously mentioned observations from this thesis study, as well as a few suggestions from literature (Søballe and Poole, 2000; Vido et al., 2005), seemed to point to a role in reducing oxidative stress by MKs in *L. lactis*.

Genetics and proteomics analysis of evolved *L. lactis* strains that showed enhanced vitamin K2 content did not reveal genetic or proteome changes that could be linked directly to vitamin K2 synthesis. However, the oxidative stress resistant phenotype could be explained from the mutations and protein level changes (Chapter 4). While it was not possible to directly link enhanced vitamin K2 content to improved resistance to oxidative stress in the evolved strains, a more direct approach was adopted by examining various gene deletion mutants with altered vitamin K2 profiles (Chapter 5). In contradiction to our assumptions, the mutant that is unable to synthesize MKs (Δ*menF*) showed the best stationary phase survival under aerobic cultivation condition. It was deduced that under aerobic condition, when heme is not supplied to enable the function of the terminal cytochrome oxidase, the electron transfer function of MKs most likely promoted the formation of reactive oxidative species (ROS), which impose extra oxidative stress on the bacterium. The statement that MKs contribute to reducing oxidative stress of *L. lactis* holds true only under the condition that exogenous heme is supplemented to activate the

terminal oxidase of the respiratory ETC. On the other hand, MKs are produced by *L. lactis* under both aerobic and anaerobic conditions, and a role of MKs in extracellular electron transfer (EET) using for example metal ions as terminal electron acceptors, has been demonstrated in *L. lactis* under anaerobic conditions (Chapter 5).

To discuss the evolutionary significance of *L. lactis* retaining the MK synthesis ability, a few hypotheses can be put forward. Firstly, although oxygen and heme are considered to be scarce in the dairy environment, the situation is different in the original habitat of *L. lactis*: plant surfaces (Cavanagh et al., 2015). Oxygen is indeed present there, and the source of heme is also diverse: not only from the plants themselves, but also from heme producing bacteria that are possibly also present in the same habitat (Espinas et al., 2012; Dailey et al., 2017). Therefore, MK producing ability would offer an advantage to *L. lactis* by heme and oxygen induced respiration. Secondly, the role of MKs in EET is of evolutionary significance for *L. lactis* under anaerobic condition too, as EET "allows for the respiration of compounds that are inaccessible in the cell membrane, such as insoluble mineral oxides" (Light et al., 2019). Finally, evolution is an everlasting process. The various species of lactic acid bacteria are considered to have experienced a series of gene loss processes for the components in the respiratory ETC (Pedersen et al., 2012). Species such as *L. lactis* lost the completeness in heme biosynthesis pathway but maintained MK biosynthesis pathway and cytochrome oxidase encoding genes; species such as *La. plantarum* lost the functionality of heme and MK synthesis but maintained the cytochrome oxidase encoding genes; species such as *Streptococcus thermophilus* have lost the ability to synthesis all three components and therefore never perform aerobic respiration (Pedersen et al., 2012). Whether MK synthesis in *L. lactis* is a result of evolutionary advantage during adaptation to its niche, or is a redundancy that can be further streamlined, can be best found out using the various MK mutants described in Chapter 5. As *L. lactis* can grow under both aerobic and anaerobic conditions regardless of the MK profiles, fitness of the various MK mutants can be examined by co-cultivation and propagation in different conditions, similar to a back-slopping process; the dynamics in the population of the various mutants can provide additional insights into the evolutionary significance of MK production in *L. lactis*.

So far, the physiological roles of MKs in *L. lactis* also cannot directly explain the observed changes in MK content under different conditions and in the evolved strains. It should be appreciated that the synthesis of vitamin K2 in *L. lactis* is a complicated process involving various pathways in both primary and secondary metabolism (Nowicka and Kruk, 2010). Therefore, this biochemical process is under the influence of a series of factors (Fig. 10.2). First, the cultivation conditions including carbon/nitrogen sources, aeration, temperature and pH, as well as the mode of metabolism all have direct impact on the primary metabolism, and therefore on the fluxes towards the vitamin K2 precursors. Moreover, the external factors may also directly influence the vitamin K2-specific biosynthesis pathway, by changing the expression level of genes involved. Finally, competing reactions, diffusion of intermediates and feedback inhibition (demonstrated for other vitamin K2 producing bacteria but very likely to be applicable in *L. lactis*) can all participate in determining the production level of vitamin K2 (Tsukamoto

et al., 2001; Bashiri et al., 2020; Ren et al., 2020). It is strongly desirable to construct a genome-scale metabolic model to understand and predict the changes in vitamin K2 levels.

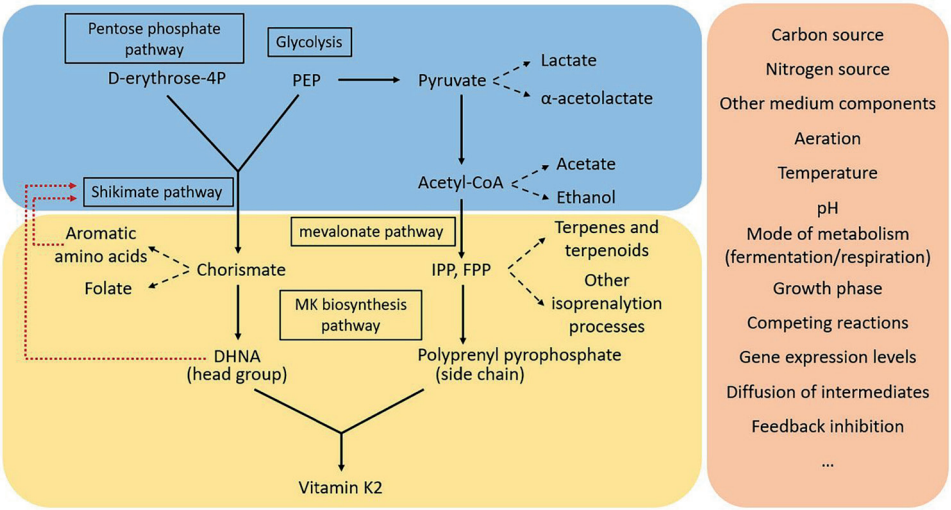

Figure 10.2. Scheme of pathways and plausible influencing factors involved in synthesis of vitamin K2 and precursors in *L. lactis*. The blue box indicate primary metabolism, and yellow box secondary metabolism. Black solid arrows indicate reactions towards vitamin K2 synthesis, black dashed arrows point to other products from competing reactions, red dashed arrows indicate possible feedback inhibitions. An arrow does not necessarily indicate a single step of reaction. Orange box on the right side shows possible influencing factors of vitamin K2 synthesis. D-erythrose-4P: D-erythrose-4-phosphate; PEP: phosphoenolpyruvate; DHNA: 1,4-dihydroxy-2-naphthoic acid; IPP: isopentenyl pyrophosphate; FPP: farnesyl pyrophosphate.

EV production in *L. lactis*: how and why

EV production in *L. lactis* has been studied in this thesis research. The role of prophage activation in EV production was revealed from phenotypical observation to molecular mechanism (Chapter 7 & 8), addressing the intriguing question of *how* EVs escape the Gram-positive bacteria with thick cell walls. Based on these observations and combining genetic information of the prophages (Chapter 6), the evolutionary significance of EV production, or the prophage-EV interaction, delivers a hypothesis answering *why* such behavior improves evolutionary success in a mixed microbial community like cheese starter cultures.

How - role of prophages in EV production

The studies of the two similar cheese starter isolates with identical prophage sequences, *L. lactis* ssp. *cremoris* strain TIFN1 and strain FM-YL11, were indeed initiated from different viewpoints. Starting with strain TIFN1, the initial intention to explain the non-lytic phage release phenomenon led to the findings of membrane enclosure of the phage particles (Chapter 7), pointing to EV-like structures. To

further understanding the mechanisms, FM-YL11 was chosen for its highly similar behavior as TIFN1. For strain FM-YL11, the stimulating role of prophage-encoded holin-lysin system in EV production was confirmed, and the cargo and composition of EVs described (Chapter 8).

The role of peptidoglycan degrading enzymes has been one of the most evidence-supported mechanism of EV production in Gram-positive bacteria (Toyofuku et al., 2017; Wang et al., 2018; Andreoni et al., 2019). The effect of prophage-encoded holin-lysin system in stimulating EV production is apparent under prophage inducing conditions, but observations on the prophage-cured strain FM-YL12 also demonstrated the presence of a prophage-independent mechanism in EV production, possibly via the action of autolysins, which play a role in cell division and cell wall remodeling (Visweswaran et al., 2013; Wang et al., 2018). In support of this assumption, the extracellular particles produced by strain TIFN1 were mainly found at the cell division sites, where the autolysins naturally accumulate; with the additional action of prophage-encoded holin-lysin, the cell division sites therefore become the weakest spots, allowing the release of large amounts of EVs. From the proteomics analysis of EVs released from strain FM-YL11, autolysins and proteins involved in cell wall synthesis were also retrieved, in line with the observation that the cell division sites are hotspots for EV release (Fig. 10.3).

The interplay between EVs and phages does not stop with prophages providing extra tools for EV production, part of the EV population also carries phage particles as cargos and provide the phages a non-lytic exit from the host. This relationship, or co-occurrence of EVs and phage/viral particles has been recently described for other bacteria and ecosystems (Soler et al., 2015; Toyofuku et al., 2017; Andreoni et al., 2019). In the marine ecosystem for example, large amounts of EVs were isolated from multiple ocean water samples, even outnumbering the viral particles found in the same environment (Biller et al., 2014). These observations bring up the awareness or concern that bacterial EVs could be easily confused with viral particles in ecological studies: the methods used for EV isolation are similar to the ones traditionally used for viral particle isolation, and the two types of particles share great similarities in terms of size, density, morphology and composition. EVs carrying DNA, including bacterial genomic DNA, plasmids and even viral DNA, are frequently reported, posing additional complexity to the effort in distinguishing EVs and viruses (Soler et al., 2015) - this struggle was also seen from this thesis research. Separating and distinguishing EVs, phage particles, EVs with DNA cargos and EVs with phage cargos is still desired for a precise description of the various extracellular particle populations to complement this thesis study, and is also recognized as a major challenge in viral ecological studies. The increasing awareness of the abundance of EVs in nature and their interplay/co-occurrence with viral particles may challenge the traditional theories on the abundance and ecological roles of viruses in nature, and also put forward higher requirement for methodology in isolating and identifying both entities in future studies.

Another intriguing observation is the encapsulation of phage particles by EVs. Although phages were occasionally reported to be the cargos in other Gram-positive bacterial EVs (Toyofuku et al., 2017), this phenomenon seemed to be very pronounced in the two strains used in this thesis study. A substantial

population of FM-YL11 EVs was indicated to carry phage particles, and in TIFN1 there even seems to be a specific membrane encapsulation process of the phage particles. Although random encapsulation is likely when the cytosol is crowded with phage particles under prophage inducing conditions, it is highly interesting to investigate whether mechanisms exist to promote this encapsulation process. In the membrane-enclosed phages such as *Cystoviridae* and *Tectiviridae,* the specific encapsulation was proposed to be secured by phage-encoded proteins that integrate/interact with the host bacterial membrane (Harrison, 2015; Mäntynen et al., 2019). Several types of naked viruses that infect vertebrates have also been reported to be packed in host-derived EVs (Feng et al., 2013; Santiana et al., 2018; Gu et al., 2020), and it is being gradually revealed that certain non-structural proteins encoded by the viruses promote the encapsulation by EVs (van Der Grein et al., 2021) – the EV enclosed viral population often shows altered infection efficiency and ability to circumvent the antiviral immunity (van der Grein et al., 2019). From the genomic analysis (Chapter 6) of proPhi1 isolated from TIFN1 (prophage in FM-YL11 showed identical sequence), membrane-associated proteins were indeed predicted (Fig. 10.3). Whether this type of phage-encoded protein promotes EV encapsulation is an extremely interesting question, as insight into such mechanism will not only contribute to the understanding of EV-phage interaction and EV roles in bacteria-phage interaction, but also is valuable for applications where specific cargo loading in the EVs is desirable.

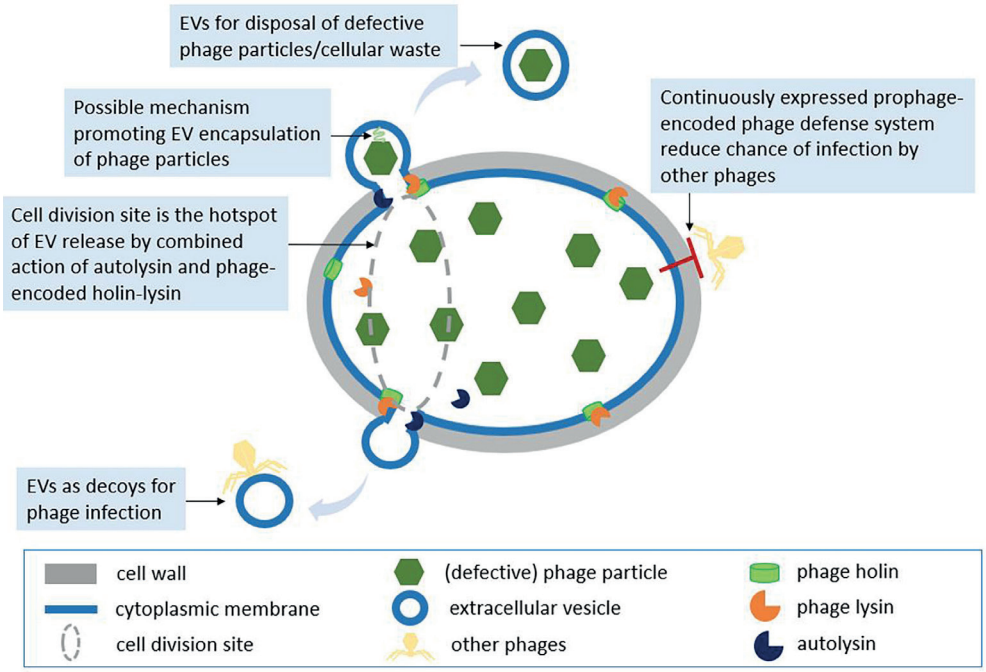

Figure 10.3. Possible interactions of bacteria, EVs and phages suggested by studies on dairy starter isolates *L. lactis* strains TIFN1 and FM-YL11.

Why - ecological and evolutionary significance of (prophage-mediated) EV release

The *L. lactis* strains TIFN1 to TIFN7 isolated from a complex dairy starter culture named "Ur" have been shown to release membrane-enclosed tailless phage particles in a non-lytic manner (Alexeeva et al., 2018; Chapter 7 of this thesis), and strain FM-YL11 isolated from artisanal cheese showed prophage-stimulated EV production where phage particles are the cargos (Chapter 8). The artisanal dairy starter cultures are results of historical use and propagation of starters that lead to successful fermentation (back-slopping), which eventually shaped the microbial community in a stable, robust form (Erkus et al., 2013; Smid et al., 2014). It is therefore reasonable to consider the strains in such an ecosystem are evolutionary successes with their strategies for interacting with other microbes and with the environment. The EV-phage interplay observed in strains isolated from either mixed dairy starters or artisanal cheeses, as well as from other complex ecosystems, is likely to be of ecological and evolutionary significance.

The prophage in TIFN1 (which is identical to the prophage in FM-YL11) was found to contain mobile elements disrupting the tail proteins, explaining the tailless phenotype of released phages (Chapter 6). The phages are therefore expected to be defective, unable to complete the infection cycle. This could be the a strategy of the bacterial host to limit phage spread during the co-evolution with phages. However, most strains found in the Ur culture were lysogenic, suggesting an advantage of harboring the prophage sequences comparing to prophage-cured strains. In addition, spontaneous phage induction was observed, without addition of any prophage-inducing factors (Alexeeva et al., 2018). An explanation could be derived from the genomic analysis of the prophage sequences: most of the prophages contain genes encoding phage defense proteins (Chapter 6). Continuous expression of these proteins contribute to defense against other incoming phage infections, and the continuous assembly of phage particles in the bacteria could also restrict the availability of reproduction for other phages. However, the cells need to provide exit to the assembled phage particles to be able to maintain normal cellular functions. This hypothesis is supported by the study on the holin-lysin knockout mutant, in which the EV release was inhibited and cell growth was retarded especially upon prophage inducting conditions (Chapter 8). It is likely that the assembled phage particles, having no efficient way of leaving the cells, cause overcrowding in the cytoplasm, which could affect protein mobility in the cells and cause stresses in translation, secretion and osmosis (Mourão et al., 2014). This assumption can be checked by proteomics analysis in the future. When the expression of cell wall modifying enzymes like endolysins is finetuned to mediate EV release without causing massive cell lysis, opportunities of getting rid of redundant, waste cellular components are offered: examples are defective phage particles as demonstrated in this thesis study, but also misfolded proteins/protein aggregates/inclusion bodies that cannot be degraded efficiently. In this aspect, EVs contribute to maintaining the cellular functions by waste disposal (Fig. 10.3).

It is also an interesting question whether the EVs play a role in phage infection. From this thesis study and available literature, there is no evidence showing that the EVs provided a novel entry route for

the phages to infect bacteria. For viruses infecting vertebrates the EVs are often found to promote the infection efficiency and circumvent the antiviral immunity (Santiana et al., 2018; van der Grein et al., 2019). In the studies on the association of EVs and phage infection, it is mostly recognized that EVs can serve as decoys for phages and contribute to the survival of bacteria (Manning and Kuehn, 2011; Kharina et al., 2015). This is plausible for the *L. lactis* EVs too, as phage receptors have been identified in the proteome of the EVs from strain FM-YL11 (Fig. 10.3). More recently it was found that the EVs spread phage receptors from sensitive strains to resistant strains, and enable phages to infect the non-host strains or even species– in which manner EVs are expected to contribute greatly to not only phage spread but also to horizontal gene transfer (Tzipilevich et al., 2017).

The production and functions of EVs, the interaction between bacteria, EVs and phages, and the impact on cell biology, ecology and phage-host co-evolution definitely deserves further insights. Complex ecosystems like those found in mixed dairy starter cultures, gastrointestinal tract or marine environment are often interesting models to examine such interactions, and understanding of these interactions will benefit research in multiple fields for example food fermentation, as well as health and environment. The knowledge on (Gram-positive) bacterial EV production can also be translated into diverse applications, which is discussed in the next section.

Good things come in small packages: EVs as the delivery vehicles

Finally, the delivery of vitamin K2 to a human cell line by *L. lactis* EVs was demonstrated in Chapter 9. Not only did the holin-lysin induced EVs contribute to the delivery of vitamin K2, EVs artificially made from *L. lactis* cells also showed the same effect, demonstrating the possibility to increase the efficiency of producing EVs as delivery vehicles. It was also evident that the long-chain vitamin K2 particularly benefits from the delivery by EVs, as shown by the increased efficiency when administrating the same amount of long-chain MKs to the cell line through EVs as compared to delivery in the solvent-dissolved form.

Although this is an *in vitro* study showing direct delivery of vitamin K2 by EVs to the cells from the target tissue, the scenarios for *in vivo* digestion and transportation of vitamin K2-loaded EVs following oral ingestion can be speculated (Fig. 10.4). The first scenario is that the EVs follow the conventional lipid digestion route, which is also expected for liposome digestion (Shearer et al., 2012; Liu et al., 2020): the vitamin K2-loaded EVs are expected to remain stable until they reach the intestine, where they get solubilized by the action of bile salts and pancreatic enzymes to form mixed micelles, which are taken up by enterocytes. The micelles are converted into chylomicrons in the enterocytes and then enter first the lacteal and then the bloodstream, where the chylomicrons are degraded by lipoprotein lipase. Vitamin K2, especially the long-chain forms, are then carried by low density lipoproteins (LDL) and transported to cells in the target tissue, such as osteoblasts, which display LDL receptors on the cell surface to facilitate the uptake of LDL and vitamin K2. Alternatively, the EVs may directly enter the

circulation system: it has been demonstrated that bacterial EVs directly pass through the intestinal wall and enter the bloodstream (Stentz et al., 2018; Haas-Neill and Forsythe, 2020). Thereafter, EVs are expected to be taken up by the host cells by endocytosis or membrane fusion, as both mechanisms have been demonstrated for the interaction of mammalian or bacterial EVs with mammalian cells (Kesty et al., 2004; Mulcahy et al., 2014; Nagakubo et al., 2020). The contribution of gut microbiota to the vitamin K2 status, which has been observed since long ago (Barnes and Fiala, 1959), is also possibly via this alternative route. The two scenarios complement each other, and EVs are expected to provide advantages for solubilization, digestion and transportation of vitamin K2 as compared to the intact bacteria.

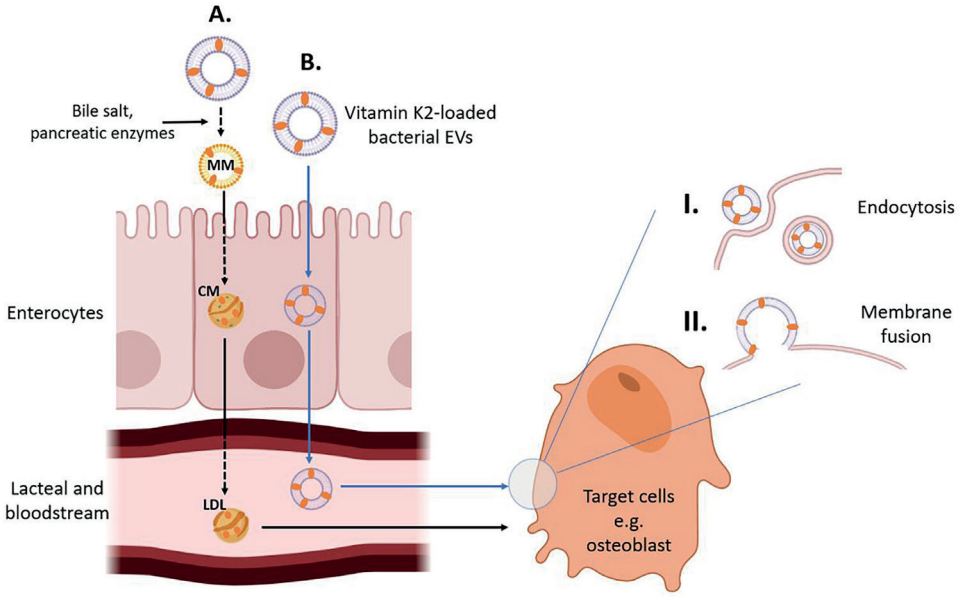

Figure 10.4. Proposed scenarios for digestion and transportation of vitamin K2-loaded EVs *in vivo*. It is expected that EVs remain stable until reaching the intestine, and then the EVs follow either a conventional lipid digestion route (A) or an alternative route (B). In the conventional route (black arrows), vitamin K2-loaded EVs are converted into mixed micelles (MM), chylomicrons (CM) and low-density lipoproteins (LDL) subsequently, and vitamin K2 is delivered to target cells, e.g., osteoblasts that display LDL-receptors to facilitate uptake of LDL. In the alternative route (blue arrows), vitamin K2 loaded EVs pass the intestinal wall and enter the bloodstream directly and get transported to recipient cells. The uptake of EVs by the host cells could be via (I) endocytosis and (II) membrane fusion. Solid arrows show transportation without conversion, dashed arrows show conversion. This figure was created with BioRender.com.

Following the uptake by the human cells, vitamin K2 needs to reach the intracellular site of function. The γ-glutamyl carboxylase (GGCX) for which vitamin K2 acts as a co-factor, is located on the endoplasmic reticulum (ER) membrane (Berkner, 2005; Gröber et al., 2014). It is logical to presume that upon taking up EVs at the host cell membrane, the membrane vesicle trafficking in the cells allow vitamin K2 to eventually reach the ER membrane (Fig. 10.5). It has been established that vesicular transport

play essential roles in cellular secretion and uptake of cargos, allowing compound exchange between plasma membrane and a series of membrane-enclosed organelles including the ER and Golgi complex (Bonifacino and Glick, 2004; O'Connor and Adams, 2010). Notably, the enzyme co-factor function of vitamin K2 on ER membrane is achieved via its electron transfer capacity (Fig. 10.5): the electron flow during the reduction of vitamin K2 by a NADH dehydrogenase/quinone reductase and the oxidation by GGCX supplies energy required for carboxylation of Glu residues, achieving maturation of Gla-proteins (Berkner, 2005; Gröber et al., 2014). This is consistent with the role of vitamin K2 in the membrane of the producing bacteria as electron carriers (Fig. 10.5), completing for instance the respiratory electron transport chain, among other discovered electron transfer routes (Brooijmans et al., 2009; Kurosu and Begari, 2010).

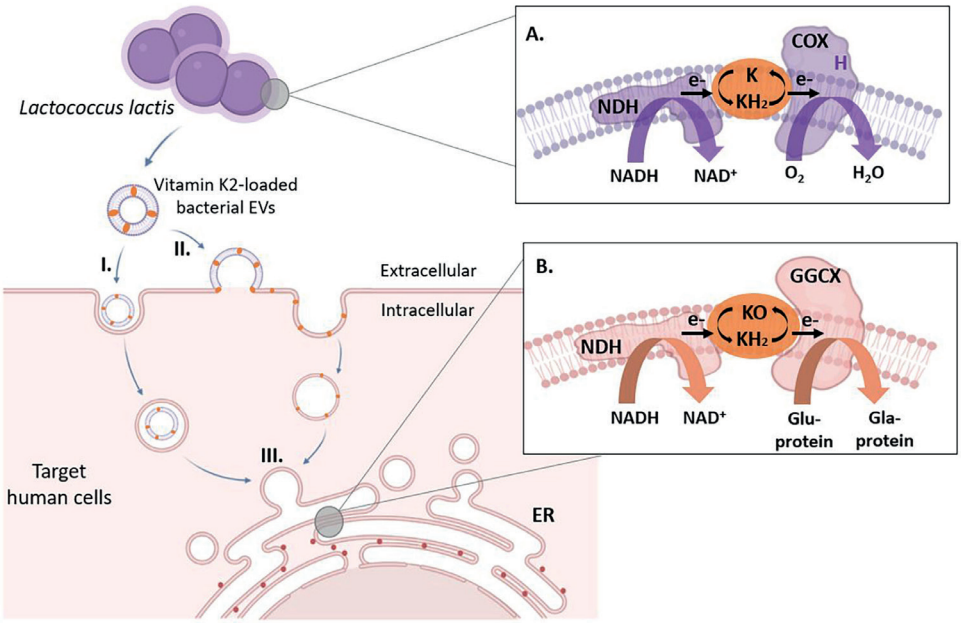

Figure 10.5. Proposed membrane interactions for vitamin K2 carried by bacterial EVs to reach the site of function, and the electron transfer function of vitamin K2 in bacteria and in human cells. After the vitamin K2-loaded bacterial EVs are taken up by the cell membrane of target human cells via either endocytosis (I) or fusion (II), vitamin K2 eventually reaches the endoplasmic reticulum (ER) membrane by vesicle trafficking (III) for exchanging components between cell membrane and membranous organelles. On the ER membrane, vitamin K2 functions as a co-factor for γ-glutamyl carboxylase (GGCX). The redox reactions of vitamin K2 in human cells allow electrons flow from a NADH dehydrogenase/quinone reductase (NDH) to GGCX, driving the carboxylation process during which Glu-proteins are transformed into Gla-proteins (B). Similarly, in *L. lactis* cell membrane, vitamin K2 transfer electrons between a NDH and a cytochrome oxidase (COX) when heme (H) and oxygen are present, forming a simple respiratory electron transport chain (A). Vitamin K2 depicted as K, oxidized form as KO, reduced form as KH_2. Orange ovals represent vitamin K2, red circles represent ribosomes. This figure was created with BioRender.com.

While the proof of principle has been obtained that bacterial EVs deliver bioactive vitamin K2 to host cells, the characteristics of *L. lactis* EVs and their influence on the delivery efficiency is an extremely interesting yet underinvestigated topic. The most outstanding factors that influence the liposomal intake pathway and its efficiency have been identified as the liposomal size and surface charge (Liu et al., 2020). The same influencing factors are likely applicable for uptake of bacterial EVs by host cells. Although not specifically examined, the electron microscopic pictures on *L. lactis* EVs produced via prophage-dependent and -independent routes were an initial indication that the producing mechanisms influence EV size (Chapter 8). For artificially produced EVs, the methods adopted naturally also influence the EV size. The size and surface charge of *L. lactis* EVs produced by different mechanisms should be characterized and the relation to vitamin K2 delivery efficiency can be established in future studies. This knowledge will be valuable not only for delivery of this specific vitamin but also for other applications of bacterial EVs.

Future perspectives and concluding remarks

Given the diverse cargos (nucleic acids, proteins, viral particles, etc.) carried by bacterial EVs and their various interactions with other microbes, host and environment (see Chapter 2), and the effectiveness of vitamin K2 delivery by EVs to host cells (see Chapter 9), offer plenty of novel opportunities for the application of bacterial EVs in food, feed and pharma.

Besides medical applications, the potential of bacterial EVs in food biotechnological applications deserves recognition (Fig. 10.6) (Liu et al., 2018). For example, the possibilities to deliver anti-microbial compounds and genome editing elements (i.e., CRISPR/Cas cassettes) by bacterial EVs can be applied not only for combating pathogens in the human gut, but also can be applied in fermentation starters to inhibit undesired strains/species or establish desired traits. Membrane-associated compounds like vitamin K2 transferred by bacterial EVs may not only contribute to human health but also to the fitness of other commensal bacteria, achieving prebiotic effects. The ability to modulate the host immune system also makes bacterial EVs ideal candidates as vaccine carriers or probiotic substitutes (Liu et al., 2018).

With many potential applications of bacterial EVs proposed, efficient production of EVs with the desired functionality could be one of the major challenges in practice. To this end, isolation and characterization of EV producing bacterial strains, understanding of the mechanisms governing natural EV production, identification of EV components and interpretation of EV functions are prerequisites to successful applications of naturally secreted bacterial EVs or the producing strains (Liu et al., 2018). Alternatively, artificial EV production by enzyme treatment/osmotic pressure or mechanical force effectively increase the yield. Compounds of interest can also be loaded to the EVs by genetic engineering of the EV producing bacteria, or by membrane insertion/encapsulation during the artificial EV production process (Fig. 10.7A-D). Notably, different compounds can be loaded in combination to

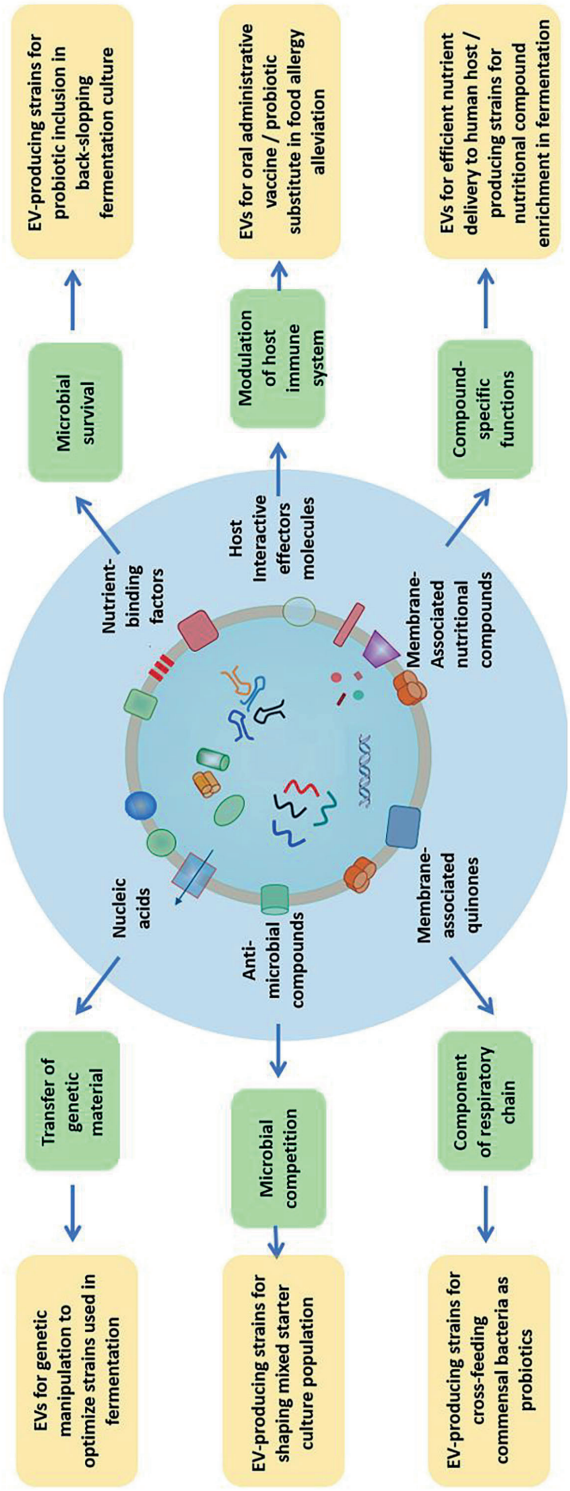

Figure 10.6. Bacterial EV cargos, roles and potential applications. Examples of EV cargos (blue circle), corresponding roles of the EVs (green box) and proposed applications of the EVs or EV-producing strains (yellow box) are presented (Liu et al., 2018).

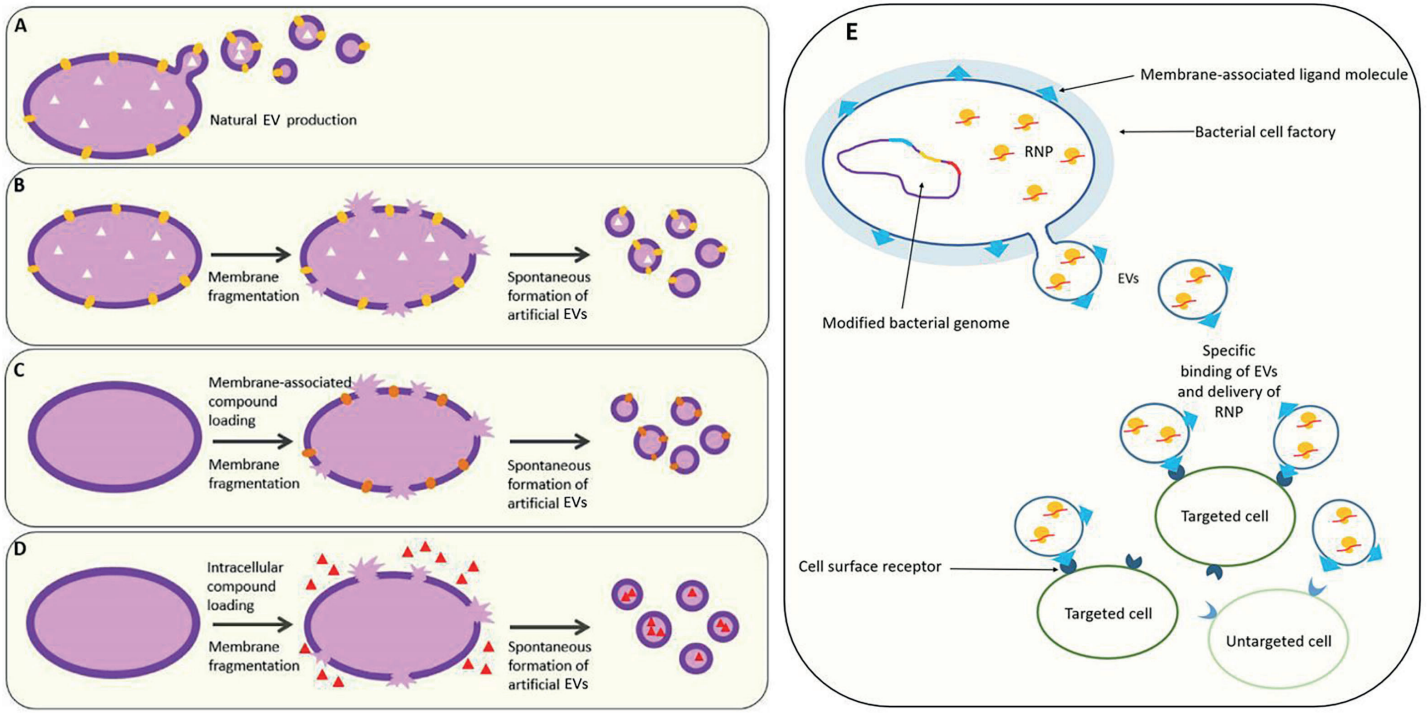

Figure 10.7. Scheme of proposed EV production methods. (A) Natural EVs produced by bacteria with desired lumenal cargos (white triangles) or membrane-associated cargos (yellow ovals). (B) Artificial EVs produced by fragmenting bacteria with desired lumenal or membrane-associated cargos. (C) and (D) Artificial EVs produced by fragmenting bacteria and artificially loading of membrane-associated cargos (orange ovals) or lumenal cargos (red triangles). (E) Designed bacterial cell factory that express ligand molecules and ribonucleoprotein complex (RNP) for targeted delivery of genome editing tools. Figure adapted from (Liu et al., 2018, 2019)

the EVs to achieve synergy: for example, bacterial cell factories can be designed to generate EVs that display ligands for specific targeting of host/microbial cells and delivery of genome editing elements (e.g. CRISPR-Cas9 ribonucleoprotein complex, RNP) (Fig. 10.7E), to achieve high-specificity delivery of genome editing tools for biotechnological and medical applications ranging from steering metabolite production to fighting pathogenic bacteria or correcting human genetic disorders (Liu et al., 2019).

Furthermore, the advantage of using Gram-positive bacteria as a source of EVs should be noted (Liu et al., 2019). Unlike Gram-negative bacteria that have an outer membrane, the Gram-positive bacteria only have a cytoplasmic membrane as the origin of EVs, and the membrane is in direct contact with cytosolic components to achieve engulfment of cargos (Toyofuku et al., 2019; Nagakubo et al., 2020). The toxicity caused by lipopolysaccharides (LPS), which hampers the application of Gram-negative bacteria (Acevedo et al., 2014), is also not of concern for EVs generated from Gram-positive bacteria. Although studies on Gram-negative bacterial EVs have thrived with a much longer history, the rapid advances in Gram-positive bacterial EVs will surely complement and further stimulate this booming research field of EVs.

In conclusion, this thesis study not only examined the fundamental mechanism of vitamin K2 and EV production in *L. lactis*, but also demonstrated the possibilities for vitamin K2 enrichment of fermented food as well as efficient delivery of vitamin K2 to the human host. Findings from this thesis are expected to contribute to the field of food fermentation, biotechnology, as well as nutrition and human health. Remaining questions and perspectives that are put forward also emphasize the requirements and potential benefits for further exploration and exploitation of microbial vitamin K2 enrichment and Gram-positive bacterial EVs.

References

Acevedo, R., Fernández, S., Zayas, C., Acosta, A., Sarmiento, M. E., Ferro, V. A., et al. (2014). Bacterial outer membrane vesicles and vaccine applications. *Front. Immunol.* 5, 1–6.

Alexeeva, S., Guerra Martínez, J. A., Spus, M., and Smid, E. J. (2018). Spontaneously induced prophages are abundant in a naturally evolved bacterial starter culture and deliver competitive advantage to the host. *BMC Microbiol.* 18, 120.

Andreoni, F., Toyofuku, M., Menzi, C., Kalawong, R., Shambat, S. M., François, P., et al. (2019). Antibiotics stimulate formation of vesicles in *Staphylococcus aureus* in both phage-dependent and -independent fashions and via different routes. *Antimicrob. Agents Chemother.* 63, e01439-18.

Barnes, R. H., and Fiala, G. (1959). Effects of the prevention of coprophagy in the rat. *J. Nutr.* 68, 603–614.

Bashiri, G., Nigon, L. V., Jirgis, E. N. M., Ho, N. A. T., Stanborough, T., Dawes, S. S., et al. (2020). Allosteric regulation of menaquinone (vitamin K2) biosynthesis in the human pathogen *Mycobacterium tuberculosis*. *J. Biol. Chem.* 295, 3759–3770.

Berkner, K. L. (2005). The vitamin K-dependent carboxylase. *Annu. Rev. Nutr.* 25, 127–149.

Biller, S. J., Schubotz, F., Roggensack, S. E., Thompson, A. W., Summons, R. E., and Chisholm, S. W. (2014). Bacterial vesicles in marine ecosystems. *Science (80-.).* 343, 183–186.

Bøe, C. A., and Holo, H. (2020). Engineering *Lactococcus lactis* for increased vitamin K2 production. *Front. Bioeng. Biotechnol.* 8, 191.

Bonifacino, J. S., and Glick, B. S. (2004). The mechanisms of vesicle budding and fusion. *Cell* 116, 153–166.

Brooijmans, R., Smit, B., Santos, F., van Riel, J., de Vos, W. M., and Hugenholtz, J. (2009). Heme and menaquinone induced electron transport in lactic acid bacteria. *Microb. Cell Fact.* 8, 28.

Cavanagh, D., Fitzgerald, G. F., and McAuliffe, O. (2015). From field to fermentation: The origins of *Lactococcus lactis* and its domestication to the dairy environment. *Food Microbiol.* 47, 45–61.

Chollet, M., Guggisberg, D., Portmann, R., Risse, M. C., and Walther, B. (2017). Determination of menaquinone production by *Lactococcus* spp. and propionibacteria in cheese. *Int. Dairy J.* 75, 1–9.

Cranenburg, E. C. M., Schurgers, L. J., and Vermeer, C. (2007). Vitamin K: the coagulation vitamin that became omnipotent. *Thromb. Haemost.* 98, 120–125.

Dailey, H. A., Dailey, T. A., Gerdes, S., Jahn, D., Jahn, M., O'Brian, M. R., et al. (2017). Prokaryotic heme biosynthesis: multiple pathways to a common essential product. *Microbiol. Mol. Biol. Rev.* 81, e00048-16.

Emami, S., Azadmard-Damirchi, S., Peighambardoust, S. H., Valizadeh, H., and Hesari, J. (2016). Liposomes as carrier vehicles for functional compounds in food sector. *J. Exp. Nanosci.* 11, 737–759.

Erkus, O., de Jager, V. C. L., Spus, M., van Alen-Boerrigter, I. J., van Rijswijck, I. M. H., Hazelwood, L., et al. (2013). Multifactorial diversity sustains microbial community stability. *ISME J.* 7, 2126–2136.

Espinas, N. A., Kobayashi, K., Takahashi, S., Mochizuki, N., and Masuda, T. (2012). Evaluation of unbound free heme in plant cells by differential acetone extraction. *Plant Cell Physiol.* 53, 1344–1354.

Feng, Z., Hensley, L., McKnight, K. L., Hu, F., Madden, V., Ping, L., et al. (2013). A pathogenic picornavirus acquires an envelope by hijacking cellular membranes. *Nature* 496, 367–371.

Gast, G. C. M., de Roos, N. M., Sluijs, I., Bots, M. L., Beulens, J. W. J., Geleijnse, J. M., et al. (2009). A high menaquinone intake reduces the incidence of coronary heart disease. *Nutr. Metab. Cardiovasc. Dis.* 19, 504–510.

Geleijnse, J. M., Vermeer, C., Grobbee, D. E., Schurgers, L. J., Knapen, M. H. J., van Der Meer, I. M., et al. (2004). Dietary intake of menaquinone is associated with a reduced risk of coronary heart disease: The Rotterdam Study. *J. Nutr.* 134, 3100–3105.

Gröber, U., Reichrath, J., Holick, M. F., and Kisters, K. (2014). Vitamin K: an old vitamin in a new perspective. *Dermatoendocrinol.* 6, e968490.

Gu, J., Wu, J., Fang, D., Qiu, Y., Zou, X., Jia, X., et al. (2020). Exosomes cloak the virion to transmit *Enterovirus* 71 non-lytically. *Virulence* 11, 32–38.

Haas-Neill, S., and Forsythe, P. (2020). A budding relationship: bacterial extracellular vesicles in the microbiota–gut–brain axis. *Int. J. Mol. Sci.* 21, 8899.

Harrison, S. C. (2015). Viral membrane fusion. *Virology* 479–480, 498–507.

Kesty, N. C., Mason, K. M., Reedy, M., Miller, S. E., and Kuehn, M. J. (2004). Enterotoxigenic Escherichia coli vesicles target toxin delivery into mammalian cells. *EMBO J.* 23, 4538–4549.

Kharina, A., Podolich, O., Faidiuk, I., Zaika, S., Haidak, A., Kukharenko, O., et al. (2015). Temperate bacteriophages collected by outer membrane vesicles in *Komagataeibacter intermedius*. *J. Basic Microbiol.* 55, 509–513.

Kim, J. H., Lee, J., Park, J., and Gho, Y. S. (2015). Gram-negative and Gram-positive bacterial extracellular vesicles. *Semin. Cell Dev. Biol.* 40, 97–104.

Kurosu, M., and Begari, E. (2010). Vitamin K2 in electron transport system: are enzymes involved in vitamin K2 biosynthesis promising drug targets? *Molecules* 15, 1531–1553.

Light, S. H., Méheust, R., Ferrell, J. L., Cho, J., Deng, D., Agostoni, M., et al. (2019). Extracellular electron transfer powers flavinylated extracellular reductases in Gram-positive bacteria. *Proc. Natl. Acad. Sci. U. S. A.* 116, 26892–26899.

Liu, W., Hou, Y., Jin, Y., Wang, Y., Xu, X., and Han, J. (2020). Research progress on liposomes: Application in food, digestion behavior and absorption mechanism. *Trends Food Sci. Technol.* 104, 177–189.

Liu, Y., Alexeeva, S., Defourny, K. A., Smid, E. J., and Abee, T. (2018). Tiny but mighty: bacterial membrane vesicles in food biotechnological applications. *Curr. Opin. Biotechnol.* 49, 179–184.

Liu, Y., Smid, E. J., Abee, T., and Notebaart, R. A. (2019). Delivery of genome editing tools by bacterial extracellular vesicles. *Microb. Biotechnol.* 12, 71–73.

Manning, A. J., and Kuehn, M. J. (2011). Contribution of bacterial outer membrane vesicles to innate bacterial defense. *BMC Microbiol.* 11, 258.

Mäntynen, S., Sundberg, L. R., Oksanen, H. M., and Poranen, M. M. (2019). Half a century of research on membrane-containing bacteriophages: bringing new concepts to modern virology. *Viruses* 11, 76.

Mourão, M. A., Hakim, J. B., and Schnell, S. (2014). Connecting the dots: the effects of macromolecular crowding on cell physiology. *Biophys. J.* 107, 2761–2766.

Mulcahy, L. A., Pink, R. C., and Carter, D. R. F. (2014). Routes and mechanisms of extracellular vesicle uptake. *J. Extracell. Vesicles* 3, 24641.

Nagakubo, T., Nomura, N., and Toyofuku, M. (2020). Cracking Open Bacterial Membrane Vesicles. *Front. Microbiol.* 10, 3026.

Nowicka, B., and Kruk, J. (2010). Occurrence, biosynthesis and function of isoprenoid quinones. *Biochim. Biophys. Acta* 1797, 1587–1605.

O'Connor, C. M., and Adams, J. U. (2010). *Essentials of Cell Biology*. Cambridge, MA: NPG Education.

Pedersen, M. B., Gaudu, P., Lechardeur, D., Petit, M. A., and Gruss, A. (2012). Aerobic respiration metabolism in lactic acid bacteria and uses in biotechnology. *Annu. Rev. Food Sci. Technol.* 3, 37–58.

Ren, L., Peng, C., Hu, X., Han, Y., and Huang, H. (2020). Microbial production of vitamin K2: current status and future prospects. *Biotechnol. Adv.* 39, 107453.

Santiana, M., Ghosh, S., Ho, B. A., Rajasekaran, V., Du, W. L., Mutsafi, Y., et al. (2018). Vesicle-cloaked virus clusters are optimal units for inter-organismal viral transmission. *Cell Host Microbe* 24, 208-220.e8.

Schurgers, L. J., Teunissen, K. J. F., Hamulyák, K., Knapen, M. H. J., Vik, H., and Vermeer, C. (2007). Vitamin K-containing dietary supplements: comparison of synthetic vitamin K1 and natto-derived menaquinone-7. *Blood* 109, 3279–3283.

Schurgers, L. J., Uitto, J., and Reutelingsperger, C. P. (2013). Vitamin K-dependent carboxylation of matrix Gla-protein: a crucial switch to control ectopic mineralization. *Trends Mol. Med.* 19, 217–226.

Schurgers, L. J., and Vermeer, C. (2000). Determination of phylloquinone and menaquinones in food. Effect of food matrix on circulating vitamin K concentrations. *Haemostasis* 30, 298–307.

Schurgers, L. J., and Vermeer, C. (2002). Differential lipoprotein transport pathways of K-vitamins in healthy subjects. *Biochim. Biophys. Acta* 1570, 27–32.

Shearer, M. J., Fu, X., and Booth, S. L. (2012). Vitamin K nutrition, metabolism, and requirements: current concepts and future research. *Adv. Nutr.* 3, 182–195.

Simão, A. M. S., Bolean, M., Cury, T. A. C., Stabeli, R. G., Itri, R., and Ciancaglini, P. (2015). Liposomal systems as carriers for bioactive compounds. *Biophys. Rev.* 7, 391–397.

Smid, E. J., Erkus, O., Spus, M., Wolkers-Rooijackers, J. C. M., Alexeeva, S., and Kleerebezem, M. (2014). Functional implications of the microbial community structure of undefined mesophilic starter cultures. *Microb. Cell Fact.* 13, S2.

Søballe, B., and Poole, R. K. (2000). Ubiquinone limits oxidative stress in *Escherichia coli*. *Microbiology* 146, 787–796.

Soler, N., Krupovic, M., Marguet, E., and Forterre, P. (2015). Membrane vesicles in natural environments: a major challenge in viral ecology. *ISME J.* 9, 793–796.

Stentz, R., Carvalho, A. L., Jones, E. J., and Carding, S. R. (2018). Fantastic voyage: the journey of intestinal microbiota-derived microvesicles through the body. *Biochem. Soc. Trans.* 46, 1021–1027.

Toyofuku, M., Cárcamo-Oyarce, G., Yamamoto, T., Eisenstein, F., Hsiao, C. C., Kurosawa, M., et al. (2017). Prophage-triggered membrane vesicle formation through peptidoglycan damage in *Bacillus subtilis*. *Nat. Commun.* 8, 481.

Toyofuku, M., Nomura, N., and Eberl, L. (2019). Types and origins of bacterial membrane vesicles. *Nat. Rev. Microbiol.* 17, 13–24.

Tsukamoto, Y., Kasai, M., and Kakuda, H. (2001). Construction of a *Bacillus subtilis* (natto) with high productivity of vitamin K2 (menaquinone-7) by analog resistance. *Biosci. Biotechnol. Biochem.* 65, 2007–2015.

Tzipilevich, E., Habusha, M., and Ben-Yehuda, S. (2017). Acquisition of phage sensitivity by bacteria through exchange of phage receptors. *Cell* 168, 186-199.e12.

van der Grein, S. G., Defourny, K. A. Y., Rabouw, H. H., Galiveti, C. R., Langereis, M. A., Wauben, M. H. M., et al. (2019). Picornavirus infection induces temporal release of multiple extracellular vesicle subsets that differ in molecular composition and infectious potential. *PLoS Pathog.* 15, e1007594.

van Der Grein, S. G., Defourny, K. A. Y., Rabouw, H. H., Goerdayal, S. S., van Herwijnen, M. J. C., Wubbolts, R. W., et al. (2021). The encephalomyocarditis virus leader promotes the release of virions inside extracellular vesicles via the induction of secretory autophagy. *bioRxiv*, 2021.05.04.442556.

Vermeer, C., Raes, J., van 't Hoofd, C., Knapen, M. H. J., and Xanthoulea, S. (2018). Menaquinone content of cheese. *Nutrients* 10, 446.

Vido, K., van Dorsselaer, A., Leize, E., Juillard, V., Gruss, A., and Gaudu, P. (2005). Roles of thioredoxin reductase during the aerobic life of *Lactococcus lactis*. *J. Bacteriol.* 187, 601–610.

Visweswaran, G. R. R., Steen, A., Leenhouts, K., Szeliga, M., Ruban, B., Hesseling-Meinders, A., et al. (2013). AcmD, a homolog of the major autolysin AcmA of *Lactococcus lactis*, binds to the cell wall and contributes to cell separation and autolysis. *PLoS One* 8, e72167.

Walther, B., Guggisberg, D., Schmidt, R. S., Portmann, R., Risse, M. C., Badertscher, R., et al. (2021). Quantitative analysis of menaquinones (vitamin K2) in various types of cheese from Switzerland. *Int. Dairy J.* 112, 104853.

Walther, B., Philip Karl, J., Booth, S. L., and Boyaval, P. (2013). Menaquinones, bacteria, and the food supply: the relevance of dairy and fermented food products to vitamin K requirements. *Adv. Nutr.* 4, 463–473.

Wang, X., Thompson, C. D., Weidenmaier, C., and Lee, J. C. (2018). Release of *Staphylococcus aureus* extracellular vesicles and their application as a vaccine platform. *Nat. Commun.* 9, 1–13.

Willems, B. A. G., Vermeer, C., Reutelingsperger, C. P. M., and Schurgers, L. J. (2014). The realm of vitamin K dependent proteins: Shifting from coagulation toward calcification. *Mol. Nutr. Food Res.* 58, 1620–1635.

Yang, J., Bahreman, A., Daudey, G., Bussmann, J., Olsthoorn, R. C. L., and Kros, A. (2016). Drug delivery via cell membrane fusion using lipopeptide modified liposomes. *ACS Cent. Sci.* 2, 621–630.

Zheng, J., Wittouck, S., Salvetti, E., Franz, C. M. A. P., Harris, H. M. B., Mattarelli, P., et al. (2020). A taxonomic note on the genus *Lactobacillus*: Description of 23 novel genera, emended description of the genus *Lactobacillus* Beijerinck 1901, and union of *Lactobacillaceae* and *Leuconostocaceae*. *Int. J. Syst. Evol. Microbiol.* 70, 2782–2858.

Summary

The fat-soluble vitamin K is essential for human health for its functions as a co-factor for maturation of proteins that play important roles in hemostasis, calcium and bone metabolism, as well as cell growth regulation. Among the different forms of vitamin K, long-chain vitamin K2 (menaquinone, MK-n) demonstrated higher bioavailability and efficacy in the human body. Additionally, dietary intake of long-chain forms of vitamin K2 has been associated with reduced risk of coronary heart disease. Therefore, vitamin K2 enrichment in the diet is of high interest for human health. As long-chain vitamin K2 (MK-5 to MK-10) is exclusively produced by bacteria, vitamin K2 producing bacteria that are commonly used in food fermentations provide unique opportunities for dietary vitamin K2 enrichment. *Lactococcus lactis* has a long history of safe use in fermented foods and produces vitamin K2 mainly in the forms of MK-9 and MK-8. Knowledge on the influence of cultivation conditions, biosynthesis pathway and physiological mechanism of vitamin K2 production in *L. lactis* is important for the development of vitamin K2-enriched fermented foods (Part I, chapter 3-5).

Initially, various *L. lactis* strains were screened for vitamin K2 content, and the impact of various cultivation conditions was examined (chapter 3). It was observed that *L. lactis* produced MK-8 and MK-9 as the major MK variants, and that significant strain diversity existed in terms of specific concentrations and titers of vitamin K2. *L. lactis* ssp. *cremoris* MG1363 was chosen for more detailed studies of the impact of selected carbon sources on vitamin K2 production in M17 media. Aerobic fermentation with fructose as a carbon source resulted in the highest specific concentration of vitamin K2: 3.7- fold increase compared to static fermentation with glucose, whereas aerobic respiration (with heme supplementation) with trehalose resulted in the highest titer: 5.2-fold increase compared to static fermentation with glucose. When the same strain was applied to quark fermentation, it was consistently observed that altered carbon source (fructose) and aerobic cultivation of the pre-culture resulted in elevated vitamin K2 concentrations in the quark product.

Next, an adaptive laboratory evolution (ALE) strategy was applied to obtain natural vitamin K2 overproducing *L. lactis* strains (chapter 4). Based on the observation (chapter 3) that aerated cultivation improves vitamin K2 content in *L. lactis*, an ALE experiment was performed on *L. lactis* MG1363 by cultivating this strain in a shake flask in a sequential propagation regime with transfers to a fresh medium every 72 hours (chapter 4). After 100 generations of propagation, three evolved strains were selected that showed improved stationary phase survival in oxygenated conditions. In comparison to the original strain MG1363, the evolved strains showed 50% - 110% increased vitamin K2 content and exhibited high resistance against hydrogen peroxide-induced oxidative stress. Genome sequencing and proteomic analysis provided explanations for the enhanced oxidative stress resistance, but the mechanisms underlying elevated vitamin K2 content in the evolved strains remain to be elucidated.

Besides the long-chain forms of vitamin K2, mainly MK-8 and MK-9, *L. lactis* also produces a detectable amount of short-chain forms, mainly represented by MK-3. The physiological significance of the various

MK forms in *L. lactis* had not been investigated extensively before. In the study described in chapter 5, *L. lactis* mutants with different MK profiles were constructed: a non-MK producer, a presumed MK-1 producer and a MK-3 producer were obtained, confirming the roles of several gene products in the MK biosynthesis pathway in *L. lactis*. Together with the wildtype strain MG1363 producing mainly MK-9 and MK-8, these strains were used to further elucidate the functionality of the long-chain and short-chain MKs in *L. lactis.* By examining the phenotypes of the MG1363 wildtype strain and respective mutants under aerobic, anaerobic and respiration-permissive conditions, we could infer that short-chain MKs like MK-1 and MK-3 are preferred to mediate extracellular electron transfer (EET) and reaction with extracellular oxygen, while the long-chain MKs like MK-9 and MK-8 are more efficient in aerobic respiratory electron transport chain (ETC). The different electron transfer routes mediated by short-chain and long-chain MKs likely support growth and survival of *L. lactis* in a range of (transiently) anaerobic and aerobic niches including food fermentations, highlighting the physiological significance of diverse MKs in *L. lactis*.

While it is of interest to improve the content of vitamin K2 in fermentation key players like *L. lactis* and eventually in the diet, the actual efficiency of delivering this vitamin to the human body is important as well. Vitamin K2 may not be readily and thoroughly absorbed by the human body due to the lipophilicity, especially for the long-chain forms like MK-9. The thick cell wall of Gram-positive bacteria like *L. lactis* could add an additional barrier for accessing vitamin K2, which is accumulated in the bacterial cell membrane. Efforts to improve the delivery of bacterial membrane-bound vitamin K2 into the human host are desired, yet not made previously.

Opportunities for bacterial membrane-bound vitamin K2 delivery are expected with extracellular membrane vesicles (EVs or MVs). EVs are produced by all domains of living organisms, including bacteria, both Gram-positive and Gram-negative. These vesicles are derived from the cell membrane, forming membrane-enclosed spheres carrying various types of cargos in the lumen or the membrane (DNA, RNA, protein, etc.) supporting exchange between cells. The impact of bacterial EVs on health and disease are being revealed gradually, and the potential of EVs in various applications has been highlighted (reviewed in chapter 2). Since vitamin K2 is present in the bacterial cell membrane, bacterial EVs are potentially ideal vehicles for efficient delivery of this vitamin to the human host with a similar principle as liposomes, namely to improve the solubility and absorption of hydrophobic compounds. Given this hypothesis, the EV-producing potential of *L. lactis* as vitamin K2 producer is of high interests (Part II, chapter 6-8).

The findings started with intriguing observations on *L. lactis* strains residing in an artisanal cheese fermentation starter (named Ur), where bacteriophages not only co-exist with bacteria but also are highly abundant. These *L. lactis* strains (TIFN1 – TIFN7) are hosts to prophages belonging to the family *Siphoviridae,* and genome analysis on most of these prophages revealed disruptions in different tail encoding genes, resulting in a common tailless phenotype of released phage particles (chapter 6). Remarkably, these *L. lactis* strains showed detectable spontaneous phage production and release (10^9-

10^{10} phage particles/mL) and up to 10-fold increases upon prophage induction, while in both cases no obvious cell lysis was observed. Intrigued by this phenomenon, the host-phage interaction was examined using *L. lactis* ssp. *cremoris* TIFN1 (harboring prophage proPhi1) as a representative (chapter 7). It was confirmed that during the massive phage release, all bacterial cells remained viable. Further, by monitoring phage replication *in vivo*, using a green fluorescence protein reporter combined with flow cytometry, it was demonstrated that the majority of the bacterial population (over 80%) was actively producing phage particles when induced with mitomycin C. The released tailless phage particles were found to be engulfed in lipid membranes, as evidenced by electron microscopy and lipid staining combined with chemical lipid analysis. Based on the collective observations, a model of phage-host interaction in *Lactococcus lactis* TIFN1 was proposed, where the phage particles are engulfed in membranes upon release, thereby leaving the producing host intact.

To further understand the mechanism of the interesting behavior of *L. lactis*, another isolate from artisanal cheese, *L. lactis* ssp. *cremoris* FM-YL11, was used that showed similar growth profiles and contained an identical prophage sequence as strain TIFN1. By applying a standard EV isolation procedure, EVs were observed in the culture supernatant of strain FM-YL11, for which the prophage-inducing condition (addition of mitomycin C) led to an over 10-fold increase in EV production in comparison to the non-inducing condition (chapter 8). In contrast, the prophage-encoded holin-lysin knock-out mutant YL11ΔHLH and the prophage-cured mutant FM-YL12, produced constantly low levels of EVs, under both prophage-inducing and non-inducing conditions. Under the prophage-inducing condition, strain FM-YL11 did not show massive cell lysis. Defective phage particles were found to be released in and associated with holin-lysin induced EVs from FM-YL11, as demonstrated by transmission electron microscopic images, flow cytometry and proteomics analysis. Taken together, evidence was provided that *L. lactis* produces EVs, and EV production is stimulated by the prophage-encoded holin-lysin system.

Finally, the possibility of using *L. lactis* EVs to deliver vitamin K2 to human cells was examined (Part III, chapter 9). It was demonstrated that EVs produced by *L. lactis* carry mainly long-chain vitamin K2 (MK-8 and MK-9). When these EVs were applied to *in vitro* grown osteosarcoma cells, the ratio of carboxylated over non-carboxylated osteocalcin increased, indicating functional delivery of bioactive vitamin K2 by bacterial EVs. The efficiency of vitamin K2 delivery by EVs was higher than adding solvent-dissolved pure compounds at similar concentrations. Therefore, this study provides proof of principle that bacterial EVs are ideal vehicles to deliver lipophilic compounds like vitamin K2 to the human host.

The results from each part of this thesis study were further discussed in chapter 10, from phenotypical observations to mechanistic insights, from current findings to future perspectives. The opportunities for the application of bacterial EVs in food, feed and pharma were highlighted, and diverse EV producing/cargo loading strategies are proposed. Given the advantages of using Gram-positive bacteria as the source of EVs, it is expected that the rapid advances in Gram-positive bacterial EVs will complement and further stimulate the booming research field of EVs.

In conclusion, this thesis study not only examined the fundamental mechanisms of vitamin K2 and EV production in *L. lactis*, but also demonstrated the possibilities for vitamin K2 enrichment of fermented food as well as efficient delivery of vitamin K2 to the human host. Findings from this thesis are expected to contribute to the field of food fermentation, biotechnology, as well as nutrition and health. Remaining questions and perspectives that are put forward also emphasize the requirements and benefits for further exploration and exploitation of microbial vitamin K2 enrichment of foods and possible therapeutic applications of Gram-positive bacterial EVs.

Acknowledgements

Growing up as a fan of the “Harry Potter” stories, I had been expecting admission letters from wizarding schools for years as a child. Until today, the owls still have not managed to find their way to me, but I think I have already found my “Hogwarts” ever since I ventured to the Netherlands at the age of 18 and stepped into the scientific world. Science is just as fascinating as magic, but what’s even more magical to me, is the connection and bonding I have with many beautiful people. Because of these people, I experienced the effect of Felix Felicis, collected powerful memories to defeat dementors, and got the wisdom and courage to face the “Voldemort” in my own mind.

I would like to take this chance and sincerely thank everyone who has been part of my magical (PhD) journey, even if I do not manage to mention every single name, please know that you are gratefully acknowledged.

First I would like to thank my promotors and supervisors, Prof. **Eddy Smid** and Prof. **Tjakko Abee**. You both are truly mentors to me. I cannot fully express how lucky I feel to be supported and coached by you ever since I was a master student until today. The encouragement, inspiration you gave me and the trust you had in me, have been energizing me the whole time. **Eddy**, I always like to listen when you explain things to me, both about science and life (sometimes about cats), in most fun and nice stories. When I face frustrations and dilemmas, you support me with the most warm, relaxing and understanding voice, and help me to see the most realistic solutions. With every step of progress and achievement I made, you never hold back in giving me positive feedback, which helped me a lot in building confidence. Your sharp eyes in spotting even the smallest errors in my manuscript and critical review have been extremely helpful for my learning progress and making solid steps. **Tjakko**, it is hard to find another person who inspired me as much as you did. I appreciate so much the endless ideas from you, the connections in various topics you helped me to see, and the interesting and helpful literatures you shared with me (usually sent on a Sunday morning), all of which kept challenging and inspiring me in the best possible way. You are the most visionary, and always look far ahead - I cannot count how many times after my experiments, analyses or reflection, I finally realized: oh, Tjakko was right when he mentioned this to me 3 months ago/last year!... Not only in scientific research, you also inspired and stimulated me in my personal growth. You always sense my moments of insecurity and powerlessness even before I realize it myself, and magically take them away with your kind words. Your knowledge and passion in science and dedication in guiding others to greater heights have been and will always be my model.

I also thank the other members of my thesis committee: Prof. **Michiel Kleerebezem**, Prof. **Egon Bech Hansen**, Prof. **Jennifer Mahony** and Prof. **Marianne Geleijnse**, thank you for taking the time to critically review my thesis, I look forward to discussing it with you.

Many analyses presented in this thesis work were performed in collaboration with colleagues from different WUR research groups. I would like to thank **Sjef Boeren** at Biochemistry for his assistance with proteomics analysis. **Sjef**, your timely help, clear communication and patient explanations were very essential for the pleasant and efficient collaboration we had, and I also see the kind considerations you have for other people, which I appreciate very much! I would also like to thank **Eric van Bennekom** and **Tina Zuidema** at Rikilt for the HPLC-MS analysis. **Eric**, you have been a great teacher to me for HPLC! And thank you for even letting me use your own work computer, so I could most efficiently process the data. **Tina**, thank you for your always timely response and openness to our collaboration! I thank **Mark Sanders** at Food Chemistry for his assistance in UPLC-MS analysis. **Mark**, your knowledge and expertise in analytical chemistry is impressive, I learned so much from you! I am also grateful towards **Marcel Giesbers** and **Jelmer Vroom** at Wageningen Electron Microscopy Centre for their assistance in EM imaging. **Marcel** and **Jelmer**, you literally helped me to see a "different world"! Moreover, I thank **Harry Baptist** at Food Physics for his kind help with the ultracentrifuge.

Now, my thoughts go to Food Microbiology – feels like home. This is where I spent the past many years, got so many beautiful memories and daily supports from all colleagues. I let my thoughts pass by the offices one by one, to thank each colleague personally.

Ingrid, before people enter the labs, they must remember your words – you also make fun of this situation yourself sometimes, but it never changes that you are fair and strict at the same time, to remind people of the safety rules and to keep labs in order. I personally think it takes much courage and assertiveness to insist doing so, and I respect you so much for that! To me you are also like a warm, caring big sister, I always like going for lunch together with you and having all the little chats with you!

Natalia, we started our PhD at similar time, took Dutch course together (remember how we giggled like teenagers haha), went to both PhD trips together, laughed about certain slogans together, and even start to become crazy about cats almost at the same time too! Thanks for being the favorite auntie for Kiwi and Koco, and I really hope I am also someone special for Miki and Luna! **Pjotr**, thank you for being my paranymph! You standing close to me on this important day is giving me the relaxing and cheerful feeling of being surrounded by good friends. You helped me a lot when I had different types of difficulties, for which I am always grateful. **Xuchuan**, so many times I am impressed by your broad knowledge and cooking skills on delicate dishes! I also remember one time you saw me very upset, and you played a nice piece of piano music for me to calm down. You are truly a gentleman! **Maren**, your cheerful laughter is the most infectious! And you have organized so many nice group activities, showed care towards other colleagues, and not to forget your great sense of humor! **Jasper B.**, you are a master of escape rooms! I always remember the moment when you were helping me practice Dutch, you spoke to me very slowly with an encouraging smile, almost like talking to a 3-year-old haha! That was so patient and kind of you!

Gerda, when I think of you, I see that calming smile you always have on your face. I cannot pinpoint how many seemingly regular things kept running properly every day at work, are because of your support and great sense of responsibility. I remember once you checked with me whether a certain issue of mine was solved, as you woke up in the middle of the night thinking about it… Recently I also shared my dream with you, in which I was too late for my defence – again I see that calming smile on your face, and you said: "I'll drive you to Aula if you really run late that day, don't worry." All of a sudden, that dream was not so horrible to me anymore, haha. Thank you for being always so supportive, Gerda!

Marcel Z., thank you for the great leadership, making FHM a working place with good atmosphere! You are always approachable, and show care and support to all colleagues by your enthusiastic participation in all group activities (that was a very impressive mask you had for the Xmas pubquiz), and you were also present in my wedding in spite of your busy schedule! In all these years, you have been giving me friendly and constructive feedback for my presentations or performance as a chairperson (Zachte heelmeesters geven stinkende wonden, I will always remember), and I can always consult you about how to handle different situations. Thank you for your guidance and support!

Marcel T., thank you for your great support in the flow cytometry analysis, and also many interesting discussions of other projects! Your knowledge, expertise and sharp eyes in identifying problems always impress me. I learned a lot from you! **Dennis**, thank you for your valuable advice on the cloning work, your kind support with IT related issues, and all the nice chats we had about science or cats! **Gerrieke**, it was nice to work in the same lab with you, and I wish you all the best!

Oscar, thank you for being my paranymph, but you should not be surprised when I invited you for this, right? – When we met each other at Dyadic, I was a bachelor student and you a master student, and every step after that I somehow followed you. I have always looked up to you, and you have also been there when I need help and advice. After so many years, it is so beautiful to see that besides the success of your work, you are now a proud father (not sure if I can follow you soon on this, haha)! I am so happy for you. **Jeroen**, Dr. Jeroen!! You made it, and you deserve it. You are a great teacher to the students, and a colleague who is always willing to offer his helping hand. Your kind help with the R script for proteomics data analysis and advice for DNA sequence database really saved me, even though the time I asked for help was also busy time for yourself. I wish you success and happiness in whatever you will take next! **Frank**, you are a role model for many of us, work hard and never complain, and you are the most kind and humble person. I wish you a smooth finalization of your PhD! **Alex**, you are one of the most intelligent persons I know! And I appreciate that you often take initiative to share with other colleagues the scripts/methods you developed. Besides your nice results in scientific research, I am also super happy for you with the little family members joining!

Andy, when a person is both intelligent and hardworking as you are, there are not many things that can stop him from his goal. During the past years we exchanged opinions on work and life, and you

could always surprise me with new insights. Thank you for all your advice on data visualization (you are so talented in this!), lab techniques, and finalization of PhD, and for all your encouragement! I wish you all the success and happiness in pursuing your dream! **Angela**, I remember so many little chats we had, we also encouraged each other many times. You are a very caring person towards others, which I really appreciate. **Ioanna**, my first office mate during the PhD! I remember all the jokes we had, and you even implemented one of them at my "Bachelor's party" haha! Hope to see you often with dinners/ballet shows! **Diego**, I miss you and you are always in my mind and heart. **Nathalia**, we exchanged a lot of opinions on career and even dancing! Thank you for encouraging me in both!

Heidy, it has been so much fun to celebrate birthday in office together with you in the past years! I was very touched by the career/life story you once shared of yourself, thank you for inspiring other (women) scientists! **James Noah**, thank you for your kind words when seeing me struggling with the final phase!

Judith and Wilma, it has been such a pleasure to be your office mate, and to work together with you on education tasks! You both helped me in setting up the facilities for cell line cultivation, thank you very much! **Judith**, you are always so friendly and understanding, efficient yet with the most pleasant approach. I could share my thoughts with you, and you responded warmly like a big sister of mine. **Wilma**, when we work on the same course, the communication with you is always super clear, and I learned a lot from your thoughtfulness. I still remember the big hugs you gave me when I passed my Dutch exam – thank you for all the encouragement!

Alberto G., my best teacher in statistics, R, and beer opening!! I cannot tell which of the three topics here is more important, but you are definitely showing passion and dedication in teaching them all, haha! But now seriously: thank you for advising me when I had doubts with statistic analyses! **Claire**, it is always nice to listen to your presentation, starting with a nice story! **Richard**, thank you for the discussion on delivery of genome editing tools, was very inspiring!

Martine, you are so kind and caring towards others, I remember you checking on me when we flew to Italy for the PhD trip (turned out I was just falling asleep haha), when I was anxious for a meeting, and when covid hit my home country…Not sure if you even remember these moments, but for me these were very heartwarming, I really appreciate it. **Denja**, I am happy to get to know you, and to have some fun musical/stretching/chatting activities with you. Your approach, or rather your nature, of being inclusive and caring with everyone at work is just beautiful! **Esther**, so glad that we are still in touch even after you left the group, and to learn about every step you made ever since. All the best with the little one! Cannot wait to meet him/her. **Mark**, **Gamze**, it has been a pleasure to work with you during practical courses!

Linda, I am still using the magical brownie recipe you shared with me. You are such a lovely person to be around with and work with, not only because of your extraordinary baking skills of course! **Alberto**

B., I like all our little chats in office and lab, and I like your sense of humor! **Rebecca**, it is always so engaging when you passionately describe the nice foods from your hometown! **Evelien**, thank you for all the discussion we had about different analyses, and your kind advice!

Svetlana, thank you for your guidance already during my master thesis, your passion and knowledge have been inspiring me also during my PhD!

Irma, **Bernard**, **Anneloes G.**, **Jennifer**, **William**, **Anneloes vB., Lise,** although it seemed short, but I have many nice memories on our interactions during the shared office time or PhD trips! **Sylviani**, **Tamara**, **Thelma**, **Jasper Z., Domiziana**, **Georgios**, wish you all the best with your work and PhD journey!

I would like to thank MSc/BSc students who conducted their internship/thesis under my PhD project. **Kyra**, you are exceptional in every positive way, it was my pleasure to work with you and I am happy that we stayed in touch until now! **Daniel**, **Yu**, **Alisha**, **Anteun**, **Joost**, **Alexios**, **Nikolaos**, **Eline**, **Hidde**, **Ioanna V.**, **Shiyu**, it has been a privilege to supervise you, and I learned also from each of you. Thank you for the good work, I appreciate all the nice personal interactions we had during and after your thesis projects, and I feel proud to see your development. I wish you all the best!

I also thank students in the groups under my supervision in MSc course Advanced Fermentation Science (2017 – 2019). Thank you for your interest in the topic, and your work has directly or indirectly contributed to insights described in this thesis.

I gratefully acknowledge **Jingjie Zhu**, **Joanna Kaczorowska**, **Thijs Kouwen**, **Herwig Bachmann**, **Jesús Adrián Guerra Martínez**, **Nataliya Yeremenko**, thank you for the contribution and collaboration, which lead to our co-authored chapters.

I would like to thank Prof. **Karin Schroën** and Dr. **Fré Pepping**, for the effort you put in the VLAG research master program. Students like myself do not only benefit from it by receiving a grant to start a PhD project, but also from the nicely designed coaching sessions on personal effectiveness and proposal writing, which has been/will be helpful throughout my career. I also thank Prof. **Ivonne Rietjens**, for the advice and inspiration you gave me.

Yvonne and **Vesna**, thank you for all the organization and administration work for the many nice VLAG courses!

During the daily work of my PhD, I always recognize elements that I have learned from all my supervisors during BSc/MSc internship/thesis projects, for which I am very grateful. Special thanks to Dr. **Franklin Nobrega** and Dr. **Jeroen van Dijk**, for your continuous encouragement during my PhD!

I thank my colleagues at Chinese Association of Life Sciences in the Netherlands, especially **Yuanjie**, thank you for your trust and guidance!

My dear friends, **Ren**, **Jiaying**, **Qinmei**, **Elaine** & **George**: we all came to the NL at a young age, and have been taken care of each other, witness the growth and development of each other, which forms a strong friendship that is extremely precious to me. Even after a long time not seeing each other, we can pick up chatting topics as if we continued from yesterday, and as if everything has not changed since the time at HAN. I always remember the beautiful times we had together, and how you all stood next to me during the difficult times I had. **Ren**, special thanks to you for drawing my thesis cover, you visualized my ideas in such a nice way, with great patience, understanding and dedication. It means a lot to me that the cover is made by a great friend like you.

Peiqing, **Qinhui**, **Li**, **Jing**, **Xinhua**... and all friends I met in Wageningen. I cherish all the beautiful memories with you, and no matter where you are now, I wish you all the best and hope to see you again very soon!

Ik wil graag mijn schoonfamilie bedanken, dankzij jullie liefde en steun ben ik me echt thuis gaan voelen in Nederland.

感谢故乡的家人，以及我成长过程中的良师益友，感谢你们对我的关爱与照顾。在天堂的爷爷奶奶，我知道你们一直都在护佑着我。

感谢我亲爱的爸爸妈妈，你们总是尊重我的决定，并给我最坚定的爱与支持。你们的健康幸福是我的心愿，也希望你们可以放心追求自己的心愿。

Dear Dustin, just like all beautiful things, our relationship comes with both the challenging and rewarding aspects. Your company, love and support have been crucial to me in both sunny and rainy days. You are at the strongest and softest place of my heart, and you are the additional motivation and inspiration in my life. May we both continue growing in this relationship, and have fun tasting the chocolates in the box of life together. I love you.

Affiliations of co-authors*

Svetlana Alexeeva, Kyra A.Y. Defourny, Yu Zhang, Jingjie Zhu, Joanna Kaczorowska, Jesús Adrián Guerra Martínez, Anteun de Groot, Nikolaos Charamis, Joost Blok, Alisha Geraldine Lewis, Marcel H. Tempelaars, Eline van Ophem, Eddy J. Smid, Tjakko Abee
Food Microbiology, Wageningen University & Research, the Netherlands

Eric O. van Bennekom
BU Veterinary Drugs, RIKILT, Wageningen University & Research, the Netherlands

Sjef Boeren
Laboratory of Biochemistry, Wageningen University & Research, the Netherlands

Thijs R.H.M. Kouwen
DSM Biotechnology Center, Delft, the Netherlands

Herwig Bachmann
NIZO B.V., Ede, the Netherlands

Nataliya Yeremenko
Department of Rheumatology & Clinical Immunology and Department of Experimental Immunology, Amsterdam UMC, University of Amsterdam, the Netherlands

*Affiliations at the time of collaboration.

About the author

Yue Liu was born on the 5th of July, 1992, in Jinan, China. She grew up, and received primary and secondary education in China.

In 2010, Yue came to the Netherlands for her BSc education in Life Sciences at HAN University of Applied Sciences (Nijmegen), and graduated *cum laude* in 2014. During the BSc education, she conducted various internships and thesis projects at companies and research institutes in the Netherlands including Synthon (Nijmegen), Rikilt (Wageningen), Dyadic Netherlands (Wageningen, currently DuPont), DSM Biotechnology Center (Delft), and participated in a variety of projects ranging from analysis of medical compounds to GMO detection and microbial strain development.

In parallel to her BSc education, Yue also completed the Analytical Science Talent Program organized by Top Institute for Comprehensive Analytical Science and Technology (TI-COAST) in the Netherlands, from which she received additional lectures and trainings in analytical chemistry.

In 2014, Yue started her MSc education in Biotechnology at Wageningen University, specialized in cellular/molecular biotechnology, and graduated *cum laude* in 2016. During the MSc education she conducted two thesis projects: a minor thesis project at the Laboratory of Microbiology, Wageningen University & Research (WUR) on modifying the host range of bacteriophages by genome recombination, supervised by Dr. Franklin Nobrega and Dr. Stan Brouns. The other thesis project was carried out at the Laboratory of Food Microbiology (WUR), focusing on understanding the bacteria-phage interactions in dairy starter cultures, supervised by Dr. Svetlana Alexeeva, Prof. Eddy Smid and Prof. Tjakko Abee.

In addition to the regular MSc courses and theses, Yue participated in the VLAG graduate school Research Master Program at WUR, from which she received trainings in proposal writing and developed a research proposal, coached by Prof. Eddy Smid and Prof. Tjakko Abee. This proposal was awarded a grant from Netherlands Organisation for Scientific Research (NWO) through the Graduate Program on Food Structure, Digestion and Health, which allowed Yue to start a PhD project at the Laboratory of Food Microbiology (WUR) in September 2016.

Yue's PhD project is entitled: "Good things come in small packages - delivery of vitamin K2 to human cells by extracellular vesicles from *Lactococcus lactis*". The results are described in this thesis. Currently, Yue is working as a postdoc at the Laboratory of Food Microbiology (WUR), and her research focuses on extracellular vesicles produced by food-associated Gram-positive bacteria and their implications in human health and disease.

List of publications

This thesis

Liu, Y., Defourny, K.A., Smid, E.J., and Abee, T. (2018). Gram-positive bacterial extracellular vesicles and their impact on health and disease. **Frontiers in Microbiology**, 9, 1502.

Liu, Y., van Bennekom, E.O., Zhang, Y., Abee, T., and Smid, E.J. (2019). Long-chain vitamin K2 production in *Lactococcus lactis* is influenced by temperature, carbon source, aeration and mode of energy metabolism. **Microbial Cell Factories**, 18, 129.

Alexeeva, S.*, Liu, Y.*, Zhu, J., Kaczorowska, J., Kouwen, T.R.H.M., Abee, T., and Smid, E.J. (2020). Genomics of tailless bacteriophages in a complex lactic acid bacteria starter culture. **International Dairy Journal**, 104900.

Liu, Y., de Groot, A., Boeren, S., Abee, T., and Smid, E.J. (2021). *Lactococcus lactis* mutants obtained from laboratory evolution showed elevated vitamin K2 content and enhanced resistance to oxidative stress. **Frontiers in Microbiology**, 12, 746770.

Liu, Y., Tempelaars, M.H., Boeren, S., Alexeeva, S., Smid, E.J., and Abee, T. (2022). Extracellular vesicle formation in *Lactococcus lactis* is stimulated by prophage-encoded holin-lysin system. **Microbial Biotechnology**, in press.

Liu, Y.*, Alexeeva, S.*, Bachmann, H., Guerra Martínez, J.A., Yeremenko, N., Abee, T., and Smid E.J. (2022). Chronic release of tailless phage particles from *Lactococcus lactis*. **Applied and Environmental Microbiology**, 88, e01483-21.

Liu, Y., Charamis, N., Boeren, S., Blok, J., Lewis, A.G., Smid, E.J., and Abee, T. (2022). Physiological roles of short-chain and long-chain menaquinones (vitamin K2) in *Lactococcus cremoris.* **Frontiers in Microbiology**, in press.

Liu, Y., van Ophem, E., Smid, E.J., and Abee, T. Lactococcal extracellular membrane vesicles deliver bioactive vitamin K2 to human cells. **Manuscript in preparation.**

* Shared first author.

Others

Liu, Y., Smid, E.J., Abee, T., and Notebaart, R.A. (2019). Delivery of genome editing tools by bacterial extracellular vesicles. **Microbial Biotechnology**, 12, 71–73.

Liu, Y., Alexeeva, S., Defourny, K.A., Smid, E.J., and Abee, T. (2018). Tiny but mighty: bacterial membrane vesicles in food biotechnological applications. **Current Opinion in Biotechnology**, 49, 179–184.

Vlot, M., Nobrega, F.L., Wong, C.F.A., Liu, Y., and Brouns, S.J.J. (2018). Complete genome sequence of the Escherichia coli phage Ayreon. **Genome Announcements**, 6, e01354-17.

Overview of completed training activities

Discipline specific activities

Courses

Genetics and physiology of food-associated micro-organisms (VLAG, Wageningen, NL)	2016
Advanced food analysis (VLAG, Wageningen, NL)	*2017
Advanced microbial physiology and fermentation technology (BioTech Delft, Delft, NL)	2019
VLAG online seminars (VLAG, online)	2020
Ecophysiology of food-associated micro-organisms: Roles in health and disease (VLAG, Wageningen, NL)	**2021

Meetings and conferences

12th International symposium on lactic acid bacteria (Egmond aan zee, NL)	*2017
International conference on microbial food and feed ingredients (Copenhagen, DK)	**2018
Fall meeting KNVM division general and molecular microbiology (Amsterdam, NL)	2019
The international society for extracellular vesicles infectious diseases meeting (ISEV, online)	2021
The international society for extracellular vesicles 10th annual meeting (ISEV, online)	**2021
13th International symposium on lactic acid bacteria (online)	*2021
Danish microbiological society's annual congress (Copenhagen, DK)	*2021
2nd International conference on microbial food and feed ingredients (Copenhagen, DK)	*2021

General courses

Transmission electron microscopy (WEMC, Wageningen, NL)	2016
Project and time management (WGS, Wageningen, NL)	2017
Supervising BSc and MSc thesis students (WUR, Wageningen, NL)	2018
Reviewing a scientific paper (WGS, Wageningen, NL)	2018
Introduction to R (VLAG, Wageningen, NL)	2018
PhD Workshop carousel (WGS, Wageningen, NL)	2018
Scientific writing (Wageningen in'to Languages/WGS, Wageningen, NL)	2018
Brain friendly working and writing (WGS, Wageningen, NL)	2019
Career perspectives (WGS, online)	2020
The Choice: Un-box your PhD process & take charge of your performance (WGS, Wageningen, NL)	2020
Philosophy and ethics of food science & technology (VLAG/WGS, online)	2021

Optional activities

Preparation of research proposal (FHM/VLAG, Wageningen, NL)	2016
PhD study tour to Italy (FHM, IT)	**2017
Weekly group meetings (FHM, Wageningen, NL)	2016 – 2020
PhD study tour to China (FHM, CN)	**2019
Organizing PhD study tour to China (FHM, Wageningen, NL)	2018 – 2019

Teaching activities

FHM-21806 Food fermentation	2017 – 2018
FHM-30806 Advanced fermentation science	2017 – 2019
Supervison of MSc- and BSc-thesis students	2017 – 2019

*Poster presentation

**Oral presentation

The research described in this thesis was subsidized by the Netherlands Organization for Scientific Research (NWO) through the Graduate Program on Food Structure, Digestion and Health.
Financial support from Wageningen University for printing the thesis is gratefully acknowledged.

Cover design by: Ren Xie & Yue Liu
Layout by: Bregje Jaspers
Printed by: ProefschriftMaken

300